Contact lens fitting characteristics and comfort with silicone hydrogel lenses

by

Jyotsna Maram

A thesis
presented to the University of Waterloo
in fulfillment of the
thesis requirement for the degree of
Doctor of Philosophy
in
Vision Science

Waterloo, Ontario, Canada, 2012

AUTHOR'S DECLARATION

I hereby declare that I am the sole author of this thesis. This is a true copy of the thesis, including any required final revisions, as accepted by my examiners.

I understand that my thesis may be made electronically available to the public.

Abstract

Purpose

To examine soft contact lens fitting characteristics using anterior segment imaging techniques and comfort. The specific aims of each chapter are as follows:

Chapter 2: To calibrate the new ZEISS Visante™ anterior segment optical coherence tomographer (OCT) using references with known physical thickness and refractive index equal to the human cornea and to compare the Visante measures to those from a previous generation OCT (Zeiss-Humphrey OCT II).

Chapter 3: The first purpose of this study was to measure the repeatability of the Visante ™ OCT in a normal sample. The second was to compare corneal thickness measured with the Visante ™ OCT to the Zeiss-Humphrey OCT II (model II, Carl Zeiss Meditec, Jena Germany) adapted for anterior segment imaging and to the Orbscan II ™ (Bausch and Lomb, Rochester New York).

Chapter 4: Conjunctival displacement observed with the edges of the contact lens, when imaged may be real or may be an artefact of all OCT imagers. A continuous surface appears displaced when the refractive index of the leading medium changes at the edge of a contact lens. To examine this effect, edges of the contact lenses were imaged on a continuous surface using the UHR-OCT. Contact lens edges on the human conjunctival tissue were also imaged to see if the lens indentation on the conjunctival tissue is real or an artefact at the edge of the lens.

Chapter 5: The main purpose of this study was to determine if we can predict end of the day discomfort and dryness using clinical predictive variables. The second purpose of the study was to determine if there

was any relationship between lens fitting characteristics and clinical complications and especially to the superior cornea and conjunctiva with a dispensing clinical trial.

Methods

Chapter 2: Twenty two semi-rigid lenses of specified thicknesses were manufactured using a material with refractive index of 1.376. Central thickness of these lenses was measured using Visante^{TM} OCT and Zeiss-Humphrey OCT II (Zeiss, Germany). Two data sets consisting of nominal measures (with a standard pachymeter of the lenses and one obtained using a digital micrometer) were used as references. Regression equations between the physical and optical (OCT) measures were derived to calibrate the devices.

Chapter 3: Fifteen healthy participants were recruited. At the Day 1 visit the epithelial and total corneal thickness, across the central 10mm of the horizontal meridian were measured using the OCT II and the Visante ^{TM} OCT. Only total corneal thickness across the central 10mm of the horizontal meridian was measured using the Orbscan II. The order of these measurements was randomized. These measurements were repeated on Day 2. Each individual measurement was repeated three times and averaged to give a single result.

Chapter 4: (2-D) Images of the edges of marketed silicone hydrogel and hydrogel lenses with refractive indices (n) ranging from 1.41-1.51 were taken placing them concave side down on a continuous surface. Five images for each lens were taken using a UHR-OCT system, operating at 1060 nm with ~3.2um (axial) and 10μm (lateral) resolution at the rate of 75,000 A-scans/s. The displacement of the glass slide beneath the lens edge was measured using Image J.

Chapter 5: Thirty participants (neophytes) were included in the study and the four lenses (Acuvue Advance 8.3, Acuvue Advance 8.7, Pure Vision 8.3, and Pure Vision 8.6) were randomly assigned for each eye. The lenses were worn for a period of two weeks on a daily wear basis for 8 to 10hrs per day. Lens performance was monitored over the 2week period. Assessment of subjective comfort was made using visual analogue scales. Total corneal and epithelium thickness was measured using the Visante OCT, the lens edge profiles of the contact lenses were observed using the ultra-high resolution OCT and the conjunctival epithelial thinning was measured using the RTVue OCT. Conjunctival blood velocity was measured at the baseline and 2 week visit using a high magnification camera.

Results

Chapter 2: Before calibration, repeated measures ANOVA showed that there were significant differences between the mean lens thicknesses from each of the measurement methods ($p<0.05$), where Visante measurements were significantly different from the other three (OCT II, MG and OP) methods ($p<0.05$). Visante thickness was significantly higher than the microgauge measures (453±37.6 µm compared to 445.1±38.2 µm) and the OCT II was significantly lower (424.5±36.1 µm both, $p<0.05$). After calibration using the regression equations between the physical and optical measurements, there were no differences between OCT II and Visante OCT ($p<0.05$).

Chapter 3: Mean central corneal and epithelial thickness using the Visante™ OCT after calibration at the apex of the cornea was 536± 27 µm (range, 563-509 µm) and 55± 2.3 µm (range, 57.3-52.7 µm), respectively. The mean corneal and epithelial thickness using OCT II at the apex was 520±25µm and 56±4.9 µm, respectively. The mean of total corneal thickness measured with the Orbscan II was 609±29µm. Visante OCT was the most repeatable for test-retest at the apex, nasal and temporal quadrants of the cornea compared to OCT II and Orbscan II. COR's of Visante OCT ranged from ±7.71µm to

±8.98µm for total corneal thickness and ± 8.72 µm to ± 9.92 µm for epithelial thickness. CCC's with Visante OCT were high for total corneal thickness for test-retest differences ranging from 0.97 to 0.99, CCC's for epithelial thickness showed moderate concordance for both the instruments.

Chapter 4: Results showed that artefactual displacement of the contact lens edge was observed when the lenses were imaged on the glass reference sphere, custom made rigid contact lenses (1.376) and on the conjunctival tissue. The displacement measured on the conjunctival tissue ranged from 7.0±0.86 µm for the Air Optix Night and Day to 17.4±0.22 µm for the Acuvue Advance contact lenses. The range of displacement with the soft lens edges imaged on the rigid contact lens was from 5.51±0.03 µm to 9.72±0.12 µm.

Chapter 5: The lenses with the steepest sag (Acuvue Advance 8.3, Pure Vision 8.3) resulted not only with the tightest fit, but with compromise to the superior conjunctiva. This was especially seen with the Acuvue Advance lenses. The steeper lenses caused more total corneal swelling, superior epithelial thinning, mechanical compression of conjunctiva, conjunctival staining, bulbar hyperemia, conjunctival indentation and reduced blood flow at the lens edge. Not many associations were observed between baseline clinical and 2 weeks sensory variables. However, significant associations were observed when comparing the baseline clinical variables to end of the day sensory variables. Baseline clinical variables compared to 2 week clinical variables also showed significant correlations.

Conclusions

Chapter 2: Using reference lenses with refractive index of the cornea (1.376) allows rapid and simple calibration and cross calibration of instruments for measuring the corneal thickness. The Visante and OCT II do not produce measurements that are equal to physical references with refractive index equal to the human cornea.

Chapter 3: There is good repeatability of corneal and epithelial thickness using each OCT for test-retest differences compared to the between instruments repeatability. Measurements of epithelial thickness are less repeatable compared to the total corneal thickness for the instruments used in the study.

Chapter 4: When contact lenses are imaged in-situ using UHR-OCT the conjunctival tissue appeared displaced. This experiment indicates that this displacement is an artefact of all OCT imagers since a continuous surface (glass slide) was optically displaced indicating that the displacement that is observed is a function of the refractive index change and also the thickness of the contact lens edges.

Chapter 5: Discomfort is a complex issue to resolve since it appears to be related to ocular factors such as the corneal and conjunctival topography and sagittal depth; to lens factors that is 1) how the sag depth of the lenses relate to the corneal/conjunctival shape and depth and therefore how well it moves on the eye. 2) Also with the lens material; whether they are high or low modulus, low or high water content, dehydration properties, wetting agents used and its resistance to deposits, lens edge profile and thickness and its interaction with the upper eyelid.

Acknowledgements

I would like express my sincere thank you to Dr Luigina Sorbara and Dr Trefford Simpson for their support, encouragement and guidance through this amazing journey. Thank you for giving me this opportunity and teaching me the art and science. Working with both of you has been a wonderful and enriching experience.

I would like to sincerely thank Prof Desmond Fonn for trusting in me and making me a part of Center for Contact lens research. Thank you ALL at CCLR for being my extended family.

I would like thank my committee members Prof Desmond Fonn, Dr Natalie Hutchings for their support and willingness to provide guidance. I am also grateful to my external examiner Prof William Joe Benjamin (University of Alabama, Birmingham, AL) and internal external examiner Dr Kostadinka Bezeheva (Department of physics and astronomy, UW) for reviewing my thesis.
I would like to thank Dr Jalaiah Varikooty for his unconditional support and guidance, can't thank you enough.
Heartfelt thanks to Emi Giddens, Gerry Giddens, Alexendra Smith, Leona Voss, Roz Exton, Marina Simpson, Jane Johnson, Grace Dong, Lynn, Diane Bandura for helping me to conduct my studies smoothly and help with data entry and analysis work.
Special thanks to Anne Weber, Krista Parsons, Kim-Tremblay Swan, Jim Davidson, Chris Matters, Andre Lowinsky, Peter Sterling, Chris Mathers and Trevor German for their help.
I thank all past and current GIVS members, staff and faculty of the school of Optometry for providing a pleasant work environment.
I am very thankful to some amazing friends: Preethi, Subam, Bharathi, Sanjay, Naveen, Renu, Maha, Taran, for your love, care and support during my tough times. Thank you to Sruthi, Priya and Lakshman for your friendship.
Special thanks to my best friend Jaya for all your love and support means a lot to me always.

I am eternally grateful to all my gurus who have *given me* the greatest *gift* of *all*, education.

Last but not the least I want to acknowledge the tremendous support from my mother, father and younger brother for their unconditional love and support of my education. In spite of the thousands of miles separating us, the love I felt in every one of their calls made it easier for me to be so far from home. Thank you for teaching me that hard work never fails and that one should be passionate about life and work to succeed.

Dedication

To my father (Sri Surendra Babu) who always encouraged me to go one step further. His words gave me light when everything seemed dark, his voice that guided me in every moment of crisis.

Dad, this is for you. I wouldn't have come this far without you!

Table of Contents

List of Figures

List of Tables

List of symbols and Abbreviations

AA	Acuvue Advance
AS-OCT	Anterior segment OCT
BOZR	Back optic zone radius
CLAPC	Contact lens papillary conjunctivitis
CEF	Conjunctival epithelial flap
CW	Continues wear
CAM	Corneal adaptor module
CCT	Central corneal thickness
COR	Coefficient of repeatability
CCC	Correlation coefficient of concordance
CCLR	Center for Contact Lens Research
Dk/t	Oxygen transmissibility
EW	Extended wear
FDA	Food and Drug Administration
HVID	Horizontal visible diameter
ICC	Intraclass correlation coefficient
LD	Lens diameter
LOA	Limits of agreement
MG	Mechanical gauge
NITBUT	Non-invasive break-up time
OCT	Optical coherence tomography
OP	Optical pachymeter
PDMS	Polydimethylsiloxane

PVP	Poly (vinylpyrrolidone)
PMMA	Polymethyl methacrylate lenses
PV	PureVision
RGP	Rigid gas permeable lens
SEAL	Superior epithelial arcuate lesion
SAI	Surface asymmetry index
SRI	Surface regularity index
SLD	Super luminescent diodes
SD-OCT	Spectral domain
SS-OCT	Swept source
TRIS	Trimethylsiloxy silane
TD-OCT	Time-domain
UBM	Ultrasonic biomicroscopy
UHR-OCT	Ultra high resolution OCT
UBM	Ultrasound biomicroscopy
UP	Ultrasound pachymetry

Chapter 1

This thesis discusses the soft contact lens fitting characteristics and the effect of the lens performance on the anterior segment of the eye. The experiments in this thesis cover a wide range of topics relating to optical coherence tomography (OCT) calibration and repeatability and soft lens fitting characteristics including their physiological effects on the bulbar conjunctiva. Contact lens edge characteristics were examined using a custom made ultra-high resolution OCT. Variables such as meridonial corneal and epithelial thickness, curvature changes and blood velocity measurements were also studied in silicone hydrogel contact lens wearers.

1.1 Introduction and literature review

Hydrogel soft contact lens wear has been associated with a number of changes to the ocular surface such as mechanical, inflammatory and hypoxic responses since their introduction in 1964.[1] Mechanical complications associated with hydrogel lenses include superior epithelial arcuate lesions (SEAL's), localized papillary conjunctivitis and conjunctival epithelial staining.[2-4] These complications are related to both lens and patient characteristics and can be minimized by altering the lens material, designs and manufacturing procedures.[5] Frequent replacement schedules, improvement in lens material and changes in contact lens solutions have been reported to minimize the inflammatory problems associated with contact lens wear.[5;6]

Sufficient oxygen should diffuse through the lens material for maintenance of normal corneal function, and according to Holden and Mertz,[7] fitting a hydrogel contact lens with high water content to maximise Dk/t is not effective in increasing the Dk/t to an appropriate level. In order to improve the oxygen transmissibility of contact lenses over that of conventional hydrogel contact lenses new silicone lens materials were developed in 1970. In the early 90's silicone hydrogel materials were developed

incorporating silicone molecules into the hydrogel skeleton.[8] Silicone hydrogel lenses have more complex monomer compositions compared to pHEMA-based materials. The most common silicone is polydimethylsiloxane (PDMS) (Figure1-1). It has been reported that the hydrophobic characteristic of PDMS induces increased lipid affinity, poor wettability and corneal adhesion.[9] To overcome this, PDMS was modified by combining the high oxygen permeability property of PDMS with the hydrophilic nature and wettability of polyHEMA.[9] The development of the silicon-containing trimethylsiloxy silane (TRIS) monomer lead to the development of the current commercial contact lenses. The two lenses that were used in the clinical experiment reported in this dissertation (chapter 5) are Purevision (Bausch and Lomb) and Acuvue Advance (Johnson and Johnson).

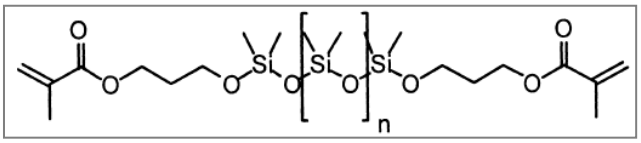

Figure 1-1 The structure of PDMS

(Image courtesy: Silicone Hydrogels the rebirth of continuous wear contact lenses, D.F Sweeney, copyright permission- appendix B)

The first commercially available silicone hydrogels adopted two different approaches. The first approach by Bausch and Lomb incorporated silicone monomers with enhanced compatibility in hydrophilic hydrogel-forming monomers.[9] The silicone monomers increased the stiffness or modulus of the lens material compared to that of HEMA lens.

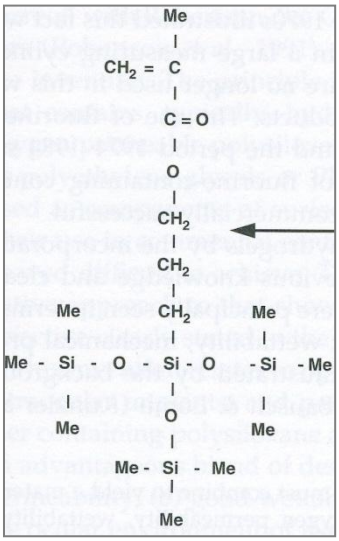

Figure 1-2 Modification site of TRIS by the introduction of hydrophilic groups

(Image courtesy: Silicone Hydrogels the rebirth of continuous wear contact lenses, D.F Sweeney, copyright permission- appendix B)

The second approach by Johnson and Johnson (J&J), was the development of siloxy macromers containing hydrophilic polyethylene oxide segments and oxygen permeable polysiloxane units, which are very hydrophilic materials and are widely used as surfactants.[9] The reduction of silicone monomers by the replacement with theses surfactants reduces the modulus of these lens materials compared to the lens approach of B&L (and Ciba Vision).

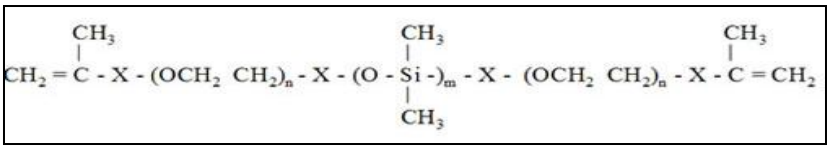

Figure 1-3 Structure of siloxy-based polyfluoroether macromer.

(Image courtesy: Silicone Hydrogels the rebirth of continuous wear contact lenses, D.F Sweeney, copyright permission- appendix B)

Silicone hydrogel contact lenses were introduced commercially in 1998 and have become the lens of first choice for practitioners, and their application for daily wear is increasing.[10;11] There are several silicone hydrogel materials currently available in the market, including balafilcon A (PureVison, Bausch 7 Lomb, Inc), lotrafilcon A and B (Focus Night and Day and O_2 Optix, respectively, CIBA Vision), galyfilcon A (Acuvue Advance, Vistakon), senofilcon A (Acuvue Oasys, Vistakon) and comflicon A (Biofinity, Cooper Vision). The introduction of the silicone hydrogel lenses has reduced most of the hypoxia related complications such as corneal swelling, and limbal and conjunctival injection in both daily and extended wear modalities.[12-14] Figure 1-4 demonstrates how the silicone hydrogel lenses have superior oxygen transmission compared to conventional hydrogel lenses and how by increasing the amount of water in the lenses reduces the oxygen permeability for silicone hydrogel lenses since the amount of oxygen bonding silicone is reduced. The J&J lenses would therefore have less oxygen permeability compared to the B&L lenses due to aforementioned material differences.

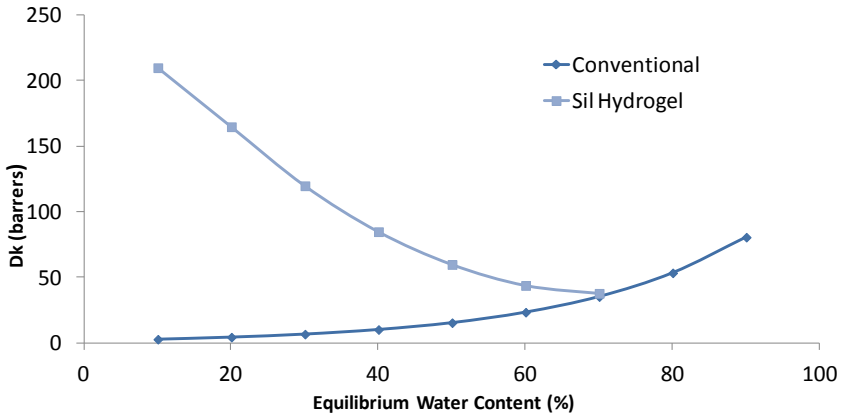

Figure 1-4 Oxygen permeability of silicone hydrogel and hydrogels

(Image courtesy: Tighe B)

Infectious and inflammatory events such as microbial keratitis, contact lens acute red eye, and infiltrative keratitis, occur at rates similar to conventional hydrogel lenses.[15-17] Mechanical complications with the

silicone hydrogel lenses such as superior epithelial arcuate lesions, localized papillary conjunctivitis and conjunctival epithelial staining and flaps occur at rates higher than conventional hydrogel lenses.[2;18]

1.1.1 Dehydration and lens material factors affecting comfort

Studies have suggested that the major cause of discontinuation with the contact lenses is poor comfort and dryness.[19-22] One report was that after 5 to 6 years of contact lens wear twelve percent of contact lens patients discontinued contact lens wear permanently, primarily because of discomfort (49%) and dryness (9%) symptoms.[23] Schlanger et al. reported that 72% of patients discontinued contact lens wear due to poor comfort, dryness being the most commonly reported symptom.[19;24] A further 20% failed because of inadequate visual acuity, with the remaining 8% failing because of inconvenience or for economic reasons.

The number of contact lens discontinuations in United States ranges between 10 and 16 million people.[25] A study by Morgan et al. reported that there are approximately 2.1 million contact lens dropouts in the UK which represents 60% of contact lens wearers.[26] One of the studies by Weed et al. has shown that the temporary discontinuation rates range from 30% to 50% and at least half of these patients may drop out for 2 years or longer.[27] The primary reasons for discontinuation were discomfort (27%), dryness (16%) and red eyes (11%). Although many treatment options exist, such as change in lens material, change in care solutions and use of rewetting drops, not many practitioners are successful in refitting their patients.[27]Also there is little literature documenting the proportion of lapsed wearers who can successfully be refitted with contact lenses.

Contact lens induced dryness is a major cause of contact lens intolerance. Symptoms of discomfort and dryness with contact lenses have been related to lens fit and movement,[28;29] edge profiles,[18;30] dehydration,[31] protein and lipid deposition,[32] modulus,[30] wettability and lubricity,[33] and solution

toxicity.[34;35] Several studies indicate that contact lenses disrupt the tear film by causing lipid and mucin abnormalities thereby changing the three layer structure of the tear film.[36-38] An increase in tear evaporation may cause evaporative dry eye, but the sensation of dryness is complex and appears to be related to a number of factors.[39] Several studies have shown the dehydration characteristics of hydrogel contact lenses during wear.[40;41] It has been reported that low water content, thick lenses dehydrate less than high water content thin lenses but the amount of dehydration seems unlikely to depend on the initial water content of the lenses.[42] It is also unclear if ionic lenses appear to dehydrate more than non-ionic lenses since *in-vitro* results perhaps show more dehydration with ionic lenses, however this observation was not supported by *in-vivo* results.[42]

Dehydration of contact lenses may be influenced by factors such as tear quality, blink rate, palpebral aperture size[43] and many environmental conditions on the eye.[44] Studies have also indicated that the dehydration of contact lenses can alter the lens parameters such as base curve,[45] diameter,[29] refractive index, thickness and oxygen transmissibility.[46] With the introduction of frequent replacement lenses many problems relating to the dehydration and dryness with contact lenses have been addressed. Few studies indicate that silicone hydrogel lens materials classified as low water content lenses (24%-36%) decrease dryness symptoms[39] but anecdotal reports also suggest that this might not be true. It has been shown that the use of frequent replacement lenses can convert previous unsuccessful contact lens wearers to successful lens wearers.[47;48]

1.2 Lens materials and wettability

In order to increase the oxygen permeability (Dk) of soft lenses, silicone is combined with the conventional hydrogel monomers. The silicone component of the material provides extremely high oxygen permeability and the hydrogel component facilitates flexibility, wettability and fluid transport which aids in lens movement. Silicone and fluoroalkyl groups are lipophilic, therefore, at the lens surface

they attract lipids and lipophilic proteins from the tear film which contribute to destabilization of the tear film, increased deposits, poor wettability, poor visual performance and perhaps increased inflammatory responses.[8;49] Therefore some silicone hydrogel lenses have to be surface treated to make them more biocompatible. The purpose of surface treatment is to increase the surface wettability of the contact lenses by masking the hydrophobic silicone from the tear film and in turn reducing the deposition from the tear film.[50]

Focus Night and Day™ lenses are permanently modified in a gas plasma reactive chamber to create a permanent, ultrathin, high refractive index and continuous hydrophilic surface.[51] PureVision™ lenses are surface treated in a gas plasma reactive chamber which transforms the silicone components on the surface of the lenses into hydrophilic silicate components.[52] However the Focus Night and Day™ lens is chemically uniform with no visible island- like appearance. Both these lenses are surface treated and not surface coated, which perhaps prevents the lenses from getting damaged while cleaning and handling on a day to day basis. Acuvue Advance™ material is the first non surface treated silicone hydrogel lens material which uses an internal wetting agent (Hydraclear™) based upon PVP and is designed to provide a hydrophilic layer at the surface of the material "shielding" the silicone at the material interface, thereby reducing the degree of hydrophobicity typically seen at the surface of siloxane-hydrogels. Studies have shown that the surface treatments used in PureVision™ and Focus Night and Day™ have been partially effective at masking the silicone and had more silicone and hydrophobic surface exposed when compared to the conventional hydrogel lenses.[53] There is only one report about the silicone exposure on the surface with the Acuvue Advance™ lenses and their wetting properties.[54]

Ideally, a contact lens must support a continuous and rupture-resistant anterior tear film and allow smooth recovery during eye closure. The term wettability refers to the ability of the tear film to cover and maintain itself over the contact lens surface. Once the contact lens is placed on the eye the pre-corneal

tear film is disrupted into pre-lens and post-lens tear film.[55] Lens wettability relates to the pre-lens tear film as the posterior side of the lens is completely immersed in the tear film.

Wettability is measured in terms of contact angle. It is basically the ability of the tear fluid to spread over the contact lens surface. A wettable contact lens is important for reducing lens deposits and for improving the optical quality of the contact lens. There have been numerous studies in the literature looking at the in-vivo and in-vitro wettability measures of contact lenses.[56-58] Wettability is assessed clinically and one method of measuring wettability is to measure the pre-lens non-invasive break-up time (NITBUT) using a Tearscope™ or a Placido ring from a corneal topographer.[59;60] Soft contact lens wear disrupts the normal tear film physiology and has an effect on the NITBUT. [60-63] that decreases dramatically in tolerant contact lens wearers and in symptomatic contact lens wearers.[60;64]

Gullion et al.[65] have shown that the *in-vivo* wettability is improved with silicone hydrogel lens wear but in a study by Maldonado-Codina[66] et al. it was shown that silicone hydrogel lenses exhibited poor wettability and shorter NITBUT compared to conventional hydrogels. Regardless, a direct correlation between comfort and *in-vivo* wettability has not yet been established and it could be hypothesised that pre-lens tear film structure i.e. quality and thickness, has greater impact on the comfort compared to NITBUT alone.[67]

As stated earlier one of the main reasons for poor wettability of the contact lens surface might be high levels of deposition. Contact lens deposition begins within minutes of lens insertion into the eye.[68] Lens surface build up is mainly composed of proteins,[69] lipids from tears,[70] carbohydrates, minerals, microbial toxins and polysaccharides.[71] Franklin and colleagues[72] examined lipid and protein deposition on human worn lenses and studied the effect of surfactant cleaning on these deposits. They assessed lipid and protein deposition using fluorescence spectroscopy and showed that lipid deposition was largely influenced by an individual's life-style, tear film composition and surrounding environment, whereas protein deposition was driven by the composition, charge and water content of the contact lens material.

Studies have shown a significant reduction in deposition levels on frequent replacement lenses and thus improving patient comfort and acceptance compared to the hydrogel lenses that have relatively rapid uptake of lipids and proteins.[73;74]

Little work has been conducted on the deposition levels of silicone hydrogels. Silicone hydrogels have exceptional transmissibility characteristics because of the incorporation of siloxane groups.[49;50] However, these groups result in materials with an increased modulus compared to conventional HEMA based materials and also results in surfaces that are significantly more hydrophobic. The hydrophobic substrates have a tendency to denature proteins and lipids. Deposition of proteins seems to be greatest on U.S. Food and Drug Administration (FDA) group IV materials (high-water content, ionic)[75;76] and group II (high-water content, non-ionic) attracts more lipid deposition.[76;77] Brennan et al. reported that with lotrafilcon A and balafilcon A lenses worn on a 30 night CW schedule, visible deposition and post-lens debris was minimal compared to traditional conventional hydrogel lens material.[78]

1.3 Non inflammatory silicone hydrogel lens complications

Developments in the contact lens industry in terms of materials, production techniques, mode of lens wear and efficacy of care systems have reduced the concern with lens deposition. Studies have been reported that show that with the advent of higher oxygen transmissible silicone hydrogel lenses there have been benefits to the ocular physiology such as reduction of hypoxia related complications including bulbar hyperaemia, limbal hyperaemia, corneal edema, epithelial microcysts and vascularisation.[79;80] However, there are still problems associated with inflammation, trauma and mechanical insult to the ocular tissue such as superior epithelial arcuate lesions (SEALs) and localized contact lens papillary conjunctivitis (CLAPC) [48;81;82] each associated with silicone hydrogel continuous wear lenses and perhaps due to the increase in the modulus of these lenses.[5;83]

The first generation silicone hydrogel lenses such as balafilcon A (PureVision, Bausch and Lomb) and lotrafilcon A (Focus Night & Day, CibaVision) have up to five times greater modulus compared to conventional hydrogel lenses. Materials with higher relative silicone content have higher oxygen permeability. The higher oxygen content will result in lower water content which generally makes the material stiffer and with a higher modulus. The second generation silicone hydrogel materials, galyfilcon A (Acuvue Advance, Johnson & Johnson), senofilcon A (Acuvue Oasys, Johnson & Johnson), comfilcon A (Biofinity, Cooper Vision) and lotrafilcon B (AirOptix, CibaVision) have relative lower moduli of elasticity but still, two to three times higher than conventional hydrogels.[84]

Excessive frictional pressure and shear force on the epithelium have been hypothesised to contribute to the formation of SEALs, although, most of the time, their presence is not associated with any symptoms. Typically the lesion is approximately 1mm from the limbus and stains with fluorescein dye. The prevalence of SEALs was around 7% with the first generation silicone hydrogel lens materials and has reduced to 4% with the second generation silicone hydrogels.[85] A study conducted at Centre for Contact Lens Research (CCLR) reported that up to 4% of people wearing continuous wear of the Focus Night and Day lenses reported the formation of SEALs.[5] Another condition commonly seen with CL wear is contact lens induced papillary conjunctivitis that is proposed to occur due to mechanical trauma to the tissue and also from perhaps immunological response to the denatured proteins deposited on the lens surface. The prevalence of CLAPC was also reduced with lower modulus lens materials compared to 6% prevalence with the first generation silicone hydrogel lenses. However, prevalence of local CLAPC is as high as 7% with silicone hydrogels compared to 0.7% with conventional hydrogel lenses.[86]

A number of patients also present with mucin balls with silicone hydrogel lens wear. Mucin balls appear as debris between the corneal epithelium and back surface of the contact lens, mainly forming during eye closure, perhaps when the lens shears the tear film and mucin rolls into small balls that get trapped under the lens.[5] They are usually most commonly seen with relatively stiffer lens materials but are flushed out

with the lens removal.[87] Mucin balls may leave dents or imprints on the corneal epithelial surface but have not been associated with any visual degradation. Morgan et al. have reported approximately 71% of Focus Night and Day silicone hydrogel lens wearers develop mucin balls compared to 45% having them when they wore PureVision lenses.[88] Therefore, perhaps modulus can affect the clinical performance of contact lenses.

1.4 Lens Design and comfort

Contact lens edges can be assigned into three groups 1) knifepoint 2) chisel and round.

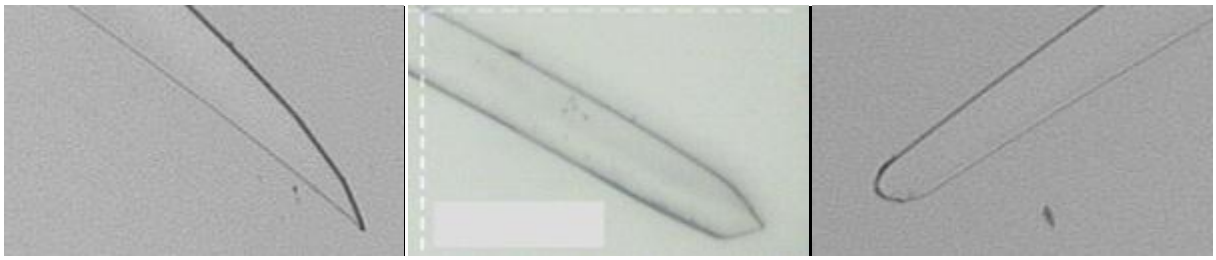

Figure 1-5: Contact lens/edge shapes: knifepoint (left), chisel (center) and round.

(With permission from Contact Lens Spectrum, copyright Wolters Kluwer Pharma Solutions, Inc.)

Silicone hydrogel lenses have higher moduli and non-rounded edge shapes and may impact the conjunctival tissue to a greater degree compared to conventional HEMA lenses. The conjunctiva is a thin, clear mucous membrane that lines the posterior surface of the eyelids (palpebral conjunctiva), and the basement membrane of the conjunctiva covers part of the sclera (bulbar conjunctiva). This membrane is composed of collagen, lymphocytes, plasma, mast cells, nerve fibers and blood vessels. The non-keratinized epithelium of the conjunctiva also secretes goblet cells which play an important role in forming the mucus layer of the tear film.

Contact lens associated conjunctival staining is seen commonly in contact lens wear and unlike corneal staining, conjunctival staining of the bulbar conjunctiva has not been extensively studied. Contact lens

wearers also present with conjunctival indentation along with staining. In lens wearers with conjunctival indentation, extra conjunctiva appears to extrude from the conjunctiva proper. This extra tissue appearing as loose folds or flaps, takes up fluorescein dye. In addition an imprint of the CL left on the conjunctiva perhaps due to poor edges or no lens movement is also visible with fluroscein.[89;90]

Løfstrøm and Kruse[91] were the first to report on the conjunctival epithelial flap (CEF). Sixteen successful silicone hydrogel lens wearers who had worn lotrafilcon A or balafilcon A lenses on continuous wear basis were examined. Thirty four percent of the 32 eyes examined were found to have CEF of varying sizes in the superior, inferior or both quadrants but no CEF was seen in nasal and temporal quadrants. They also reported that the majority of the participants wearing lotrafilcon lenses presented with conjunctival indentation and staining and sometimes just conjunctival staining hypothetically due to the chisel-shaped edge design compared to the contact lens wearers with the rounded edge design in the balafilcon A lens. A similar study conducted by Santodomingo et al. also reported higher incidence of CEF with lotrafilcon A lenses compared to balafilcon A lenses. The author also reported higher prevalence of CEF with continuous wear modality compared to daily wear and also flatter fitting lenses had higher prevalence of conjunctival epithelial flaps.[92] Figure 1-6 shows conjunctival epithelial flap with contact lens overnight wear.

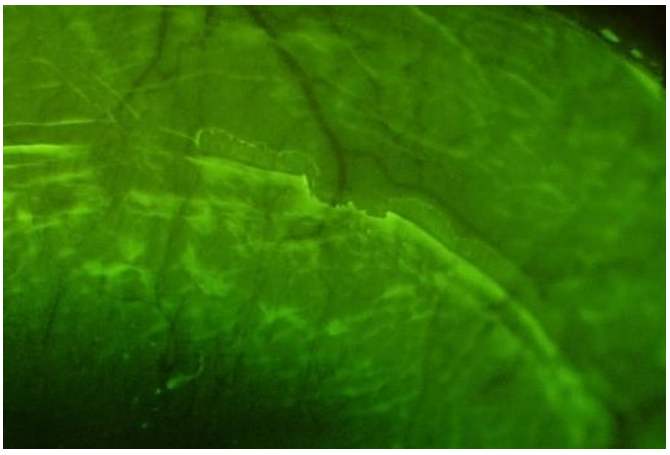

Figure 1-6 Conjunctival epithelial flap

Løfstrøm and Kruse et al. suggested that the lens edge perhaps might be digging into the superficial conjunctival tissue during eye closure, and subsequent movement upon eye opening may irritate the conjunctival epithelial tissue and increases the conjunctival epithelial cell production that the authors hypothesised to be hyperplasia of the conjunctival epithelium resulting in a conjunctival flap.[93] However, as the authors indicated, the small sample size in their study did not help in determining the prevalence rates of CEF. The paper also did not report the patient factors involved such as eye shape, lid tension and age and also subjective comfort.

Another study comparing galyfilcon A and lotrafilcon A by Maldonado-Codina and colleagues[66] found a minimal difference in the physiological response to the two lenses. Increased conjunctival staining was reported in wearers of the galyfilcon A lens and this was attributed to the design features of these lenses.

1.5 Evaluation of soft contact lens fit

Optimisation of lens fit and proper lens selection may be important to improve patient satisfaction and long term success with contact lens wear. The relative stiffness of the silicone hydrogel contact lenses compared to conventional hydrogel lenses suggests that clinicians should take more care in examining the lens/cornea relationship with silicone hydrogels compared to the conventional hydrogels.[29] Most silicone hydrogel lenses are available in one or two base curves and all the rules and procedures that apply to hydrogel lens fitting broadly apply to silicone hydrogel lens fitting.[94] Veys et al. have reported that most of the patients can be fit with flatter base curves which is usually the lens of first choice.[95] Although the fitting rules remain the same for silicone hydrogels and conventional hydrogel lenses, the modulus of the material is higher for silicone hydrogels compared to conventional hydrogel lenses which indicate that the material resists deformation and as a consequence these lenses do not drape over the cornea as much.[94]

The resulting lens fluting and foreign body sensation may perhaps may be the basis of discontinuation of lens wear.[96]

Evaluating the fit of the soft contact lens such as assessment of the stability of vision, evaluation of keratometry mires, and subjective comfort of the patient and slit lamp examination are the most commonly used techniques.[94;97;98] Judging the fit of the contact lens involves evaluating both static and dynamic fit of the lens; lens centration, lens movement on blink, lens lag in primary gaze and lens tightness or looseness assessed with the push up test.[94] The dynamic fit of the lens is very important to maintain the ocular integrity[94]; the contact lens should be fitted so that there is a proper exchange of tears enabling, among other things, the metabolic debris from underneath the lens to be flushed out. Proper lens movement is also important for corneal oxygenation and the ideal lens movement has been suggested to be approximately 0.2mm to 0.4mm.[88;94]

The movement of thick high water and low modulus lenses is less compared to thick low water content lenses.[94] It is sometimes difficult to judge the fit of the lens with just looking at the movement of the lens; the lens push-up test gives a better idea about the dynamic fit of the lens. In the push up test, the practitioner assesses the tightness of the lens by moving the lens vertically up by applying pressure on the lower lid and then allowing the lens to re center. The relative ease with which the lens returns to its original position and the speed of recovery is graded with 100% representing a lens that fits very tight or steep and 0% representing a loose lens that falls off the eye.[94]

1.6 Sagittal height and lens fit

Although the practitioner assesses the lens fit using the guidelines recommended by the manufacturer, Young et al. have reported that these variables may perhaps have little predictive value in deciding if the fit is successful.[99] For example a lens showing good centration and tightness might not move adequately

on the eye but still have a satisfactory appearance. Therefore apart from the fitting characteristics of the lenses, a variety of ocular dimensions affect the lens fit such as corneal sagittal height, corneal diameter, corneal asphericity and scleral shape. Keratometry readings are the gold standard measurements for selection of contact lens trials but studies have indicated that keratometry measures are poor indicators of soft lens fit.[100] Dumbleton et al. reported that K measurements are not sensitive enough and are an oversimplified predictor of soft contact lens fit.[28] They showed that steep K was a useful predictor of the base curve of first choice when fitting lotrafilcon A high-DK silicone hydrogel lens. They also showed that comfort improved when a flatter (8.6mm) base curve lens was replaced by the steeper lens (8.4mm).[29]

Traditionally, hydrogel contact lenses are also fit in reference to back optic zone radius (BOZR). [28;94;99;101;102] In order to increase the movement of the lenses, the BOZR is increased and to reduce the movement, the BOZR is reduced, however there are reports that an report that an alteration in the BOZR has a minimal effect on the fit of the lens.[28] However, this does not imply that changing the base curve does not affect the movement but only that it might not show the predicted effect on lens fit. Changes in the lens diameter (LD) is a better predictor of lens fit and appears to impact the fit of the lens to a greater extent than changes made to BOZR.[94]

Increasing the total diameter of the lens increases the sag of the lens and theoretically tightens the lens. Decreasing the total diameter will have an opposite effect on the fit. Altering the diameters of the lenses and in turn the sag will also hopefully improve lens centration. Lowther and Tomlinson studied the effects of the BOZR and total lens diameter on clinical fit and reported that relatively large changes were required in the parameters to produce a significant modification to the clinical performance of the lens.[103]

In order to understand why corneal diameter is so critical in soft lens fitting it is important to understand the concept of sagittal height or the sag value.

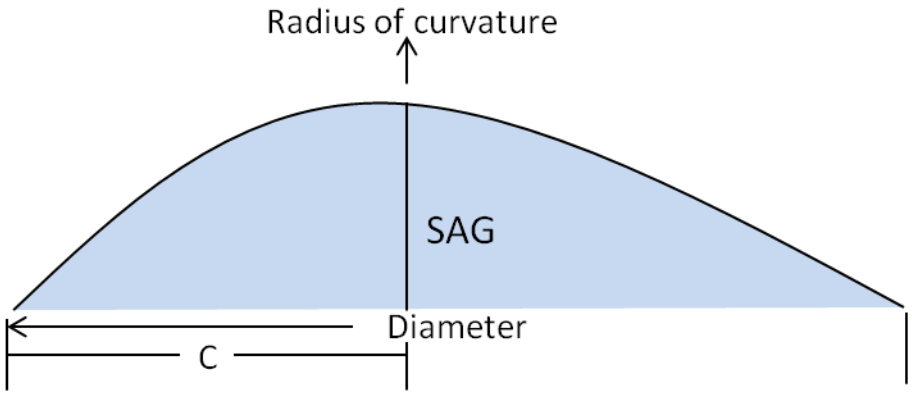

Figure 1-7: Illustration of sagittal height

The sagittal depth of an aspherical curve is the perpendicular distance from the apex of the curve to the chord defined by the two ends of the aspherical curve. The distance between the two ends of the curve represents the diameter and the radius of curvature is equal to the radius of the center of the aspheric surface. Changing the radius or the diameter would alter the sagittal height and in turn, the fit of the lens. A normal healthy cornea with a radius of 7.85 mm and a diameter of 12.9 mm has a sag value of approximately 3.12 mm with a p-value of 0.76 (horizontal) and 0.82 (vertical). Garner et al. have reported that for a successfully fitting lens, the back surface sagittal height is greater than the curvature of the anterior segment of the eye.[104] During clinical evaluation, a tight fitting lens is considered to have too great a sagittal height compared to the curvature/sagittal height of the cornea and for a loosely fitting lens the sagittal height is too low. Ocular sagittal height is not just the function of the diameter and the radius of corneal curvature but also a function of the corneal shape factor (amount of flattening from the centre to the periphery) and curvature and shape factor of the para-limbal sclera.

The amount of asphericity or rate of flattening (e) also plays an important role in the determining the sagittal height of the eye. The average asphericity/eccentricity in the normal population is an e value of 0.5. Young et al. have reported that variation in corneal eccentricity and diameter have greater effects on

corneal sag than the radius of curvature.[105] This study also reported that with a lens of 14.00 mm diameter, a change in 0.40 mm BOZR corresponded to approximately 0.30 mm difference in sagittal height or depth. Again this suggests that considering the corneal curvature measurements with keratometry alone to predict the BOZR does not optimise the lens selection. Corneal diameter and corneal shape factor are important parameters in predicting BOZR.

Young et al. reported an increase in the overall value of the corneal sagittal measurement with increasing corneal radius, but changes in the scleral radius were insignificant (1mm change in the scleral radius changes the sagittal height by only 0.05 mm).[105] A recent study by Sorbara et al. measured the shape of the corneal/scleral area using a high resolution Visante™ OCT (Carl Zeiss Meditec, Dublin, California) essential for large diameter semi scleral or large diameter gas permeable lens fitting. In this study measurements of nasal and temporal angles were measured tangentially to the sclera at 15 mm chord length to describe the flatter scleral shape. They reported a mean corneal/scleral depth of 3.47 ± 0.19 mm when measured with the Visante™ OCT at a 15 mm chord length and as expected, due to the individual changes in the scleral shape beyond the limbus, there was significant but poor association between the corneal/scleral sagittal depth and the nasal/temporal angles at 15mm.[106]

Horizontal visible diameter (HVID) is also one of the fitting parameters that optimize the soft contact lens fit. A recent study[94] reported a range of HVID of 10.2 mm to 13.0mm when measured on 200 normal corneas. Patients who had HVIDs between 11.6 to 12 mm appeared to have a higher percentage of success using the traditional fitting approach. However, the study also reported that the eyes that have a small HVID may need a smaller diameter or flatter base curve, and eyes that have a large HVID may require a larger diameter or steeper base curve. Ideally the HVID must be at least 1mm less than the total diameter of the lens for optimal fit.[94]

Initial comfort during trial lens fitting greatly influences the patient's perception of contact lenses[29;107] and with the introduction of higher modulus silicone hydrogel lenses manufacturers and practitioners must take utmost care in streamlining the lenses and achieving optimal lens fit through trials for ultimate success of contact lens wear. Newer technologies, such as topographical mapping systems, may provide sagittal values for each contact lens design to make sagittal height measurements as commonly accepted as are base curve and lens diameter.

1.7 Physiological and vascular response to contact lens wear

Contact lenses interact mechanically with the cornea and potentially compromise its function.[2;81;108;109] A major consequence of contact lens wear is lens-induced chronic hypoxia and corresponding hypercapnia.[109;110] Polymethyl methacrylate lenses (PMMA) contact lenses caused varying degrees vascular responses on the eye until high oxygen permeable silicone hydrogel lenses were introduced.[111 112;113]

Holden et al.[82] studied the effect of long term (5years) extended unilateral hydrogel lens wear compared with the non-lens wearing fellow eye in the subjects. The results of the study were significantly thinner corneal epithelium, greater number of corneal epithelial microcysts, thinner corneal stroma, greater amounts of limbal and bulbar hyperaemia and neovascularisation.[82] However this study also reported that many of changes to corneal epithelium were reversed over a one month period after removal of lenses and also that its oxygen consumption improved over a period of time. They hypothesised that chronic-lens induced hypoxia was the underlying cause of the physiological effects on the cornea.

1.7.1 Limbal response

Limbal hyperaemia represents one of the first signs of tissue response to hypoxia associated with daily and extended wear of hydrogel contact lenses.[17;114;115] Chronic limbal vessel dilation provides an active

vascular plexus adjacent to the cornea which provides access to blood–borne defence mechanisms. Papas et al. have reported an association between hypoxic effects of low-Dk hydrogel lens wear and limbal hyperaemia. They reported that the mean peripheral Dk/t required to avoid a change in limbal redness was $95x10^{-9}$ (cm/second) (mlO_2/mL.mm Hg) the amount almost equal to the CL oxygen transmissibility in that region. Currently it is believed that soft contact lenses with $125x10^{-9}$ (cm/second) (mlO_2/mL.mm Hg) reduce limbal hyperaemia.[114]

Wearing high oxygen transmissible silicone hydrogel lenses should reduce limbal hyperaemia substantially. Dumbleton et al. found a significant reduction in limbal hyperaemia when comparing an extended wear (EW) high Dk/t silicone hydrogel lens to a low Dk/t hydrogel lens for over a period of 9 months.[115] Papas et al. have also indicated that reducing the flow of oxygen to the cornea without using contact lenses can also produce limbal hyperaemia.[116] They have also showed that negative powered lenses used to correct myopia are of more concern as these lenses have thicker lens edges compared to positive powered lenses and therefore hinder the amount of oxygen supplied to the limbal region.[116] They report a Dk/t reduction of about 80% and this is of serious concern as the hypoxic damage to limbal stem cells can have serious long term effects on the cornea.[116]

1.7.2 Neovascularization and bulbar hyperaemia

Neovascularization is produced as a response to a metabolic or an angiogenic factor released by blood vessels. New blood vessels form from existing vasculature and disturb the dynamic equilibrium of pro and anti-angiogenic factors responsible for maintaining the normal corneal avascularity.[117] Neovascularization is presumed to be a response to contact lens wear and hypoxic stress created by the lens wear. Studies have shown that the vessels refill when the hypoxia is relieved after a period of contact

lens discontinuation. [17] Additional studies have reported the prevalence of neovascularization to be higher with low Dk/t lenses and significantly less neovascularization with high Dk/t silicone hydrogel lenses.[115] Contact lens wear has also been reported to induce bulbar hyperaemia.[85;118;119] Brennan et al.[78] and Coles et al.[120] found reduced bulbar conjunctival hyperemia in high Dk/t lens silicone hydrogel lens wearers compared to low water thin hydrogel lenses.

1.7.3 Formation of epithelial microcysts

Epithelial microcysts form with daily and extended wear contact lenses and are most reliable indicator of chronic hypoxic stress. They usually appear within 2 to 3 months of lens wear, are usually asymptomatic, and were first observed in PMMA lens wearers.[121;122] Epithelial microcysts are small (10 to 50 µm) and non-inflammatory translucent and irregular dot like structures. Epithelial microcysts are hypothesised to be the result of chronic hypoxia with EW of low-Dk hydrogel lenses.[123] Slit lamp examination using retro-illumination can identify microcysts. Microcysts have been hypothesised to consist of degenerative cellular material produced in the basal layer of the epithelium and that they move towards the surface during epithelial turnover.[123;124]

Keay et al. have indicated that there is a rebound effect when patients were refitted with high Dk/t lenses, as microcyst numbers appear to increase for a short period of time until the epithelium returns to its previous metabolic state.[124]

1.8 Effects of contact lenses on corneal epithelium, corneal shape alterations.

1.8.1 Rate of exfoliation

The normal epithelium is a self-renewing tissue undergoing relative rapid and continuous cell turnover throughout life (see Figure 1-7). Epithelial stem cells are of utmost importance in maintaining long term

health of the corneal epithelium. Stem cells are slow cycling, divide infrequently and give rise to mature cell types that further differentiate under normal conditions.[125] The stem cells of the corneal epithelium are exclusively located in the basal cell layer of the limbal epithelium.[126]

Hypoxia and the physical presence of the contact lens on the eye significantly reduce and slow the turnover of the corneal epithelium by suppressing epithelial cell proliferation[127], migration[128] and also by decreasing the rate of exfoliation.[129] The conditions observed due to these changes include microcysts,[82;124]compromise in epithelial junctional integrity,[130;131]epithelial defects,[82] neovascularization[115;132] and reduced corneal sensation [108;133;134]. The effects on the epithelial structure also include reduced nerve density, edema, epithelial thinning and abnormal cell shapes.[135]

Extended lens wear of soft and rigid gas permeable lenses is characterized by significant thinning of central corneal epithelium, an increase in the surface cell size and a decreased rate of exfoliation.[136] Ren et al. reported that in extended soft contact lens wear, the epithelial metabolism is perhaps reduced because of the 15% decrease in the oxygen avaliablity.[137] During overnight RGP lens wear, rabbits' central corneal epithelial proliferation rate was significantly decreased by 47% centrally.[138] Others have shown that lens related variables such as oxygen transmissibility, material rigidity and wear schedule[129] decreases cell exfoliation [136;137].

The rate of exfoliation and apoptotic driven cell death in central corneal epithelium is similar in contact lens wearers to the rate under closed eye conditions.[139] The increase in the cell size at the corneal surface during contact lens wear is hypothesised to slow exfoliation and therefore the cells reside on the cornea for longer. Stapleton et al. reported that after 3 months of extended silicone hydrogel lens wear the sizes of exfoliated corneal epithelial cells was similar to the sizes of the cells found in non-lens wearing eyes. In addition the cell sizes increased significantly after 6 to 9 months of lens wear. However, with silicone

hydrogel lens wear, Ladage et al. have shown that after long term wear (up to 3 years), the cell size recovers to pre-lens wearing levels.[140]

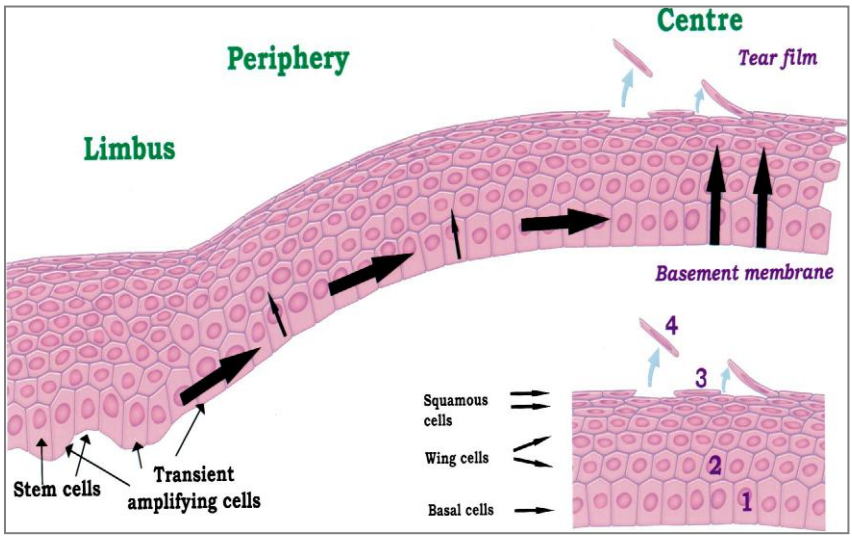

Figure 1-8 : Represents the renewal and replacement of the corneal epithelium (X, Y, Z hypothesis) proposed by Throft and Friend.

1.8.2 Epithelial thinning

The degree of central corneal epithelium thinning is affected by the lens type, oxygen transmissibility and duration of contact lens wear and is not affected by short term hypoxia.[141;142] Studies have shown that higher oxygen transmissible silicone hydrogel lenses have less pronounced effects on the ocular health than hydrogel lenses of lower oxygen transmissibility or rigid gas permeable lenses of equal oxygen transmissibility and a greater adaptive recovery during long term extended wear.[88;143 110] In a 5 year study conducted on 27 participants unilaterally wearing high water content hydrogel lenses[110] a reduction of epithelial thickness of 6% was reported.. However the corneal epithelial thickness returned to normal within one week after lens removal.

Ren et al. reported that hydrogel lenses of lower oxygen transmissibility cause more epithelial thinning than hydrogel lenses of higher oxygen transmissibility during the first year of lens wear. They reported that the corneal epithelium reached a maximal thinning after the first month of extended wear and thereafter partial adaptive recovery occurred.[137] This was questioned by Gonzalez et al. who reported that the recovery of the epithelium would never be complete.[144] In another study by Patel et al. the thinning of the epithelium was reported to occur in the temporal epithelium and not in the central epithelium of long term daily contact lens wearers.[145]

Studies of the effects of CL wear on epithelial homeostasis in animals and humans have suggested inhibition of cell shedding as a possible mechanism for epithelial thinning. Increased epithelial cell surface area[129;146] and reduced epithelial cell desquamation[129] have been shown to occur in all types of contact lens wearers.[127;137] Studies on soft contact lens wearing monkeys[147] and rigid contact lens wearing rabbits[139]show similar epithelial cell flattening,[138;139] reduced surface epithelial cell death through apoptosis and reduced central basal cell proliferation.[127] Based on these findings Ladage et al. have suggested that contact lens wear causes reduced demand for new surface cells. They reported that the contact lens forms a shield protecting the surface cells especially during the blink, and this leads to a decrease in the shedding rate and an increase in the epithelial cell size.[148] Insufficient basal cell proliferation and movement of epithelial cells to the corneal surface is associated with central corneal thinning.[148] This study also showed a decreased, central basal cell proliferation (-33.8%) with silicone hydrogels and -40.8% with low oxygen transmissible hydrogel lenses. They reported basal cell recovery in silicone hydrogel lens wearers but it was not clear if this phenomenon was due to the physiological adaption of the epithelium or caused by delay of cells entering the cell cycle.[148]

They also reported that corneal epithelial thinning perhaps could be due to the direct physical pressure by the contact lenses. Studies have shown a significant thinning effect on the epithelium when subjects were fitted with a high DK rigid gas permeable CL's compared to the thinning effect caused by soft contact

lens of similar oxygen transmissibility.[148] Localized corneal and epithelial thinning is also observed in ortho-keratology lens wearers where the direct pressure of the lens may involve in epithelial thinning and shape change.[149]

In summary, the central corneal epithelium thinned by 5.6% in unilateral, long-term, extended-wear contact lens wearers.[110] A thinning of 4.6 % with conventional hydrogel lens wear, 2.9% with weekly silicone hydrogel lens wear and 3.2% with monthly silicone hydrogel lens wear was reported.[137] A central thinning of 10% at 12 months of RGP lens wear was also reported.[144]

1.8.3 Corneal shape alterations

Corneal shape alterations have been noted with various imaging techniques revealing that all types of contact lenses are capable of changing the corneal topography. Montenegro et al. reported a change in topography of normal corneas to be around 8% compared to relatively large percentages such as 75% with PMMA lens wear, 57% with RGP lens wearers and 31% with daily wear hydrogel lenses. Central corneal steepening or flattening, changes in regular or irregular astigmatism, loss of radial symmetry,[150] and changes in optical higher order aberrations are some of the topographic patterns resulting from contact lens wear. The most commonly reported change was a flattening of the cornea in areas of lens bearing resulting in a flattening of the corneal topography.[150-154] It has been reported that there is increased corneal curvature with contact lens wear [155] although in overnight wear of high DK GP lenses as well as long term wear of PMMA lenses, a decrease or no change in the curvature of the cornea has been reported.[156-158]

The only modality that was widely available for monitoring the topographical changes and measuring corneal curvature was the keratometer. A major limitation of the keratometer is that it assumes the cornea to be a sphero-cylindrical surface and provides no information of the central and peripheral topography.

This makes the keratometer a measurement technique for fitting contact lenses on normal cornea and provides limited topographical information for irregular corneas such as keratoconus and post refractive surgeries.[159]

Orbscan™ (Bausch & Lomb, Rochester, NY) corneal topography is a relatively new and widely used slit scanning technique that provides pachymetry measures of the cornea. This system[160] is capable of measuring the entire corneal thickness by calculating the difference in elevation between anterior and posterior corneal surface. However, Yaylali et al. reported that the Orbscan™ system measures the corneal thickness 23 to 28 µm greater than that obtained by ultrasound pachymetry and argued that one possible reason for this may be the non contact nature of the Orbscan™ topography system compared to the ultrasound pachymetry which is invasive.[161] Liu et al. reported that the mean corneal thickness measured with the Orbscan™ was reduced by 30-50 µm with long term wear of contact lenses compared to normal eyes without contact lenses. They have also reported significant corneal and epithelial thinning in long term contact lens wearers who wore the lenses for more than 13 years. They stated that no specific reason for corneal and stromal thinning has been established in contact lens wearers but gave a possible explanation for both corneal epithelium and stromal thinning that perhaps is due to chronic edema of the corneal stroma and biochemical changes in corneal stromal composition.[162]

The Medmont E300™ corneal topography system provides information on the dynamics of tear-film behaviour and corneal topography. This instrument enables us to acquire multiple dynamic sequences of images and the user can choose the best map that shows the most appropriate alignment. Cho et al. have reported the repeatability and reproducibility of the apical radius, eccentricity and elevation to be better than other commercially available topographers.[163] Wilfred et al. have reported that the Medmont™ corneal topographer shows high repeatability in measuring six different test surfaces such as a sphere, an asphere, a multicurve, and three bicurve surfaces. The Medmont™ was reported to be the most repeatable instrument in the study comparing a number of topographers.[164] Cho et al. have reported that the

repeatability of Medmont™ and Humphrey Atlas™ were consistently higher with intraclass correlation coefficient (ICC) values ranging from 0.94 to 0.99 compared to the Orbscan II™ and Dicon CT200™ topography imaging systems. The Orbscan II™ was the poorest performer with ICC's ranging from -0.0095 to 0.69. They reported poor repeatability to be an indicator of the poor image capture by the Orbscan™, due to poor fixation and focusing as the patients have difficulty keeping their eyes open during the image acquisition process.[165]

1.8.4 Corneal swelling with soft contact lens wear

Hypoxia induced corneal swelling is a normal phenomenon that is the result of reduced availability of oxygen. In humans, contact lens wear and eye closure with and without contact lens wear is an effective model of measuring hypoxia and is one of the primary indices of corneal physiological change.[108] Holden et al. have shown that corneal swelling is inversely proportional to contact lens oxygen transmissibility.[7] Short term hypoxia can lead to thickening of the corneal stroma and long term hypoxia can lead to thinning of the corneal stroma. In general the cornea swells 2 to 4% with overnight eye closure and recovers the following morning.[7;166;167] It has also been shown that cornea swells regionally and the highest swelling occurs in the anterior and posterior stroma due to perhaps altering the physiological pump and disruption of the stromal barrier function .[141]

Holden and Mertz[7] showed that the minimum oxygen transmissibility (DK/t) of 87±3.3 barrer/cm was required to avoid overnight corneal swelling, and in a recent study, Harvitt et al.[168] theorized that a (DK/t) of 125 barrer/cm was required to reduce lens induced overnight corneal swelling. Moezzi et al. studied 16 non-lens wearers before and after wearing conventional hydrogel and PMMA contact lenses and reported that corneal swelling was significantly greater in those using soft lenses compared to when PMMA lenses were worn, and this was attributed to the larger diameter of the soft contact lenses and less tear mixing beneath the lenses.[160]

Holden et al. [169] measured corneal edema along the horizontal meridian after contact lens wear and reported that the periphery of the cornea swelled significantly less than the center and they suggested that this was due to the physical restraint in the limbal region. Moezzi et al. also showed a greater swelling centrally and reported that the flattening of the posterior surface of the cornea is independent of the lens type.[160] This observation was supported by Bergenske et al. who demonstrated that there was an increase in the central and mid-peripheral corneal thickness with contact lens wear and eye closure.[170] Fonn et al. reported a peculiar finding of corneal swelling of the contralateral control eye, that was influenced by the swelling of the fellow high-DK lens wearing eye, suggesting a sympathetic physiological response.[166]

Conventional hydrogel lenses have shown to cause more overnight corneal swelling compared to silicone hydrogel lenses. Hydrogel lenses are characterized by several factors such as their water content, ionicity, and oxygen permeability (Dk). Hamano et al. studied two hydrogel lens materials (nelfilcon A and etafilcon A) and three silicone hydrogel lens materials (galyfilcon A, senofilcon A, and lotrafilcon A) and showed that after just one hour of dozing, a significant physiological effect on the cornea was seen with hydrogel lens wear but not after silicone hydrogel lens wear.[171] In an another study reported by Steffen et al., twenty five subjects were fitted with four different types of silicone hydrogel lenses (balafilcon A, etafilcon A, lotrafilcon A, senofilcon A) and the other eye did not wear a lens. The swelling response was measured after 8 hours of closed eye wear and the silicone hydrogel materials produce little corneal swelling when worn on an overnight basis. Induced corneal swelling also did not significantly differ from the eye without the lens.[172] Therefore, theses data provide support for the idea that silicone hydrogel lenses have less physiological effects on the cornea

Changes in meridonial corneal thickness have also been reported in orthokeratology. With reverse geometry lens designs, changes in thickness have been reported, with central corneal thinning and mid-peripheral corneal thickening occurring when compared to the baseline corneal thickness. This change in

the corneal thickness has been suggested to be due to the redistribution of the epithelial tissue during lens wear.[149;173]

1.9 Instruments and imaging of the cornea

Although many of the following devices are not directly used in my experiments much of the work has used one of many devices, therefore theses devices will be reviewed in the following sections.

1.9.1 Ultrasonic methods

Ultrasonic pachymetry is used for measuring corneal thickness in the center and periphery of the cornea. The ultrasonic pachymeter is an A-scan ultrasonography instrument consisting of a hand-held probe and a digital display console. The probe generates and directs ultrasound waves into the cornea and then detects the reflected ultrasound waves. When high frequency sound waves are propagated through soft tissues, the acoustic reflection of these waves is recorded in one dimension in the path of the beam.[174] The thickness can be estimated from the time delay between these boundaries. Reinstein et al. have reported the repeatability of the hand-held ultrasound pachymetry to be about ±20µm. [175]

High-frequency ultrasonic biomicroscopy (UBM) is a new ultrasonic method which in addition applies image processing in imaging microstructures in 2D and 3D.[176] In UBM, high-frequency (50-100 MHz) polymer transducers are used, which have resolutions from 20 to 60 µm and depth of penetration of approximately 4mm.[177]

Pavlin et al. measured various features including corneal thickness, anterior chamber angle of the eye, and imaged iris and anterior segment tumours using UBM. They defined the term ultrasonic biomicroscopy as the production of images at true microscopic resolution in living tissues using ultrasound.[177] Newer fourth generation UBM models with 100-MHz transducers have sufficient penetration depth to be capable of

imaging the entire anterior chamber. However, the axial resolution does not match other optical techniques.[178]

1.9.2 Specular microscopy

The principle technique of specular microscopic pachymetry is to focus on the specular reflection from the anterior and the posterior corneal surfaces with a microscope and measure the distance between these two layers.[179] The Topcon SP-2000P is a commercially available non-contact specular microscope that images the endothelium, and provides specular images from which corneal thickness is calculated simultaneously. Specular microscopy has been used to study corneal endothelial morphology in addition to measure the corneal thickness. The measurements, with the specular microscopy have been reported to be reproducible for measures of cell morphology and corneal thickness.[180;181]

1.9.3 Optical pachymetry

Optical pachymetry has been used to measure the corneal thickness since its introduction in 1952.[182;183] The optical pachymetry system typically consists of an image splitting device, inserted into one eyepiece of the slit lamp. This device consists of two glass plates that split the image of the cornea. A slit beam is projected perpendicularly to the cornea through the narrow diaphragm of the instrument and the right-sided split image eyepiece replaces the regular eye piece of the slit-lamp. By moving the scale of the instrument, the focused upper half of the corneal image is positioned so that its posterior surface is in apposition with the anterior surface of the lower image.[184]

The optical pachymeter has been used to measure the corneal thickness profiles in the peripheral cornea with soft contact lens wear. They are also used to measure the epithelium across the entire cornea and to evaluate changes to the cornea in orthokeratology lenses.[169;185]

1.9.4 Orbscan II

The Orbscan™ is a non-contact optical topographer that measures anterior and posterior corneal elevation (relative to a best-fit sphere), surface curvature, and corneal thickness using a slit scanning mechanism. Elevation maps of the anterior cornea enable clinicians to visualize the shape of abnormal corneas, which helps in accurate diagnoses and consistent surgical results. The instrument was designed to acquire the elevation information directly, but was mostly used for deriving the curvature information. The Orbscan II™ incorporated a placido disk (Figure 1-8).

Figure 1-9: The Orbscan™ II topographer (Bausch & Lomb, Rochester, NY)

(Image courtesy: Sameena Haque)

During the acquisition, the placido disk used for corneal curvature data is illuminated and the mire's reflection from the anterior corneal surface is stored. Subsequently, 40 slits, 20 from the right and 20 from the left are projected on the cornea at an angle of 45 degree to the instrument axis. As the light from these slits passes through the cornea, it is scattered and the backscattered component is captured by the digital video camera. [186-189]

This device can also be used to study cornea during refractive surgery and contact lens wear and also to measure corneal thickness post orthokeratology.[190-193] Cho et al. reported that central corneal thickness measurements acquired using the Orbscan™ was perhaps more repeatable than measurements from the peripheral cornea.[194] Since the Orbscan II™ appeared to produce higher corneal thickness measures compared to ultrasonic pachymeters, an acoustic factor of 0.92 was introduced to "correct" the final measurements of the corneal thickness.[195]

1.9.5 Optical Coherence Tomography

Optical coherence tomography (OCT) is a recently developed non-contact imaging technology for performing high-resolution cross-sectional images (Figure 1-9).[196] Its principle is similar to ultrasonic imaging, but the magnitude of reflected (backscattered) light is measured instead of reflected sound waves. OCT uses low coherence Michelson interferometry to compare a partially coherent reference beam to one reflected from the tissue. The two beams are combined at the beam splitter and interference between the two optical beams occurs only when their path lengths match to within the coherence length of the light source. Because interferometry measures optical paths, which is the product of the physical distance traversed by the optical beam and the refractive medium it travel through, OCT effectively maps the spatial variation of the tissue refractive index. If the average refractive index of biological tissue is known (has been measured with other techniques), then OCT can be used to measure precisely the physical dimensions of different morphological. Because the tissue refractive index is wavelength

dependent, and OCT uses broad spectral bandwidth to achieve high axial imaging resolution. Proper calibration of the OCT system is required for precise measurements of the physical dimensions of morphological features in biological tissue.

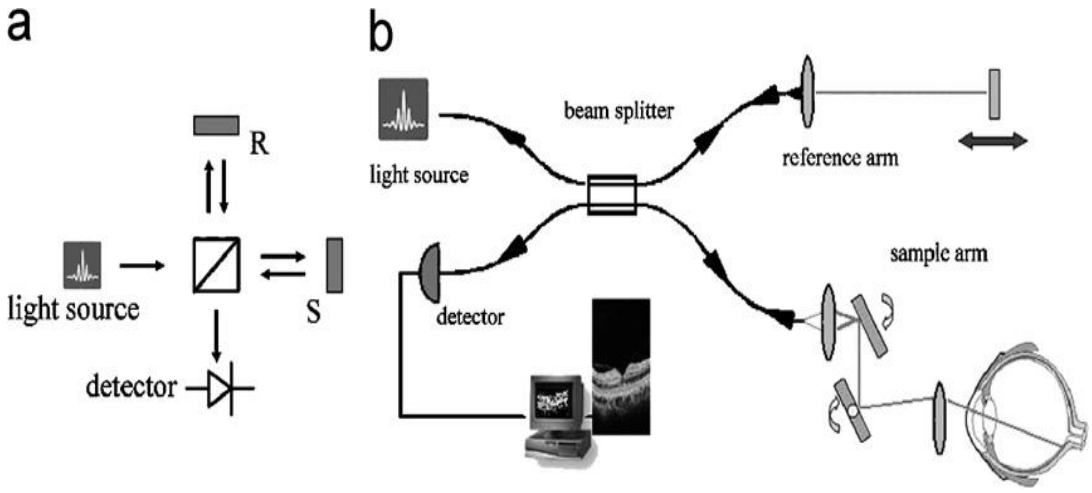

Figure 1-10: Schematic diagram of Michelson interferometer.

(With permission from: Recent developments in optical coherence tomography for imaging the retina)

The OCT provides ultrasound-A-scan-like information at a single point. The resolution of the OCT ranges from 1 µm to 15 µm and the instrument is capable of scanning a large area (up to 20mm scan diameter).[197] OCT technology has been applied to address a wide range of problems in fiber optics, interferometry, high-speed optical detection and biomedical imaging. The OCT has also been used for a variety of biomedical applications including measuring the thickness of cartilage around joints[198], retinal imaging [199-202], anterior segment imaging [203-207] and in gastroenterology [208], dentistry [209], urology[210] and neurology.[211]

The OCT image is a grey scale or false color two dimensional representation of backscattered light intensity in a cross-sectional plane; in medical imaging, the OCT image represents differential backscattering contrast between tissue types on a micron scale. OCT was originally developed for

imaging the transparent tissue of the eye and has been extensively used for imaging the retina and anterior eye. Various studies have reported the benefits of OCT imaging system in diagnosis and monitoring of disease such as glaucoma .[197;212] OCT has been widely used in the study of glaucoma, in macular diseases such as age related macular degeneration, in systemic diseases such as diabetes and to examine structural changes such as hole formation.[197;213-216] OCT can also be applied to the non invasive, *in vivo* assessment of retinal blood flow.[217] OCT imaging was extended to *in vitro* pathology in non transparent tissue such as skin and blood vessels .[218;219]

In OCT, the lateral (transverse) resolution is a function of the optics of the device (among others) and may be achieved by using a large numerical aperture, and focusing the beam to a small spot size.[197] Commercially available OCT's lateral resolutions range from 10-60 µm. The theoretical lateral resolution of the OCT system can be calculated using the following formula $\Delta x = 1.22\ \lambda/2NA$ where NA is the numerical aperture of the imaging lens if the eye optical imaging probe. Higher numerical aperture improves the lateral resolution, though this improvement comes at the price of reduced depth of focus, which can introduce detrimental image contrast variation with depth in the OCT images. Axial resolution is determined by the central wavelength and bandwidth of the light source.[212] High axial resolution can be obtained by using broad bandwidth and a light source with higher wavelength.[212] formula $lc = 21n(2)/\pi \times \lambda_0^2/n\Delta\lambda$ where λ_0 is the central wavelength of the light source and n is the refractive index of the sample under investigation.

OCT systems such as the Humphrey™ OCT II and some custom OCT imaging devices use super luminescent diodes (SLD's) as a partial-coherence light source. SLDs are commonly used because they are compact with high efficiency and low noise. However, the output power is limited to only several hundred microwatts and available bandwidth permits imaging with 10-15 micron resolution.[197] Other superluminescent sources such as fluorescence from organic dyes and $Ti:Al_2O_3$ have been used to achieve higher resolution.[197]

The earliest clinical devices were time domain OCT.[220] Recently, a new class of OCT instruments employing spectral (Fourier) domain technology has been developed. An alternative way to obtain a spectrogram is to use a frequency-swept laser or a tuneable laser with just a single detector which is referred as swept source OCT (SS-OCT). In SS-OCT as in SD-OCT no moving parts are required for axial scan; however this system has been mostly used as a research grade system and not as a commercial OCT.

1.10 Time-domain OCT

Basic principles

The generally referred to time–domain OCT (TD-OCT) is a system in which the position of reference mirror is systematically changed to match the optical path from reflections within the sample, and like other OCT's the light in the interferometer is split into two paths. One path is directed to the eye through the scanning mirrors and the other path is directed to a moving reference mirror (Figure 1-10). Light is then reflected back from the reference mirror and the eye and it is combined in the interferometer and this combination is analyzed by a detector and an "A-scan" is created. This process is then repeated with another scanning system slightly displacing each sagittal scan in order to create the cross sectional "B-Scan" image.

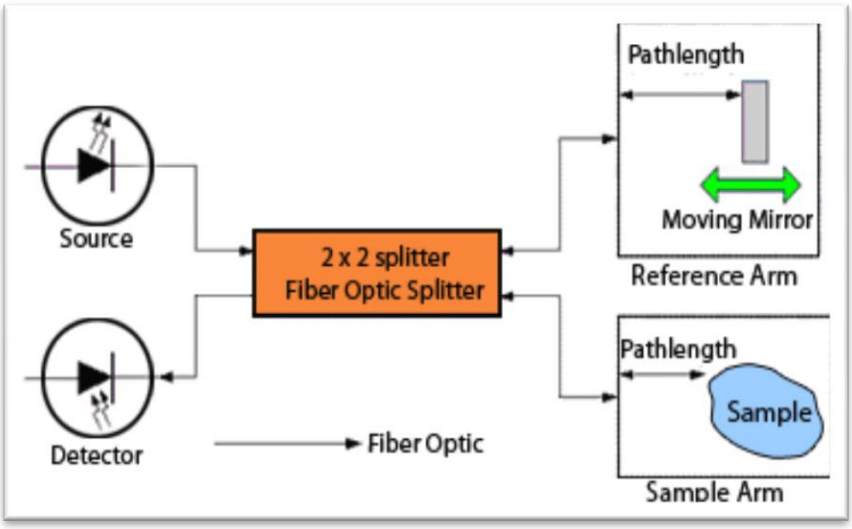

Figure 1-11: Schematic diagram of a TD-domain OCT.

Diagram courtesy of the National Research Council, Canada.

1.11 Spectral domain OCT/ Fourier domain OCT

Basic principles

In the spectral-domain (SD) OCT the reference mirror is stationary, and the OCT signal is acquired as a function of wavelength, either by using a spectrometer as a detector or by varying the (narrowband) wavelength of the light source in time (Figure 1-11). The light reflected back from the eye is combined with the light from the stationary reference mirror in the interferometer. The signal is then split up by a grating into wavelength components and each of these wavelengths is then analyzed by a spectrometer to create a spectro-interferogram. A Fourier transform is then performed on the spectro-interferogram to create an A-scan.

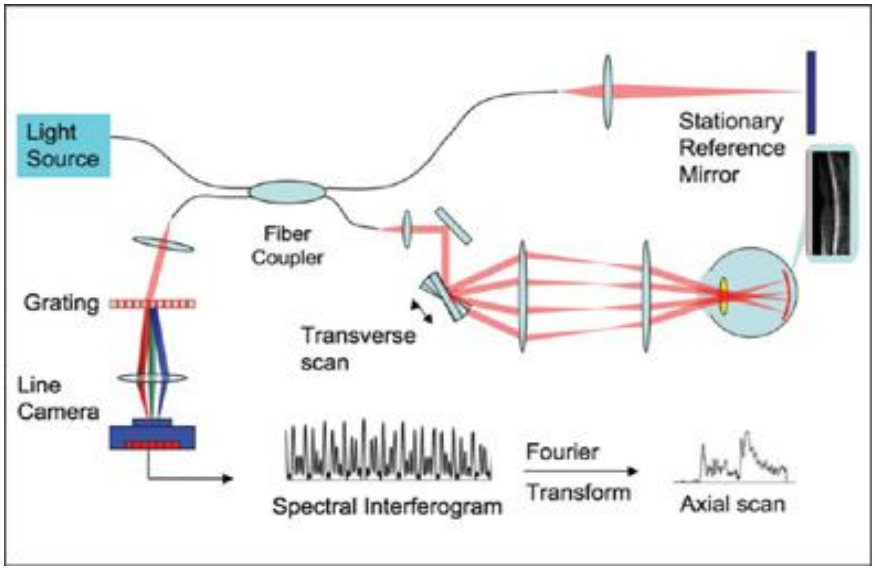

Figure 1-12: Schematic diagram of a SD-domain OCT

(Image courtesy: Huang D)

1.12 Anterior segment optical coherence tomography

Corneal and anterior segment OCT imaging was first reported by Joseph Izatt et al. in 1994 using light with a wavelength of 830 nm.[212] Most early corneal OCT studies used the commercially available retinal scanners OCT1, OCT2, and Stratus OCT (Carl Zeiss Meditec, Dublin, CA).[207;221-225] These early retinal OCT systems acquired only 100 to 400 axial scans (A-scans) per second. At this low speed, the anterior and posterior segment OCT images had motion artefacts and did not enable visualization of angle structures such as the scleral spur and important landmarks for anterior chamber biometry.

To overcome these limitations, commercial OCT technology for the anterior segment has become available and the growth of literature on anterior segment OCT imaging has increased remarkably.[226-236]

An important step in the development of high performance anterior segment OCT designed specifically for imaging the angle of the anterior chamber was longer wavelength sources at 1310-nm.

Light at the 1310-nm wavelength is strongly absorbed by water. Less than 7% of the 1310-nm light incident on the cornea reaches the retina, compared to 93% transmitted for 830-nm light. So a much higher power level can be used at 1310 nm and this ability to use more power for corneal and anterior segment OCT imaging makes it twenty times faster. A high-speed OCT using 1.3 µm wavelength was first reported by Radhakrishnan et al.[204] with an acquisition speed of 4000 axial scans per second.

1.13 Clinical Utility

1.13.1 Anterior Chamber imaging

The anterior chamber angle imaging is an important aspect in diagnosis and management of glaucoma. The current way of viewing the angle is gonioscopy, an invasive procedure that requires direct contact with the patient's eye, unlike anterior segment OCT. Also, anterior segment OCT provides quantifiable measurements of the angle.[237] Commercially available OCT's such as the Zeiss Stratus™ OCT, have been used for imaging the anterior chamber angle. For example Kalev-landoy et al. have reported on the clinical utility of the instrument in patients with different angle configurations [238] and the Visante™ OCT has been effective in imaging the anterior chamber angle in glaucomatous eyes. [239] AS-OCT has been shown to be an important screening tool for glaucoma.[237;240]

Nemeth et al. reported a good anterior chamber depth measurement repeatability with the Visante™ OCT than with immersion ultrasound.[241] Sorbara et al. have reported the use of Visante™ OCT in measuring the sagittal scan images of the anterior chamber to derive the chords and the sagittal depth measurements for fitting large diameter semi scleral contact lenses.[106]

1.13.2 Cornea

Corneal thickness has been traditionally measured by optical or ultrasound pachymetry.[242-245] Ultrasound pachymetry remains the gold standard because of its reliability, ease of use and relative low cost.[246;247] Mean corneal thickness is reportedly higher when measured using ultrasonic devices when compared to measurements using the optical pachymetry.[246] Central corneal thickness measured using the modified retinal OCT.[248-250] Wang et al.[248] were able to measure a chord of the cornea of approximately 10mm and plot corneal and epithelial thickness at baseline and after 3 hours of hydrogel lens wear in closed eye conditions. This study demonstrated the hypoxic swelling occurred mostly in the central cornea, but no apparent change was seen to the epithelial thickness.[248]

The corneal layers that are imaged by the OCT can be differentiated into epithelium and stroma including Descemets membrane and the endothelium. The Descemets membrane around 8 microns thick and the endothelium is about 5 microns in thickness. The instruments used in this thesis for examining the corneal thickness have axial resolutions ranging from 10-18 microns and at this larger resolution compared to the thickness of the tissue the Descemets membrane and the endothelium cannot be differentiated from the stroma due to the limitations in OCT imagers.

Haque [225] et al. reported the meridonial corneal and epithelial changes in subjects who wore Ortho-Keratology lenses. They showed a significant decrease in central thickness but an increase in paracentral thickness.

More recently, an anterior segment OCT (AS-OCT) instrument has been developed that offers high resolution cross-sectional imaging of the cornea and allows both central and peripheral pachymetry. A recent study by Hutchings et al.[251] used this UHR-OCT operating in the 1060 nm range to evaluate the changes in thickness of the anterior, stromal, and posterior corneal laminae in response to hypoxia induced corneal swelling. The results from this study showed a regional swelling due to hypoxic

provocation. On removal of the hypoxic stimulus, the rate of recovery was different for different layers except the endothelium-Descemets membrane complex that exhibited a biphasic recovery.

Central corneal thickness and LASIK flap thickness measurements were commonly reported using these devices.[252-254] A limitation of the OCT when imaging the cornea is that the image degrades in contrast from the center to the periphery. There are two factors that affect the quality of the images at the periphery. The first factor is the lack of compensation for the change in curvature towards the periphery this induces an error in the peripheral corneal thickness due to Snell's law and due to non paraxial incident rays. The second factor relates to the change in refractive index and thickness from the center to the periphery which is not accounted for.

High resolution corneal pachymetry images from anterior segment OCT's have been reported to be useful for refractive surgeons to be able to image the cornea pre-operatively and also be able to assess the post-operative results.[255] AS-OCT produces pachymetry maps that may reveal keratoconus, ectatic or corneal thinning prior to laser refractive surgery.

1.13.3 Tear film thickness

The estimates of the human tear film thickness vary from 3 to 40 microns.[256-258] Some reasons for the lack of agreement include the difference between instruments used and the invasive or non-invasiveness of the techniques used.[259-261] Prydal and Campbell[261] reported that the mean thickness measured using confocal microscopy was 34 to 45 microns, and King-Smith et al.[260] reported the tear film thickness measured using reflection spectra to be approximately 3 microns.

Wang et al. have shown that it was possible to measure the pre-corneal tear film thickness with a modified commercial retinal OCT, but due to the limited axial resolution of the their device these measurements had to be indirect. They reported tear film of approximately 3.3 microns, in agreement with

the results reported by King-Smith et al.[260;262] Wang et al. have shown that they are able to measure the tear film thickness at the upper and lower meniscus statically and dynamically. [263]

The post-soft lens tear film space has been recently imaged using the spectral-domain OCT. The spectral-domain OCT has a very short acquisition time approximately 100 times faster than time-domain instruments which eliminates motion artefacts and produces high resolution images.

1.14 Humphrey Zeiss retinal OCT II adapted for anterior segment imaging

Initially designed to image the retina, the Zeiss Humphrey retinal OCT II™ was adapted to perform anterior segment imaging. Figure 1-12 shows the OCT II instrument.

Figure 1-13: Zeiss Humphrey retinal OCT II™

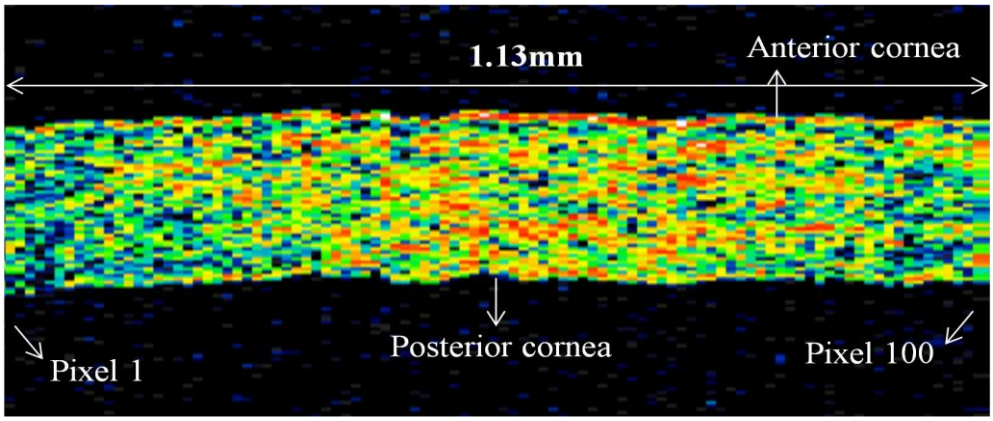

Figure 1-14: An OCT image of the central cornea with a 1.13 mm scan length. The image consists of 100 axial scans

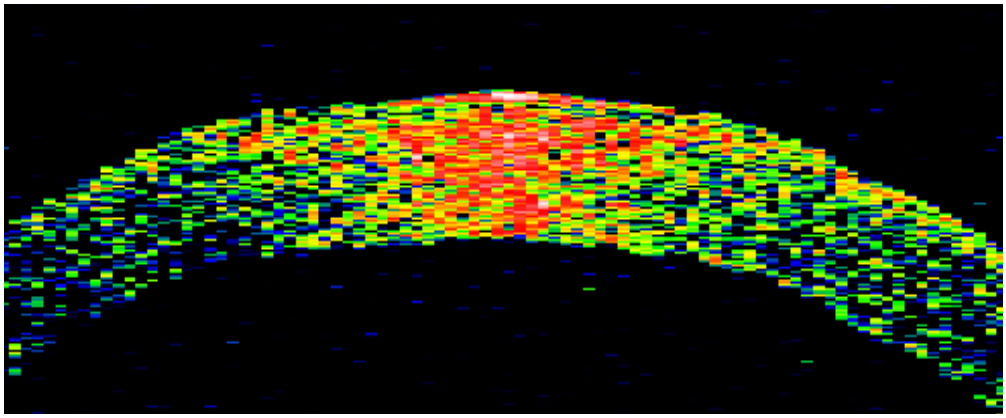

Figure 1-15: An OCT image obtained with a larger scan length of 5mm (100 axial scans)

The OCT II uses a near infrared light source operating at the wavelength of 820nm. The nominal axial resolution of the instrument is 10 microns. Each image consists of a set of 100 axial scans. The OCT image is shown as a pseudo color representation of backscatter intensity (Figure1-13). Each column of pixels represents a single axial scan. Figure 1-14 shows an OCT image obtained over 5mm (but still 100 axial scans), and can be compared in terms of detail with the previous image (Figure 1-13). The axial

resolution of OCT II is inadequate for imaging the cornea at the cellular level, but can distinguish the epithelial layer from the stroma.[197]

1.15 Visante optical coherence tomography

The Visante™ OCT was the first commercially available OCT system with sufficient speed to map in a single image acquisition epoch (Figure 1-15). It is a time domain OCT (TD-OCT) that produces cross-sectional tomograms of the eye without contact. The light source is a 1,310 nm SLD with axial resolution of 18µm and the transverse resolution of 60µm. The scan dimensions are 6mm by 16mm wide for the anterior segment scans and 3mm by 10mm for the pachymetry scans.[264;265]

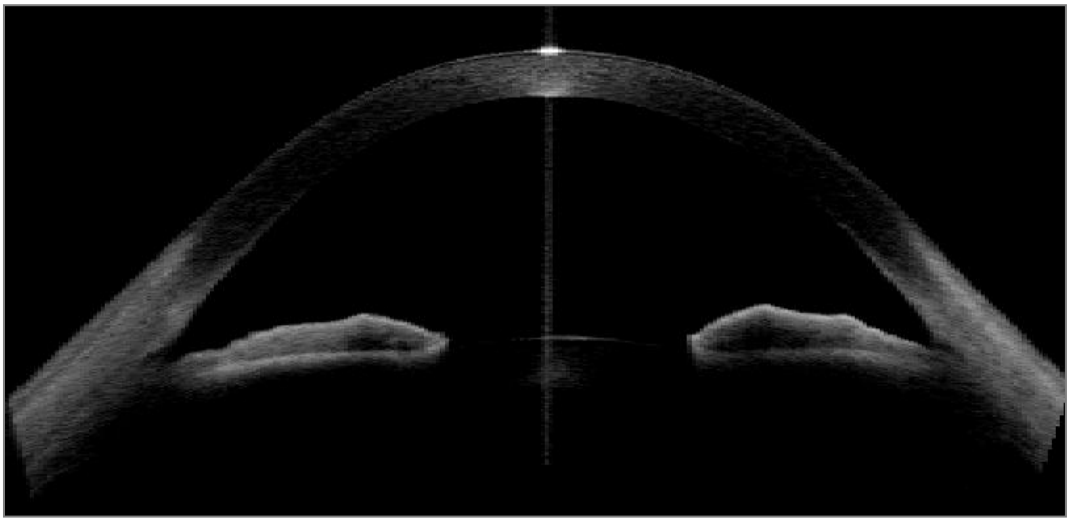

Figure 1-16: A Visante™ anterior segment scan.

The pachymetry map (Figure 1-16) from the Visante™ OCT comprises 10-mm radial lines on eight meridians centered on the apex. Each meridonial scan consists of 128 A-scans and can be visualized as a cross-sectional image. The entire scan takes approx. 0.5 seconds to acquire.

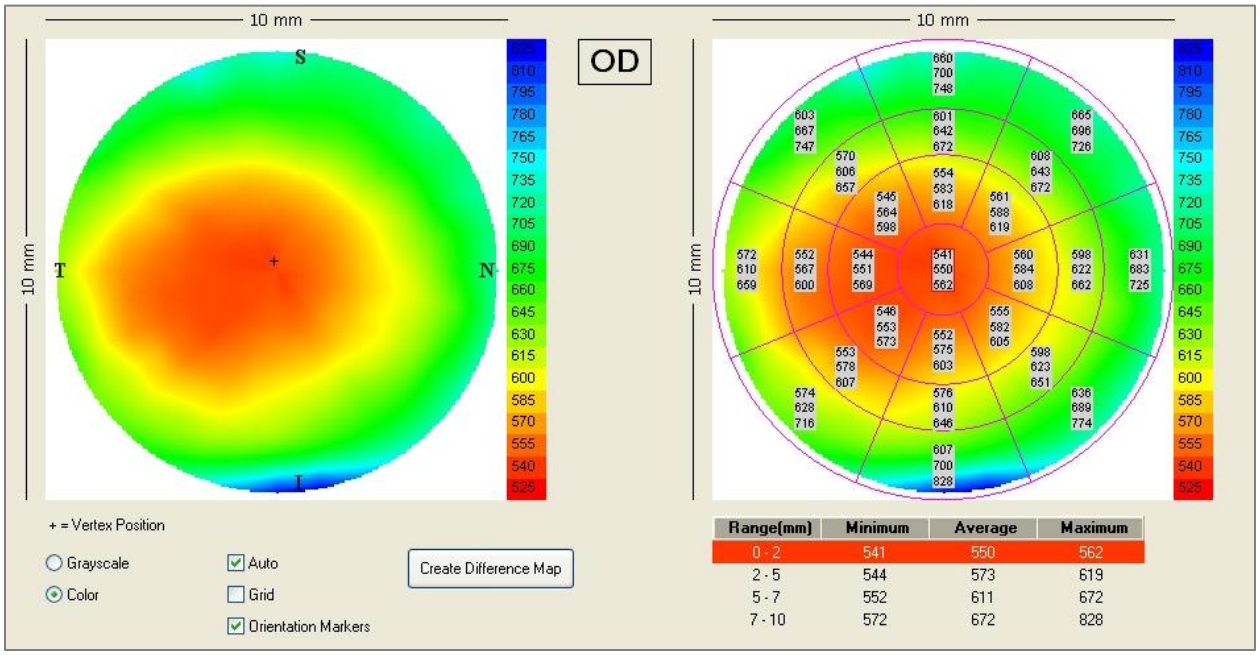

Figure 1-17: Corneal pachymetry map.

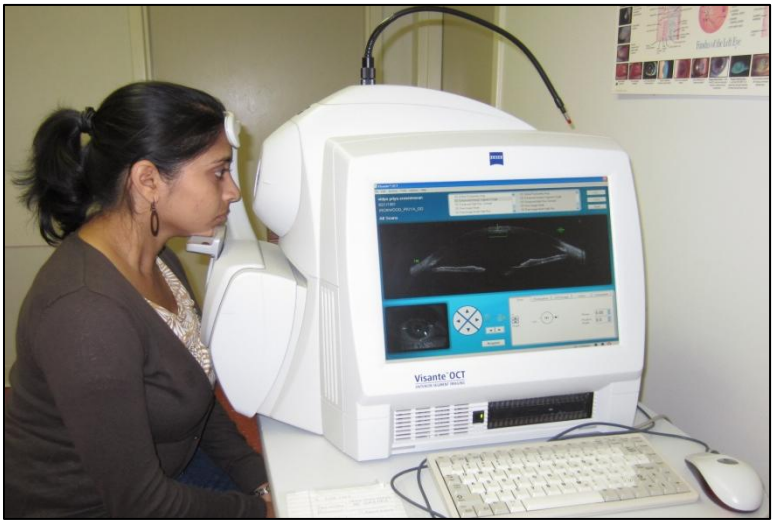

Figure 1-18: A participant at the Visante™ OCT

In the Visante™ OCT software, different tools are available for measurement depending on capture mode of the image. In any of the high resolution corneal imaging modes, thickness callipers, a flap measurement and/or an annotation tool can be used (Figure 1-18). The flap tool consists of a calliper that

is automatically placed on the boundaries delineating anterior/posterior surfaces of the cornea with an operator- moveable marker that can be placed at the putative surgical flap/stroma interface.

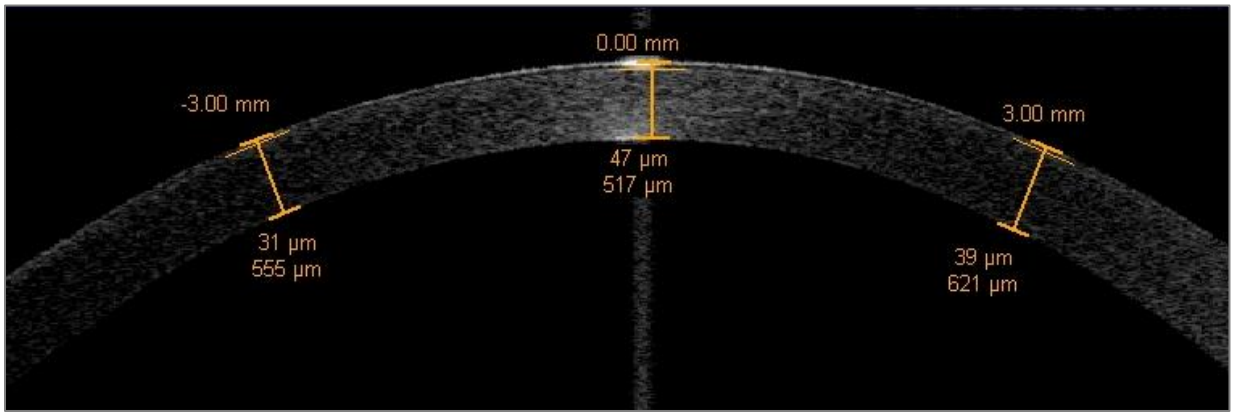

Figure 1-19: High resolution corneal single map with measurement tools.

1.16 RT-Vue Optical Coherence tomography

The RTVue™ is a Fourier/spectral domain OCT system that can image both the anterior and posterior segments of the eye (Figure 1-19). The RTVue™ OCT obtains 26,000 axial scans per second with an axial resolution of 5 microns. The higher resolution of the instrument allows detailed corneal and anterior segment cross sectional images. The RTVue™ operates at a shorter wavelength of 830 nm that allows the instrument to be used in both anterior and posterior segment imaging.

The corneal mapping pattern of RTVue™, consist of 8 high definition meridonial scans acquired in 0.31 seconds. An algorithm detects the anterior and posterior corneal boundaries on a cross sectional image. Prakash et al.[266]reported that the RTVue™ provided repeatable measures of corneal thickness in 100 healthy subjects and reported a mean central thickness of 521 ± 34.7 microns.

Figure 1-20: A participant on the RT-Vue™ Optical Coherence Tomographer

Corneal Anterior Module

To obtain corneal and anterior segment images with the RTVue™, a corneal adaptor module (CAM) was developed. The CAM lenses of the RTVue™ were designed to provide images from the device's telecentric scanning system. There are two adaptor lenses 1) a wide angle lens 2) a high magnification lens. The wide angle lens allows a scan width of 6mm and a transverse resolution of 15 microns (Figure 1-20) and the high magnification lens allows a scan width of 4mm and a transverse resolution of 10 microns (Figure 1-20). The adaptor lens is placed in front of the retinal objective lens to focus the OCT beam on the anterior segment.

Figure 1-21: Corneal Anterior Modules

The basic functions of the CAM lens are to control the focusing, the reference arm delay, and corneal and anterior segment imaging software. The CAM software also automatically "dewarps" the images to recover the shape so that measurements can be made on the corrected image. With the CAM addition one is able to capture anterior segment images illustrated in Figure 1-21 (contact lens edge on the bulbar conjunctiva).

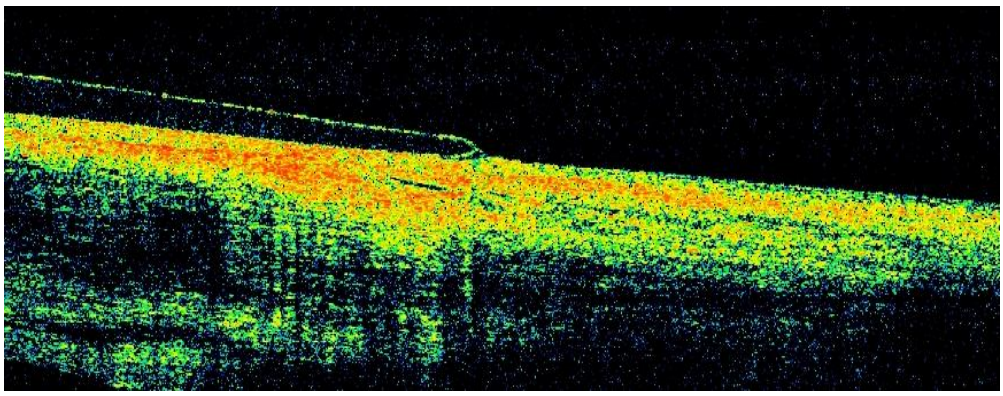

Figure 1-22: Profile of CL edge and bulbar conjunctiva

1.17 Custom built Ultra high resolution OCT

The UHR-OCT system[251;267;268] is based on a compact fibre optic Michelson interferometer, connected to a SLD (Superlum Ltd.; λc =1020 nm, Delta λ=110nm). The sample arm of the system is connected to an optical imaging probe, consisting of three achromatic lenses and a pair of galvanometric scanners, mounted on a modified slit lamp biomicroscope. The interference signal is detected with a custom, high-performance spectrometer (P&P Optica, Inc.), interfaced to a 1024 pixel array InGaAs camera (SUI,

Goodrich Corp.) with 92 kHz readout rate (Figure 1-22). The UHR-OCT system provides 3 micron axial and 10 micron lateral resolution. In this system the acquired images do not require post-processing for dispersion compensation since water has a null in the 1 micron spectral region.[267-269] Images are processed with MATLAB ® (Mathworks) and Amira (Visage Imaging, Inc.)

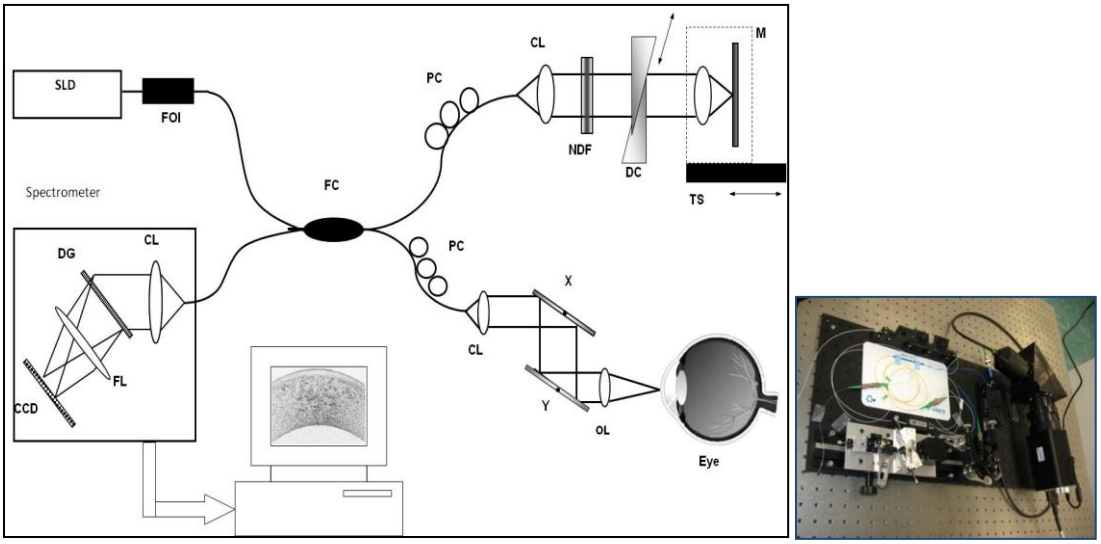

Figure 1-23: A schematic diagram of the UHR-OCT system.

CCD – InGaAs camera, CL – collimator lens, DG - diffraction Grating, FL- focusing lens, OL - ocular lens, PC - polarization controllers, SLD – super luminescent diode, TS – computerized translation stage, X,Y – galvanometric scanning mirrors.

This UHR-OCT imaging system has been applied to imaging of the anterior structures of the human eye, this system has an advantage over the high resolution OCT's operating at 800 nm or 1300 nm.

1.18 Medmont E300™ Corneal Topographer

The Medmont E300™ is a computerized video-keratometer, using placido rings to map the surface of the human cornea (Figure 1-23). This instrument uses 32 rings with 9,600 measurements at 102,000 analysis points and the coverage of each image extends from a minimum ring diameter of 0.25mm to beyond 10mm.

Figure 1-24: Positioning of a participant at Medmont E300™ Corneal Topographer

The data can be used to assist in contact lens fitting, refractive surgery, orthokeratology and general assessment of the cornea.[270-272] Chui et al. compared the performance of three topographers Medmont E300™, Keratron Scout™, and Humphrey Atlas 991™ to measure apical radius, flattest corneal curvature, eccentricity (e) on children. They found that the repeatability of the measurements from the Medmont™ and the Atlas™ were good.[273] In another study, Tang et al. evaluated the repeatability of three placido disc videokeratoscopes (Keratron™, Medmont™ and TMS™). Six test surfaces were measured; a sphere, an asphere, a multicurve and three bicurve surfaces. The repeatability of measures from the Keratron™ and the Medmont™ instruments were the highest.

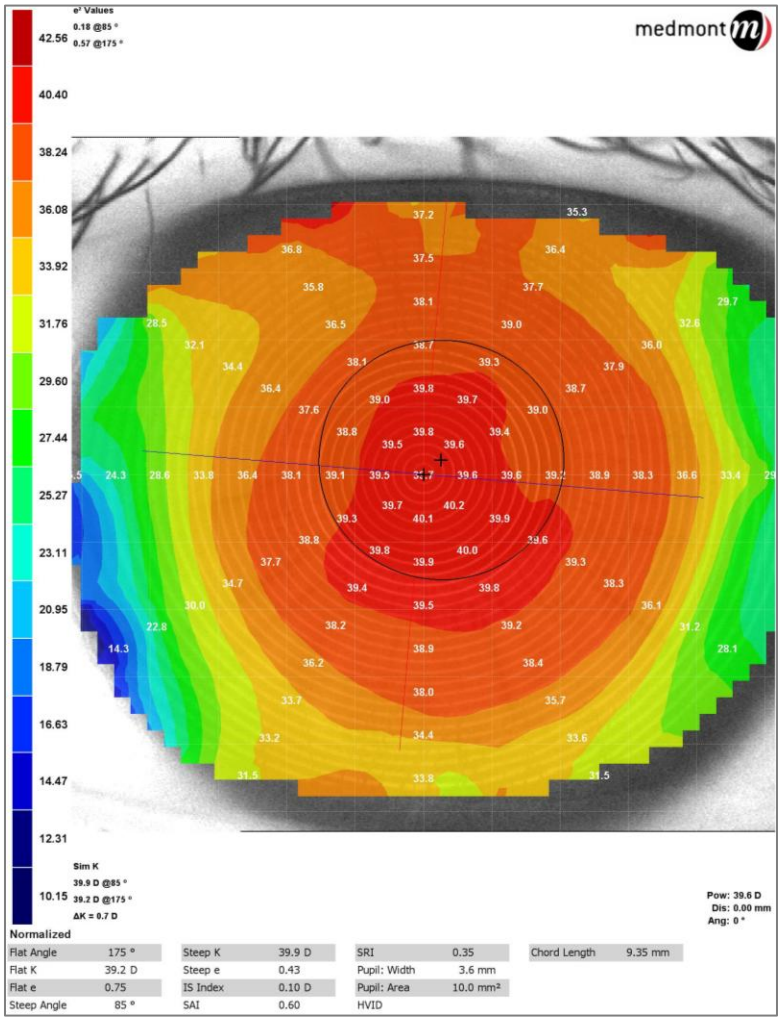

Figure 1-25: Medmont E300™ curvature map

1.19 Red blood cell velocity measurement

There are several studies reporting various quantitative and the qualitative aspects of blood flow measured at the posterior segment of the eye,[274-279] including microcirculatory hemodynamic state of the retina.[280-283] There have been reports of red blood cell (RBC) velocity obtained using measurements from in vivo microscopy videos. This requires precise tracking of each RBC to estimate the velocity in large blood vessels were the blood moves at right angles to, and along the long axis (among others) of the vessel.

Imaging micro vessels (5-10 microns), although more challenging because of high magnification required, is less complex because the red blood cells (which are in the range of 6-8 microns) line up in a single file and move along the vessel long axis.[284;285]

There is not much literature on hemodynamics of the bulbar conjunctiva. This is perhaps surprising because the bulbar conjunctiva is one of the few regions of the body in which the circulation of the blood can be viewed directly and noninvasively in humans. Blood flow in conjunctival capillaries is comparable to the blood flow in other capillaries of the body especially to blood flow in the brain.[286] Red blood cell movement can be observed clinically using a slit lamp but the low magnification and contrast between the red blood and the paler sclera makes the tracking of the RBC movement quite challenging. Processing of video images, from cameras with high spatial and temporal resolution and high dynamic range, enable tracking of RBC movement and provides more usable qualitative information of the conjunctival blood flow.

Duench measured bulbar conjunctival red blood cell velocity in a group of hydrogel lenses wearers and compared it to non lens wearers. She reported that the participants in the lens wearing group had significantly lower blood velocities, compared to the control group. This result supports the notion that contact lens wear has an effect on the bulbar conjunctival vasculature by effecting the content of the blood vessel.[287]

The present study uses Handy Alpha, Hyper Micro Color CCD Camera with LED lighting (Figure 1-25) which was mounted on a modified slit-lamp (Figure 1-26).

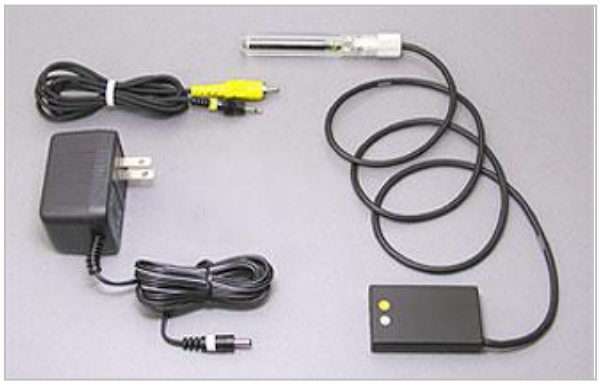

Figure 1-26 The Handy Alpha camera with accessories

Figure 1-27 A participant at a modified slit-lamp with camera

Chapter 2

Accuracy of Visante and Zeiss-Humphrey Optical Coherence Tomographers and their cross calibration with optical pachymetry and physical references

2.1 Introduction

The measurement of corneal thickness has various important clinical and research applications. Some of these may be to measure corneal swelling after overnight wear of continuous wear contact lenses,[1] after overnight orthokeratology,[2] to monitor thickness changes in patients with thinning disorders such as keratoconus[3] or for refractive therapy techniques.[4;5] Corneal thickness can be measured optically[6;7] or using ultrasound techniques among others.[8;9] One of the advantages of optical measures over ultrasound is the non-contact nature of the technique (except for the confocal microscopy). Despite the reported accuracy of ultrasound measures, corneal contact and the use of anaesthetics makes these methods more inconvenient.[10;11] Also, the indentation of the cornea has been hypothesised to result in an under-estimation of corneal thickness when compared to other methods.[11]

Optical Coherence Tomography (OCT) is a newer non-contact optical imaging technique that can measure biological tissue thickness with higher nominal resolution, ranging from 2 to 20 microns.[12-16] OCT works on the Michelson interferometry principle and images are typically two-dimensional data sets which represent optical backscattering in a cross-sectional plane through the tissue.[17;18] Time domain OCT (TdOCT) has been useful in the visualization of different ocular tissues including the cornea.[12] Its main disadvantage is a longer acquisition time causing a decrease in image quality and thus limiting its clinical applications. On the other hand, the spectral domain OCT (SOCT) has a shorter acquisition time eliminating many of the motion artefacts and have been used for cross sectional imaging of the cornea.[12;19-21]

Previous work has suggested that corneal and epithelial thickness can be measured using the Zeiss–Humphrey retinal OCT II (Zeiss Humphrey Systems, Dublin, CA), a posterior segment instrument, that has been adapted to measure the anterior segment.[2;22;23] The OCT II uses a partially coherent superluminescent light source (SLD) with the wavelength peak at 830-850 nm and band width of 32 nm. The axial resolution is about 10 microns.[24]

A recently marketed anterior segment Td-OCT instrument, the Visante OCT (Zeiss Meditec, Dublin, CA) calculates corneal thickness throughout the entire cornea (in eight meridians nearly simultaneously) something that is advantageous in characterizing the whole corneal structure.[25;26] The Visante OCT uses a source with a peak wavelength of 1310nm. This longer wavelength theoretically allows better delineation of the anterior and posterior surfaces of the cornea and the better penetration enables clearer imaging particularly of the limbus. Its high speed scanning system enables the generation of pachymetry maps in addition to linear cross-sectional images, in seconds. The axial resolution of the device is 18µm and the transverse resolution is 60µm. Each scan is in a zone 6mm by 16mm for anterior segment scans, 3mm by 10mm for the pachymetry.[25;27 28]

Anterior segment OCTs are now more commonly being used for a range of diagnostic and post-surgical analyses.[7;29-32] For instance, there are a number of reports of the assessment of patients prior to and after surgery examining such things as corneal oedema and ectasia.[7;33-37] Despite strong associations, between devices measuring corneal thickness,[10;26;38] there is no gold standard to cross calibrate these instruments and to assess their accuracy, although attempts have been made.[39;40]

Although there is abundant literature on the precision of instruments for measuring corneal thickness,[10;23;26;38;41-43] very few studies have reported accuracy of these methods.[39;40]

Measurements could be repeatable and not accurate and therefore, in addition to precision, a measurement technique should also be demonstrably accurate. The purpose of this study was first, to measure the accuracy of the Visante OCT as it compared to a direct measure with mechanical gauge (MG). The

materials used to mimic the cornea were transparent plastic lenses made with a refractive index similar to the cornea, that is n= 1.376. The second purpose was to compare these results with an Optical Pachymeter (OP) and the Zeiss–Humphrey retinal OCT II. In order to calibrate the two OCT's (Visante OCT and Zeiss–Humphrey retinal OCT II) the measurements using the MG were taken as true measurements.

2.2 Methods

2.2.1 Lenses

Twenty two rigid lenses with varying thicknesses were manufactured using a plastic material with a refractive index of 1.376±0.0005 (at 589 nm), verified by the manufacturer. This plastic material was developed by Optical Polymer Research, Inc., Gainesville, Florida. All the lenses were made with plano power (parallel anterior and posterior surfaces) with a base curve of 8.6mm and no prism. The physical center thickness of the calibration lenses (ranging from 100 to 764μm) was measured four times and then averaged. (Table 2.1)

2.2.2 Instrumentation

The central thickness of the same set of lenses was also measured using the following three instruments: a computerized optical pachymeter (OP) mounted onto a Zeiss 30 SL-M biomicroscope, Zeiss–Humphrey retinal OCT II, and Visante OCT.

Table 2.1 The actual central thickness of twenty-two lenses

Actual lens center thickness (µm)	
1	301
2	580
3	420
4	350
5	470
6	560
7	360
8	630
9	489
10	527
11	312
12	470
13	650
14	700
15	240
16	450
17	150
18	580
19	100
20	500
21	190
22	764
Mean	445
Standard deviation	179

The Visante OCT "high resolution" mode was used to scan the rigid contact lenses. The image of the Visante OCT comprises 512 axial scan and the scan dimensions were 10 mm by 3 mm. The scanned image was considered to be optimally aligned when the specular reflex, which is a high intensity reflection from the center of the front surface of the contact lens, was visible (Figure 2-1).

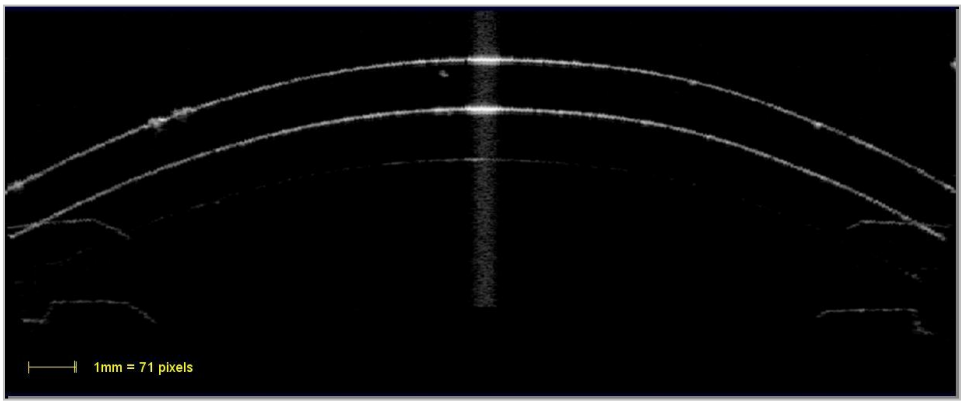

Figure 2-1 Visante OCT image of the contact lens with n=1.376

Scans were judged to be of adequate quality based on the following criteria: good demarcation of the anterior and posterior boundaries of the contact lens and absence of artefacts. Instead of using the built in callipers provided by the instrument, custom software was used which automatically delineated the anterior and posterior borders of the cross-sectional images of the contact lens and the radial distance between the anterior and posterior surface were obtained, that is, the thickness of the contact lens.

Version 2.0 of the Visante OCT software was used and the raw unaltered binary image file (*.bin) was exported for analysis. To convert pixels obtained from the binary image, to millimetres, a conversion factor was used (71 pixels=1mm).

With the Zeiss–Humphrey OCT II similar methods were used and one hundred axial scans (1.13-mm width) were processed. The same custom software was used to analyse the data. Averages of the thicknesses were then used. (Figure 2-2)

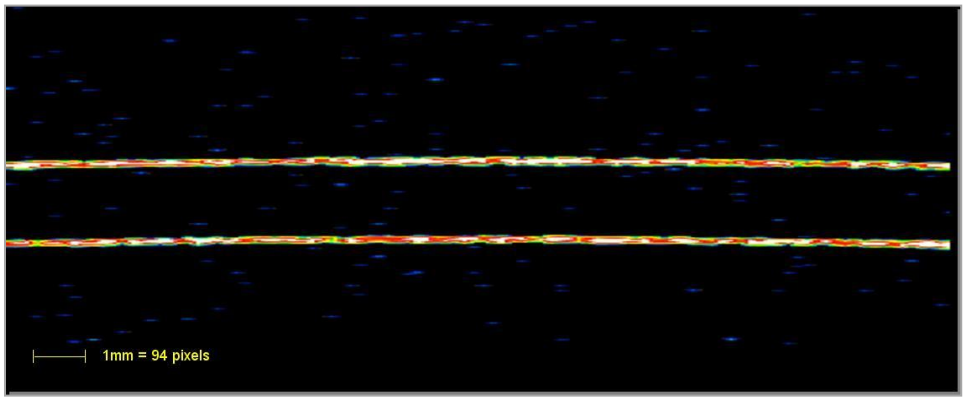

Figure 2-2 Zeiss-Humphrey retinal OCT II of the contact lens with n=1.376

2.2.3 Procedure

The lenses were installed on a circular holder in a random order. A number was assigned to each with no reference to the thickness of the lens. All the measurements using the MG, OP, OCT II and the Visante OCT were performed by me. Each lens was measured four times and the average of the four readings was calculated. Multiple measurements were necessary in order to minimize measurement variability.[41;44] The measurement order with the instruments was randomized in the study. The accuracy of the measurements of the optical instruments was determined by comparison of the physical CT of the lenses obtained using the MG to those from the optical devices.

2.2.4 Data analysis

Using a repeated-measures analysis of variance, the effects of measurement devices were examined. (P values < 0.05) were considered statistically significant. Post-hoc Tukey tests (significant level $p< 0.05$) were used to determine the significance of specific pairs. Regression equations between the MG and all

optical measures were derived to calibrate the devices. The Bland & Altman recommendations were used to examine the limits of agreement between pre and post calibration.[45]

2.3 Results

Using repeated measures ANOVA, there was a significant difference in the lens thickness between each of the instruments calibrating them, as shown in Figure 2-3. Please note the graph shows the means and the 95 % confidence intervals of the estimate of the mean whereas the significance testing is whether the means of the differences are equal to zero: These are not the same thing. Tukey post hoc testing revealed that the Visante OCT measurements were significantly higher than the other three (OCT II, OP and MG) methods (p=0.001). The Visante thickness was 453.0±37.6 µm compared to 445.1±38.2 µm with the microgauge and the OCT II was significantly lower (424.5±36.1µm) compared to the other three methods of measurement both (p=0.001). There was no statistically significant difference (p>0.05) between thickness measured using the MG (445.1±38.2 µm) and the OP (444.2±38.2 µm).

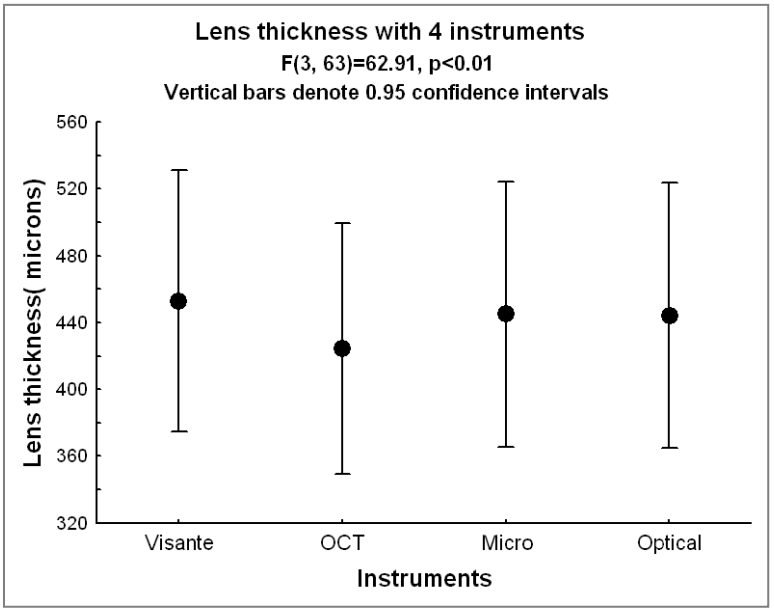

Figure 2-3 Center thickness (µm, Mean ± 95 % CI) of lenses prior to calibration measured with each instrument

The following figures compare the standard microgauge measures to each of the measurements made by the three instruments (using Bland-Altman plots). Figure 2-4 compares the microgauge versus the optical pachymeter before calibration and illustrates how little difference there was between these two instruments. Figure 2-5 demonstrates the differences between the OCT II and the microgauge and indicates that the thickness of thicker lenses (450 um and up) were over-estimated by the instrument. On the other hand, the Visante OCT overestimated the thickness especially when lenses were thinner (250 to 400 um) in comparison to the microgauge measurements (Figure 2-6).

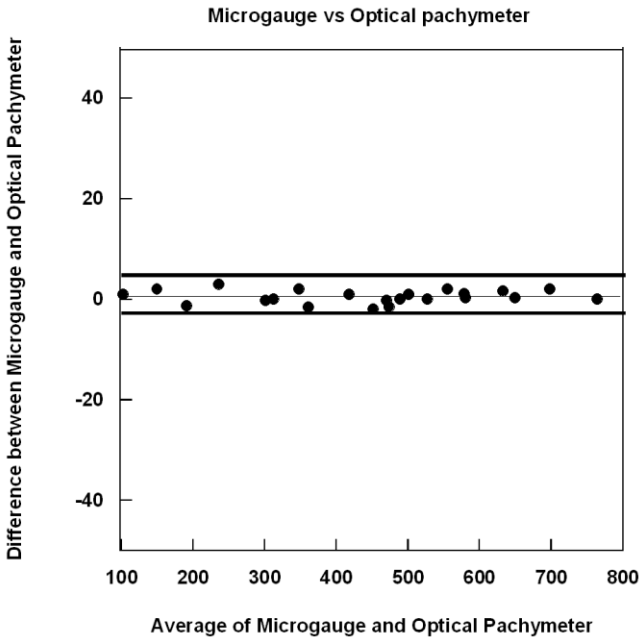

Figure 2-4 The means of microgauge and optical pachymeter thickness measures versus the differences between the microgauge and optical pachymeter measures. The thin line represents the mean difference and the thick lines represent the 95% limits of agreement.

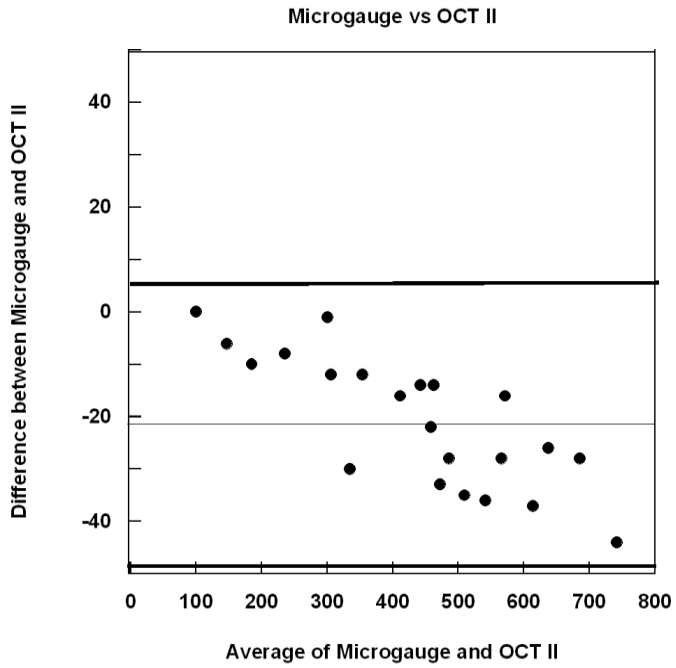

Figure 2-5 The means of microgauge and OCT II thickness measures versus the differences between the microgauge and OCT II measures. The thin line represents the mean difference and the thick lines represent the 95% limits of agreement.

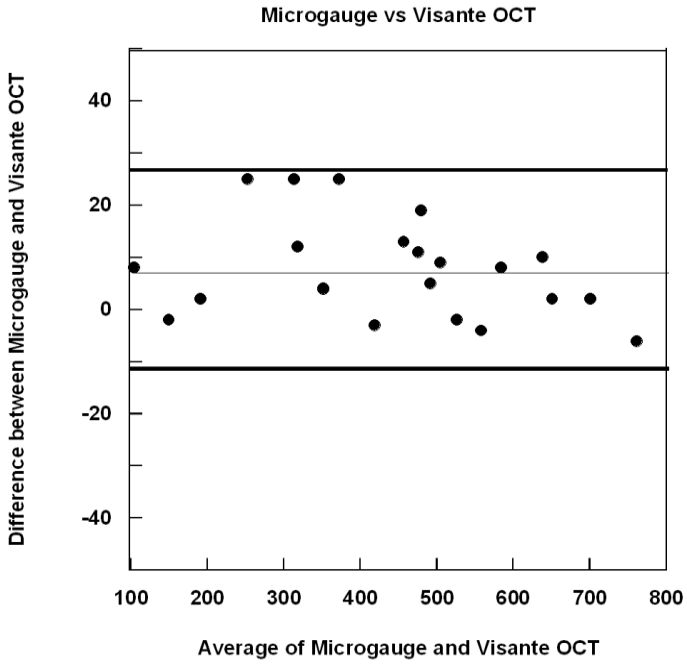

Figure 2-6 The means of microgauge and Visante OCT thickness measures versus the differences between the microgauge and Visante OCT measures. The thin line represents the mean difference and the thick lines represent the 95% limits of agreement.

The relationship between the OP and MG lens thickness measurements is shown in Figure 2-7.

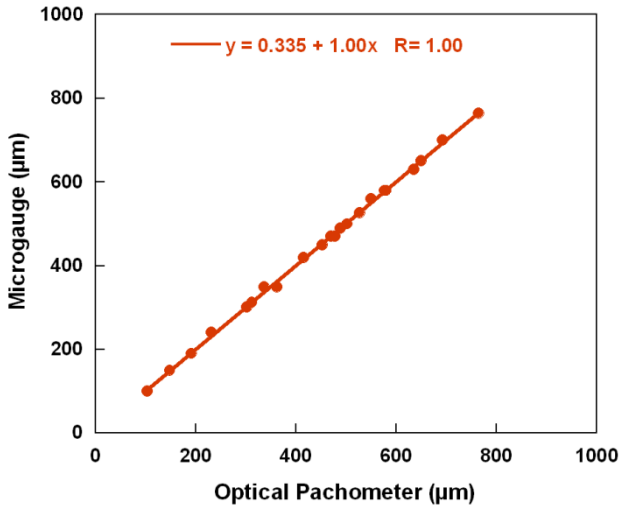

Figure 2-7 Comparison (regression equation) of microgauge and Optical Pachometer thicknesses prior to calibration.

The correlations of pre calibrated OCT II and the Visante OCT to the MG were significant (R=0.99 p=0.001, for both, Figures 2-8 and 2-9). The calibration equations that were derived from the regression analysis were then used to calibrate the instruments.

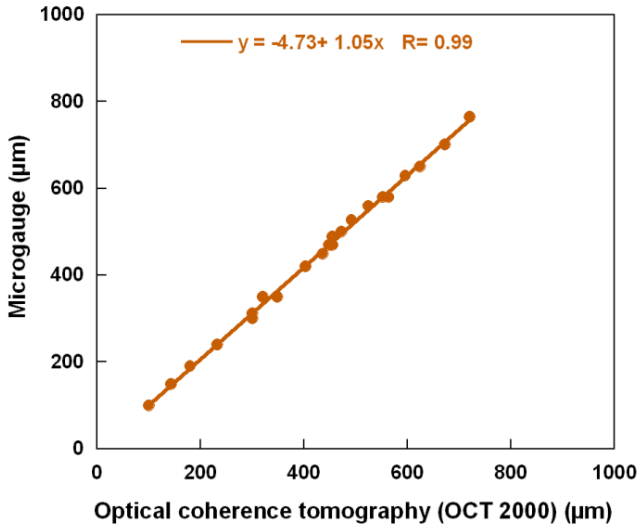

Figure 2-8 Comparison (regression equation) of microgauge and Zeiss-Humphrey OCT II thicknesses prior to calibration.

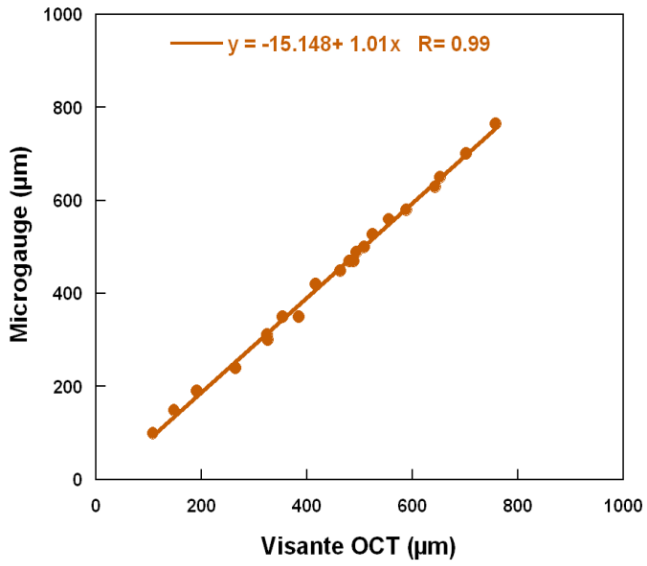

Figure 2-9 Comparison (regression equation) of microgauge and Visante OCT thicknesses prior to calibration.

The differences between the two OCT instruments and the MG were eliminated after applying the calibration equations to each of these devices. (Table 1.2)

	Mean	SE	CI -95%	CI +95%	N	Calibration Equation
Microgauge (µm)	445.1	38.2	365.7	524.6	22	N/A
Visante OCT(µm)	453.0	37.6	374.8	531.3	22	-15.15+1.01 X Measured CT
OCT II (µm)	424.5	36.1	349.5	499.6	22	-4.73+1.05 X Measured CT
Optical pachymeter (µm)	444.2	38.2	364.7	523.7	22	0.34+1.00 X Measured CT

Table 2.2 The average central thicknesses of the twenty-two lenses for each of the instruments and the respective calibration equations.

The difference between pre and post calibration versus the average of the pre and post calibration thickness values of the Visante OCT is shown in Figure 2-10. The results indicate that the overestimation of the thickness of the thinner lenses is reduced post calibration.

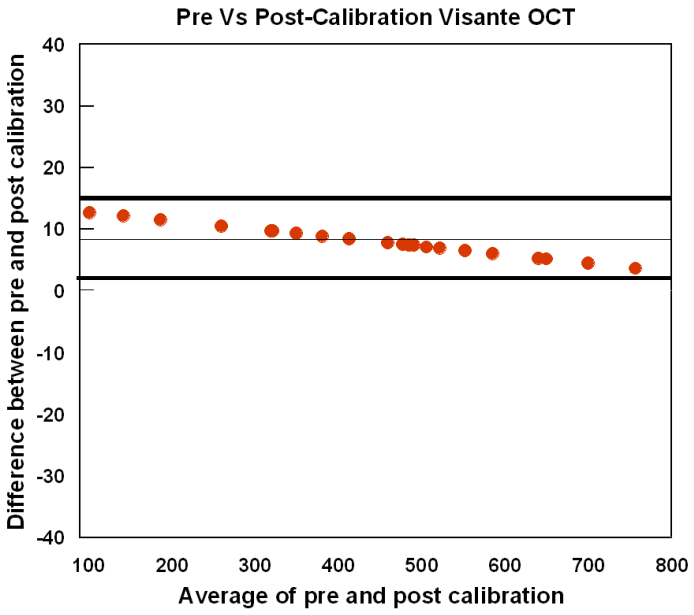

Figure 2-10 The means of pre and post calibrated Visante OCT thickness measures versus the differences between pre and post calibrated Visante OCT measures. The thin line represents the mean difference and the thick lines represent the 95% limits of agreement.

2.4 Discussion

My intent in doing this experiment was to explore whether there are differences among the optical devices that are used to perform pachymetry. There *were* differences and so the method proposed by Moezzi et al. [39] was used to remove the differences. The calibration equations that were derived enable the direct comparison among devices so that the commonly reported differences among pachymetric methods are now unimportant.[46]

Accurate (post-calibrated) corneal thickness measured with any of these devices is perhaps important for a number of reasons including understanding corneal hypoxia[47;48] in CL wearers and or in diabetics,[49] for accurate IOP measurements,[50] in cases of pre-surgical patients for refractive surgery,[4] pre[51] and post-surgical[52] keratoconus patients and in patients wearing ortho-keratology lenes.[22]

Many instruments that are used to measure corneal thickness have calibration methods based on imaging the front surface of a reference sphere or an asphere, but, the posterior surface typically cannot be calibrated with these devices. The calibration method I used required only a transparent contact lens (that is with a visible posterior surface), with a similar refractive index to the human cornea. Cross -calibrating various optical pachymeters can therefore be easily implemented.

Although previous studies show regional variation of corneal refractive index as well as variation of refractive index between different layers of the cornea,[53] an average refractive index of 1.376 is reasonable based on the current evidence of corneal refractive index.[54;55] Using reference lenses with the refractive index of the cornea (1.376) allows rapid and simple calibration and cross calibration of these optical instruments for measuring corneal thickness, although of course the assumption is that it is refractive index is constant across subjects and across cornea.

The calibration I used demonstrates that when measuring lenses within the "normal" corneal thickness range (from 375 to 550microns) the instruments are quite accurate, but, with thicker or thinner reference lenses, the error is increased. Thinner measures are over-estimated and thicker measurements are under-estimated with the Visante OCT (Figure 2-10). The internal calibration of the Visante OCT using its own solid calibration sphere is perhaps limited in range of thicknesses which it operates.

Central corneal thickness differences outside of the average range can be clinically significant if decisions regarding refractive surgery are being made and regarding correction factors for the measurement of IOP.[56;57] When decisions are made about eligibility for surgery using a thickness criterion, it is perhaps not clear that the recommended $\pm$ 20 microns used to define the range of uncertainty is appropriate; it might be considered to be much less.[58]

Calibration requires that our 'phantom corneas' have two optical characteristics. The first is that the refractive index is as specified by the manufacturer and that this index is the "same" as the cornea. The second is that the refractive index is constant over the samples we used. Problems with the former (e.g. misspecification of refractive index) would result in the absolute measures of central corneal thickness obtained after calibration of each device being fractionally in error (the amount being a function of the misspecification). However, the calibration between devices would still be valid. Assuming that the cornea has a homogeneous refractive index is in itself an approximation since refractive index varies in depth and extra-axially.[53;59] Therefore, in a sense, the phantom corneas with a single refractive index are only a first approximation. The second problem of heterogeneity of the refractive index across the sample lenses, provided it was non-systematic, would not be expected to affect the calibration equations other than diminishing the goodness-of-fit.

Dunne et al. examined the inaccuracy of the Visante OCT using ray tracing through images of contact lenses with a refractive index of 1.493 and centre thicknesses ranging from 0.3 to 0.7mm (in 0.1mm steps). Their results indicated that there was no variation in accuracy with thickness.[56] My approach was

different to theirs, with differences in measured/assumed refractive indices and also how the images were acquired; they used the "anterior segment map" (with custom software callipers) while I used the "high resolution map" (also with custom software callipers) .

A potential drawback of my study is perhaps that only central thickness accuracy was examined and not peripheral. These lenses had parallel front and back surfaces and therefore there should be no differences in the lens thickness in the center and the periphery. Since this is a comparison of devices there is no specific reason that one device's peripheral measurement is more or less accurate than another, I believe that the results can be generalized to the periphery. In addition, the range of the thickness of the rigid reference lenses included what might be expected for peripheral *corneal* thickness [60] and so, again the results apply to peripheral measurements.

Finally, there was no compensation for the difference in the two wavelengths that each OCT (OCT II and Visante OCT) uses. The former uses 820 nm and later 1300nm. Most instrument comparisons do not take into account this difference in wavelength which results in difference in index of the tissue examined perhaps due to the relatively small effect.

Chapter 3

Repeatability and comparative study of corneal thickness using the Visante™ OCT, OCT II and Orbscan II™

3.1 Introduction

Imaging of the ocular adnexa has evolved significantly since its conception. The early forms of capturing images began with the use of film based slit lamp cameras. Ultrasound A scan and B scans gave axial length, position and thickness of the crystalline lens, anterior chamber depth and information about the posterior pole.[1] Although these forms of imaging still hold value, computer technology has allowed for advancements in the imaging field. Various imaging techniques have been used over the past few years to improve identification, characterization and quantification of the ophthalmic disorders. In recent studies optical coherence tomography (OCT) has been used as a microscopic imaging technique for *in vivo* examination of the posterior and the anterior segment.[2-7]

Techniques for measuring central corneal thickness (CCT) include ultrasound pachymetry (UP),[8] confocal microscopy,[9] ultrasound biomicroscopy (UBM),[10] scanning slit imaging (Orbscan II ™)[11] and OCT.[12-14] Optical coherence tomography is a non-invasive, non-contact imaging technique that typically uses infrared light to obtain high resolution cross-sectional images *in vivo*.[14] Although the technique has been used primarily in the diagnosis of optic nerve and retinal pathology, more recently it has been shown to be valuable for the study of the cornea.[13-16]

The Visante ™ OCT (Zeiss Meditec, CA) is time domain OCT (TD-OCT), utilizing optical coherence tomography to image the anterior segment. The Visante ™ OCT Model 1000 can provide detailed in vivo examination of the anterior segment of the eye without eye contact. It provides high resolution cross-

sectional images. The axial resolution of the Visante™ OCT image is 18µm and the transverse resolution is 60µm.[17;18] The Visante ™ OCT and Stratus ™ OCT devices allow the scanning probe to move transversely, thus enabling for the reconstruction of a 2-dimentional image form a series of transversely displaced axial scans. The difference between the Stratus ™ OCT and the Visante ™ OCT is in the wavelength of light that is used in the device.[15;19] The Stratus ™ OCT uses a near-infrared light with a wavelength of 820 nm, whereas the Visante ™ OCT uses a wavelength of 1310 nm. By increasing the wavelength of light, the amount of signal scattering is reduced, and this potentially facilitating better penetration past the limbus and sclera.

The first purpose of this study was to measure the repeatability of the Visante ™ OCT in a normal sample. The second was to compare this instrument with other measures of topographic total corneal and epithelial thickness as measured with the Zeiss-Humphrey OCT II (OCT II) (model 2000, Carl Zeiss Meditec, Jena Germany) adapted for anterior segment imaging [20] and the Orbscan II ™ (Bausch and Lomb, Rochester New York).

3.2 Methods

3.2.1 Study Design

Ethics clearance was obtained from the Office of Research Ethics at the University of Waterloo prior to commencement of the study and the study was conducted according to the Tenets of Helsinki. Fifteen healthy participants (9 women, 6 men) were recruited and their eligibility was determined at a screening appointment. The age range of the participant was 20 and 32 years. They were free of any ocular disorder, with no history of eye surgery, ocular trauma, or current systemic disease. Informed consent was obtained from all participants prior to enrolment in the study. The measurements for each eye (randomized) approximately the same time on each day with the same instructions and procedures by myself.

Subjects were positioned on the chin and fore headrest and were encouraged to keep their eyes open as wide as possible but were allowed to blink as needed. At the screening visit (Day zero), visual acuity was measured and biomicroscopy was performed. At the Day 1 visit the epithelial and total corneal thickness, across the central 10mm of the horizontal meridian was measured using the OCT II and the Visante ™ OCT. Total corneal thickness across the central 10mm of the horizontal meridian was measured using the Orbscan II ™. Three measurements were taken across the cornea at the center, nasal and temporal cornea with the Visante ™ OCT, OCT II and the Orbscan II ™. Nasal and temporal corneal measurements were 3mm away from the center. Because of a limited scanning range of the OCT II, an external fixation target was used to control eye position to enable measurement of nasal and the temporal corneas \with the device. Measurements were taken 3 mm nasally and temporally from the central corneal scan with the OCT II using the external fixation target and were compared to the total corneal and epithelial thickness in same area for the Visante ™ OCT and the Orbscan II ™. The order of these measurements was randomized. These measurements were repeated on Day 2. Each individual measurement was repeated three times on both day 1 and day 2 and the measurements were averaged to give a single result.

3.3 Instruments

3.3.1 Visante™ optical coherence tomographer

The Visante™ OCT uses a wavelength of 1310nm and has a nominal axial resolution of 18µm and transverse resolution of 60µm. The participant was comfortably positioned at the chin rest and aligned for the scan. The participant was asked to fixate at the start burst fixation pattern inside the instrument. A high resolution corneal single map was acquired for the study. The scanned image was considered to be optimally aligned when the specular reflex, which is a high intensity reflection from the front surface of the cornea, was visible on the screen. Data were analyzed using the inbuilt calliper tool that automatically places itself on the boundaries delineating anterior/posterior surfaces of the cornea. Measurements of

corneal and epithelial thickness at day 1 and day 2 for central, nasal and temporal locations on the cornea were taken using the Visante™ OCT.

3.3.2 OCT II

The OCT II adapted for anterior segment imaging [21-23] was used to obtain thickness data of the cornea and the epithelium. A scan width of 1.13mm was used to acquire images.

Study participants were seated comfortably at the OCT instrument with their chin and forehead on the headrest and the participants were asked to fixate the peripheral fixation lights of the fixation target. The incident beam was aligned with the fixation light of the target on the corneal surface, and the specular reflection confirmed that the scan was perpendicular to the cornea.

Once the specular reflection was obtained at the 3mm nasal and temporal locations from the center of the cornea, an optimal image and the raw data were captured. Central corneal and epithelial thickness was obtained using custom analysis software. Custom software read the raw files consisting of position vs. reflected intensity for each of the 100 sagittal scans. The software imported the raw data from the instrument and then located the peak reflectance that corresponded to front and back surface of the cornea. From the curves fit to these surfaces, thicknesses were calculated for each pixel point along the front surface (the shortest distance between the anterior and posterior surfaces).The averages of these thicknesses were then used.

3.3.3 Orbscan II ™

The Orbscan II ™ (Bausch & Lomb, Rochester, NY) provides topographic images of both the on and front and the back surface of the cornea and also provides pachymetric thickness measurements of the cornea. The Orbscan II™ is based on Placido disk technology. The instrument is used to acquire and

analyze the elevation and curvature measurements on both the anterior and posterior surfaces, on and off the axis of the cornea.

The patient was positioned with a chin and forehead rest and asked to look at a fixation target. The device projects 40 slits, 20 from the right and 20 from the left at an angle of 45 degrees to the instrument axis. As the light from these slits passes through the cornea, it is scattered in all directions which is backscattered toward the digital video camera of the device, which records the appearance in 2-dimensional images.[11;24;25]

3.3.4 Data management and analysis

Data analysis was conducted using Statistica (Version 7). The coefficient of repeatability (COR), Bland-Altman limits of agreement[26] and the correlation coefficient of concordance (CCC) were used.[27] The COR was 1.96 x test-retest differences. CCC describes concordance between repeated measurements by analyzing the deviation of test and re-test measures from a perfect 45°-line through the origin (i.e. CCC=1). CCCs <1 represent deviations from this perfect line and correspond to a weaker repeatability. P-values less than 0.05 were considered to indicate statistical significance. Analysis of measurements taken from the center and ±3mm on either side are reported. In addition, measures from pairs of instruments were compared using t-tests.

3.4 Results

There were nine females and six males enrolled in the study, ranging from 20 to 32 years. The measurements were taken on two separate days, but, at the same time of day ±60mins. Mean central corneal thickness imaged by the Visante™ OCT at the center of the cornea was 536± 27 µm (range, 563-509 µm) and the mean epithelial thickness using the Visante™ OCT was 55± 2.3 µm (range, 57.3-52.7 µm). Table 3-1 represents the mean corneal and epithelial thickness at the center imaged by the Visante™

OCT and OCT II and the mean corneal thickness using the Orbscan II. A t-test showed that there was a significant difference in apical corneal thickness imaged by the Visante™ OCT and OCT II ($p<0.05$). Significant difference was also found in corneal thickness ($p<0.05$) between measures using the Visante™ OCT and the Orbscan II ™ at the center. There was no statically significant difference between the epithelial thickness measured with Visante™ OCT and the OCT II ($p>0.05$).

Table 3-1 Mean corneal and epithelial thickness at center (mean± 95 % CI) for Visante OCT, OCT II and Orbscan.

Central thickness	Visante OCT	OCT II	Orbscan II
Total thickness	536± 27µm	520±25µm	609±29µm
Epithelial thickness	55± 2.3µm	56±4.9µm	Not applicable

The mean corneal and epithelial thickness at the temporal location imaged by the Visante™ OCT was 554± 26 µm and 53± 0.7µm respectively, the 5th and 95th percentiles for corneal and epithelial thickness were between 580 to 528 µm and 53.7 to 52.3 µm respectively. Table 3-2 represents the mean corneal and epithelial thickness at the nasal position imaged using the OCT II the Visante™ OCT, and the Orbscan II ™. Nasally there was no significant difference in the corneal and epithelial thicknesses between measurements from the Visante™ OCT and OCT II ($p>0.05$), but there was a difference between measures from the Visante™ OCT and Orbscan II ™ ($p<0.05$).

Table 3-2: Mean corneal and epithelial thickness at the nasal position (mean± 95 % CI) for Visante OCT, OCT II and mean corneal thickness using the Orbscan II™

Nasal thickness	Visante OCT	OCT II	Orbscan II
Total thickness	554± 26µm	599±36µm	609±27µm
Epithelial thickness	53± 0.7µm	56±3.4µm	Not applicable

Table 3-3 shows the mean corneal and epithelial thickness at the temporal location acquired using the Visante™ OCT, OCT II and Orbscan II ™. There was no significant difference in the corneal thickness at the temporal location between data from Visante™ OCT and OCT II ($p>0.05$). Epithelial thickness at the temporal location measured using the Visante™ OCT and OCT II was statistically significantly different ($p<0.05$).

Table 3-3: Mean corneal and epithelial thickness at the temporal location (mean± 95 % CI) for Visante ™ OCT, OCT II and Orbscan II ™

Temporal thickness	Visante OCT	OCT II	Orbscan
Total thickness	565± 26µm	555±39µm	600±29µm
Epithelial thickness	53± 0.8µm	54±2.2µm	NA

Table 3-4 and table 3-5 presents the COR of the corneal thickness and the epithelial thickness for the three instruments (Visante™ OCT, OCT II and Orbscan II ™). There is better repeatability of corneal and epithelial thickness measured with Visante™ OCT between the sessions when compared to the OCT II and Orbscan II ™ imaging systems.

Table 3-4: Coefficient of repeatability of corneal thickness with Visante ™ OCT , OCT II and Orbscan II ™

COR	Total corneal thickness (Test/Retest)		
Instruments	**Center**	**Temporal (3mm)**	**Nasal (3mm)**
OCT II	± 13.31µm	± 13.98µm	± 19.94µm
Visante OCT	± 8.98µm	± 8.62µm	± 7.71µm
Orbscan II	±10.71µm	± 13.66µm	± 11.53µm

Table 3-5: Coefficient of repeatability of epithelial thickness with Visante ™ OCT, OCT II and Orbscan II™.

COR	Epithelial thickness (Test/retest)		
Instruments	**Center**	**Temporal (3mm)**	**Nasal (3mm)**
OCT II	± 8.81µm	± 9.68µm	± 9.49µm
Visante OCT	± 8.72 µm	± 9.92 µm	± 9.72 µm
Orbscan II	NA	NA	NA

Coefficient of Concordance (CCC) was also estimated between sessions for the Visante™ OCT, OCT II and Orbscan II ™ imaging systems. There was good concordance of total corneal thickness with the Visante™ OCT (0.90-0.99 at either center, temporal or nasal locations), the OCT II (0.97-0.99 at either

center, temporal or nasal locations) and the Orbscan II ™ (0.97-0.98 at either center, temporal or nasal locations) between sessions (Table 3-6).

Table 3-6: Correlation coefficient of concordance of total corneal thickness with Visante™ OCT, OCT II and Orbscan II ™.

CCC	Total corneal thickness		
Instruments	**Center**	**Temporal (3mm)**	**Nasal (3mm)**
OCT II	0.97	0.98	0.99
Visante OCT	0.99	0.90	0.97
Orbscan II	0.98	0.97	0.98

There is moderate concordance of epithelial thickness measurements for both Visante™ OCT and the OCT II with CCCs ranging between 0.52 and 0.81 respectively (Table 3-7).

Table 3-7: Correlation coefficient of concordance of epithelial thickness with Visante™ OCT and OCT II.

CCC	Epithelial Thickness		
Instruments	**Center**	**Temporal (3mm)**	**Nasal (3mm)**
OCT II	0.70	0.58	0.52
Visante OCT	0.81	0.53	0.54
Orbscan II	NA	NA	NA

The CCC was estimated between instruments comparing the measures of corneal and epithelial thickness from the Visante ™ OCT with the OCT II and for corneal thickness and epithelial thickness measures (Tables 3-8 & 3-9). There was good concordance of corneal thickness measures on day 2 (range 0.86-0.97 center, temporal and nasal cornea) comparing Visante™ OCT and the OCT II measurements and moderate concordance on day 1 (ranging between 0.66 to 0.68 at the center, nasal and temporal cornea).

Table 3-8: Correlation coefficient of concordance of total corneal thickness between instruments comparing the Visante ™ OCT and OCT II.

CCC	Total corneal thickness		
Visante OCT Vs OCT II	**Center**	**Temporal (3mm)**	**Nasal (3mm)**
Day 1	0.68	0.68	0.66
Day 2	0.97	0.88	0.86

Table 3-9: Correlation coefficient of concordance of epithelial thickness between instruments comparing the Visante ™ OCT and OCT II.

CCC	Epithelial Thickness		
Visante OCT Vs OCT II	**Center**	**Temporal (3mm)**	**Nasal (3mm)**
Day 1	0.54	0.75	0.53
Day 2	0.34	0.54	0.57

CCC's were also estimated from corneal thickness measures obtained using the Visante ™ OCT and the Orbscan II ™ (Table 3-10). Measures were moderately concordant on either day 1 or day 2 (ranging between 0.55-0.78 center, nasal and temporal cornea). Visante™ OCT and the OCT II epithelium thickness measures also demonstrated moderate concordance on either day 1 or day 2 (range; 0.53-0.75 center, nasal and temporal cornea).

Table 3-10: Correlation coefficient of concordance of total corneal thickness between instruments comparing the Visante ™ OCT and Orbscan.

CCC	Total corneal thickness		
Visante OCT Vs Orbscan	**Center**	**Temporal (3mm)**	**Nasal (3mm)**
Day 1	0.59	0.59	0.73
Day 2	0.67	0.55	0.78

In summary, the CCC's revealed good agreement between measures of corneal and epithelial thickness within all the three instruments compared to between the instruments where the CCC was moderately concordant.

Agreement between the measurements of the three instruments was also examined with Bland-Altman plots and limits of agreement (LOA) were calculated.[26] These plots of the difference between measures on the y-axis versus the averages of the corneal or epithelial thickness measures from the Visante ™ OCT, OCT II and Orbscan II ™ on the x-axis on different days are shown from Figures 3-1 to 3-18.

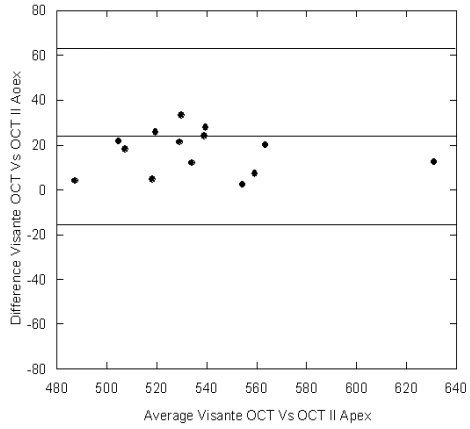

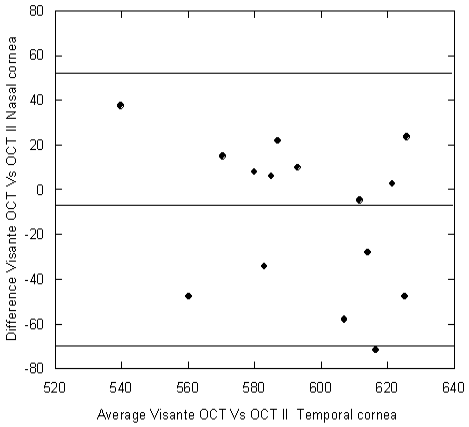

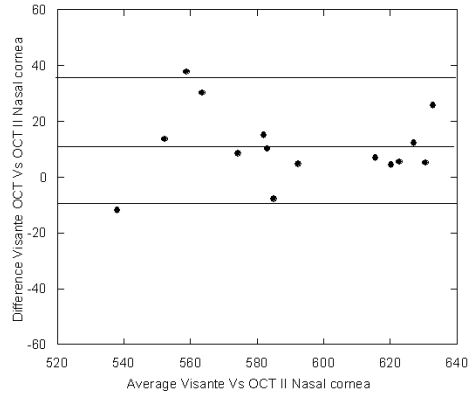

Figure 3-1: Bland and Altman graph of Visante ™ OCT vs OCT II at the center (corneal thickness day 1).

Figure 3-2: Bland and Altman graph of Visante ™ OCT vs OCT II at the nasal cornea (corneal thickness day 1).

Figure 3-3 Bland and Altman graph of Visante ™ OCT vs OCT II at the temporal cornea (corneal thickness day 1).

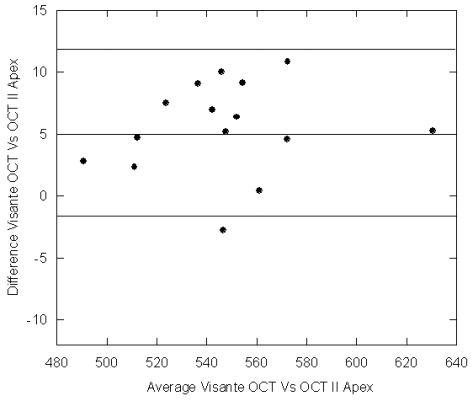

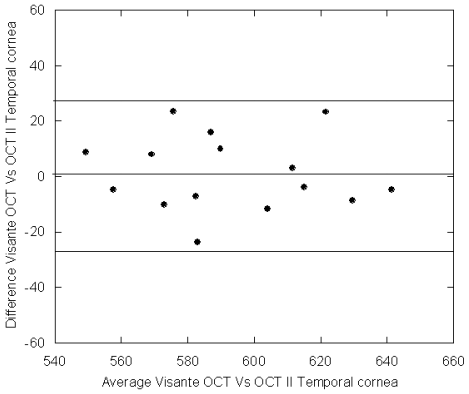

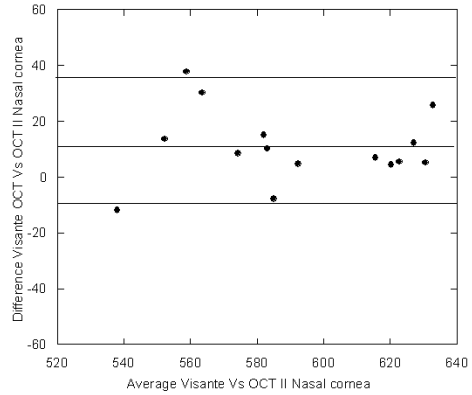

Figure 3-4: Bland and Altman graph of Visante ™ OCT vs OCT II at the center (corneal thickness day 2).

Figure 3-5: Bland and Altman graph of Visante ™ OCT vs OCT II at the nasal cornea (corneal thickness day 2).

Figure 3-6: Bland and Altman graph of Visante ™ OCT vs OCT II at the temporal cornea (corneal thickness day 2).

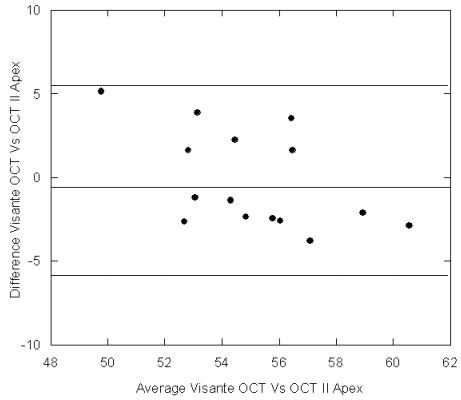

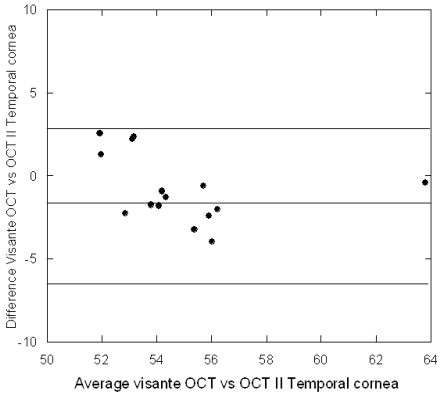

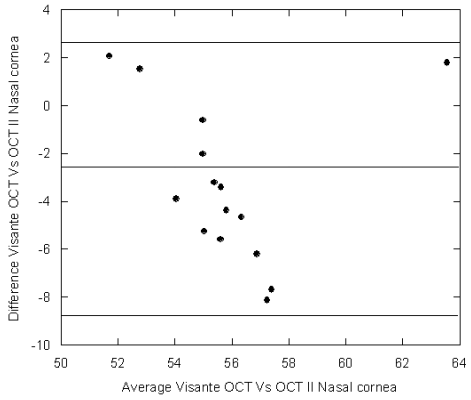

Figure 3-7: Bland and Altman graph of Visante ™ OCT vs OCT II at the center (epithelial thickness day 1).

Figure 3-8: Bland and Altman graph of Visante ™ OCT vs OCT II at the nasal cornea (epithelial thickness day 1).

Figure 3-9: Bland and Altman graph of Visante ™ OCT vs OCT II at the temporal cornea (epithelial thickness day 1).

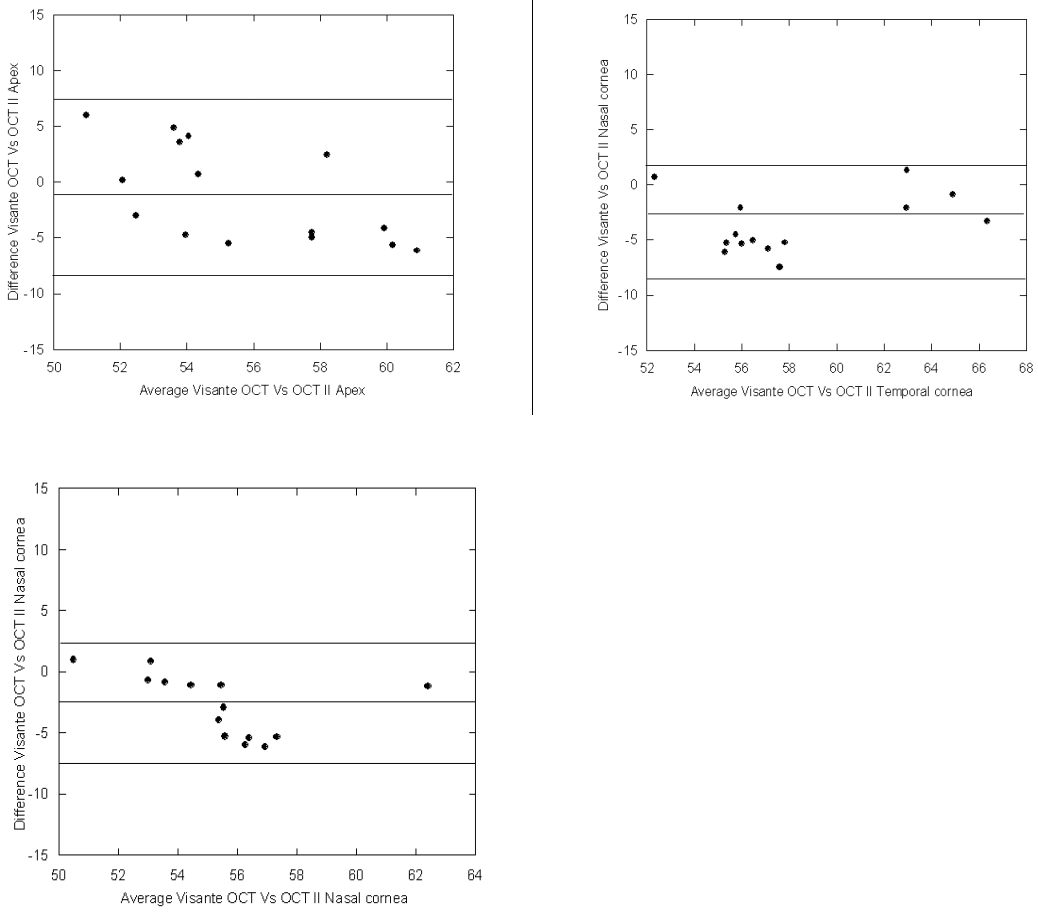

Figure 3-10: Bland and Altman graph of Visante ™ OCT vs OCT II at the center (epithelial thickness day 2).

Figure 3-11: Bland and Altman graph of Visante ™ OCT vs OCT II at the nasal cornea (epithelial thickness day 2).

Figure 3-12: Bland and Altman graph of Visante ™ OCT vs OCT II at the temporal cornea (epithelial thickness day 2).

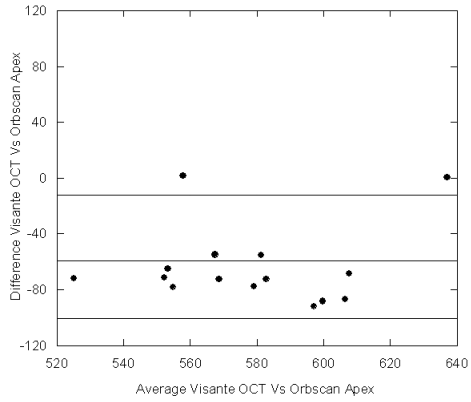

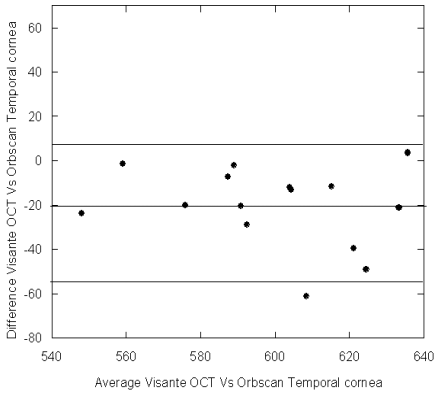

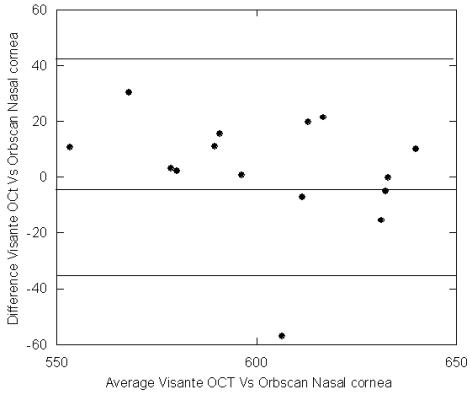

Figure 3-13: Bland and Altman graph of Visante ™ OCT vs Orbscan at the center (corneal thickness day 1).

Figure 3-14: Bland and Altman graph of Visante ™ OCT vs Orbscan at the nasal cornea (corneal thickness day 1).

Figure 3-15: Bland and Altman graph of Visante ™ OCT vs Orbscan at the temporal cornea (corneal thickness day 1).

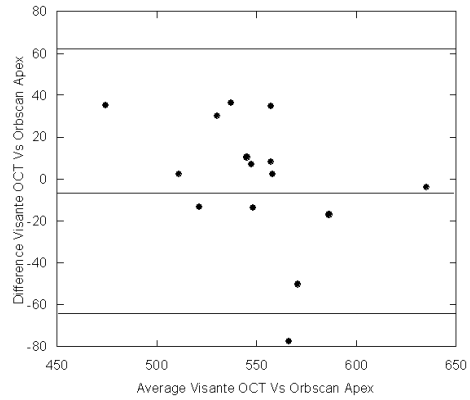

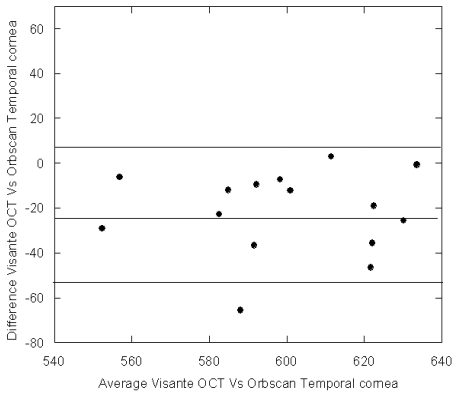

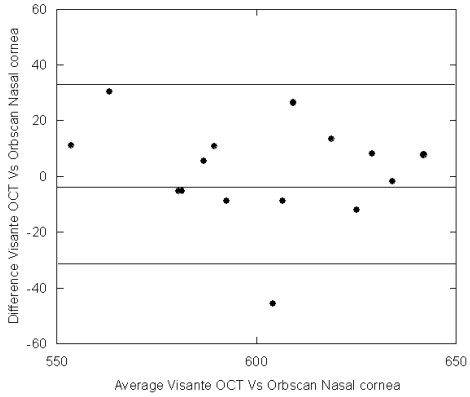

Figure 3-16: Bland and Altman graph of Visante ™ OCT vs Orbscan at the center (corneal thickness day 2).

Figure 3-17: Bland and Altman graph of Visante ™ OCT vs Orbscan at the nasal cornea (corneal thickness day 2).

Figure 3-18: Bland and Altman graph of Visante ™ OCT vs Orbscan at the temporal cornea (corneal thickness day 2).

3.5 Discussion

Ultrasound pachymetry has been the gold standard for central corneal thickness measurement because of its established reliability, but no corneal contact and high speed anterior segment OCT provides a promising alternative. Izatt et al. [28] were the first to show the potential for corneal imaging and they demonstrated that epithelium and endothelium layers could be distinguished in an OCT image. Bechmann et al. and Wong et al. have reported that ultrasound pachymetry overestimates corneal thickness by approximately 49 microns and 31.9 microns respectively. [14;29] Commercial anterior segment OCT's have been most commonly used for examining corneal and epithelial thickness,[30] diurnal variation in corneal thickness,[20] measurement of tear film thickness, [31]measurement of corneal thickness pre and post refractive surgery [32] and also to assess corneal morphological effects of corneal edema.[23]

In this study we compared repeatability of two commercially available TD-OCT (Visante™ OCT and the adapted Zeiss–Humphrey retinal OCT II) and examined the measures of total corneal and epithelial thickness across central, temporal and nasal locations on the cornea. Repeatability of Orbscan II ™ was also examined for the total corneal thickness at the same three locations on the cornea. The average corneal thickness for day 1 and day 2 at the center of the cornea was 536±27 µm, the nasal and temporal corneas were 554±26 µm and 565 ±26 µm respectively using the Visante™ OCT. When these results are compared to the Orbscan II ™, there is a significant difference with Orbscan producing higher average corneal thickness measurements of 609±29µm, 609±27µm and 600±29µm for the central, nasal and temporal corneas respectively. The nasal measurement of corneal thickness with the OCT II was higher by 45 microns compared to the Visante™ OCT. The average CCT with the OCT II at the center was 520±25µm, which is very similar to the results obtained by Muscat et al. and Bechmann et al. of 526±28µm and 530±32µm respectively.[13;29]

Muscat et al. evaluated the repeatability of CCT using Humphrey-Zeiss OCT found an CCC of 0.998 which is comparable to the results of my study.[13] The repeatability of the central corneal thickness was similar for all the three instruments although the Visante™ OCT produced the highest CCC of 0.99, similar to the results in other recent studies with reported CCC's of 0.962[33] and 0.998.[34] The range of corneal thickness CCC's for all the three instruments was 0.97 to 0.99. The nasal and temporal locations measured with both the instruments showed less repeatability compared to the center with CCC ranging from 0.52 to 0.58. The epithelial thickness measures showed poor repeatability with Visante™ OCT and OCT II with CCC ranging from 0.34 to 0.75.

Peripheral corneal pachymetry measurements were difficult to repeat. Some of the previous studies have also shown similar results; Li et al. reported thinner and less reliable measurements in the peripheral zone of 7mm diameter or greater.[35] Sin et al. have also reported central corneal epithelial thickness repeatability to be much lower compared to the corneal thickness measure repeatability and have emphasised the importance of averaging images and the requirement of increasing sample size to potentially overcome poor repetability.[30]

The ***within*** device repeatability was generally good, excluding some epithelial measures. There was poorer concordance ***between*** the instruments compared to within instrument test-retest. The highest CCC of 0.97 was between the Visante™ OCT and the OCT II for measures of central corneal thickness on day 2. The range of between-device central corneal thickness CCC's was 0.66 to 0.97. The epithelial measures were less repeatable, ranging from 0.53 to 0.57, similar to the report by Muscat et al.[13]

In this chapter I have reported that the Visante™ OCT has the most repeatable measurements of corneal and epithelial thickness, with COR's approximately ranging from 7.71 µm to 9.92 µm. Similarly, Muscat et al.[13] have shown a COR of 11 µm averaged for 6 radial scans and COR of 10 µm for central corneal thickness [30].

The Orbscan II ™ corneal thickness measures were significantly higher ($p<0.05$) compared to the Visante™ OCT and OCT II but their repeatability was similar to the other three instruments. The COR's I estimated using the measures from the Orbscan II ™ were ± 11 µm , similar to that of apical measures reported by Marsich and Bullimore.[36]

An important reason for performing the repeatability studies is to get insight about the measurements themselves. My results were that the test-retest and between-device measurements were generally consistent and that the within-device Visante™ OCT repeatability was the best. On the other hand the repeatability of the epithelial thickness measurements was poorer; this variability can be minimized by averaging multiple images. This was also suggested by Sander et al. who showed that averaging OCT images enables recovery of detailed structural information. [37] My results are similar to this and also to those reported by Sin et al. Because clinicians typically do not collect multiple images and average them, they perhaps could be a little more careful when interpreting these measurements.

Chapter 4

Lens edge artefact occurring when imaged with an ultra-high resolution Optical coherence tomographer

4.1 Introduction

The lens edge has been identified as a possible source of contact lens discomfort. Conjunctival staining, indentation and conjunctival flaps outside the limbus, which are associated with the lens edge, are examples of complications observed with contact lenses.[1-3] Although the slit-lamp examination perhaps is the standard technique for contact lens examination and is irreplaceable in the assessment of contact lens fit, by itself it gives limited information about the relationship between the surface of the eye and the posterior surface of the contact lens. Partly for this reason, fluorescein pattern analysis was introduced and became part of the routine procedure in contact lens practice. However, recent studies have shown that slit-lamp examination with fluorescein may not always be sufficiently sensitive.[4;5] Better assessment of the fitting relationship between a contact lens and the ocular surface could be helpful to achieve an optimal fit thus, to improve success rates.[6] This has been demonstrated especially in eyes with astigmatism [7] and in ortho-keratology.[8-10]

Optical coherence tomography (OCT) is an imaging method that allows for non-invasive imaging of the morphology of the biological tissue with micrometer scale resolution.[11-14] Over the past two decades OCT has found numerous medical applications, and in particular in ophthalmology for non-invasive, imaging of the human retina [15-18] and the anterior eye chamber.[18-22]

Recent advances in laser and infrared camera technologies have led to the development of spectral domain OCT (SD-OCT)[23-26] and swept source OCT (SS-OCT)[20;27-29] which offer significantly improved sensitivity

and reduced image acquisition time as compared to Time domain OCT (TD-OCT). The faster image acquisition speed results in OCT tomograms free from distortions that are typically observed in TD-OCT images and are caused by the motion of the object.[30;31]

In the present study, we demonstrate the application of a research grade high speed, ultra high resolution optical coherence tomography (UHR-OCT) system, operating in the 1060nm spectral range that can acquire high resolution images of the contact lens edge on a continuous surface and on human conjunctival tissue. This UHR-OCT system provides approximately 3 micron axial and 15 micron lateral resolution in the corneal tissue. Imaging the anterior segment with the 1060nm spectral range has major advantages over the similar systems operating at other 800nm and 1300nm – it provides similar resolution to 800nm OCT anterior segment systems, without the necessity for hardware or software dispersion compensation.[32]

4.2 Methods

4.2.1 Imaging

The UHR-OCT system used in this study is based on a compact fibre optic Michelson interferometer, connected to a super luminescent diode (SLD; Superlum Ltd.; λc =1020 nm, Delta λ=110nm) (Figure 4-1). The reference arm consists of an achromatic collimator (Edmund Optics), a custom tuneable dispersion unit based on a pair of BK7 glass prisms, a focusing achromat lens and an Ag mirror mounted on a translation stage. The corneal imaging probe is comprised of 3 achromat doublet lenses (Edmund Optics, f_1 = 20mm, $f_2 = f_3$ = 35mm) and a pair of galvanometric scanners (Cambridge Technologies). The interference signal is detected with a custom, high-performance spectrometer (P&P Optica, Inc.), interfaced to a 1024 pixel array InGaAs camera (SUI, Goodrich Corp.) with 47 kHz readout rate. The UHR-OCT system provides 3.2 micron axial and 15 micron lateral resolution in biological tissue. All tomograms were processed with Matlab (Mathworks).

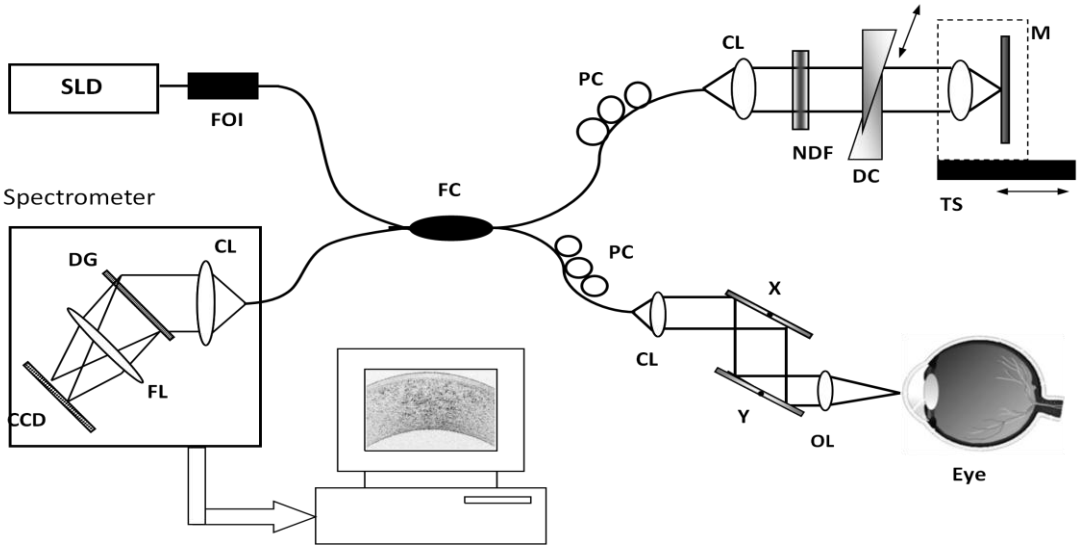

Figure 4-1: A schematic diagram of the UHR-OCT system.

CCD – InGaAs camera, CL – collimator lens, DC – dispersion compensation unit, DG - diffraction Grating, FL- focusing lens, OL - ocular lens, PC - polarization controllers, SLD – superluminescent diode, TS – computerized translation stage, X,Y – galvanometric scanning mirrors.

Two dimensional tomograms (2-D) of a selection of marketed silicone hydrogel and hydrogel lenses (refractive indices ranging from 1.41 to 1.51) were acquired using the UHR-OCT. Images were acquired after placing the lenses concave side down on a glass spherical reference sphere (n=1.52), and on a rigid contact lens manufactured with a refractive index similar to that of the human cornea (n=1.376). The contact lenses used in the study were J&J: 1-day Acuvue Moist™, Acuvue Advance™, Ciba Vision: Air Optix Night and Day™, and Bausch and Lomb: PureVision™. All lenses imaged were of the same power (-3.00 D) and with similar base curves. Images of the glass spherical reference sphere and the custom made rigid contact lens were acquired without the lens for comparison purposes. All contact lens images were acquired at room temperature and within ~1minute after removal from the original package to minimize distortions in the images resulting from dehydration of the lenses. A total of 5 cross-sectional

OCT images were acquired from each of the soft contact lenses while the lenses were placed on the glass sphere and on the contact lens.

OCT images were acquired after 5 minutes to adaption to the lens. During the imaging procedure, the imaging probe was initially aligned with the corneal center. Subsequently, the position if the imaging probe was adjusted laterally to acquire images of the edge of the lenses. Figures 4-2 and 4-3 show the lens edge imaged on the glass surface and human conjunctiva respectively.

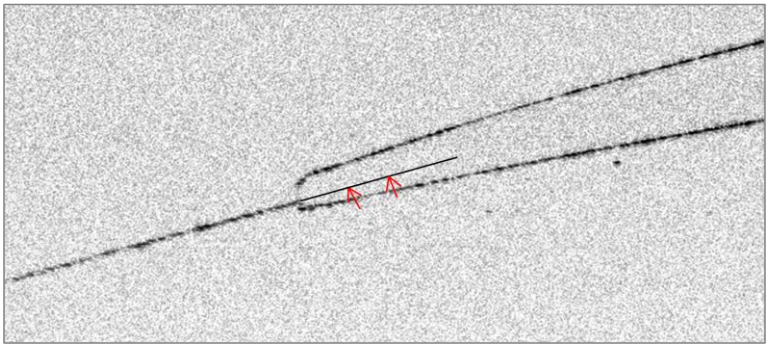

Figure 4-2: Soft contact lens edge on a continuous glass surface.

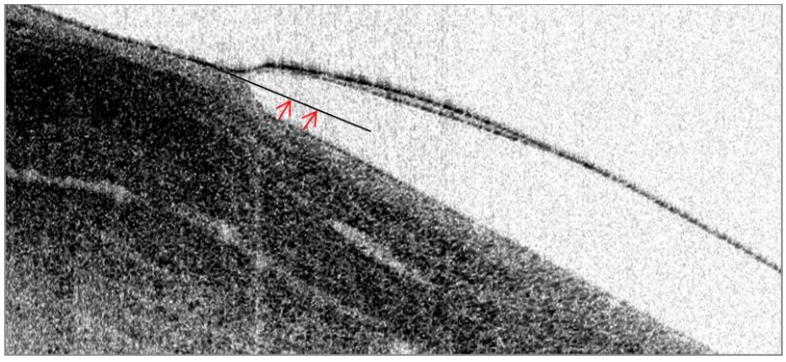

Figure 4-3: Soft contact lens edge on human conjunctival tissue.

In order to derive the estimates of displacement illustrated in figures 4-2 and 4-3 the following method was used using the constants defined in figure 4-1.

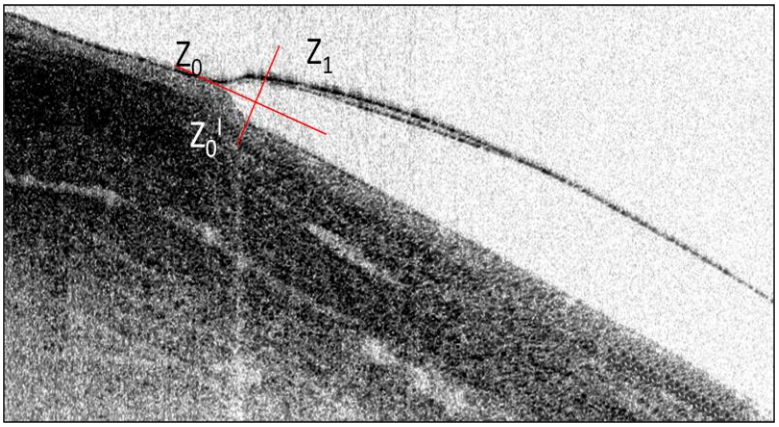

Figure 4-4: Measurement method- A (2-D) UHR-OCT tomogram (1000 A-scans x 512 pixels) Bausch & Lomb Pure Vision contact lens (-3.00D ; n= 1.426) on conjunctival tissue.

Physical thickness of the lens edge is $Z_1 - Z_0$ equation 1

Optical thickness of the contact lens is $Z_1 - Z_0^I$ equation 2

and an increase in the path length difference is $Z_0 - Z_0^1$ equation 3

Optical thickness = physical thickness x refractive index (n).

Or $Z_1-Z_0^1=Z_1-Z_0 \times n$ equation 4.

And by rearrangement of one can obtain;

$$n = \frac{Z_1-Z_0^1}{Z_1-Z_0}$$

And we can obtain Physical thickness= Z_1-Z_0 / n

The optical displacement was measured as the difference between the optical thickness and the physical thickness in microns using Image J software.

4.3 Results

Displacement of a continuous surface was observed when the lenses were imaged on the glass reference sphere and also on the rigid contact lenses.

Figures 4-5, 4-6, 4-7, 4-8 are (2-D) UHR-OCT images of the soft contact lens edges on the glass reference sphere (n=1.52).

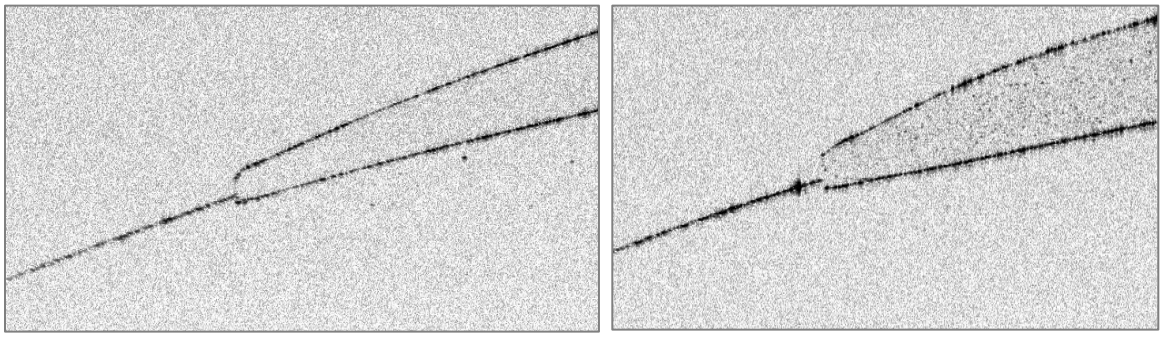

Figure 4-5: (2-D) UHR-OCT tomogram of Air Optix (-3.00D; n=1.42).

Figure 4-6: (2-D) UHR-OCT tomogram of PureVision (-3.00; n=1.426).

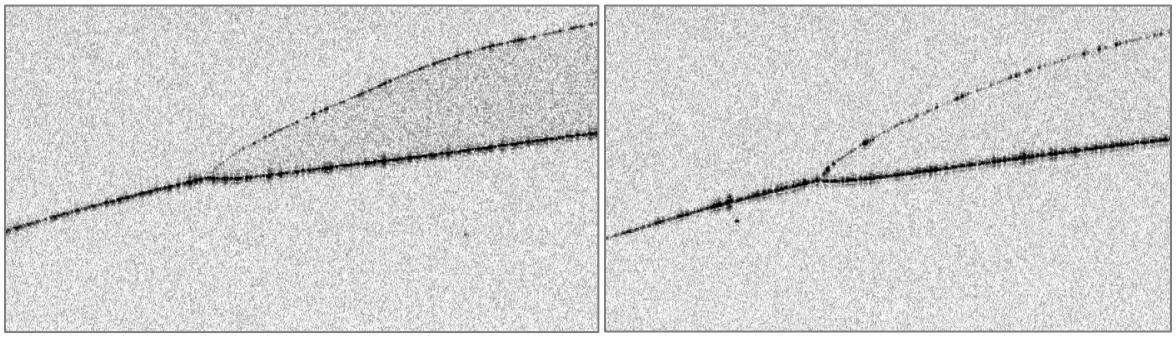

Figure 4-7: (2-D) UHR-OCT tomogram of 1-day Acuvue Moist (-3.00D; n=1.509).

Figure 4-8: (2-D) UHR-OCT tomogram of an Acuvue Advance (-3.00D; n=1.405).

Figures 4-9, 4-10, 4-11, 4-12 are images of soft contact lens edges on rigid contact lenses with refractive index of the cornea (n=1.376).

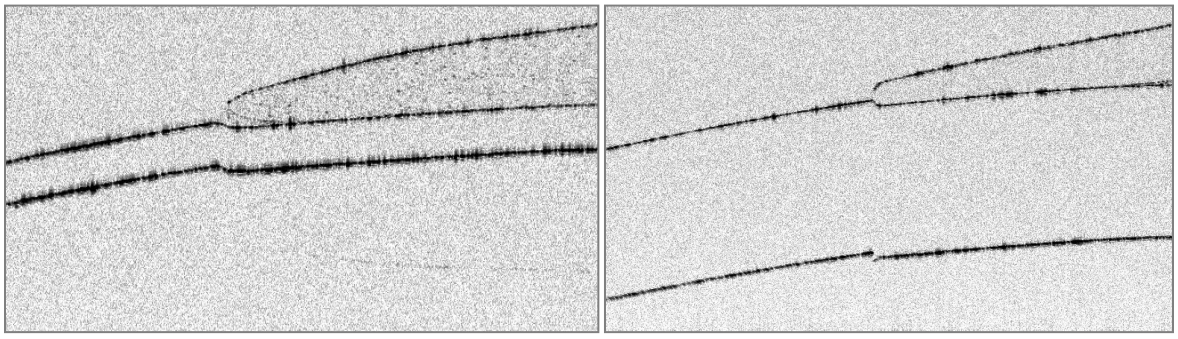

Figure 4-9: (2-D) UHR-OCT tomogram of Air Optix (-3.00D; n= 1.42).

Figure 4-10: (2-D) UHR-OCT tomogram of PureVision (-3.00D; n= 1.426).

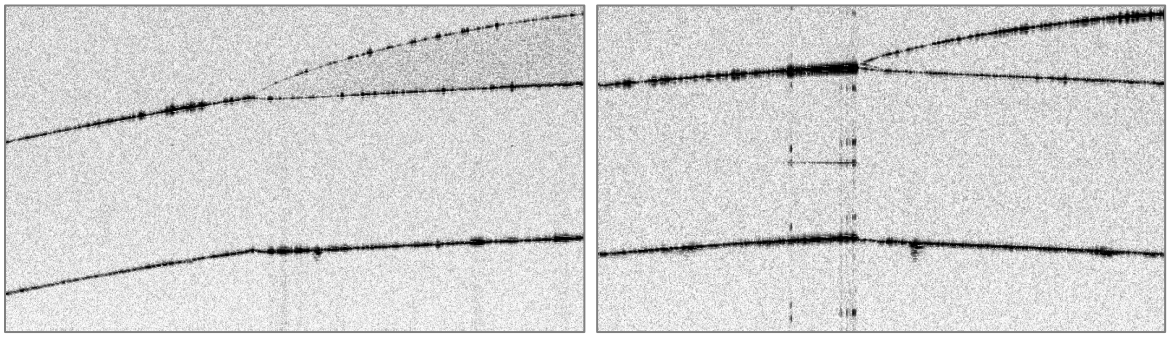

Figure 4-11: (2-D) UHR-OCT tomogram of a 1-day Acuvue Moist (-3.00D; n= 1.42).

Figure 4-12: (2-D) UHR-OCT tomogram of a Acuvue Advance (-3.00D; n=1.405).

Representative images of contact lens edges on the conjunctiva are shown in Figures 4-13 to 4-16.

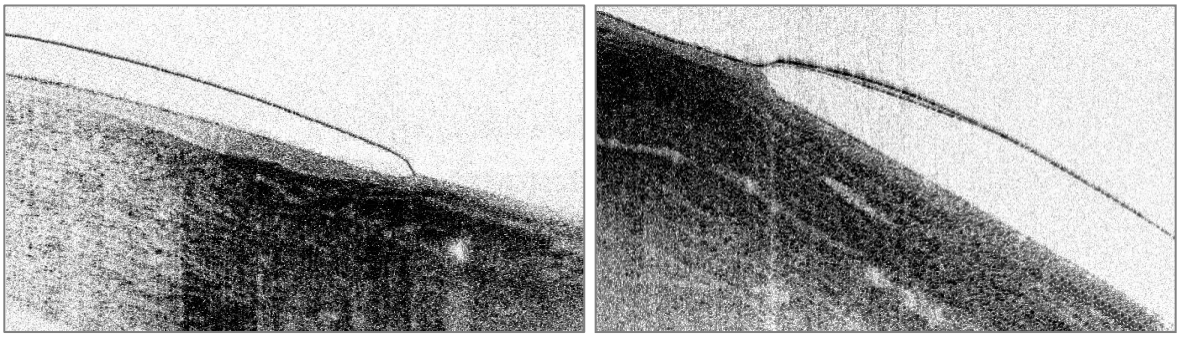

Figure 4-13: (2-D) UHR-OCT tomogram of Air Optix (-3.00D; n= 1.42).

Figure 4-14: (2-D) UHR-OCT tomogram of PureVision (-3.00D; n= 1.426).

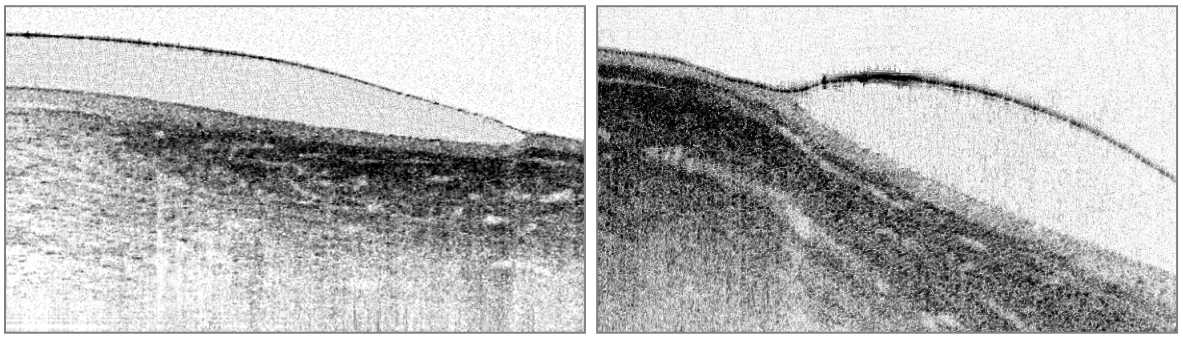

Figure 4-15: (2-D) UHR-OCT tomogram of an 1-day Acuvue Moist (-3.00D; n= 1.42).

Figure 4-16: (2-D) UHR-OCT tomogram of an Acuvue Advance (-3.00D; n=1.405).

In each of the figures above it appears that the lens is indenting the surface on which it is placed. This perhaps makes sense for the conjunctiva because of the softness of the tissue but is obviously impossible when the substrate on which the lens is positioned is glass or plastic. Therefore, this discontinuation present in the images on the continuous substrate (glass or plastic) is an artefact.

Table 4-1 shows the displacement artefact of the contact lens edge on the glass spherical reference sphere (n=1.52) derived from images using ImageJ. A t-test showed a significance difference between measured (physical) and calculated (optical) results ($p<0.05$).

Table 4-1: Displacement measurements on a glass reference sphere (n=1.52)

Lens type	Power	Refractive Index	Measured (µm)	Calculated (µm)	Difference (Optical displacement)
1-day Acuvue Moist	-3.00 D	1.509	30.93 µm	24.79 µm	6.14±0.06 µm
Air Optix Night and day	-3.00D	1.405	44.95 µm	32.96 µm	11.99±0.18 µm
Acuvue Advance	-3.00D	1.426	25.83 µm	20.44 µm	5.39±0.06 µm
Purevision	-3.00 D	1.42	44.33 µm	38.05 µm	6.28±0.17 µm

Table 4-2 shows the displacement artefact of the contact lens edge on rigid contact lenses with a refractive index of the cornea (n=1.376). A t-test showed a significance difference between measured (physical) and calculated (optical) results ($p<0.05$).

Table 4-2: Displacement measurements on rigid contact lens with a refractive index of the cornea (n=1.376).

Lens type	Power	Refractive Index	Measured (µm)	Calculated (µm)	Difference (Optical displacement)
1-day Acuvue Moist	-3.00 D	1.509	31.00 µm	24.10 µm	6.9±0.14 µm
Air Optix Night and day	-3.00D	1.405	51.66 µm	41.94 µm	9.72±0.12 µm
Acuvue Advance	-3.00D	1.426	35.13 µm	29.4 µm	5.73±0.10 µm
Purevision	-3.00 D	1.42	47.53 µm	42.02	5.51±0.03 µm

Table 4-3 shows the displacement measured conjunctival tissue at the edge of the lens. The t-test showed a significance difference between measured (physical) and calculated (optical) results ($p<0.05$).

Table 4-3: Displacement measurements on human conjunctival tissue

Lens type	Power	Refractive Index	Measured (µm)	Calculated (µm)	Difference (Optical displacement)
1-day Acuvue Moist	-3.00 D	1.509	60.47 µm	44.13 µm	16.34 ± 0.31µm
Air Optix Night and day	-3.00D	1.405	45.42 µm	38.4 µm	7±0.86 µm
Acuvue Advance	-3.00D	1.426	51.17 µm	33.06 µm	17.4±0.22 µm
Purevision	-3.00 D	1.42	47.70 µm	32.54 µm	15.16±0.07 µm

The range of displacement when measured with the glass reference sphere ranged from 5.39±0.06 µm with Acuvue Advance to 11.99±0.18 µm with Air Optix Night and day.

The range of displacement when measured on a rigid contact lens with a refractive index of the human cornea (1.376) ranged from 5.51±0.03 µm for Pure Vision to 9.72±0.12 µm with Air Optix Night and day. The displacement of the conjunctiva ranged from 7.0±0.86 µm for the Air Optix Night and Day™ to 17.4±0.22 µm for the Acuvue Advance™ contact lenses.

4.4 Discussion

UHR-OCT technology has great clinical potential since it allows non-contact *in vivo* examination of the anterior segment of the eye, may be a useful tool in aiding in contact lens fitting and can provide insight into complications arising from contact lens wear.[33;34]

This study has shown that clinicians might be more careful at interpreting any conjunctival indentation reported to be caused when imaged with optical imagers.

I believe that the conjunctival displacement and/or compression observed with the edges of the contact lens when imaged with the UHR-OCT is partly an artefact of the OCT imaging systems where a continuous surface appears displaced when the refractive index (n) of the leading medium changes from air to the edge of the contact lens. The displacement was not just observed when the contact lens edges were imaged on the human conjunctival tissue but especially when the contact lenses were imaged on continuous surfaces.

The artefact is visible when imaging the lenses and can be quantified by subtracting the baseline curve of the glass plate (without the contact lens) from the images with the lenses. The size of the artefact is proportional to (n x d) where n is the refractive index and d is the physical thickness. This displacement artefact of the surface (due to the incident medium refractive index difference) not only affects the measurements with contact lenses but also could affect, for example, tear film volume measurement using the OCT devices. Morphometric characteristics of tissue are not always simple attributes of the tissue alone, but are also affected by the imaging device.

In addition, of course, we do not actually know that the nominal lens refractive index is correct near the lens edge and secondly, the thickness of the lens is also measured with error (the lens does not have the same RI as the tissue RI assumed by the OCT). These two conspire to making the actual artefact very difficult to actually quantify *in vivo*.

In summary, this study has demonstrated that when contact lenses are imaged in-situ using UHR-OCT the conjunctival tissue was optically displaced beneath the edge of the contact lens and some of this displacement is perhaps an artefact of OCT (and other optical) imagers where a continuous surface is imaged discontinuous. This displacement is a property of the thickness and refractive index of the contact lens edges.

Chapter 5

Relationship between lens fitting characteristics, corneal and conjunctival response and comfort

5.1 Introduction

Soft contact lenses are preferred by both practitioners and wearers because of the relative ease of fitting, patient comfort and quick adaption. Sub-optimal fits can lead to discomfort and potentially physiological changes and subsequent discontinuation.[1-3] Soft contact lens fitting involves the selection of the most appropriate lens materials, dimensions and wearing modality to match the ocular characteristics and patient needs, whilst giving the best fit and visual acuity.[4;5]

Safety and comfort of the contact lens fitting is determined on the eye. The performance is judged using both static and dynamic criteria, including lens centration, corneal coverage and lens movement in response to blinking. The factors that influence lens performance include corneal topography, lens base curve and peripheral curve radius, lens diameter, edge design, lens material and modulus and lens dehydration.[6-10]

Effects of contact lenses on the anterior surface of the eye are subjective discomfort, dryness, etc.[11-15] These symptoms may ultimately lead to either temporary or permanent discontinuation of contact lens wear.[16] Up to fifty percent of hydrogel lens wearers report symptoms of dryness [14] and while several strategies have been employed to reduce these symptoms, for example comfort drops,[17;18] interchanging material characteristics etc, the actual symptoms have not been thoroughly investigated.

Assessment of subjective discomfort relating to contact lens wear is generally made using psychophysical methods such as visual analogue scales.[19] Objective measures of dry eye are usually based on the Schirmer test or phenol red thread test, tear break up time and biomicroscopy.[20-22]

Tear exchange has been hypothesised to play an important role in reducing complications associated with extended wear of soft contact lenses and it is not obvious which soft lens variables have the greatest influence on tear exchange.[23] Factors may include the diameter, base curve radius or the peripheral lens geometry and all of these can have a substantial impact on the tear exchange.[23] Young's modulus of elasticity has been shown to have an effect on lens performance [24]; a material with a lower modulus will offer improved comfort in comparison to a stiffer material of higher modulus[25] however, there would be greater lens flexure on the cornea especially toric corneas.[25] With the advent of silicone hydrogel lenses, attention has started to focus on the mechanical properties and the ocular complications that can arise as a result of stiffer, less flexible materials.[26;27] When silicone hydrogel contact lenses are worn on an extended wear basis there are several complications that are hypothesised to arise as a result of mechanical irritation, such as superior epithelial arcuate lesions, contact lens related papillary conjunctivitis and mucin ball production.[28]

There has been a great deal of research focusing on the impact of soft contact lens on the cornea such as corneal neovascularisation,[29] corneal staining,[30] topographical changes, microbial keratitis [31]etc. Due to the proximity of the upper eyelid to the superior cornea, additional physiological changes might perhaps be expected in this region dependent on the lens material, lens design and eyelid pressure. Certainly, eyelid pressure has been reported as a factor in corneal changes due to downward gaze angle,[32] eye movements[32] and different visual tasks including reading, and computer work.[33] The superior eyelid has been associated with various complications with extended soft contact lens wear due to mechanical [28;34-36] and hypoxic stress[37-42] on the superior cornea and this is said to affect the risk of complications with soft contact lens wear. In terms of the hypoxic stress, Holden et al. [43] reported that wearing contact lenses on

an extended wear basis mimics prolonged eye closure; swelling of 12% overnight and 4% during the day was reported in subjects during continuous wear of hydrogel contact lenses. Studies have shown that immediately after retracting the upper eyelid the oxygen uptake of the cornea significantly increases compared to the central and inferior cornea. [44-46] Benjamin et al.[45] reported that the uptake in oxygen is reduced and reversed when exposing the entire cornea uniformly. Their results provide support to the view that superior cornea is perhaps chronically hypoxic[45]. Hypoxia and mechanical complications of lens wear affecting the superior cornea include super arcuate epithelial lesion, neovascularization, epithelial folds, limbal hyperemia, and conjunctival indentation.[28;39;47-49]

Silicone hydrogel contact lenses transmit more oxygen to the eye compared to the conventional hydrogel lenses and are supposed to lower the risk of hypoxia related complications. [50-52] Studies have reported improvement in general ocular health, including the cornea and conjunctival tissue, with silicone hydrogel lenses and hence these lenses have become the preferred lens for clinical fitting compared to the low oxygen permeable lenses (low Dk).[53-55] It has been reported that the risk of corneal infections and inflammatory reactions have been reduced with the silicone hydrogel wear. [54;56;57] However, there are conflicting reports suggesting that wearing these lenses is still associated with risk of infalmation.[49;58;59]

The main purpose of this study was to determine if we are able to predict end of the day comfort and dryness using clinical predictor variables. In addition, to examine the relationship between the soft contact lens fitting characteristics and clinical complications observed. The superior cornea and conjunctiva were examined to explore regional differences.

5.2 Objective

The main purpose of this study was to determine if we are able to predict end of the day discomfort and dryness using clinical predictive variables. The second purpose of the study was to determine if there was any relationship between lens fitting characteristics and clinical complications, especially to the superior

cornea and conjunctiva. All observations were made with a higher modulus (PureVision) and lower modulus (Acuvue Advance) silicone hydrogel contact lenses that were fitted steeper (AA 8.3, PV 8.3) and flatter on the eye (AA 8.7, PV 8.6).

5.3 Materials and Methods

5.3.1 Participants

Thirty participants (neophytes) were recruited. Study lenses were worn for two weeks on a daily wear basis for 8 to 10 hours per day. Neophytes were selected so that any physiological (or other) response to the experimental lenses would not be influenced by any previous contact lens wear. Those study participants who could not be fitted with all four designs of lenses were excluded from the study. The participants were recruited for the study using Centre for Contact Lens Research records with the use of an advertisement circulated on the University of Waterloo campus and local residential community. Eligibility was determined using the inclusion and exclusion criteria detailed below.

5.3.2 Inclusion and Exclusion criterion

A person was eligible for inclusion in the study if he/she:

1. Was a non contact lens wearer for at least 6 months
2. Was a spectacle wearer with the power range from -12.00 to +8.00 DS.
3. Was at least 17 years of age and has full legal capacity to volunteer.
4. Had read and signed an information consent letter.
5. Was willing and able to follow instructions and maintain the appointment schedule.
6. Had an ocular examination in the last two years.

A person was excluded from the study if he/she:

1. Had any ocular disease.

2. Had any systemic disease affecting ocular health.

3. Was using any systemic or topical medications that may affect ocular health.

4. Was known to be sensitive to the diagnostic pharmaceuticals to be used in the study.

5.3.3 Study lenses

The lenses used for the study were Purevision (8.3 and 8.6 base curve) and Acuvue Advance (8.3 and 8.7 base curve). Table 5.1 summarize the lens parameters.

Table 5.1 Lens parameters

	Acuvue Advance	**PureVision**
Manufacturer	Vistakon	Bausch & Lomb
Material	Galyfilcon A	Balafilcon A
FDA classification	I	III
Health Canada license #	67836	64120
Stiffness (g/mm^2)	43	110(150)
EWC (%)	47%	36%
Dk/t (-3.00D)	86	99
BOZR (mm)	8.40, 8.80	8.30, 8.60
Diameter (mm)	14.00	14.00
Spherical powers (D)	+8.00 to -12.00D	+6.00 to -10.00D

5.3.4 Study visits

There were two phases to the study. In phase one, subjects were randomly assigned to wear higher or lower modulus lens that was steep or flat for each eye. Thus different lenses were worn in each eye. In phase two, the other combinations of modulus and base curves were worn. The examiner was masked to the lens type worn in each eye. Figure 5-1 shows the study design flow chart.

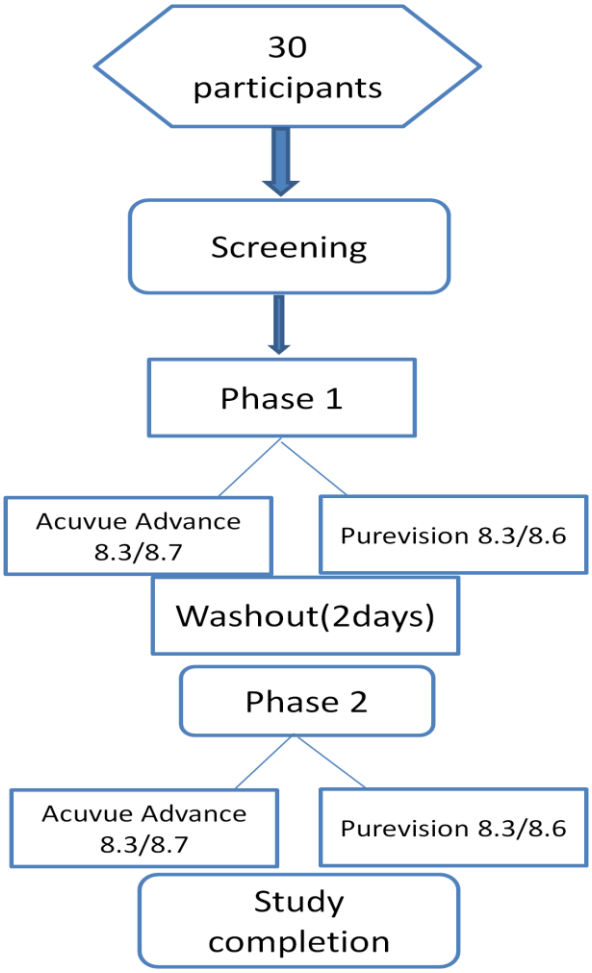

Figure 5-1: Study design flow chart

This study had a screening assessment and 4 measurement visits. The visits consisted of the following.

i. **Screening** (0.5 hours per visit)

   Subject eligibility for this study was determined.

ii. **Study visits at baseline for each phase** (2 hours per visit) – Randomization of lenses was assigned. Lenses were fitted and assessed. Visante™, Soft contact lens analyzer, Medmont E300™, RT-Vue OCT and RBC velocity (one eye) measurements were obtained.

iii. **Study visits at 2 week follow up for each phase** (2 hours per visit) – Randomization of lenses was assigned. Visante™, Soft contact lens analyzer, Medmont E300™, RT-Vue OCT and RBC velocity (one eye) measurements were obtained.

Participant eligibility was determined at a screening appointment according to the inclusion and exclusion criteria outlined below. Informed consent was obtained for all participants prior to their enrolment in the study. This protocol was approved by the Office of Research Ethics at the University of Waterloo. Informed consent was obtained from all participants prior to the study.

5.3.5 Visante™ optical coherence tomography (OCT)

A Visante™ OCT was used to obtain pachymetry scans of the cornea to measure corneal and epithelial thickness. The participants exam experience with the Visante™ OCT was brief and comfortable, with no direct contact by the instrument. Patients were instructed to look at an internal fixation target during scanning. Rough alignment was achieved by centering the cornea on the real-time video display. The scanned image was considered to be optimally aligned when the specular reflex, which is a high intensity reflection from the center of the front surface of the contact lens, was visible on the screen. They were also instructed to keep their eyes wide open during scanning and when necessary, the lids were gently held apart to ensure that the lids did not block the measurement of the central 10mm (diameter) of the cornea. Acceptable scans were judged to be of adequate quality based on the following criterion: good demarcation of the anterior and posterior boundaries of the cornea, and absence of artefacts. Three pachymetry scans per each eye were performed and averaged for corneal and epithelial thickness measures. The procedure took approximately 3 minutes per eye.

The Visante™ OCT software (Version 2.0) automatically processed the OCT image and calculated the corneal pachymetry map. The maps were divided into zones by octants (superior, superotemporal, temporal, inferotemporal, inferior, inferonasal, nasal, superonasal) and annular rings (2mm, 5mm, 7mm

and 10mm distance). The minimum, average, and maximum corneal thickness of each zone were listed in the pachymetry map and in the data table.

The Visante™ OCT software was also used to export the raw unaltered binary image file (*.bin) for analysis. Custom software was used to obtain all values of corneal and epithelial thickness. This was measured for all the study lenses at baseline and at the 2 week visit. The software imported the raw data from the instrument and then located the peak reflectance that corresponded to the front and rear corneal surfaces. From the curves fit to these surfaces (the shortest perpendicular distance to the posterior surface) were calculated for each pixel point along the front surface. This procedure was followed for each of the three images obtained and the average thickness from the three images was used for analysis.

Thickness was determined along 5 meridians (0, 45, 90, 135, and 180) degrees and for 7 points on each meridian. The points on each meridian were at the apex and at three measurement points on each side at 1mm intervals.

The Visante™ OCT comes equipped with the built-in callipers, which were used in the study to measure the sagittal depth at the diameter of the contact lens on a high resolution anterior segment image. Three images were acquired and the average sagittal depth of the three measurements was used in the analysis. Figure 5-2 represents the sagittal height measurements in the enhanced anterior segment mode using the Visante™ OCT.

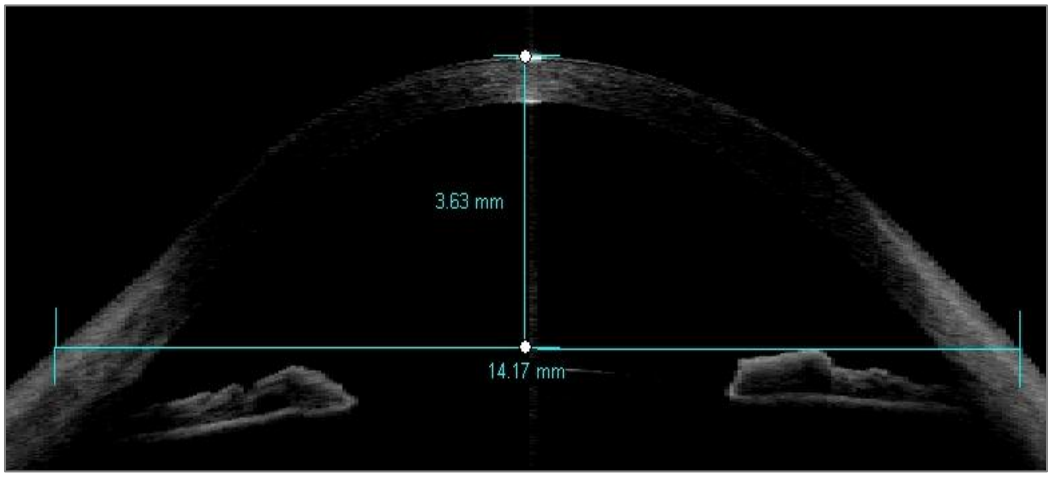

Figure 5-2 Sagittal height measurements with Visante™ OCT

5.3.6 Soft contact lens analyzer

A soft contact lens analyzer (Chiltern Optimec Limited, Malvern, UK) was used in this study to determine the dimensions of the soft contact lenses, including sagittal depth and diameter. Prior to the measurement, the saline compartment of the analyzer was filled with preserved saline. Using tweezers, the contact lenses were placed onto the mantle inside the saline compartment of the analyzer with the concave lens surface facing down. A letter-sized paper was placed on the lens projection screen and the image of the contact lens was projected onto the paper covering the screen. The contours of the magnified lens image (edges and lens apex) were manually sketched on the paper. Using a ruler, the magnified dimensions of diameter and sagittal depth were measured and converted into the actual size by considering the magnification factor. Three images were taken for the sagittal depth measurements over a period of three days and the results were averaged for further analysis. Figure 5-3 shows the soft contact lens analyzer.

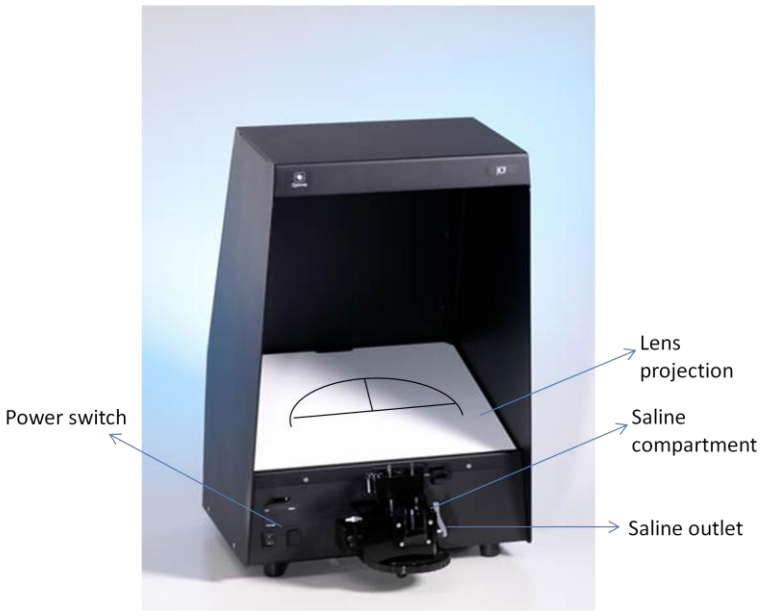

Figure 5-3 Soft contact lens analyzer

5.3.7 Medmont E300™ corneal topographer

The Medmont E300™ is a computerized video-keratometer, using Placido rings to map the surface of the human cornea. The instrument uses 32 rings with 9,600 measurements and 102,000 analyzed points, and the Medmont E300™ provides detailed topographic data over a wide range of the cornea by reflection. Participants were instructed to rest their forehead and chin firmly and look at the green fixation target. The target, along with the ring patterns of the Medmont E300™ defines the video-keratoscope axis.

Tangential curvature of the cornea at the baseline and 2week visit with the study lenses was measured at three corneal locations; 2mm, 4mm and 6mm zone from the apex (in 1mm steps) and along the five meridians (0, 45, 90, 135 and 180 degrees). Three repeated captures of corneal topography were done with the topographer and an average of the measurements was used for subsequent analysis.

5.3.8 Optovue™ optical coherence tomography

The Optovue™ (RT-Vue OCT) was used to examine the effect of the lens edge on the bulbar conjunctiva. During the examination the patient was instructed to look into the imaging aperture with the starburst fixation target against a dark background and a scan was performed.

5.3.9 Image analysis

The lens edge *in vivo* was observed using the RT-Vue OCT. Conjunctival epithelial tissue thickness was measured within 100 microns of lens edge using ImageJ software (Version 1.44p; National Institutes of Health, USA). The conjunctival epithelial thickness was measured at the lens edge and at three 1mm steps on either side as shown in Figure 5-4.

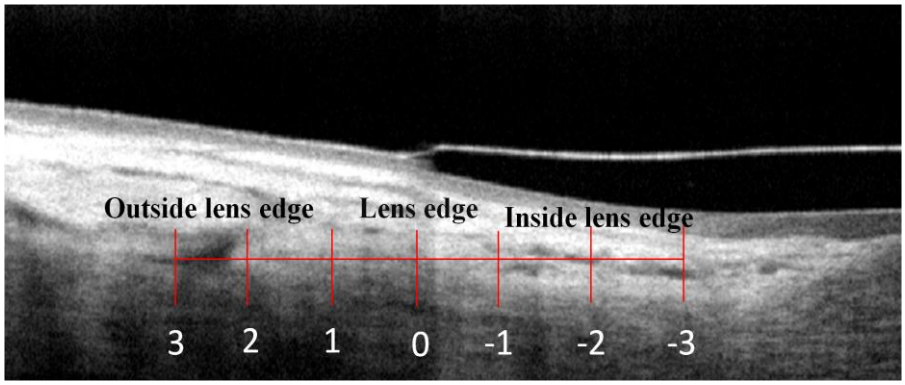

Figure 5-4 RT-Vue OCT image of a lens edge and the measurement increments at which epithelial thickness was obtained.

5.3.10 Red blood cell (RBC) velocity measurement

Videos of the conjunctival blood vessels were taken with the Hyper Micro Color CCD Camera (Plumnet Co. Ltd, Japan), which was mounted on a modified slit-lamp. The camera was connected to a PC via USB and AVI movies were recorded at a frame rate of 30fps, with a resolution of 720 x 480 pixels (24bits/pixel). In order to record the position of the observation and the illumination arms of the slit-lamp a protractor was designed and attached to the slit lamp base. At each subsequent visit the illumination arm was rotated precisely to the same position for recording the red blood cell velocity. One eye of each subject was randomly assigned for video measurement.

Videos were obtained for the temporal conjunctiva and vessel of interest (VOI) was identified. I recorded several minutes of video in order to ensure good quality and an ample number of frames. To ensure consistent results, the participant's head was restrained with a Velcro strip across the back of their head in addition to being supported with a chin rest. During video acquisition the participant was instructed to look at a target to their right or left depending on which eye was randomly assigned for video measurement.

The conjunctival vessels were digitally imaged with high enough magnification to clearly resolve movement of the blood within the vessel. For each video one vessel was selected and the cell shift along the vessel center line was evaluated using the semi automated analysis software (described in section 1.4.7) to estimate mean red blood cell velocity. A graticule was used for calibration. It was calculated that 1mm in the graticule corresponded to 331.5 pixels per mm. Flow rate was calculated using the formula:

flow = distance * mm/pixel * (frame rate)

5.3.11 Image analysis macro

A macro was written for Fiji (Version 1.46a; National Institutes of Health, USA) that extracted velocity from adjacent frames by examining shifts in peak intensity and shifts in groups of peaks. The following steps were taken to obtain RBC velocity measurements.

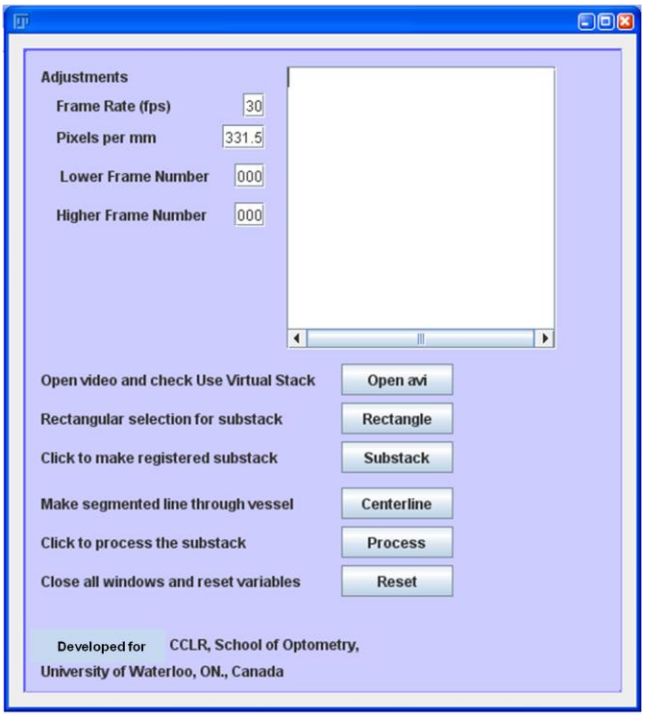

Figure 5-5 Interface of the macro for RBC velocity measurements

- The avi. Video file opened in the macro.
- A series of frames was selected by reviewing the video file and excluding any frames where there was obvious uneven illumination, blink and/or large eye movements. The remaining frames were examined to ensure that movement was visible along the VOI centerline. The frame numbers were entered into the macro (Figure 5-6) for analysis.
- The pixels per/mm (331.5) was entered. And a rectangular selection (Figure 5-5;"Rectangle" button) around the VOI was manually drawn (Figure 5-7).
- For the rectangular selection the consecutive frames were registered using "Rigid body" transformation in StackReg and a centerline was drawn for the VOI (Figure 5-8)
- The centerline was analyzed to obtain the RBC velocity estimates (Figure 5-9).

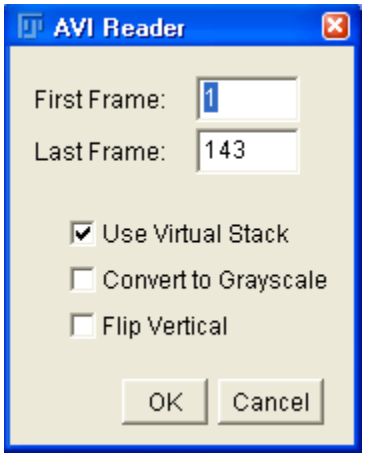

Figure 5-6 Tab to enter frames

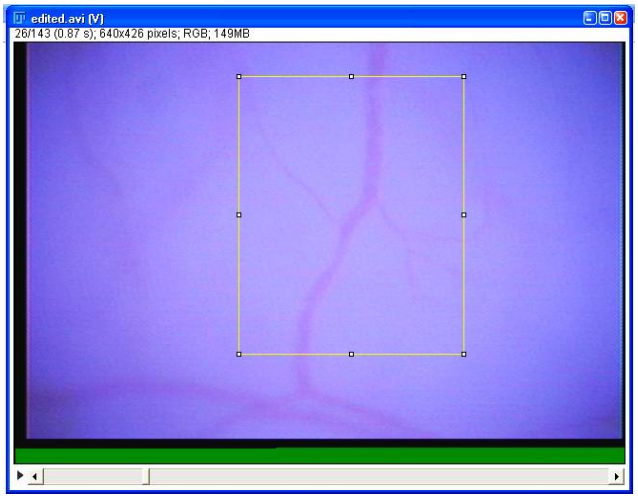

Figure 5-7 Rectangular isolation of region of interest

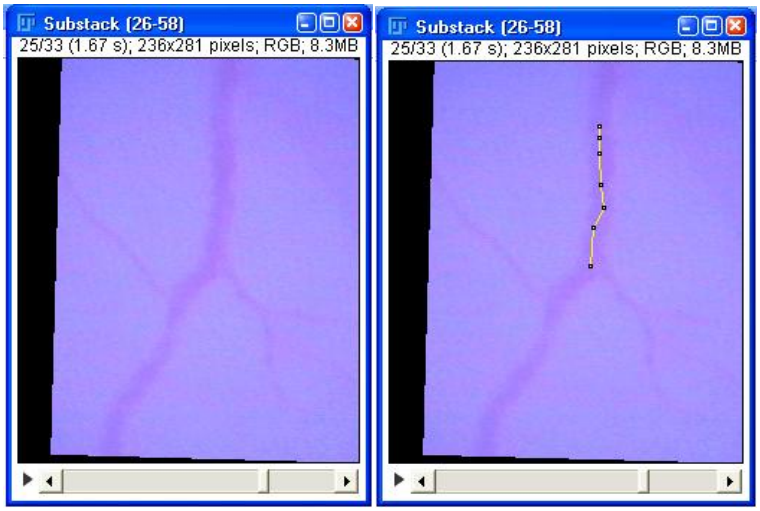

Figure 5-8 Substack registration using StackReg (left image) and centerline through vessel of interest (right image).

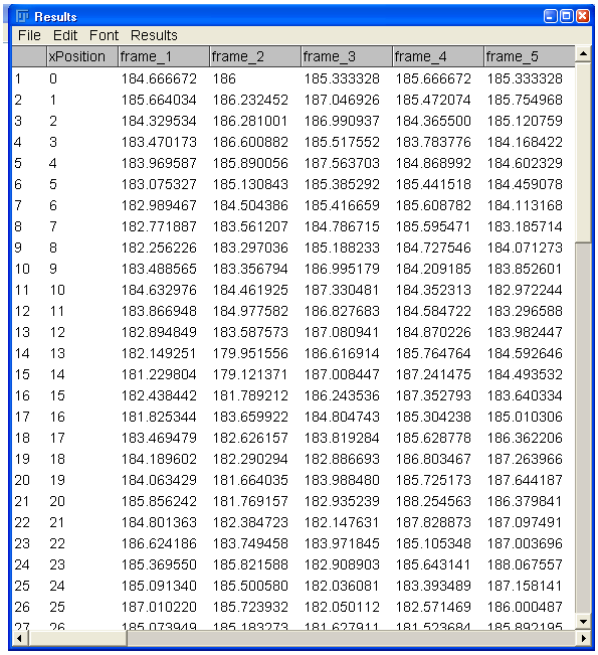

Results

File Edit Font Results

	xPosition	frame_1	frame_2	frame_3	frame_4	frame_5
1	0	184.666672	186	185.333328	185.666672	185.333328
2	1	185.664034	186.232452	187.046926	185.472074	185.754968
3	2	184.329534	186.281001	186.990937	184.365500	185.120759
4	3	183.470173	186.600882	185.517552	183.783776	184.168422
5	4	183.969587	185.890056	187.563703	184.868992	184.602329
6	5	183.075327	185.130843	185.385292	185.441518	184.459078
7	6	182.989467	184.504386	185.416659	185.608782	184.113168
8	7	182.771887	183.561207	184.786715	185.595471	183.185714
9	8	182.256226	183.297036	185.188233	184.727546	184.071273
10	9	183.488565	183.356794	186.995179	184.209185	183.852601
11	10	184.632976	184.461925	187.330481	184.352313	182.972244
12	11	183.866948	184.977582	186.827683	184.584722	183.296588
13	12	182.894849	183.587573	187.080941	184.870226	183.982447
14	13	182.149251	179.951556	186.616914	185.764764	184.592646
15	14	181.229804	179.121371	187.008447	187.241475	184.493532
16	15	182.438442	181.789212	186.243536	187.352793	183.640334
17	16	181.825344	183.659922	184.804743	185.304238	185.010306
18	17	183.469479	182.626157	183.819284	185.628778	186.362206
19	18	184.189602	182.290294	182.886693	186.803467	187.263966
20	19	184.063429	181.664035	183.988480	185.725173	187.644187
21	20	185.856242	181.769157	182.935239	188.254563	186.379841
22	21	184.801363	182.384723	182.147631	187.828873	187.097491
23	22	186.624186	183.749458	183.971845	185.105348	187.003696
24	23	185.369550	185.821588	182.908903	185.643141	188.067557
25	24	185.091340	185.500580	182.036081	183.393489	187.158141
26	25	187.010220	185.723932	182.050112	182.571469	186.000487
27	26	185.073949	185.183273	181.627911	181.523684	185.892195

Figure 5-9 Raw data post processing.

- A contour map describing the pixel intensity (color) for a position on the centerline (y-axis) for each frame in the series (x-axis) was generated using STATISTICA (Figure 5-10).
- The contour maps were smoothed (3 x 3 pixel blur) in Fiji for better visualization.
- The angle tool was used to determine the slope (θ) of similar intensities over time.
- $Tan^{-1}(\theta)$ was calculated and converted to mm/sec for the RBC velocity measurement.

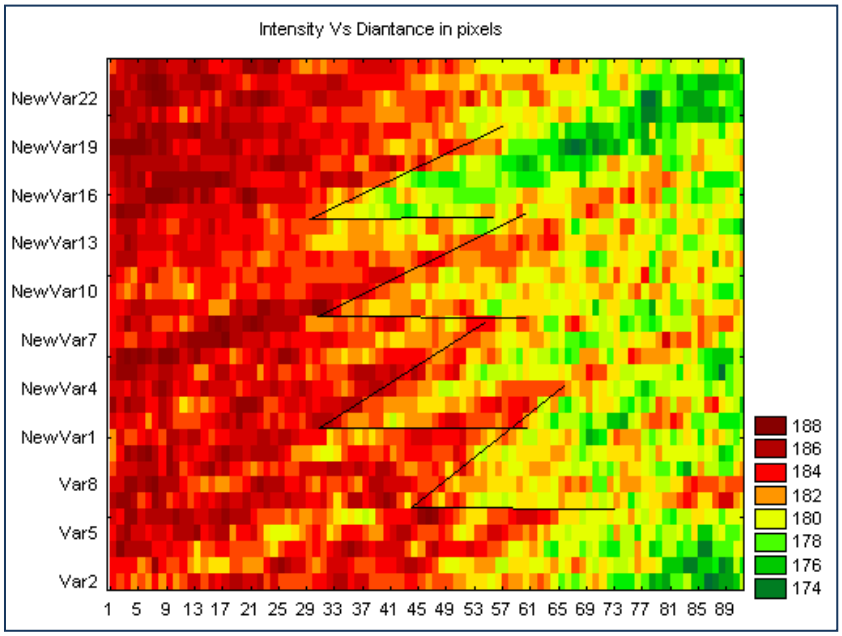

Figure 5-10 Graph illustrating RBC velocity measurements

5.3.12 Assessment of subjective comfort

Subjective comfort was assessed using 0-100 visual analogue scales (VAS) for symptoms of comfort, vision and dryness. These were assessed by each participant in the morning at insertion, after 2 hours and 6 hours of lens wear on day 1 and similarly at day 14. These subjective symptoms were assessed for each eye separately in both phases of the study.

5.3.13 Clinical outcome measures

The following clinical outcomes were obtained at each measurement visit: Lens movement; Lens lag on up gaze; Lens tightness; Horizontal and vertical lens centration; corneal, conjunctival and limbal staining; bulbar and limbal hyperemia, and conjunctival indentation.

5.3.14 Data analysis

Data analyses were done using STATISTICA v7 (Stat Soft Inc., Tulsa, OK). An alpha level of ≤ 0.05 was considered statistically significant. Data are presented in tables as mean ± standard deviation and in figures as the mean with 95% confidence intervals. Repeated measures ANOVA (RM ANOVA) was employed for the main outcome variables and Tukey HSD Post-hoc testing ($\alpha \leq 0.05$) was used to examine pair-wise differences.

Data was also analyzed using correlation matrices to compare the sensory variables (dryness, discomfort and vision) with the clinical outcomes at baseline and 2 weeks. The results were reported as Pearson correlation coefficient values (r) with $\alpha \leq 0.05$.

5.4 Results

5.4.1 Study sample

Forty participants were screened for the study and 30 participants completed both phases of the study (22 female, 8 male). Sample size estimations are problematic because of the relatively large number of new outcome variables that were studied: Unfortunately, for most of the novel ones, there are no historical data to use to rationally calculate effect sizes (means, within and between variances etc.). Nevertheless, power calculations were used to examine, for fixed α and β, what effect size the sample size used would be able to "detect". This illustrated in Figures 5-11 and 5-12 below. For the paired test, the interpretation is relatively straight forward (and applies to many comparisons used in this thesis). For the sample used (n=30), the effect size is 0.46 and so the mean difference needs to be just a bit less than half the standard deviation of the difference for this to be significant. Unfortunately, the greater complexity of the repeated measures ANOVA precludes as straight forward an interpretation. Nevertheless, as will become apparent, the large effect sizes reported in subsequent sections illustrate how large the effect sizes were and so this sample size provided more than enough power to obtain statistical significance.

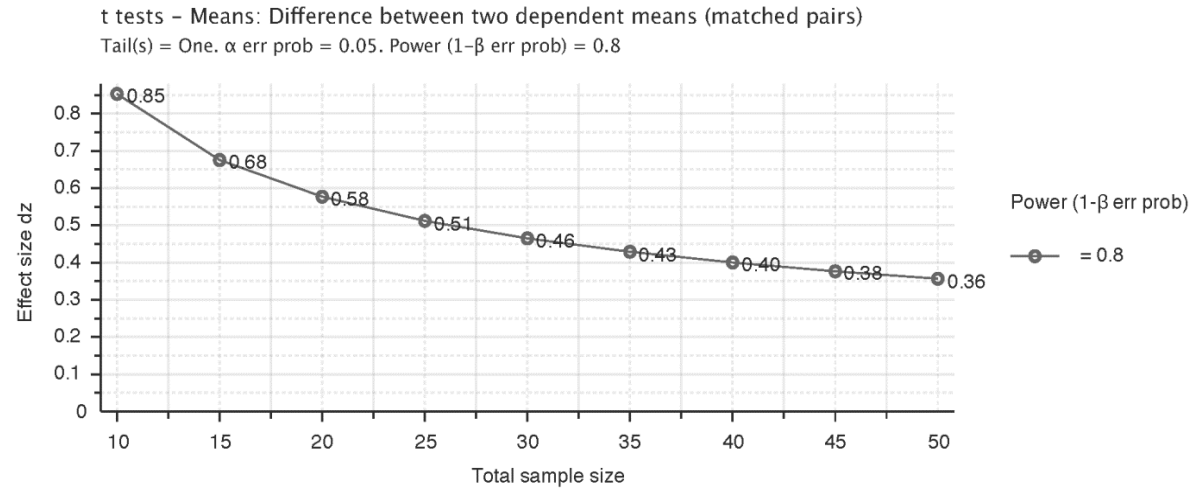

Figure 5-11 Effect size graph estimation for paired t test (effect size=0.46, n=30, power= 0.8)

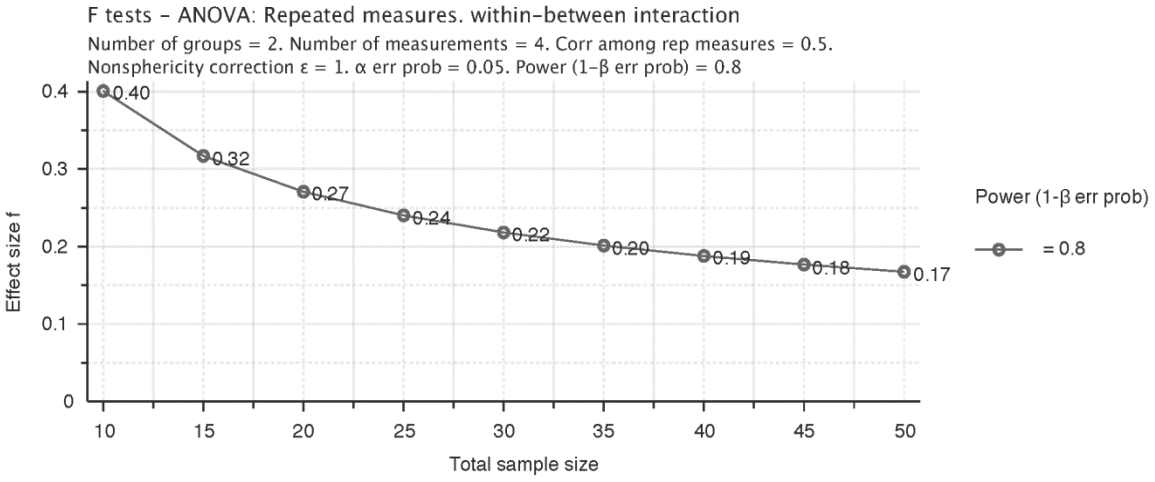

Figure 5-12 Effect size graph estimation for repeated measures ANOVA (effect size=0.22, n=30, power= 0.8)

Table 5.2 summarizes the screening outcome.

Table 5.2: Screening outcome

Participants screened	40
Did not meet incl./excl. criteria	5
Chose not to participate (personal reasons)	4
Participants enrolled for dispensing	31
Discontinued prior to dispensing	1
Participants completed	30

The mean age ± SD of the completed participants was 28 ± 1.5 years (ranging from 29.5 to 26.5 years).

Table 5.3 summarizes few ocular characteristics of the eligible study participants.

No adverse events were reported over the course of the study.

Table 5.3 Ocular characteristics

		OD	OS
K-readings	Flat K Steep K	42.93±1.34 43.58±1.35	42.92±1.30 43.66±1.41
Corneal cylinder		-0.40±0.21	-0.44±0.37
Refractive error	Sphere Cylinder	-1.95±1.67 -0.40±0.26	-2.05±1.65 -0.40±0.28

5.4.2 Lens fitting characteristics

For each fitting characteristic, RM ANOVA was run with visit (baseline, 2 weeks), modulus (AA=low, PV=higher) and fit (steep, flat) as simple effects.

Lens movement

The results of lens movement for each lens and each time point are shown in Table 5.4 and Figure 5-13.

Table 5.4 Mean and standard deviation of subjective lens movement (mm) at baseline and 2 weeks.

Lens	Baseline	2 weeks
AA 8.3	0.30 ±0.07	0.26±0.06
AA 8.7	0.30±0.09	0.31±0.07
PV 8.3	0.29±0.07	0.28±0.07
PV 8.6	0.31±0.07	0.30±0.08

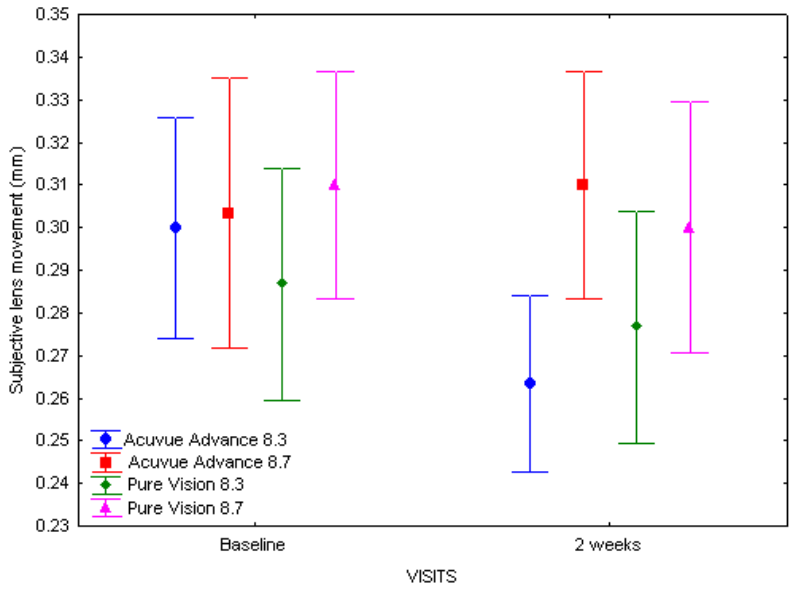

Figure 5-13: Mean subjective lens movement (mm) at baseline and 2 weeks with AA 8.3, AA 8.7, PV 8.3 and PV 8.6 (error bars represent mean ± SD).

Lens movement was significantly different between steep and flat lenses (RM ANOVA, Fit p=0.035). The least movement was shown by the AA 8.3 lens (multiple pair wise comparisons, Tukey p=0.028). Modulus, visit and the other interactions were not significantly different for lens movement (RM ANOVA, all p>0.05). All the lenses decreased in movement by the end of 2 weeks except for AA 8.7.

Lens lag on primary position of gaze

The results of lens lag for primary gaze for each lens and each time point are shown in Table 5.5 and Figure 5-14. Lens lag for primary gaze showed no significant difference in any main effects or their interactions (RM ANOVA, all $p>0.05$).

Table 5.5 Mean and standard deviation of lens lag (mm) for primary gaze at baseline and 2 weeks.

Lens	Baseline	2 weeks
AA 8.3	0.17±0.05	0.15±0.05
AA 8.7	0.16±0.06	0.16±0.06
PV 8.3	0.17±0.06	0.14±0.05
PV 8.6	0.16±0.06	0.16±0.05

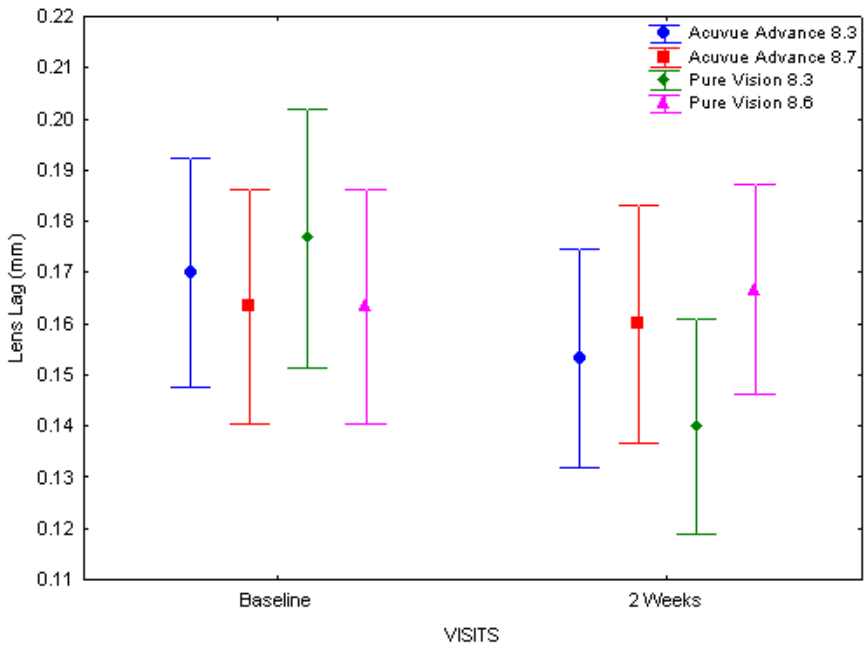

Figure 5-14 Mean Lens lag in primary position at baseline and 2 weeks with AA 8.3, AA 8.7, PV 8.3 and PV 8.6 (mm) (error bars represent mean ± SD).

Lens lag with up gaze

The results of lens lag with up gaze for each lens and each time point are shown in Table 5.6 and Figure 5-15.

Table 5.6 Mean and standard deviation of lens lag with up gaze (mm) at baseline and 2 weeks.

Lens	Baseline	2 weeks
AA 8.3	0.16±0.06	0.13±0.04
AA 8.7	0.18±0.07	0.17±0.06
PV 8.3	0.15±0.06	0.14±0.06
PV 8.6	0.17±0.08	0.15±0.06

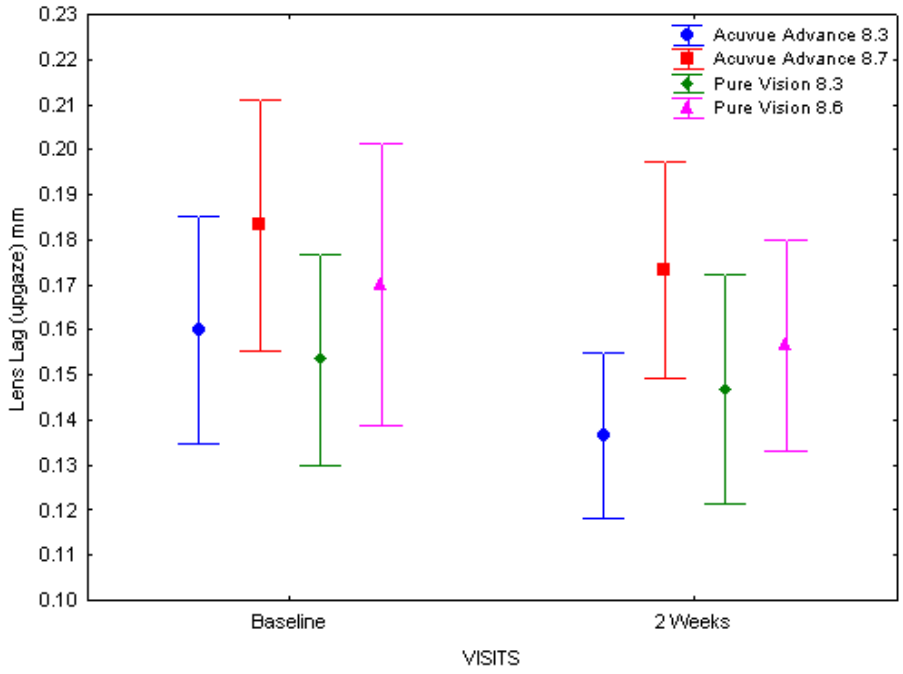

Figure 5-15 Mean Lens lag with up gaze (mm) at baseline and 2 weeks with AA 8.3, AA 8.7, PV 8.3 and PV 8.6 (error bars represent mean ± SD).

Lens lag with up gaze was significantly different between steep and flat lenses (RM ANOVA, Fit p=0.011), with flatter lenses showing greater lens lag with up gaze. Modulus, visit and all the interactions were not significantly different for lens lag with up gaze (RM ANOVA, all p>0.05).

Lens tightness grading

The results of lens tightness with up gaze for each lens and each time point are shown in Table 5.7 and Figure 5-16.

Table 5.7 Mean and standard deviation of lens tightness (%) at baseline and 2 weeks.

Lens	Baseline	2 weeks
AA 8.3	50.03 ±6.32	52.00±6.77
AA 8.7	44.7±6.17	45.93±6.55
PV 8.3	46.5±7.08	45.83±4.92
PV 8.6	48.4±7.42	47.00±4.84

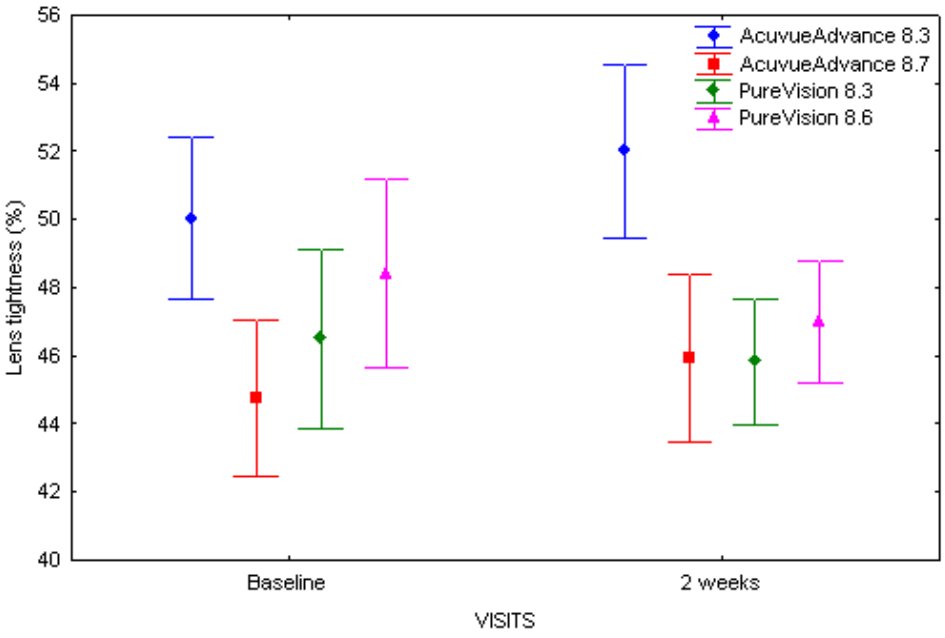

Figure 5-16 Mean lens tightness (%) at baseline and 2 weeks with AA 8.3, AA 8.7, PV 8.3 and PV 8.6 (error bars represent mean ± SD).

There was a significant interaction between modulus and fit for lens tightness (RM ANOVA, modulus*fit $p=0.021$). Steeper AA lens (lower modulus) had greater lens tightness than flatter AA lenses and both PV lenses. The PV (high modulus) steeper lenses had less lens tightness than PV flatter lenses (Tukey, all $p<0.05$).

Horizontal lens centration

The results of horizontal lens centration for each lens and each time point are shown in Table 5.8 and Figure 5-17.

Table 5.8 Mean and standard deviation of horizontal centration (mm), temporal (-) and nasal (+) at baseline and 2 weeks.

Lens	Baseline	2 weeks
AA 8.3	0.27±0.23	0.17±0.22
AA 8.7	0.28±0.28	-0.02±0.30
PV 8.3	0.25±0.28	0.16±0.26
PV 8.6	0.26±0.20	0.19±0.23

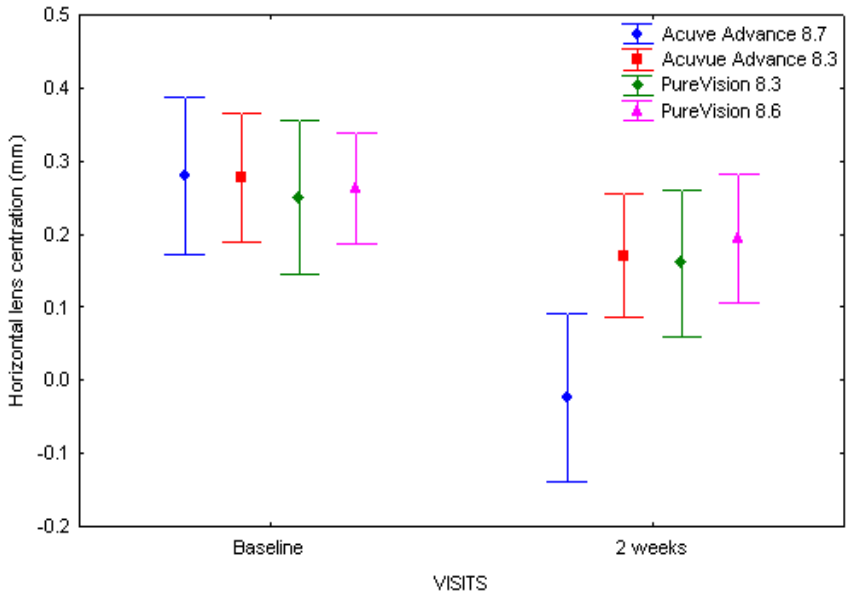

Figure 5-17 Mean horizontal lens centration (mm) at baseline and 2 weeks with AA 8.3, AA 8.7, PV 8.3 and PV 8.6 (error bars represent mean ± SD).

There was a significant interaction between visit and modulus for horizontal lens centration (RM ANOVA, visit*modulus p=0.002) (Figure 5-18). Both AA and PV lenses shifted towards a more central position at 2 weeks compared with baseline, and the shift was greater in the AA lenses (Tukey, $p<0.05$).

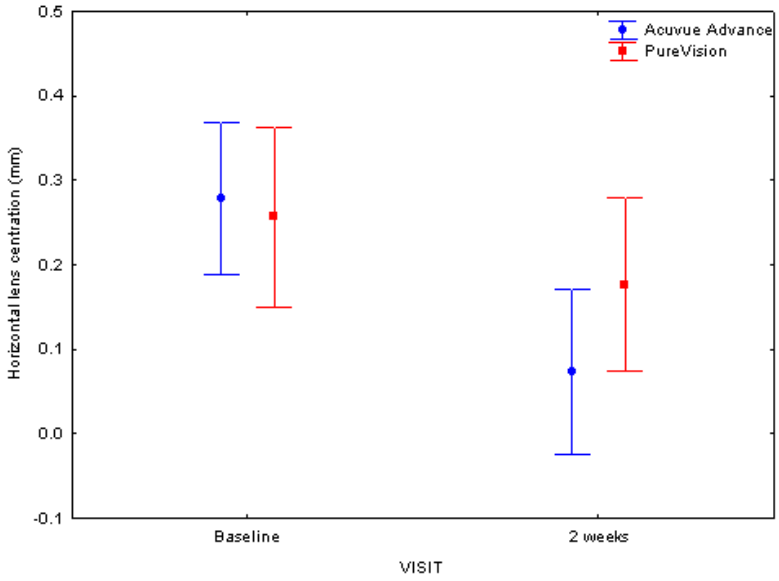

Figure 5-18 Horizontal lens centration (mm) with AA and PV lenses at baseline and 2 weeks (error bars represent mean ± SD).

Vertical lens centration

The results of vertical lens centration for each lens and each time point are shown in Table 5.9 and Figure 5-19.

Table 5.9 Mean and standard deviation of vertical lens centration (mm), inferior (-), superior (+) at baseline and 2 weeks.

Lens	Baseline	2 weeks
AA 8.3	-0.05 ±0.43	-0.02±0.30
AA 8.7	0.05±0.32	-0.04±0.20
PV 8.3	0.11±0.30	0.11±0.23
PV 8.6	-0.03±0.32	-0.08±0.22

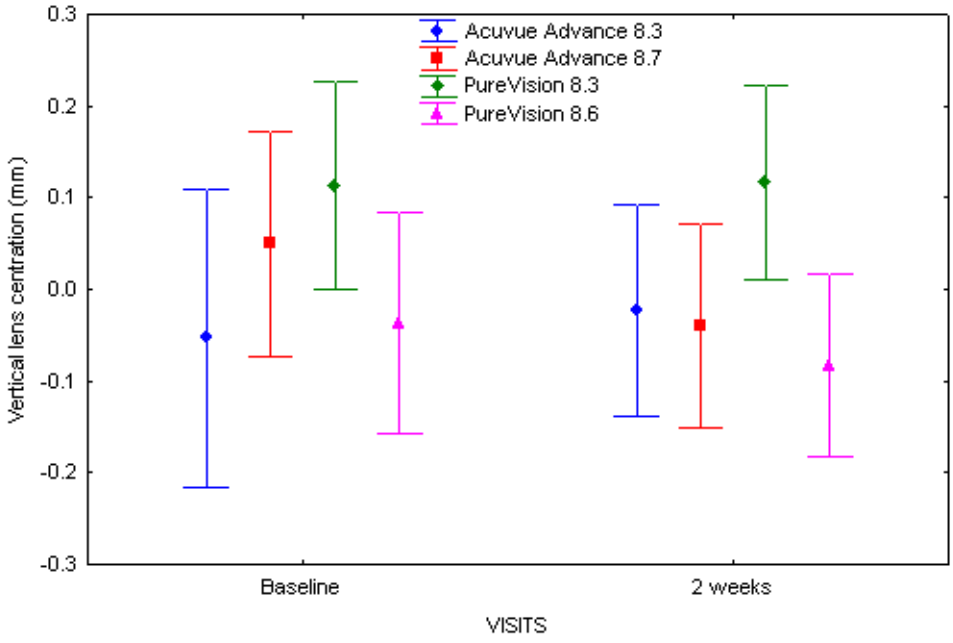

Figure 5-19: Mean vertical lens centration (mm) at baseline and 2 weeks with AA 8.3, AA 8.7, PV 8.3 and PV 8.6 (error bars represent mean ± SD).

Vertical lens centration was significantly different between steep and flat lenses (RM ANOVA, Fit $p=0.033$). Modulus, visit and all the interactions were not significantly different for vertical lens centration (RM ANOVA, all $p>0.05$). Flatter lenses of both AA and PV lenses significantly decentred vertically (RM ANOVA, vertical lens centration $p<0.05$).

Lens sagittal height at actual lens diameter on the eye vs. sag of the eye

Table 5.10 and 5.11 shows the mean sagittal height of the eye at the chord of the measured diameter of the contact lens. Table 5.11 shows the sagittal depth of the contact lens at the chord of its measured diameter. Figure 5-2 represents the measurement technique for sagittal height measurements on the eye using the Visante OCT.

Comparing the sag of the cornea to the sag of the lens there was a significant difference ($p<0.05$). There is no difference in the sagittal height comparing AA 8.3 and PV 8.3 lenses ($p>0.05$) but there is a significant

difference in the sag of AA 8.7 and PV 8.6 lenses ($p<0.05$). The AA 8.7 lenses had the least sag. The sagittal depth of both steeper lenses was 0.46mm greater than the sagittal depth of the eye at the lens diameter chord. The flatter lenses of AA 8.7 and PV 8.6 were 0.14 and 0.22mm respectively greater than the sagittal depth of the eye.

Table 5.10 Mean and standard deviation corneal sagittal depth at lens diameter.

Lens	Diameter (lens) mm	SAG (cornea) mm
AA 8.3	14.18±0.11	3.41±0.16
AA 8.7	14.21±0.18	3.39±0.19
PV 8.3	14.12±0.15	3.38±0.15
PV 8.6	14.32±0.24	3.43±0.16

Table 5.11 Mean and standard deviations sagittal depth of the lens.

Lens	Diameter (lens) mm	SAG (lens) mm
AA 8.3	14.18±0.11	3.87±0.16
AA 8.7	14.21±0.18	3.53±0.08
PV 8.3	14.12±0.15	3.84±0.03
PV 8.6	14.32±0.24	3.65±0.06

Corneal topography

For corneal topography, RM ANOVA was run with visit (baseline, 2 weeks), modulus (AA=low, PV=higher), fit (steep, flat), meridian (0, 45, 90, 135, 180) and location (+2, +4, +6 mm) as simple effects. The results of corneal topography (tangential curvature) for each lens, meridian, location and time point are shown in Table 5.12 to 5.14 and Figures 5-20 to 5-22.

Table 5.12 Mean and standard deviation of radius of tangential curvature at 2mm location from the apex at baseline and 2 weeks visit.

Lens	Baseline					2 weeks				
	2mm					2mm				
	T-0	ST-45	S-90	SN-135	N-180	T-0	ST-45	S-90	SN-135	N-180
AA 8.3	7.88±0.25	7.84±0.23	7.79±0.24	7.85±0.22	7.88±0.23	7.87±0.25	7.84±0.24	7.80±0.24	7.84±0.24	7.88±0.25
AA 8.7	7.95±0.34	7.90±0.32	7.85±0.33	7.84±0.28	7.89±0.27	7.89±0.24	7.84±0.24	7.85±0.30	7.84±0.24	7.95±0.34
PV 8.3	7.87±0.25	7.83±0.24	7.77±0.24	7.82±0.23	7.85±0.25	7.89±0.25	7.85±0.25	7.79±0.24	7.84±0.24	7.87±0.24
PV 8.6	7.89±0.25	7.84±0.25	7.76±0.26	7.84±0.25	7.90±0.27	7.88±0.23	7.84±0.24	7.79±0.27	7.86±0.25	7.89±0.25

Table 5.13 Mean and standard deviation radius of tangential curvature at 4mm location from the apex at the baseline and 2 week visit.

Lens	Baseline					2 weeks				
	4mm					4mm				
	T-0	ST-45	S-90	SN-135	N-180	T-0	ST-45	S-90	SN-135	N-180
AA 8.3	7.96±0.28	7.92±0.29	7.86±0.32	7.99±0.31	8.02±0.26	7.97±0.28	7.92±0.28	7.87±0.39	7.98±0.29	8.01±0.25
AA 8.7	8.01±0.22	7.95±0.25	7.89±0.25	7.97±0.32	7.99±0.32	8.03±0.26	7.95±0.32	7.83±0.37	7.95±0.35	7.98±0.28
PV 8.3	7.98±0.27	7.94±0.28	7.87±0.31	7.90±0.29	7.99±0.24	7.99±0.28	7.95±0.29	7.85±0.48	7.99±0.32	7.98±0.25
PV 8.6	7.99±0.26	7.91±0.27	7.78±0.46	7.98±0.34	8.00±2.67	7.99±0.25	7.95±0.29	7.86±0.34	8.00±0.33	8.05±0.28

Table 5.14 Mean and standard deviation radius of tangential curvature at 6mm location from the apex at the baseline and 2 week visit.

Lens	Baseline					2 weeks				
	6mm					6mm				
	T-0	ST-45	S-90	SN-135	N-180	T-0	ST-45	S-90	SN-135	N-180
AA 8.3	8.28±0.37	8.21±0.47	8.28±0.98	8.296±0.42	8.42±0.36	8.37±0.41	8.32±0.57	9.00±3.96	8.34±0.49	8.42±0.36
AA 8.7	8.36±0.34	8.27±0.43	8.25±1.28	8.15±0.54	8.32±0.45	8.47±0.32	8.39±0.42	8.07±1.23	7.95±0.35	8.29±0.42
PV 8.3	8.36±0.40	8.22±0.47	8.27±0.97	8.19±0.46	8.35±0.29	8.34±0.42	8.39±0.63	8.34±2.92	8.19±0.39	8.28±0.34
PV 8.6	8.36±0.34	8.19±0.47	7.98±0.56	8.21±0.53	8.34±0.38	8.35±0.35	8.25±0.38	8.09±0.81	8.38±0.45	8.40±0.41

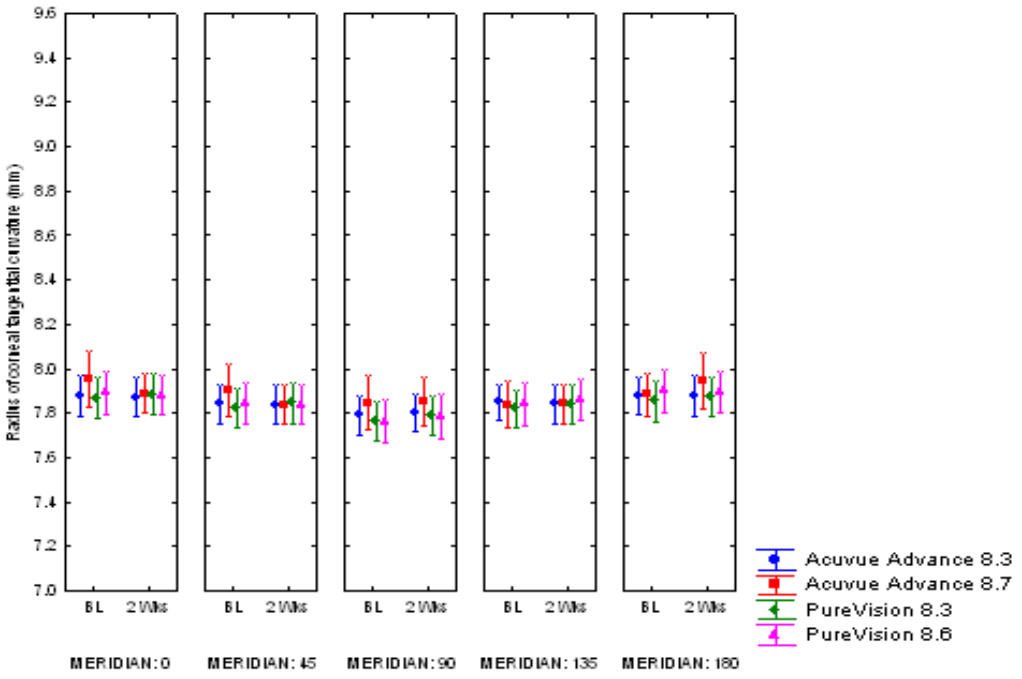

Figure 5-20 Mean tangential radius of corneal tangential curvature (mm) at 2mm from the apex for baseline and 2 weeks with AA 8.3, AA 8.7, PV 8.3 and PV 8.6 at (0,45,90,135,180) meridians (error bars represent mean ± SD).

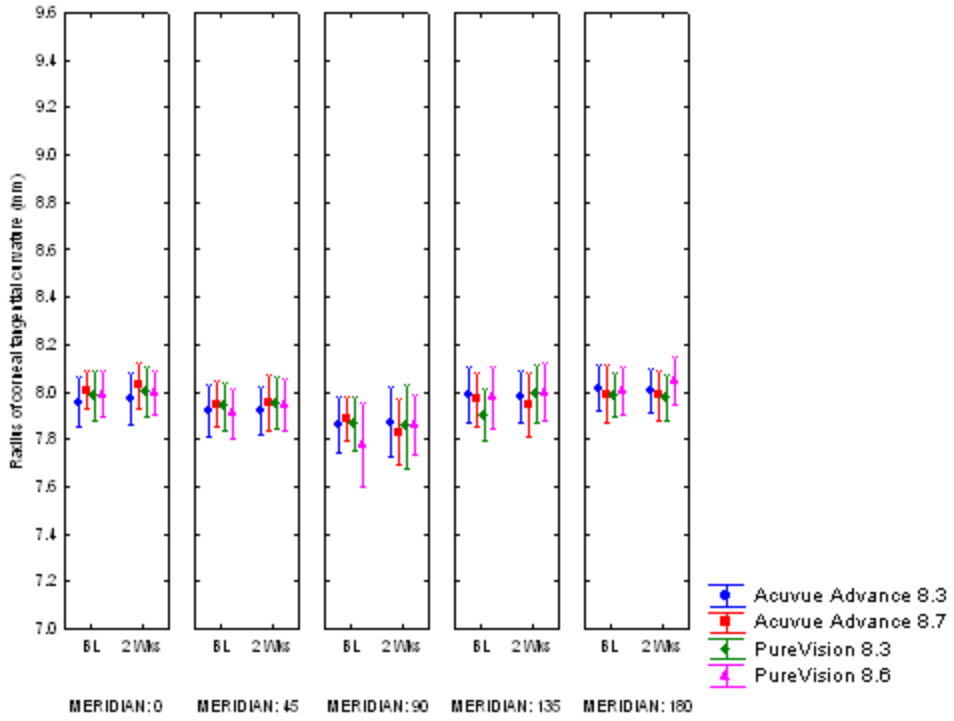

Figure 5-21 Mean tangential radius of curvature (mm) at 4mm from the apex for baseline and 2 weeks with AA 8.3, AA 8.7, PV 8.3 and PV 8.6 at (0,45,90,135,180) meridians (error bars represent mean ± SD).

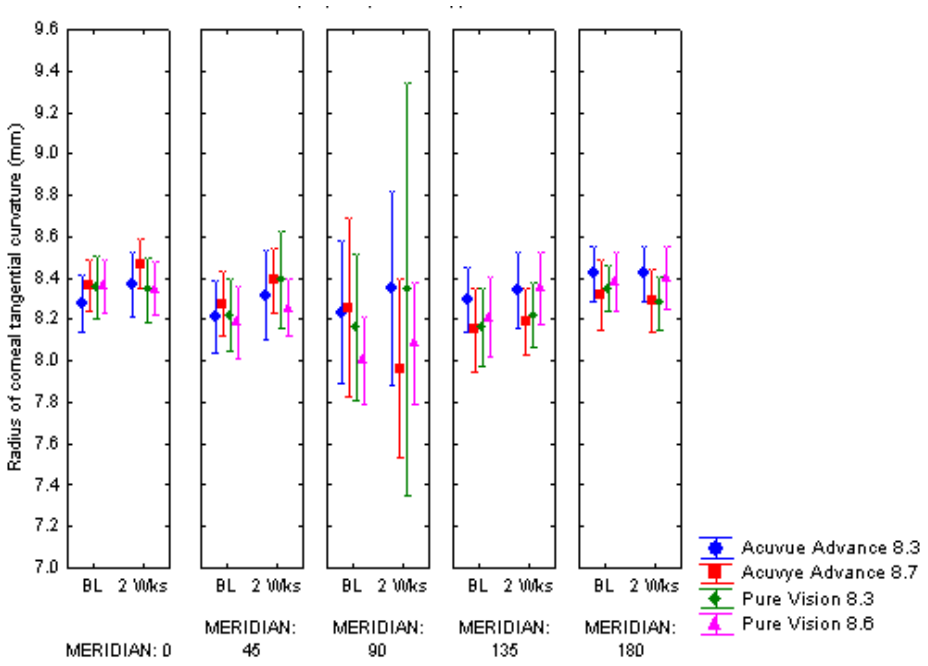

Figure 5-22 Mean tangential radius of curvature of the cornea curvature (mm) at 6mm from the apex for baseline and 2 weeks with AA 8.3, AA 8.7, PV 8.3 and PV 8.6 at (0,45,90,135,180) meridians.

There was no significant change in tangential curvature over time (RM ANOVA, p=0.168), no change with base curve (RM ANOVA, p=0.741) and no change comparing higher and lower modulus lenses (RM ANOVA, p=0.237).

There was a significant difference in tangential curvature between meridians (RM ANOVA, meridians p=0.001), and between locations for different fits (RM ANOVA, fit*location p=0.036). The tangential curvature was significantly steeper superiorly than the nasal and temporal cornea by the end of 2 weeks (Tukey, both p=0.001). All the flatter and steeper lens fits showed a flatter tangential curvature at locations more distant from the apex by the end of 2 weeks (Tukey, all $p<0.05$). At similar distances from the apex there was no significant difference in tangential curvature between fit types (Tukey, $p>0.05$).

Corneal and epithelial thickness

For both corneal and epithelial thickness, RM ANOVA was run with visit (baseline, 2 weeks), modulus (AA=low, PV=higher) and fit (steep, flat) at central (0), temporal locations (-1, -2, -3) and nasal locations (1, 2, 3) along four meridians (0, 45, 90 and 135 degrees). Data was analysed for the central and peripheral location at +3 in the vertical (superior) meridian. Comparisons were made using the Fisher LSD post-hoc tests and were Bonferonni corrected. The total corneal and epithelial thickness has been tabulated for baseline and 2 weeks and reported in Appendix A and B.

Corneal thickness

Figures 5-23 and figure 5-24 illustrates corneal thickness at the superior and central quadrants with lower (AA) and higher (PV) modulus lenses comparing the steeper and flatter fit along the vertical meridian.

There was a significant interaction between visit, modulus, fit, meridian and location (RM ANOVA visit*modulus*fit*location, p=0.002) for total corneal thickness. At baseline with the PV lens there was a significant difference in corneal thickness for each base curve (Fisher LSD, both p=0.001). In the central location there were significant changes for both steep AA and PV lenses indicating corneal thinning at 2 weeks (Fisher LSD, all p=0.002).Comparing the baseline with 2 weeks for both AA and PV lenses, the steeper base curves of both lenses and flatter base curve of the AA, in the superior meridian had a significant amount of corneal thinning (Fisher LSD, both p=0.014 respectively)

At 2 weeks comparing the superior and central cornea with the higher modulus lens (PV) with the steeper base curve indicated that there was no difference (Fisher LSD, p=0.119)

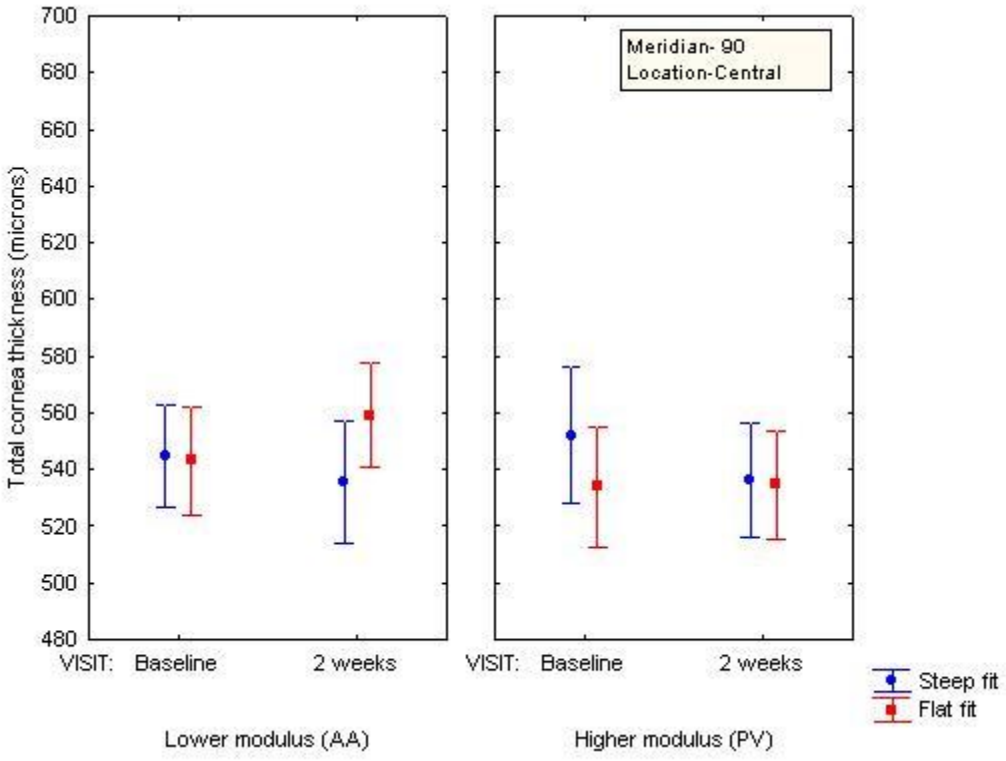

Figure 5-23 Mean central corneal thickness with lower (AA) and higher (PV) modulus lenses comparing the steeper and flatter fit. Error bars represent mean ± SD.

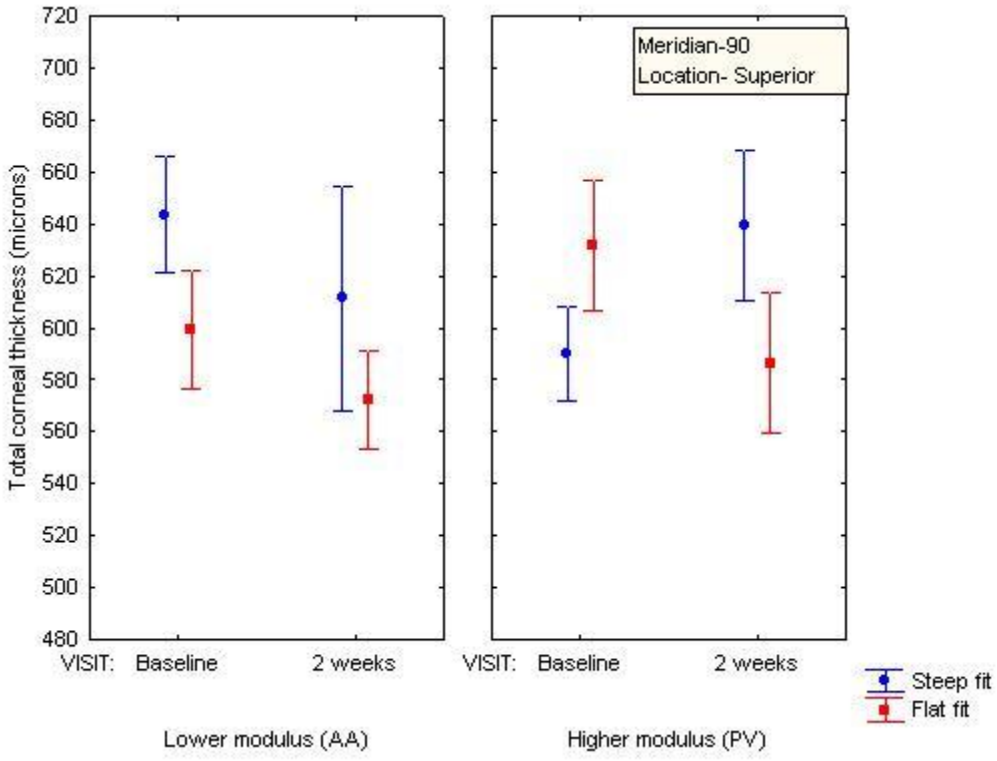

Figure 5-24 Mean corneal thickness along the 90 degree meridian for superior cornea with lower (AA) and higher (PV) modulus lenses comparing the steeper and flatter fit. Error bars represent mean ± SD.

Epithelial thickness

There was a significant interaction between modulus, fit and location (RM ANOVA, modulus*fit*location $p=0.042$) for epithelial thickness (Figure 5-25). Steeper AA lens (lower modulus) had greater epithelial thinning than flatter AA lenses and both PV lenses in the superior location (Tukey, all $p<0.05$). Figure 5-25 illustrates epithelial thickness data at central, superior, inferior, nasal and temporal locations with lower (AA) and higher modulus (PV) lenses comparing the steeper and flatter fit.

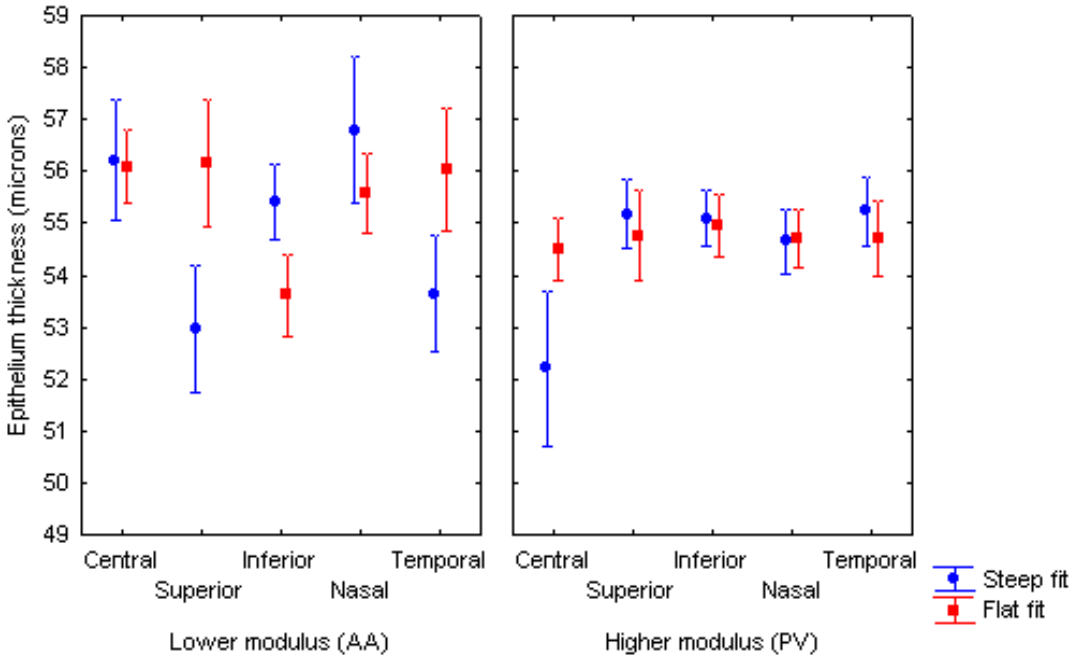

Figure 5-25 Mean epithelial thickness at central, superior, inferior, nasal and temporal locations for lower modulus (AA) and higher modulus (PV) lenses comparing the steeper and flatter fit. Error bars represent mean ± SD.

Comparing the superior and inferior locations for epithelial thickness for the lower modulus lenses (AA) with the steeper BC there was a significant thinning of the epithelium superiorly (Tukey, p=0.038). Comparing the superior and central location with the higher modulus lens (PV) with the steeper base curve indicated that there was more epithelial thinning occurring centrally (Tukey, p=0.037). Nasal and temporal comparisons showed a significant thinning temporally for the lower modulus lenses (AA) with the steeper base curves (Tukey, p=0.014).

5.5 Biomicroscopy

For each biomicroscopy finding, RM ANOVA was run with visit (baseline, 2 weeks), modulus (AA=low, PV=higher), fit (steep, flat) and location (temporal, superior, nasal, inferior) as simple effects.

Corneal staining

Corneal staining was rated on a scale of 0 (negligible) to 100 (severe) for each quadrant (nasal, temporal, superior and inferior) and the central region. The results of corneal staining for each lens and each time point are shown in Table 5.15 and Figure 5-26.

From the product of severity and percent coverage, global staining score (GSS) was calculated as the mean of the five quadrants. Corneal staining showed no significant difference in any main effects or their interactions (RM ANOVA, all $p>0.05$).

Table 5.15 Mean and standard deviation of corneal staining at baseline and 2 week visit

Lens	Baseline	2 weeks
AA 8.3	33.83±68.24	45.16±69
AA 8.7	65.83±92.07	47.50±74.0
PV 8.3	52.33±76.57	48.00±65.2
PV 8.6	50.67±108.65	47.0±73.3

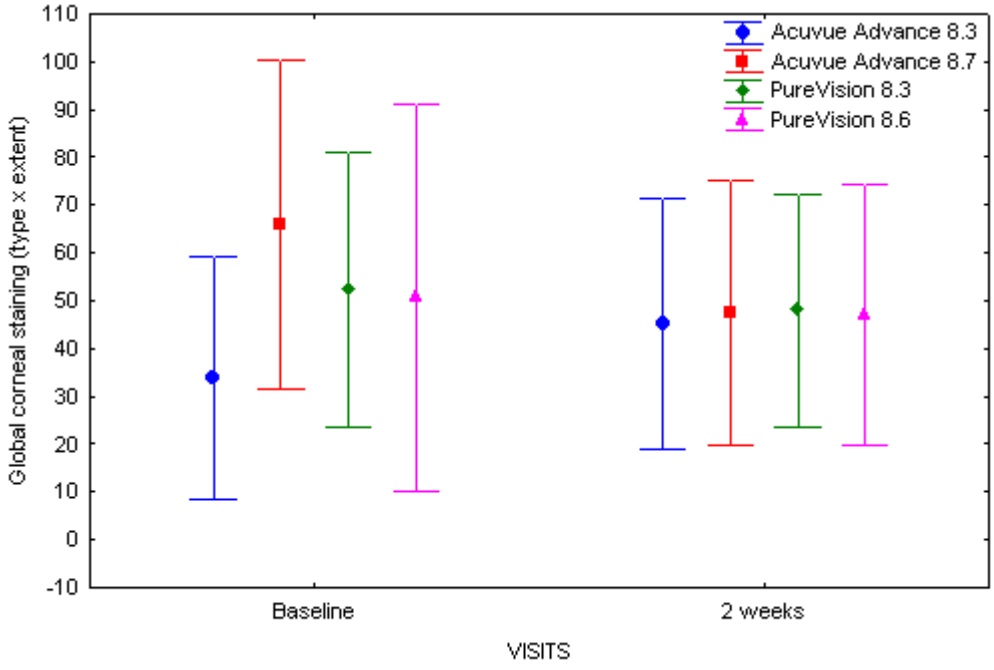

Figure 5-26 Mean global corneal staining (average of five locations) at baseline and 2 weeks with AA 8.3, AA 8.7, PV 8.3 and PV 8.6 (error bars represent mean ± SD).

Bulbar Hyperemia

Bulbar hyperemia was rated on a scale of 0 (negligible) to 100 (severe) for each quadrant (nasal, temporal, superior, and inferior) and averaged over all quadrants to derive an average bulbar hyperemia. The results of bulbar hyperemia for each lens and each time point are shown in Table 5.16 and Figure 5-27.

Table 5.16 Mean and standard deviation of bulbar hyperemia (0-100) at baseline and 2 week visit

Lens	Baseline				2 weeks			
	Temp	Superior	Nasal	Inferior	Temporal	Superior	Nasal	Inferior
AA 8.3	25.6±3.8	21.6±3.03	26.1±3.6	22.1±2.81	27.0±3.89	23.27±4.28	27.24±4.14	23.45±4.03
AA 8.7	24.1±3.41	21.1±3.10	24.3±3.80	20.8±2.90	26.9±3.64	23.28±4.49	25.17±5.09	23.28±3.84
PV 8.3	25.83±8.6	21.10±2.89	25.5±3.31	21.33±2.60	25.10±5.11	23.17±3.07	26.67±3.79	23.00±2.82
PV 8.6	27.00±9.1	21.50±3.25	24.5±3.56	21.67±3.79	26.33±4.34	21.83±4.63	25.83±3.73	21.83±4.45

There was a significant interaction between fit and location for bulbar hyperemia (RM ANOVA, modulus*fit $p=0.034$) (Figure 5-27). There was a significant increase in bulbar hyperemia at the nasal and temporal locations for both baseline and 2 weeks with AA (lower modulus) and PV (higher modulus) lenses (Tukey, all $p<0.05$). However, there was a significant decrease in the bulbar hyperemia with PV (higher modulus) lenses at 2 weeks compared to the baseline at the temporal location. (Tukey, $p<0.05$)

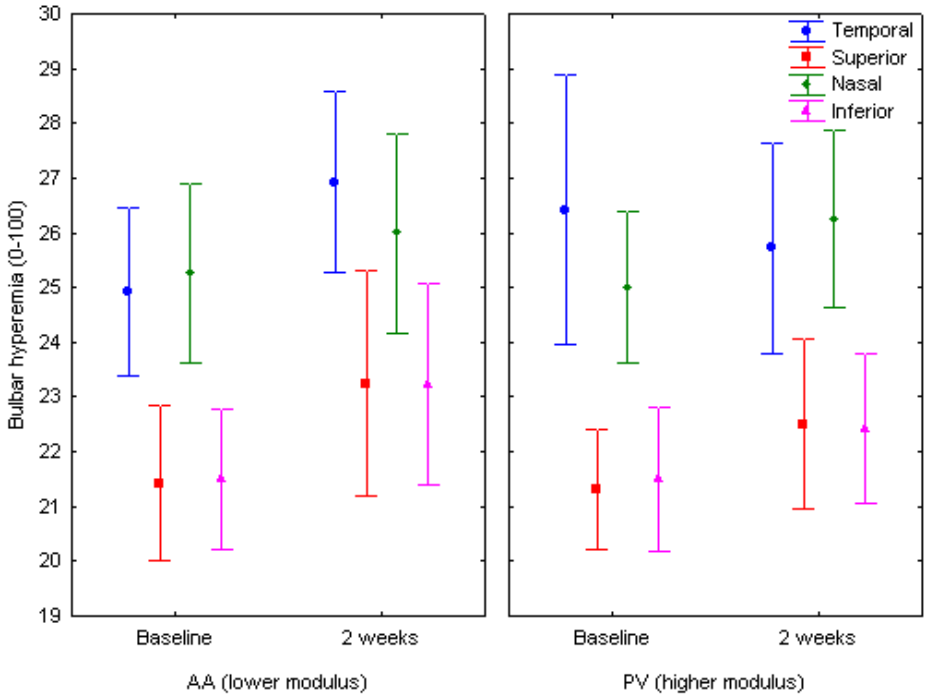

Figure 5-27 Mean bulbar hyperemia (0-100) at baseline and 2 weeks with AA (low modulus) and PV (high modulus) at temporal, superior, nasal and inferior locations (error bars represent mean ± SD).

Limbal hyperemia

Limbal hyperemia was rated on a scale of 0 (negligible) to 100 (severe) for each quadrant (nasal, temporal, superior, and inferior). The results of limbal hyperemia for each lens and each time point are shown in Table 5.17 and Figure 5-28.

Limbal hyperemia was significantly different over time (RM ANOVA, a p=0.007) and by location (RM ANOVA, p=0.029). There was an increase in limbal hyperemia at 2 weeks which was found mainly in the nasal and temporal quadrants.

Table 5.17 Mean and standard deviation of limbal hyperemia (0-100) at baseline and 2 weeks.

Lens	Baseline				2 weeks			
	Temporal	Superior	Nasal	Inferior	Temporal	Superior	Nasal	Inferior
AA 8.3	10.17±4.99	8.00±2.82	10.33±4.34	7.83±3.13	11.55±4.03	8.96±3.09	11.89±4.10	9.31±4.95
AA 8.7	10.33±4.34	8.33±3.55	11.50±4.76	7.83±3.13	12.07±4.12	10.00±3.54	13.10±4.10	11.03±4.89
PV 8.3	10.37±4.06	8.67±3.19	11.73±4.60	8.83±3.13	10.83±3.49	8.83±3.39	11.5±3.26	9.33±4.49
PV 8.6	10.67±4.30	8.33±3.30	10.33±2.92	8.83±3.87	11.0±4.03	8.67±3.46	11.83±5.17	9.50±3.79

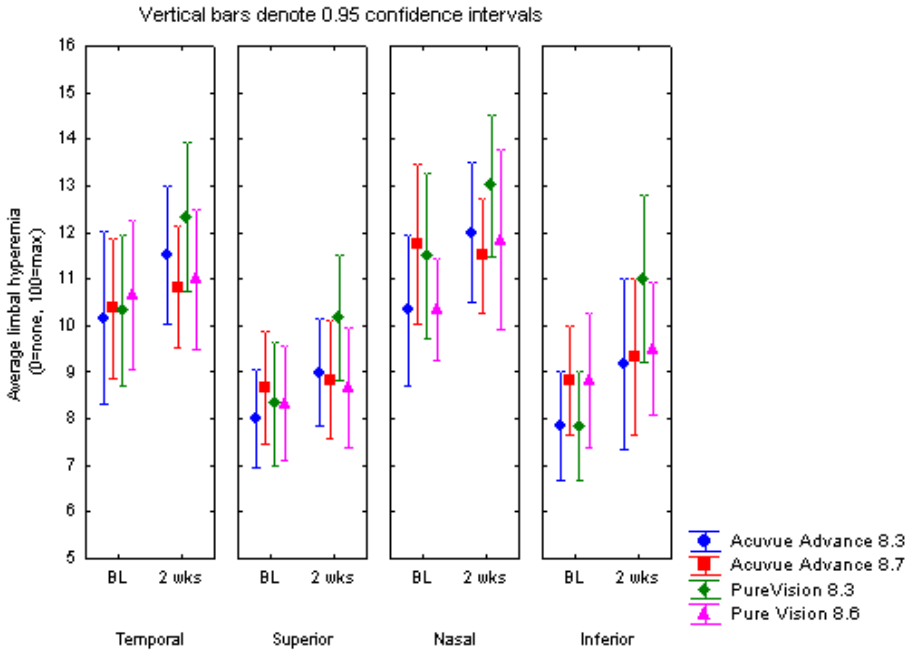

Figure 5-28 Mean limbal hyperemia at baseline and 2 weeks with AA 8.3, AA 8.7, PV 8.3 and PV 8.6 (0-100) (error bars represent mean ± SD).

Conjunctival staining

Conjunctival staining with a fluorescein stain was graded on a scale of 0(none) to 100 (severe) for nasal, temporal, superior and inferior quadrants. The results of conjunctival staining for each lens and each time point are shown in Table 5.18 and Figure 5-29.

Table 5.18 Mean and standard deviation of global conjunctival staining at baseline and 2 weeks.

Lens	Baseline				2 weeks			
	Temporal	Superior	Nasal	Inferior	Temporal	Superior	Nasal	Inferior
AA 8.3	5.83±7.55	4.67±8.80	6.17±10.06	3.00±6.90	17.93±13.40	16.03±16.11	17.59±13.60	25.28±16.91
AA 8.7	7.00±8.50	2.50±6.66	7.50±9.35	2.50±5.53	19.35±16.69	16.55±14.46	18.45±14.83	24.48±15.89
PV 8.3	7.00±10.39	1.67±5.14	4.17±7.08	1.17±3.13	14.50±12.27	5.50±8.55	9.83±9.78	10.00±11.14
PV 8.6	7.33±8.88	3.83±9.44	6.50±10.01	5.83±10.99	13.00±12.08	5.50±12.48	10.00±10.51	11.83±13.55

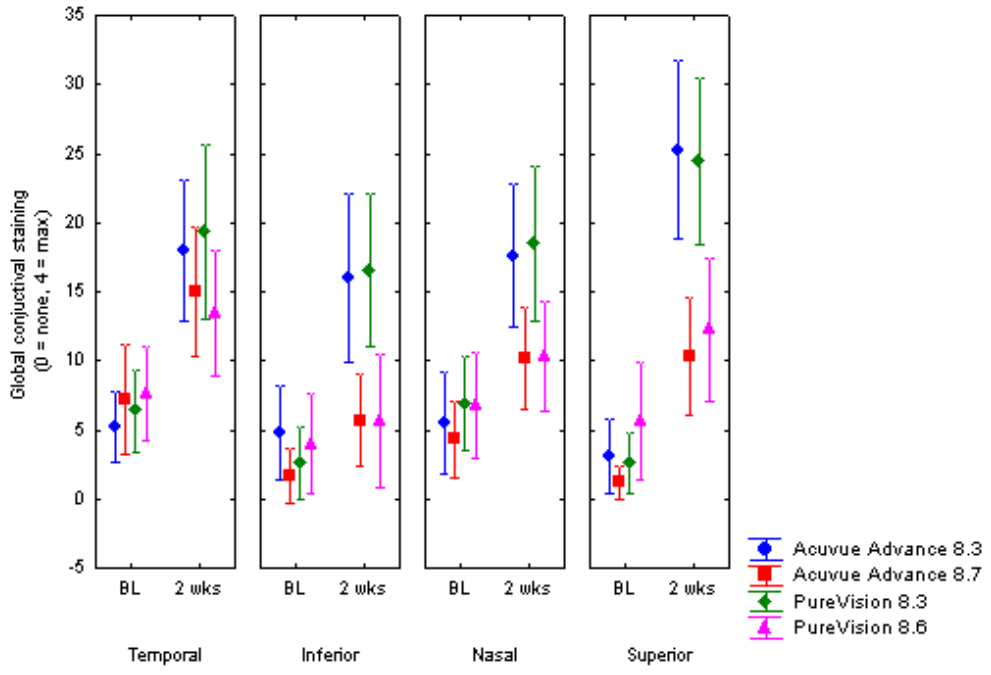

Figure 5-29 Global conjunctival staining at baseline and 2 weeks with AA 8.3, AA 8.7, PV 8.3 and PV 8.6 at temporal ,inferior, nasal and superior conjunctiva (error bars represent mean ± SD).

There was a significant interaction between visit, fit and location for conjunctival staining (RM ANOVA, visit*fit*location p=0.029) (Figure 5-30). Steeper fitting lenses of AA and PV showed a significantly higher conjunctival staining for all the lenses at the 2 week visit (Tukey, p<0.05).

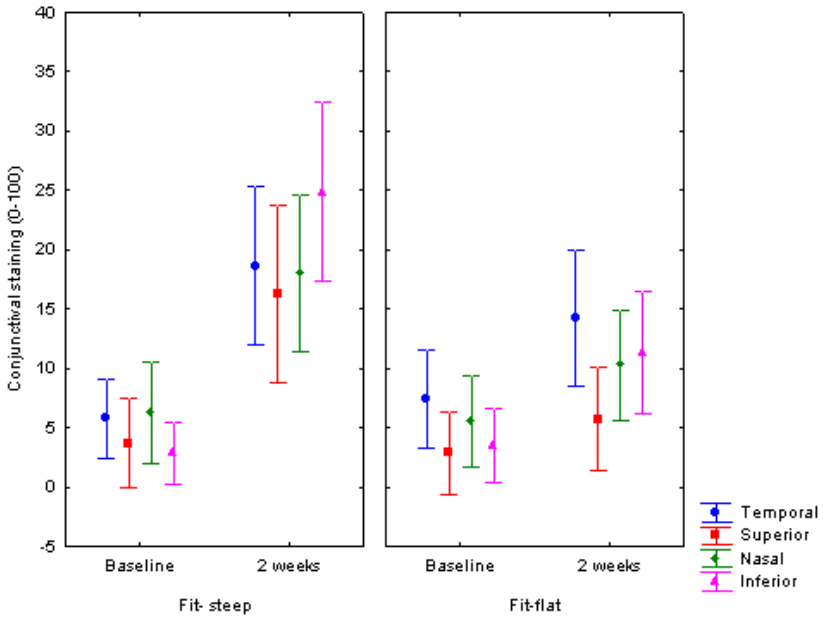

Figure 5-30 Global conjunctival staining at baseline and 2 weeks with fit and steep fitting lenses at temporal, inferior, nasal and superior conjunctiva (error bars represent mean ± SD).

5.5.1 Limbal staining

Limbal staining, visualized with sodium fluorescein was rated on a scale of 0 (negligible) to 100 (severe) for each peripheral quadrant (nasal, temporal, superior, and inferior) and was averaged to derive global limbal staining. The results of limbal staining for each lens and each time point are shown in Table 5.19 and Figure 5-31.

There was minimal limbal staining with both AA and PV lenses for baseline and 2 weeks. Data was only analysed for the 2 week visit as there were multiple visits at baseline where staining was 0 and had no variance.

Table 5.19 Mean and standard deviation of limbal staining (0-100) at baseline and 2 weeks.

Lens	Baseline				2 weeks			
	Temporal	Superior	Nasal	Inferior	Temporal	Superior	Nasal	Inferior
AA 8.3	1.17±3.13	0.33±1.83	0.67±2.86	2.17±7.84	2.07±4.91	0.86±3.01	2.24±5.60	3.79±6.22
AA 8.7	0.67±2.17	0.00±0.00	1.17±3.40	0.67±2.54	2.41±4.15	0.69±2.21	3.45±6.14	3.79±5.12
PV 8.3	1.50±5.11	0.00±0.00	0.17±0.91	0.00±0.00	2.33±6.12	0.33±1.27	0.67±1.73	2.17±5.52
PV 8.6	1.50±3.51	0.50±1.53	1.33±3.93	2.00±5.19	1.33±3.20	0.17±0.91	1.17±4.68	1.83±3.83

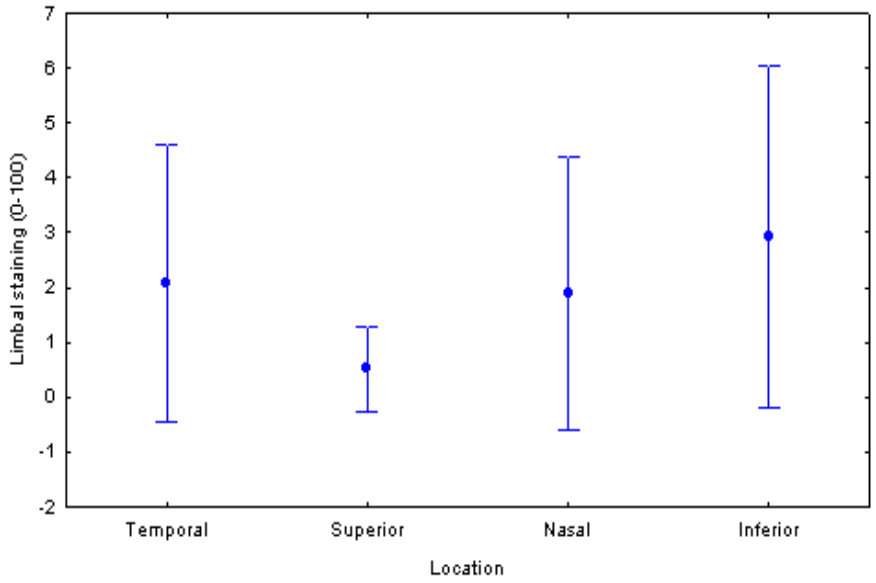

Figure 5-31 Limbal staining at temporal, superior, nasal and inferior location at 2 weeks (error bars represent mean ± SD).

A significantly higher limbal staining was observed with higher modulus lenses (RM ANOVA, p=0.231). A significantly lower limbal staining was observed in the superior quadrant compared to the other locations (RM ANOVA, p=0.024).

Conjunctival indentation

Conjunctival indentation, visualized with sodium fluorescein was rated on a scale of 0 (negligible) to 100 (severe) for each peripheral quadrant (nasal, temporal, superior, and inferior) and was averaged to derive global conjunctival indentation. The results of conjunctival indentation for each lens and locations are shown in Table 5.20.

On a 0-100 scale very little indentation was observed across all lenses, fits and visits. RM ANOVA could not be carried out because many variables were 0 and had no variance. Examining only the superior conjunctiva at the 2 week visit it was noted that there was a significant difference comparing the low and high modulus lenses. The low modulus lenses induced more indentation (ANOVA, p=0.047).

Table 5.20 Mean and standard deviation of conjunctival indentation at baseline and 2 weeks

Lens	Baseline				2 weeks			
	Temporal	Superior	Nasal	Inferior	Temporal	Superior	Nasal	Inferior
AA 8.3	0.00±0.00	0.00±0.00	0.00±0.00	0.00±0.00	0.86±4.64	3.45±9.07	0.35±1.86	2.41±7.51
AA 8.7	0.33±1.83	0.00±0.00	0.00±0.00	0.00±0.00	1.38±4.20	5.00±11.57	1.38±4.41	3.97±8.28

PV 8.3	0.33±1.83	0.33±1.83	0.33±1.826	0.00±0.00	1.67±5.47	1.33±5.24	0.00±0.00	0.17±0.91
PV 8.6	0.33±1.83	0.00±0.00	0.33±1.83	0.67±3.65	0.33±1.83	1.00±5.48	0.00±0.00	0.83±3.24

Conjunctival epithelial thinning (RTVue-OCT)

For conjunctival epithelial thickness, RM ANOVA was run with visit (baseline, 2 weeks), modulus (AA=low, PV=higher), fit (steep, flat), location -3 (inside the lens edge), 0 at apex, +3 (outside the lens edge) and quadrant (temporal, nasal, superior, inferior) as simple effects. The results of conjunctival epithelial thickness for each lens, location, and quadrant are shown in Tables 5.21 and 5.22 and Figures 5-33 to 5-35.

Conjunctival epithelial thickness was measured in three positions (1/3 mm steps) on either side of the lens edge and the difference in conjunctival thickness from the baseline at each study visit was calculated.

A significantly higher conjunctival epithelial thinning was seen with modulus, fit and location (RM ANOVA, p=0.003), significant conjunctival thinning was also seen with visit, modulus and quadrant (RM ANOVA, p=0.008). Interaction of visit, modulus, fit and location also showed a significant conjunctival epithelial thinning (RM ANOVA, p=0.018). Overall, steeper fitting AA lenses showed a significantly greater thinning at the 0.33mm inside location compared to the PV lenses for steep and flat fit (Tukey, p=0.003). Conjunctival epithelial thinning was greater in the inferior quadrant at baseline and 2 weeks with the AA lenses (Tukey, p=0.008). The conjunctival thinning was a change of 13.6% for the AA 8.3 and 13.3% for the AA 8.7 lenses compared to 12.8% with PV 8.3 and 3.37% with PV 8.6 from baseline to 2 weeks.

Table 5.21 Mean and standard deviation of conjunctival epithelial thickness at nasal (Nas), temporal (Temp), superior (Sup) and inferior (Inf) quadrant at baseline.

Lens	Loc	Position						
		-3	-2	-1	0	1	2	3
AA 8.3	Temp	54.06±13.9	49.88±12.3	51.43±15.3	60.74±12.9	50.64±12.4	55.90±12.8	56.85±14.0
	Nas	57.20±17.3	53.80±13.9	50.30±13.0	53.47±16.3	51.26±20.6	48.68±12.8	50.24±14.2
	Sup	63.49±18.2	66.35±22.1	59.70±19.7	63.32±25.4	59.22±20.9	61.87±19.4	57.80±18.1
	Inf	57.89±22.1	51.01±16.9	50.84±18.3	54.61±18.4	52.20±15.3	49.69±15.4	58.89±18.0
AA 8.7	Temp	49.38±12.4	46.50±14.4	52.97±15.6	54.99±15.1	45.93±15.0	53.86±17.8	59.56±23.5
	Nasal	62.02±20.6	55.57±14.8	50.69±12.5	48.39±10.4	49.40±13.8	47.74±11.9	51.31±16.2
	Sup	66.18±24.1	66.95±21.3	60.29±20.9	59.74±21.3	58.53±16.3	59.25±17.9	55.99±16.6
	Inf	58.99±18.6	58.00±18.1	52.79±16.0	60.91±18.7	58.14±20.6	56.96±22.6	54.81±22.2
PV 8.3	Temp	48.99±11.1	54.08±11.2	50.24±11.8	54.45±14.9	52.62±19.7	56.07±18.3	60.86±20.1
	Nasal	54.46±18.0	52.45±15.6	47.24±12.3	49.12±12.2	45.74±9.7	45.74±12.9	46.38±12.4
	Sup	56.13±16.0	59.22±14.1	59.23±17.7	58.66±20.7	56.21±20.7	58.30±15.2	62.19±19.5
	Inf	61.89±25.3	56.12±19.2	48.93±16.2	54.65±14.4	53.14±17.6	57.92±16.4	60.36±20.6
PV 8.6	Temp	57.19±12.8	54.12±13.2	51.40±11.6	57.13±14.3	50.42±13.7	56.49±14.8	60.39±19.2
	Nas	72.61±62.8	51.86±14.9	47.79±14.4	48.71±14.7	48.32±10.7	47.75±12.5	46.27±14.4
	Sup	66.94±20.2	68.03±25.8	64.82±24.5	60.23±16.7	58.70±20.1	60.44±24.2	75.64±28.3
	Inf	57.08±19.1	49.67±17.2	51.70±19.2	61.76±16.3	53.44±16.6	51.90±20.3	54.29±21.6

Table 5.22 Mean and standard deviation of conjunctival epithelial thickness at nasal (Nas), temporal (Temp), superior (Sup) and inferior (Inf) at 2weeks.

Lens	Loc	Position						
		-3	-2	-1	0	1	2	3
AA 8.3	Temp	52.88±37.8	52.19±37.2	49.67±36.7	51.22±35.9	50.36±36.1	48.97±36.3	53.09±35.8
	Nas	50.13±35.9	54.23±36.7	55.53±40.2	55.20±42.9	50.10±39.4	47.07±38.5	49.45±36.0
	Sup	70.20±41.8	62.06±39.7	59.11±38.5	56.47±36.8	52.66±37.9	53.87±39.8	60.45±34.1
	Inf	52.89±38.1	51.10±38.0	46.03±37.5	51.18±38.4	52.38±35.7	51.99±37.2	50.23±36.9
AA	Temp	52.42±34.8	51.94±35.0	51.29±35.3	47.74±36.3	50.74±37.8	45.23±36.6	49.85±35.7

8.7								
	Nas	53.56±37.5	49.93±38.6	49.37±36.9	45.49±38.6	45.82±36.9	46.04±36.6	43.86±38.5
	Sup	59.74±37.5	62.39±37.5	55.82±36.8	55.16±39.0	51.28±36.6	55.04±36.9	51.78±36.8
	Inf	50.26±36.6	52.05±38.9	49.26±37.4	46.96±38.2	47.94±38.2	48.73±38.1	50.06±38.9
PV 8.3	Temp	54.12±35.7	54.61±35.5	53.24±35.9	52.44±35.9	50.45±35.6	51.46±36.2	52.74±35.9
	Nas	50.15±36.9	46.18±37.5	46.47±37.1	46.29±38.0	46.96±37.4	47.05±36.6	45.73±37.5
	Sup	56.65±35.5	55.22±36.1	51.95±35.9	54.87±35.7	53.78±36.1	55.25±36.6	64.95±37.0
	Inf	49.16±37.6	48.23±38.3	50.26±37.8	49.31±37.8	50.00±37.7	46.51±37.1	50.96±36.1
PV 8.6	Temp	50.84±36.3	50.39±35.9	47.50±36.7	52.34±36.3	46.62±37.0	47.44±37.2	51.22±37.3
	Nas	51.53±36.4	48.19±36.0	47.70±38.8	49.67±38.9	46.40±38.5	44.10±37.7	46.52±36.8
	Sup	58.34±37.0	63.16±37.1	58.85±36.04	60.01±40.0	58.65±37.0	58.65±37.9	60.37±37.8
	Inf	54.66±35.9	53.79±37.1	50.74±37.3	51.40±36.4	57.30±38.9	53.49±37.1	58.62±37.2

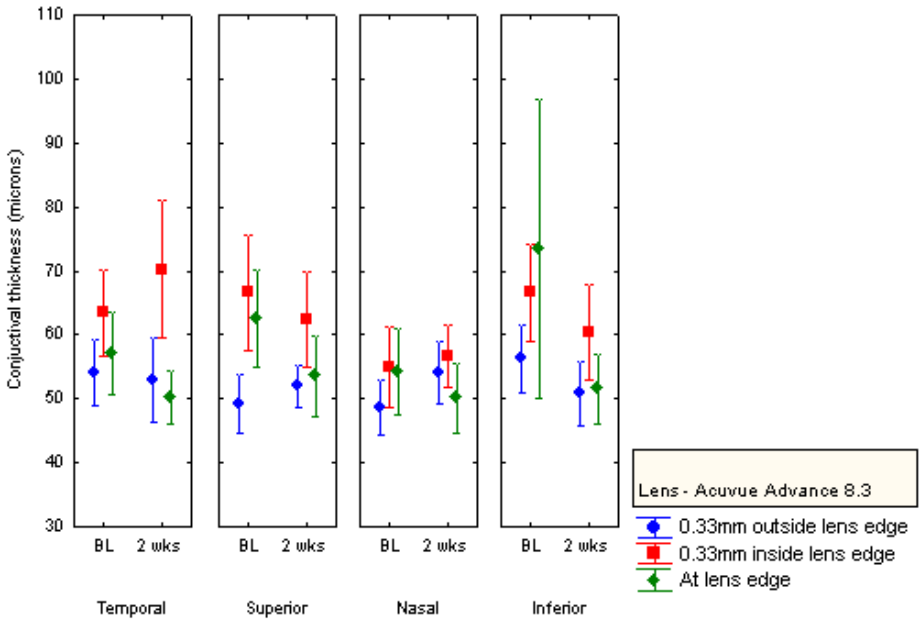

Figure 5-32 Mean conjunctival thickness -Acuvue Advance 8.3 at baseline and 2 weeks at temporal, superior, nasal and inferior conjunctiva (error bars represent mean ± SD).

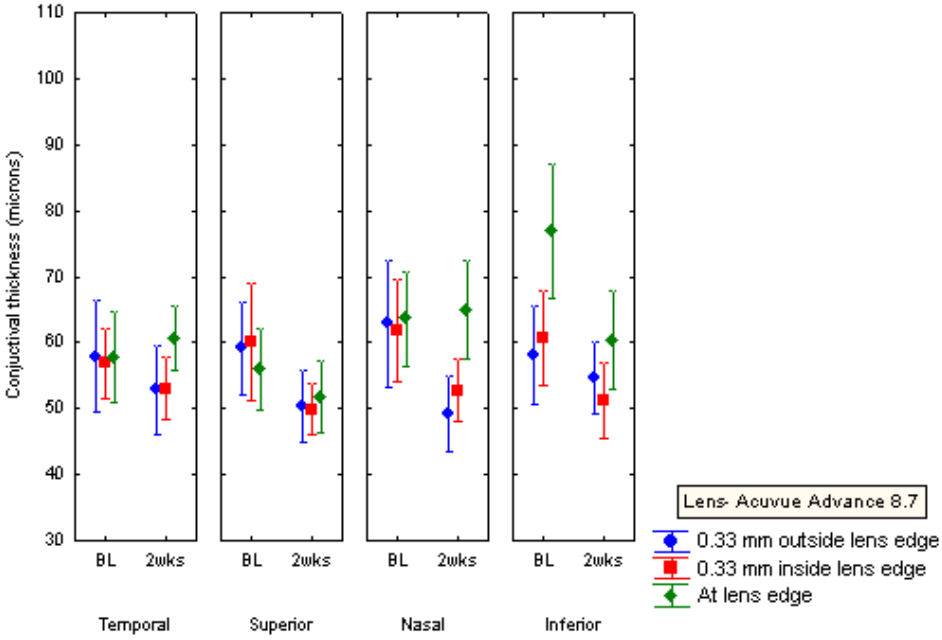

Figure 5-33 Mean conjunctival thickness -Acuvue Advance 8.7 at baseline and 2weeks at temporal, superior, nasal and inferior conjunctiva (error bars represent mean ± SD).

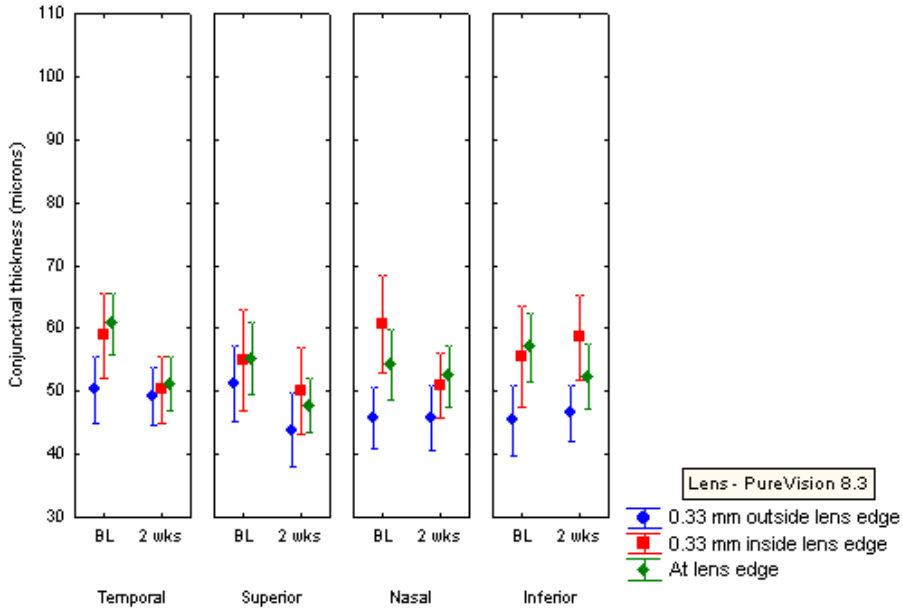

Figure 5-34 Mean conjunctival thickness- Purevision 8.3 baseline and 2 weeks at temporal, superior, nasal and inferior conjunctiva (error bars represent mean ± SD).

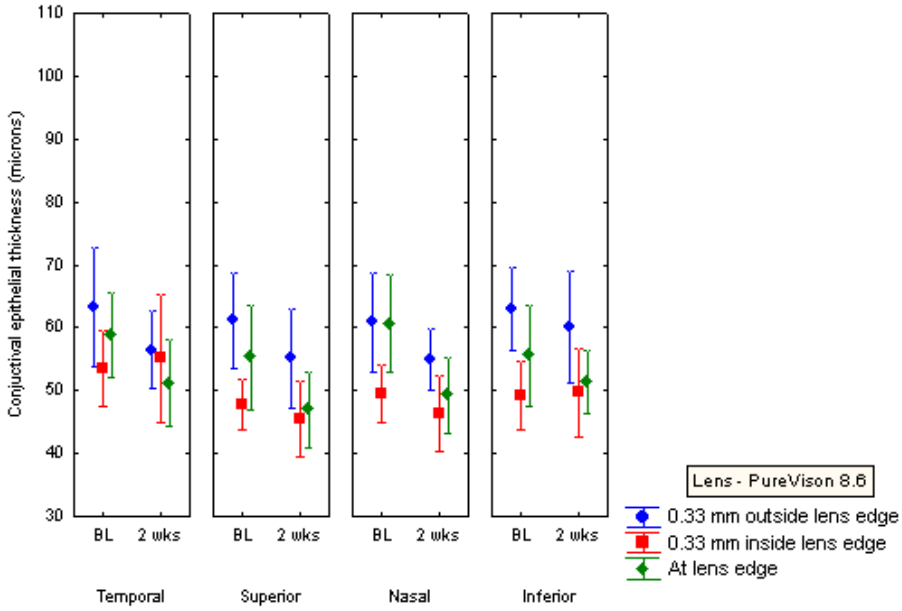

Figure 5-35 Mean conjunctival thickness- Purevision 8.6 baseline and 2weeks at temporal, superior, nasal and inferior conjunctiva (error bars represent mean ± SD).

5.6 Conjunctival blood velocity

Mean (±SD) velocity of conjunctival blood velocity contents ranged from 0.114± 0.04 mm/sec for the AA 8.7 lens to 0.195±0.07 mm/sec for the PV 8.6 lenses at the 2 week visit. The results of red blood cell velocity at baseline and 2 weeks are shown in Table 5.23 and Figure 5-36.

There was no effect of lens fit over time on blood velocity. No interactions were observed. There was a significant difference in blood velocity with lens types (RM ANOVA, p=0.001). There was a significant increase in blood velocity with higher modulus PV lenses compared to lower modulus AA lenses (Tukey, p=0.021).

Table 5.23 Mean and standard deviation of RBC velocity measurement (mm/sec) at baseline and 2 weeks.

Lens	Baseline(Blood velocity) (mm/sec)	2 Weeks(blood velocity) (mm/sec)
AA 8.3	0.156±0.15	0.153 ±0.11
AA 8.7	0.114± 0.04	0.127±0.05
PV 8.3	0.161±0.047	0.170±0.05
PV 8.6	0.173±0.29	0.195±0.07

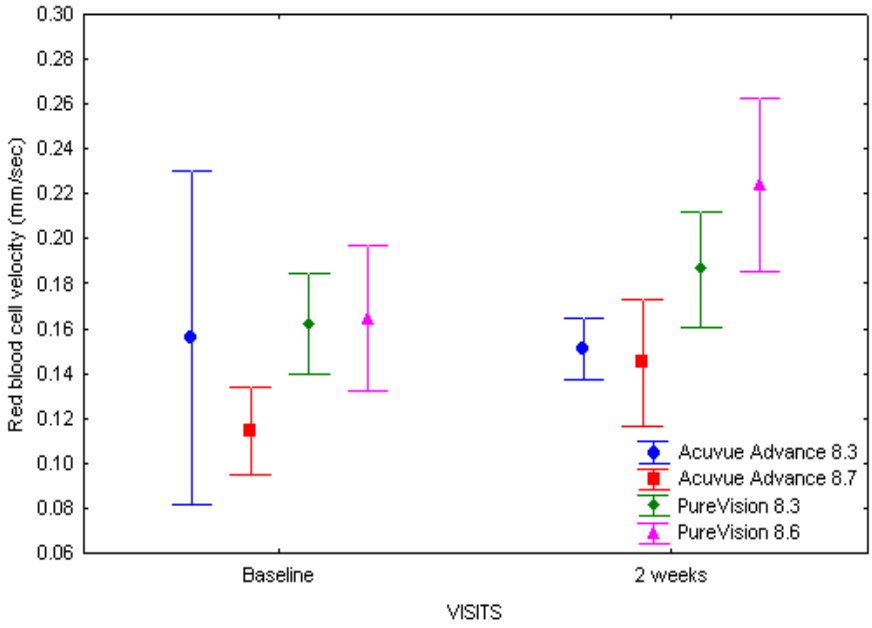

Figure 5-36 Mean red blood cell velocity (mm/sec) at baseline and 2 weeks with AA 8.3, AA 8.7, PV 8.3 and PV 8.6 (error bars represent mean ± SD).

5.7 Subjective ratings

For each subjective rating, RM ANOVA was run with visit (baseline, 2 weeks), modulus (AA=low, PV=higher), fit (steep, flat) and assessment (insertion, +2 hours, +6 hours) as simple effects.

Comfort

Participants rated comfort on a scale of 0 (very poor comfort) to 100 (excellent comfort). The results of comfort scales for each lens and each time point are shown in Table 5.24 and Figure 5-37.

Table 5.24 Mean and standard deviation of comfort ratings (0-100) at insertion, 2 hrs and 6 hrs at baseline and 2 weeks.

Lens	Baseline			2 Weeks		
	Insertion	2 Hours	6 Hours	Insertion	2 Hours	6 Hours
AA 8.3	90.97±12.94	84.04±36.45	81.76±36.38	83.28±36.54	90.72±12.01	80.17±37.99
AA 8.7	88.57±9.85	82.70±35.92	79.67±36.83	88.90±14.11	91.28±11.10	85.52±16.64
PV 8.3	87.86±9.07	90.14±9.31	85.14±10.79	87.11±12.23	87.89±11.12	80.96±15.03
PV 8.6	86.48±11.86	88.89±9.67	81.74±16.00	80.04±37.86	87.04±11.77	73.31±38.74

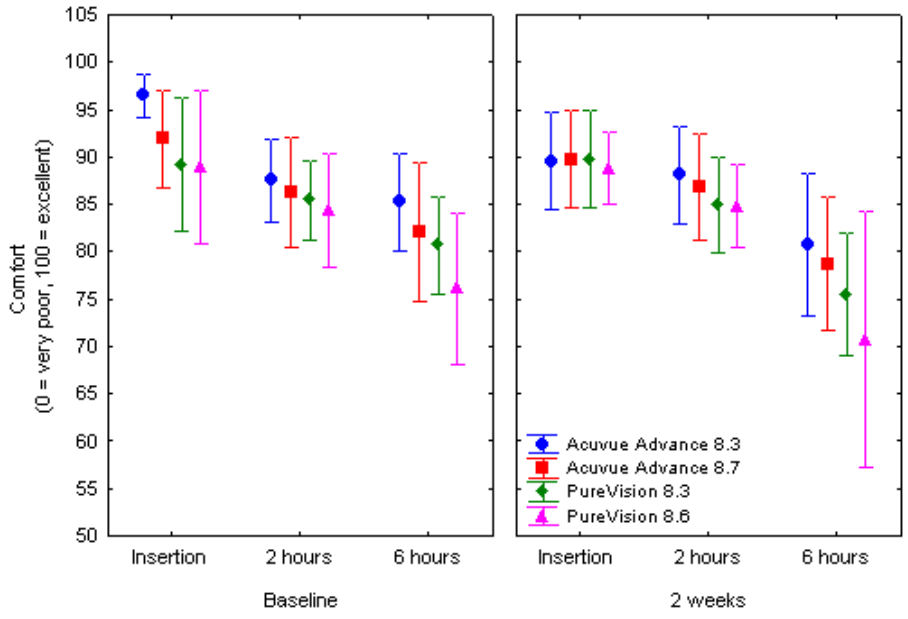

Figure 5-37 Mean subjective comfort at baseline and 2 weeks with AA 8.3, AA 8.7, PV 8.3 and PV 8.6 at insertion, 2hrs and 6hrs (error bars represent mean ± SD).

Lower modulus lenses were more comfortable overall when compared to lenses of higher modulus (RM ANOVA, modulus p=0.041). There was a decrease in comfort from the time of insertion to 6 hours later (RM ANOVA, assessment p=0.021). Overall the steep lenses were more comfortable at baseline compared to steep lenses at 2 weeks, and compared to flat lenses at baseline and 2 weeks (Tukey, all p<0.005).

Dryness

Participants rated dryness on a scale of 0 "very dry" to 100 "not dry at all". The results of dryness scales for each lens and each time point are shown in Table 5.25 and Figure 5-38.

Table 5.25 Dryness ratings (0-100)

Lens	Baseline			2 Weeks		
	Insertion	2 Hours	6 Hours	Insertion	2 Hours	6 Hours
AA 8.3	96.31±6.22	87.32±12.13	84.89±14.24	90.25±13.69	88.21±13.98	74.14±39.04
AA 8.7	91.90±13.63	86.45±15.84	82.17±20.10	90.10±14.03	87.79±14.44	79.034±19.22
PV 8.3	89.11±19.67	85.46±11.40	80.89±14.35	89.75±14.12	85.07±14.14	74.79±17.64
PV 8.6	88.89±22.67	84.44±16.21	75.67±22.26	89.96±10.31	86.27±11.40	68.08±38.22

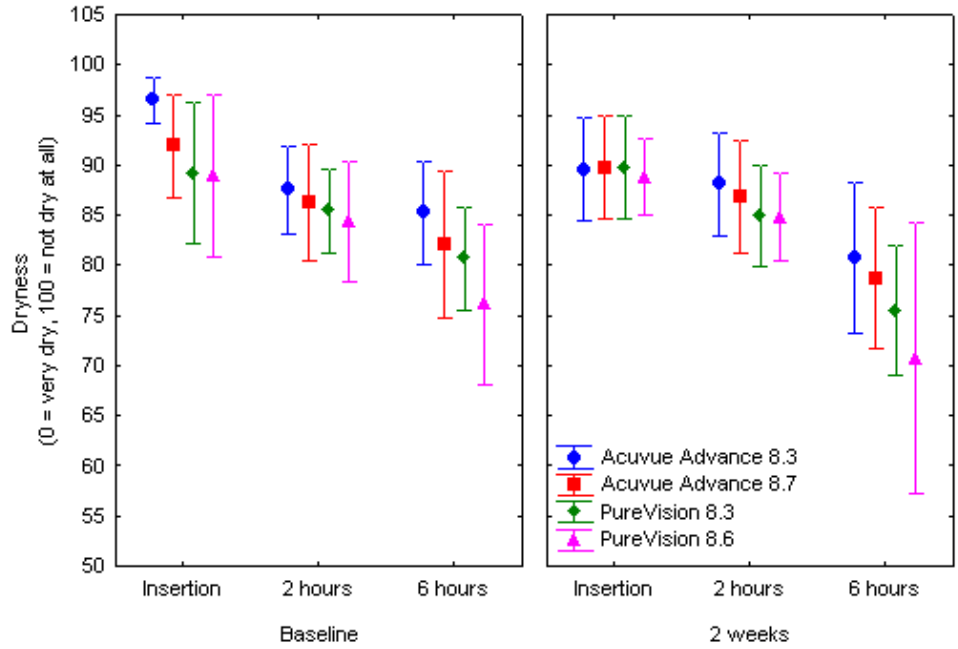

Figure 5-38 Subjective dryness ratings at baseline and 2 weeks with AA 8.3, AA 8.7, PV 8.3 and PV 8.6 at insertion, 2hs and 6hrs (error bars represent mean ± SD).

Lower modulus lenses were overall rated as less dry when compared to lenses of higher modulus (RM ANOVA, modulus p=0.007). There was also a significant difference in dryness at different times of assessment (RM ANOVA, assessment p=0.002) and showed increasing dryness between insertion, 2 hours and 6 hours (Tukey, all $p<0.05$).

Burning

Participants rated burning on a scale of 0 (no burning at all) to 100 (severe burning). The results of dryness scales for each lens and each time point are shown in Table 5.25 and Figure 5-39.

There is no significant difference in the burning ratings for any of the main effects or their interactions (RM ANOVA, all $p>0.05$).

Table 5.26 Mean and standard deviation in burning rating (0-100) at insertion, 2 hrs and 6 hrs at baseline and 2 weeks.

Lens	Baseline			2 Weeks		
	Insertion	2 Hours	6 Hours	Insertion	2 Hours	6 Hours
AA 8.3	98.14±6.02	93.32±18.64	93.11±18.92	96.46±6.98	97.14±5.57	98.86±6.10
AA 8.7	91.93±18.38	93.21±18.79	91.97±19.10	94.93±13.93	96.03±11.50	94.38±13.80
PV 8.3	96.11±10.64	97.71±3.91	94.50±10.38	94.14±12.44	94.93±13.07	93.68±13.82
PV 8.6	95.11±9.63	94.26±12.76	92.56±14.66	94.28±13.73	97.00±5.69	94.60±8.84

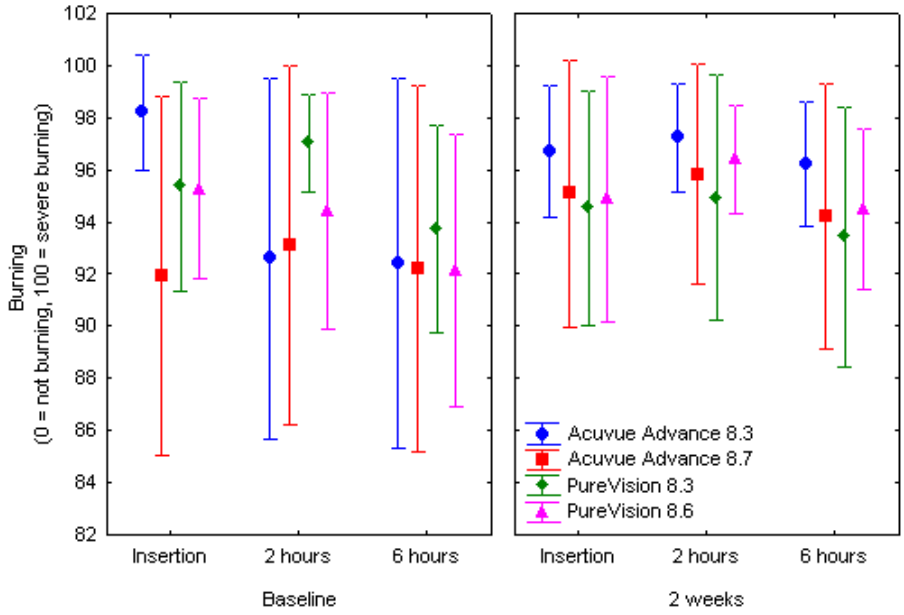

Figure 5-39 Mean subjective burning ratings (0-100) at baseline and 2 weeks with AA 8.3, AA 8.7, PV 8.3 and PV 8.6 at insertion, 2hs and 6hrs (error bars represent mean ± SD).

Subjective vision rating

Participants rated vision on a scale of 0 (poor vision) to 100 (clear vision) and the results in summarized in Table 5.27 and Figure 5-40.

Table 5.27 Mean and standard deviation of subjective vision rating (0-100) at insertion, 2 hrs and 6 hrs at baseline and 2 weeks.

Lens	Baseline			2 Weeks		
	Insertion	2 Hours	6 Hours	Insertion	2 Hours	6 Hours
AA 8.3	89.76±14.50	89.11±15.80	87.21±13.77	87.68±15.24	85.07±16.03	82.79±18.87
AA 8.7	86.87±18.39	88.10±15.60	86.90±13.49	86.24±15.40	84.52±16.24	81.83±20.40
PV 8.3	90.32±15.19	90.18±11.91	84.04±17.14	90.18±10.31	87.32±12.39	80.54±19.95
PV 8.6	92.23±10.61	91.78±9.36	85.85±14.01	88.40±15.05	86.92±11.97	81.08±16.61

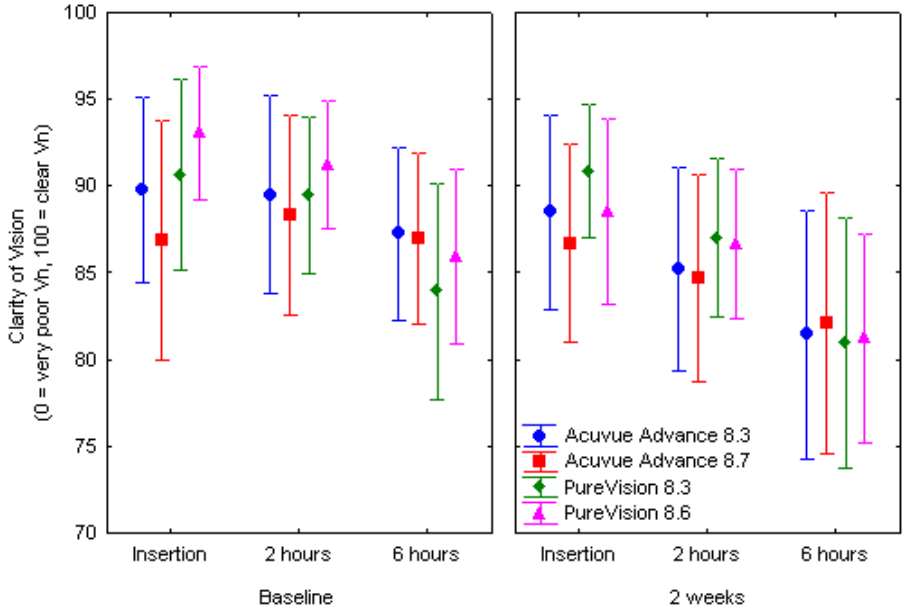

Figure 5-40 Mean subjective vision rating (0-100) at baseline and 2 weeks with AA 8.3, AA 8.7, PV 8.3 and PV 8.6 at insertion, 2hs and 6hrs (error bars represent mean ± SD).

The subjective rating of vision was significantly different dependent on modulus and the time after insertion of assessment (RM ANOVA, modulus*assessment p=0.047). The subjective ratings of vision did not change significantly between times of assessment with lower modulus (AA) lenses (Tukey, all

p>0.05). The rating of vision was highest for the higher modulus (PV) lenses at insertion and decreased 6 hours after insertion (Tukey, all p<0.05).

5.8 Correlations between sensory and clinical variables at the baseline and 2 weeks

In this experiment, sensory variables of end of the day discomfort, dryness, burning and vision at the baseline and the 2 week visit were compared to clinical variables (lens performance) using correlation statistics in order to see if we can predict the end of the day sensory variables.

Baseline clinical variables vs end of the day sensory variables

Baseline clinical variables were correlated to end of the day sensory variables for the baseline visit and the results are that there are a number of variables that are associated with the sensory variables measured at the end of the day. In wearers of the AA 8.3 lens, horizontal centration, topography along 90 degree meridian (4mm from apex), and blood flow were significantly correlated to the sensory variables of burning (r=0.53) ,discomfort (r= 0.30), and vision (r=0.43) at the end of the day. In AA 8.3 lens wearers there was a significant correlation between blood flow and end of the day discomfort (r = 0.54).

In lens wearers of AA 8.7, there were a significant associations between vision at the end of the day and lens movement, lens lag and horizontal centration (r=0.58, r=0.43, r=0.41 respectively). There was also a significant correlation between blood flow and end of day dryness (r=0.55) in these subjects.

Subjects wearing PV 8.3 and PV 8.6 showed mechanical effects, there were significant correlations between conjunctival compression, corneal thickness and epithelial thickness and end of the day discomfort (r=0.52), burning (r=0.57) and vision (r=0.52).

Number of variables correlated (clinical vs. sensory) for the 2 week visit was less compared to the number of variables correlating at the baseline visit. Corneal thickness measured with Visante^{TM} OCT along the 90 degree meridian and at the 3 mm vertical location had a negative correlation with the burning at the

end of the day (r=-0.36) with AA 8.3 lens wearers. PV 8.3 lens wearers showed a significant correlation between bulbar hyperemia in the superior quadrant and end of the day discomfort (r=0.40). There was no correlation seen in lens wearers with PV 8.3 and PV 8.6 lenses comparing the clinical and end of day sensory variables for the 2 week visit.

Clinical variables at baseline visit vs 2 week sensory variables

Correlations were also performed between the clinical variables measured at the baseline visit and 2 week sensory variables; there appeared to be a cluster of vascular effects. Subjects wearing AA 8.3 lens showed a significant correlation between superior limbal staining, superior bulbar hyperemia with end of the day dryness (r=0.46) and burning (r=0.44). Red blood cell velocity measurements in AA 8.3 lens wearers was correlated with dryness symptoms at 2 weeks (r=0.91).

In study participants fitted with AA 8.7 lenses there was a significant correlation between horizontal lens centration and end of the day symptoms of dryness (r=0.48) and burning (r=0.65). There was also a significant correlation between corneal epithelial thickness measured with the Visante^{TM} OCT and end of the day discomfort (r=0.56) after two weeks of lens wear.

In wearers of PV 8.3 lenses there was a correlation between horizontal lens centration and burning (r=0.62), superior bulbar staining and discomfort (r=0.53), superior limbal staining and dryness (r=0.60) and superior limbal hyperemia and burning (r=0.62). In wearers of PV 8.6 lenses there was a significant correlation with the lens fitting parameter of horizontal lens centration and vision (r=0.46) at 2 weeks.

Sensory variables at the baseline vs clinical variables at 2 weeks

Analysis was done to examine if there were any correlation between the sensory variables at the baseline and the clinical variables examined at 2 weeks. There was a significant correlation between tangential curvature data along the 90 degree meridian (4mm away from the apex) and discomfort (r=0.47), burning (r=0.53) and vision (r=0.37) for study participants wearing AA 8.3 lens. Those wearing AA 8.7 lens

showed a significant negative correlation of lens centration with discomfort (r=-0.37) and dryness (r=-0.51).

There was a significant correlation between sensation of burning at the baseline and lens lag (r=0.38) observed at the 2 week visit with study studies wearing PV 8.3 lens, there was also a significant correlation observed between the sensation of end of the day dryness and conjunctival staining (r=0.43) and bulbar hyperemia (r=0.41) observed at 2 weeks. Sensory variables like dryness and discomfort at baseline correlated with superior bulbar hyperemia (r=0.456) for study participants wearing PV 8.6 lens.

Clinical variables at baseline and clinical variables at 2 weeks

The number of clinical variables collected in the study at baseline and 2 weeks were compared to see if they correlate. Conjunctival compression observed in the superior quadrant at the baseline visit seemed to correlate with the conjunctival indentation ratings (r=0.47) and the superior bulbar hyperemia ratings (r=0.57). The horizontal centration with study wearing AA 8.3 lens correlated with the topographic change (r=0.53) measured at the 90 degree meridian (4mm away from apex).

Significant correlations were also observed with study subjects wearing AA 8.7 lens. A correlation was seen between superior bulbar hyperemia observed at the 2 week visit and superior conjunctival indentation (r=0.46) seen at the baseline. The conjunctival indentation observed superiorly at the 2 week visit had a significant correlation with the superior bulbar hyperemia observed at the baseline visit (r= 0.46). There was also a significant correlation between the lens movement at the baseline visit and the Visante epithelial thickness measured at the superior cornea along 90 degree meridian (3mm away from the apex). Lens movement and corneal topography along 90 degree meridian (4mm location away from the apex) at 2 weeks also showed a significant correlation comparing the lens movement (r=0.63) and topography (r=0.64) at the baseline visit for study subjects wearing AA 8.7 lens.

5.9 Summary of results

The results confirm that the flatter base curve lenses moved more than the steeper lenses. There was a significant difference for the two base curves of the AA lenses, the flatter lens having more movement. The primary gaze lens lag showed no significant difference in any main effects or their interactions. Lens on lag up-gaze was significantly different with fit, with flatter lenses showing greater lens lag with up gaze.

Horizontal centration results indicated that both AA and PV lenses shifted more centrally at the 2 week visit compared to the baseline. The shift was greater with the AA compared to the PV lenses. For vertical centration the flatter fitting lenses for both AA and PV decentred more vertically. The steeper AA lenses had the best centration in the vertical direction.

There was a significant effect of the lens modulus for lens tightness and centration where the lower modulus lens had more resistance with the push-up test and was less decentred, but the modulus difference was not seen for lens movement and lag. In vitro it was also observed that flatter AA had the least sagittal depth values when measured at the diameter of the contact lens (14mm). This indicates a better match with the corneal sagittal depth and therefore the best fitting relationship which is supported by the previous results. Both the AA and steeper PV lenses had a higher sagittal depth compared to the cornea at the same lens diameter, indicating the steepest fitting relationship.

Subjective grading for comfort and dryness were reduced for flatter fitting PV lens which did not align with the better fitting lens observation. This indicates that the subjects rated the steeper fitting AA as the most comfortable lens and the PV lens that moved the most were rated the least comfortable. Comfort and dryness perhaps appears to be associated with lenses that move the least. This observation is well supported in the literature. The lower modulus lens was also found to be more comfortable and less dry, which perhaps aligns with the previous findings on tightness and centration. There was no significant difference in burning with any of these lenses.

The results from the corneal topography showed that neither the steep nor the flat fitting lenses have any effect on the corneal tangential curvature at all the three locations along the five meridians. Perhaps, these results may be due to small sample size and short wearing period of two weeks. Another consideration is that the back surface curvature of the cornea could be changing instead of the front surface.

Results from corneal staining showed no significant difference with the lenses. This result perhaps indicates that non-preserved peroxide care system being used was gentle to the cornea. The steeper fitting lenses of AA and PV showed a significantly higher conjunctival staining at the 2 week visit compared to the baseline. Lenses that fit steeper did in fact correspond to more conjunctival staining. There was no lens effect on limbal staining; however there was trace amounts of limbal staining with the 2 weeks of silicone hydrogel lens wear especially in the superior cornea.

The mechanical effect of the lens edge of the silicone hydrogel lenses on the conjunctival tissue at the 2 week visit was assessed with the slit lamp. There was a significant difference in indentation comparing the low and high modulus lenses at the superior conjunctiva where the AA lenses induced more indentation compared to the PV lenses.

In addition, the lens edge effect of silicone hydrogel lenses on the conjunctival tissue at the baseline and 2 week visit was imaged and measured using the RTvue OCT by measuring the conjunctival epithelial thickness. There was a BOZR difference where the flatter PureVision lens induced the least amount of conjunctival epithelial thinning. The most thinning was found with steeper fitting Acuvue Advance lens in the inferior quadrant under the lens edge.

Hyperaemic response and corneal thickness changes with 2 weeks of silicone hydrogel lens wear were also observed. There was a significant interaction between fit and location for bulbar hyperemia. Nasal and temporal conjunctiva showed more bulbar hyperaemia. There were no significant bulbar hyperaemic effects under the lid at the superior cornea, seen with the two silicone hydrogel lenses with different

BOZRs. However, bulbar hyperemia was significantly reduced with higher modulus PV lenses at 2 weeks compared to the baseline at the temporal quadrant. Limbal hyperemia was significantly greater in temporal and nasal locations at the 2 week visit.

Total corneal and epithelial thickness profiles with daily wear of silicone hydrogel lenses for 2 weeks were measured. A significant difference in the total corneal thickness in the superior meridian was observed comparing the baseline with 2 weeks for steeper base curves of both lenses and flatter base curve of the AA indicating corneal thinning. Overall the AA steep lens caused more epithelial thinning compared to the AA flat lens and both PV lenses at the 2 week visit in the superior cornea.

There was a significant difference in the red blood cell velocity with lenses of different modulus. However, no difference of lens fit over time on blood velocity. Purevision lenses with higher modulus showed an increase in blood flow compared to the Acuvue Advance lenses. This perhaps indicates that the modulus or the stiffness of the contact lenses do play a role in reducing the blood velocity, the lens with the lower modulus and tighter fit did impede the blood flow the most.

The other important objective addressed in this study was to determine if we are able to predict end of the day discomfort and dryness using clinical predictive variables at baseline. Discomfort and dryness are the most commonly cited reasons for discontinuation of contact lens wear.[15;60;61] From the results of this study I found that when comparing the clinical and end of the day sensory variables at the baseline visit, there were many variables that showed significant correlations with the lenses used in this study. The clinical variables such as blood flow, horizontal lens centration, corneal topography, superior conjunctival compression seemed to affect the end of the day sensory variables like discomfort, dryness and vision. However, when comparing the clinical variables on 2 week visit to the sensory variables at the end of the day, there were very few variables that were correlated and this could possibly be due to an adaptation effect by the end of two weeks.

This study also provides information regarding the sensory effects such as end of the day discomfort and dryness at the end of two weeks and their ability to predict the clinical observations that were see at the baseline visit. The limbal staining, conjunctival staining, superior bulbar hyperemia, blood flow, horizontal centration all had a significant effect on discomfort, dryness and burning by the end of 2 weeks. This could be a very important relationship that contact lens practitioners who have been dealing with the problem of contact lens related discomfort and dryness over the years can use as indicators. Measuring blood velocity is not a common practise by contact lens practitioners due to the lack of clinical instrumentation and also due to the lengthy chair time. However, the measurement of blood flow in this study at baseline was highly correlated with the sensation of dryness at the end of the two week visit.

The results from this study also emphasise the point that grading of clinical variables such as limbal hyperemia, staining and the lens fitting characteristics are important. Increased staining and indentation effects on the cornea and conjunctiva would probably lead to more symptoms of discomfort with lens wear at the end of 2 weeks but this study did not confirm this association since the most comfortable lens possessed the poorest fitting characteristics.

Clinical variables collected at the baseline were also correlated to see if any change over time can be predicted. A number of significant associations were seen when correlating clinical variables at baseline to clinical variables at the end of two weeks for study subjects wearing AA 8.3, AA 8.7, PV 8.3 and PV 8.7. AA 8.3 was the tightest fitting lens and the conjunctival epithelial thinning measured superiorly with this lens at the baseline visit had the most correlation to clinical variables such as superior bulbar hyperemia, superior conjunctival indentation at the 2 week visit. The lens centration also seemed to affect the tangential curvature measurements of the cornea at 2 weeks.

Study subjects wearing AA 8.7 lens had shown a significant correlation to the lens fit such as lens lag and movement to the physiological changes to cornea and conjunctival such as superior limbal staining,

limbal hyperemia and superior bulbar hyperemia at the end of 2 weeks. Superior conjunctival indentation observed with these lenses seemed to have a significant correlation to bulbar hyperemia in the superior quadrant and this could be possible due to the mechanical effects and also the fitting relationship under the lid with the contact lenses. The loosest fitting Pure Vision 8.6 lens correlated significantly to horizontally lens centration at the end of 2 weeks of lens wear. This indicates the importance of choosing the lens of the correct parameters for trial fitting and if one assumes that the lens would center better by the end of two weeks, the poor centration may still be a cause of discomfort depending on the material used. Systematic associations of blood flow with vascular and staining effects was seen at the end of 2 weeks with all the lenses indicating the potential hypoxic and mechanical effects with the lenses.

Chapter 6

General discussion

The experiments in this thesis cover a wide range of topics relating to optical coherence tomography (OCT) calibration and repeatability and soft lens fitting characteristics including their physiological effects on the bulbar conjunctiva. Contact lens edge characteristics were examined using a custom made ultra-high resolution OCT. Variables such as meridonial corneal and epithelial thickness, curvature changes and blood velocity measurements were also studied in silicone hydrogel contact lens wearers.

The clinical application of theses lenses that is described in chapter 5 demonstrates that prescribing contact lenses with the appropriate material, lens dimensions and wearing modalities is the key to successful contact lens wear but the most critical factor is the optimization of lens fit. Sub optimal fit or poorly fitting lenses can alter ocular physiology and can contribute to lens discontinuation.[1-3] This thesis examined parameters such as base curve, modulus and lens edge designs and investigated their effects on a few specific aspects of the ocular physiology and compared it to subjective comfort.

Slit lamp biomicroscopy has been the standard technique for evaluating lens fit.[4;5] In this thesis I have demonstrated the use of wide range of imaging techniques that can be used to examine some components of the physiological changes of the anterior segment. Commercially available optical coherence tomographers were used in quantitatively characterizing the lens fit and to look at the topographic alteration in the conjunctiva with lens wear. A custom built ultra high resolution OCT was also used in the study. The physiological effects of corneal swelling and topographical curvature changes were also assessed.

In order to measure the lens effect on the corneal thickness using the Visante™ OCT, the instrument needed to be calibrated and assessed for repeatability. In addition, the experiment that was done determined that there are differences in measurements among optical devices that are used to perform pachymetry. Corneal thickness measures can be repeatable but might not be accurate. It is very important to have accurate measures of corneal thickness when physiology is disrupted normally (e.g. hypoxia under the lid, in numerous pathological conditions and pre and post surgery) and a number of devices are used to assess theses effects. This study examined at the calibration of the Visante™ OCT and Zeiss–Humphrey retinal OCT II and optical pachymetry. Central thickness of semi rigid lenses with known physical thicknesses and with a refractive index similar to that of the cornea (n=1.376) was measured with the two OCT's and they were compared to measurements with a mechanical gauge and the pachymeter. Calibration equations were derived using these comparisons, so that the difference between the instruments could be eliminated. The method used was proposed by Moezzi et al. [6] The importance of having accurate (post-calibrated) corneal thicknesses when measured with any of these devices is that they are necessary for measurement of thickness in case of corneal hypoxia[7;8] in CL wearers and in diabetics[9] and for accurate IOP measurements,[10] in cases of pre-surgical patients for refractive surgery,[11] pre[12] and post-surgical[13] keratoconus patients and contact lens wearing patients for ortho-keratology among many others.[14]

Many instruments that are being used to measure corneal thickness cannot be calibrated. Part of the difficulty might be in imaging the posterior surface but the refractive index of the cornea is a variable common to all techniques for measuring corneal thickness by optical methods, that needs to be controlled.[15] Therefore, a remedy, at least for the optical measurement techniques, would be to calibrate the instruments using a transparent material with a similar refractive index as the human cornea in the form of a contact lens (that is with a visible posterior surface).[6]

Although previous studies show regional variation of corneal refractive index as well as variation of refractive index between different layers of the cornea,[16] a refractive index of 1.376 is regarded as the overall corneal refractive index.[17-22] Using reference lenses with refractive index of the cornea (1.376) allows rapid and simple calibration and cross calibration of these optical instruments for measuring central corneal thickness. This method demonstrates that in measuring lenses within the "average" corneal thickness range (from 375 to 550 microns) the instruments are quite accurate, but, with thicker or thinner reference lenses the error is increased. Thinner measures are over-estimated and thicker measurements are under-estimated with the Visante™ OCT (Figure 2-10). Possibly the internal calibration of the Visante using its own solid calibration sphere is limited in the range of accuracy. These central thickness differences outside this average range can be clinically significant if decisions regarding refractive surgery are being made and when correcting the measurement of IOP for corneal thickness.[23;24] On the other hand, when decisions are made about eligibility for surgery using a thickness criterion, it is not at all clear that $\pm$ 20 microns is used to define a range of uncertainty; it might be considered to be much less.[25]

Dunne et al. examined the inaccuracy of the Visante™ OCT using ray tracing of contact lenses with a refractive index of 1.493 and centre thicknesses ranging from 0.3 to 0.7mm (in 0.1mm steps). Their results indicated that there was little variation in accuracy of thickness although other errors were reported.[23] Our approach was different to theirs in that there were differences in measured/assumed refractive indices. Also how the images were acquired differed; they used the Visante's anterior segment map (with custom software callipers) while I used the high resolution map (with custom software).

The results from chapter 2 also addresses a perhaps important point that attention should be given to corneas that are thinner or thicker than average as in cases of keratoconus and post-refractive surgery as well as post-penetrating keratoplasty. These measurements may not be accurate when acquired using the Visante, OCT II and optical pachymeters.

Commercially available anterior segment OCT's have been used for measuring the corneal and epithelial thickness,[26] diurnal variation in corneal thickness,[27] tear film thickness, [28] corneal thickness pre and post refractive surgery [29] and also to assess corneal morphological effects of corneal edema.[30]

In order to assess the repeatability of the Visante OCT a second experiment was done where the measures of repeatability of two commercially available TD-OCT (Visante™ OCT and Zeiss–Humphrey retinal OCT II adapted for anterior segment imaging) were assessed. Corneal and epithelial thickness across 10 mm of central, temporal and nasal cornea was measured using the two OCT's and repeatability of the Orbscan II was also included in the study. These measurements were repeated on two days and each individual measurement was repeated three times and averaged.

The mean corneal thickness with the Visante™ OCT was the most repeatable at the corneal apex, nasal and temporal cornea. The epithelial thickness was found to be less repeatable compared to the total corneal thickness. In addition to this, the study also demonstrated the importance of averaging multiple measurements to improve the repeatability of the thickness measures. This was also suggested by Sander et al. who showed that OCT averaging enables recovery of detailed structural information about the retina and averaging helps in improved imaging of the retina and also that averaged images correlate well with known pathology.[31]

The average corneal thickness with the OCT II at the apex in the studies reported in chapter 2 and 3 was 520±25µm and it was very similar to the results obtained by Muscat et al. and Bechmann et al. of 526±28µm and 530±32µm respectively.[32;33] The first study by Muscat et al. that evaluated the repeatability of corneal thickness using OCT II found an CCC of 0.998 which is comparable to the results of my study.[32] The repeatability of the central corneal thickness in my study was similar for all the three instruments, with the Visante™ OCT showing the highest CCC of 0.99 similar to the results in reported recent studies with CCC's ranging between 0.962[34] and 0.998.[35] The range of CCC between the three instruments in my study was from 0.97 to 0.99.

The epithelial thickness repeatability (CCC) of the Visante™ OCT and OCT II was of 0.81 and 0.70. The nasal and temporal locations measured by both the instruments were less repeatable compared to the apex with CCC values ranging from 0.52 to 0.58. The results from chapter 3 were that peripheral corneal pachymetry measurements were more difficult to repeat than apical ones. Some of the previous studies have also shown similar results. Li et al. reported the thickness measurements are thinner and are not reliable when measured in a peripheral zone of 7mm diameter or greater.[36] Sin et al. have also reported central corneal epithelial thickness repeatability to be much lower compared to the corneal thickness measures and have emphasised the importance of averaging images and the suggested increasing image numbers to overcome poor repatability.[26]

Chapter 3 showed that there was good repeatability of corneal thickness measures between days (test/retest) at all the locations with the Visante™ OCT, OCT II and the Orbscan II ™. The best concordance (estimated using CCC) between the Visante™ OCT and the OCT II for central corneal thickness on day 2 was 0.97. The range of between-device central corneal thickness CCC's was 0.66 to 0.97. The epithelial thickness repeatability was also relatively poor when compared with the corneal thickness and clinicians and scientists could perhaps be a little more careful when interpreting these measurements and take the variability into consideration.

Examination of the features of the lens edge and their interaction with the conjunctival surface was performed using the ultra-high resolution OCT (chapter 4). The conjunctival displacement observed at the edges of the contact lenses when imaged with the OCT imagers may be real or an artefact of the imaging system. This study used an ultra-high resolution OCT system to acquire two dimensional images of edges of hydrogel lenses with varying refractive indices. To examine this displacement effect of the refractive index change from air to contact lens material, images of lens edges were taken on continuous surfaces (e.g. glass reference sphere, rigid lenses (n=1.376)) and also on the human conjunctiva. ImageJ software was used to measure the physical and optical thickness at the edges of these lenses and displacement was

measured. There was a range of displacements from 7.0±0.86 µm for the Air Optix Night to 17.4±0.22 for Acuvue Advance when measuring the lens edges on the glass/plastic. The results from this study have implications since there is very little literature regarding the lens edge and conjunctival interaction and the mechanical and physiological changes such as indentation, staining and epithelial folds caused by the lens edge and lid interaction. Results from Chapter 3 emphasised that it is important to understand that the morphometric characteristics of tissue imaged at the lens edge are not always simple attributes of the tissue alone, but are also affected by the imaging device and that the displacement observed is a property of the thickness and the refractive index of the contact lens edges.

Studies have shown that the most common reason for lapsed contact lens wear is discomfort.[3] The patient's experiences of inadequate comfort may have arisen from a variety of sources. Among them, one of the most important is inappropriate lens fit.[1;37] Silicone hydrogel lenses have improved the physiological responses to contact lens wear [38-40] but not much has been done to look at the conjunctival tissue responses with these lenses. The study reported in chapter 4 showed that care is needed when interpreting the indentation imaged using OCT or optical imagers.

The results from chapter 5 confirm those from the previous studies; soft contact lenses rarely conform to the ideal fit described in fitting guides.[41-43] Subjective lens movement was reduced in eyes fitted with the steeper base curves (BOZR) of both the lenses. PureVision (PV 8.6) appeared to be flat and had the most lens movement at baseline and at 2 weeks and Acuvue Advance (AA 8.3) moved the least. Lag on up gaze and lateral gaze are considered to be sensitive indicators of soft contact lens fit.[2;4;41;44] On up gaze, both flatter AA and PV lenses showed a significant lag suggesting a flat fit.

The assessment of fit by the push-up test has been reported to provide useful information about lens fit especially for tight fitting lenses compared to loose fitting lenses.[2;4;45] There was a significant difference in tightness with the four different types of lenses. Wearers of AA 8.3 experienced increasing graded tightness of lens fit at baseline and 2 weeks indicating a steep fitting lens and wearers of AA 8.7 appeared

to have the lowest graded lens tightness. Horizontal and vertical lens centration helps in the interpretation of the lens fit and is more likely to indicate a loose and tight fitting lens on the eye where the loose fitting lens is generally more decentered.[2;4] There was a significant difference in horizontal lens centration among the wearers of all lenses over time. Both AA and PV lenses shifted more centrally at the 2 week visit compared to the baseline and the AA lens resulted in better centration.

Central corneal curvature measurement has been used to select the appropriate soft contact lens base curve[2;45;46]. However, several studies have confirmed that the optimal base curve does not correlate with central corneal curvature.[47;48] Young et al. have reported that the relationship between the sagittal depth (sag) of the lens and the sagittal depth of the anterior segment of the eye at the lens diameter determines the fit of the lens.[46] It has been reported that if the lens sag is greater than the ocular sag the lens will fit steeper and so we need a steeper base curve, and if the lens sag is smaller than the ocular sag the lens will fit flat.[46] There are reports that suggest that not only sagittal depth but other ocular dimensions such as corneal asphericity and diameter will also affect soft contact lens fit.[46;49;50] For successful contact lens wear and to reduce the sagittal differences between the lens/cornea it is important to choose the lens with appropriate parameters and this can be done by matching the corneal sag and the lens sag.[51-53] I used Visante™ OCT to measure the ocular sagittal depth of eyes fitted with the two different types of silicone hydrogel lenses at the lens diameter. The sagittal depth and the diameter of the contact lenses were measured using the Chiltern (Optimec) metrology instrument. Despite hypotheses about the ocular and lens shapes characterised by sags being important (e.g., flat lenses are more uncomfortable), these ideas were not generally supported and only in wearers of steeper AA lenses was there any correlation with comfort (albeit relative poorly).

Silicone hydrogel lenses have higher modulus compared to the conventional hydrogel lenses and this is perhaps one of the reasons why the fit of the silicone hydrogel contact lenses can alter the corneal topography.[42;54;55] In this thesis I examined whether these stiffer lenses induced a change in ocular

topography. Regional curvature measurements have been used in fitting rigid lenses but are not a common practise in soft lens fitting. In the present study I evaluated the effect of base curve and modulus on changes in corneal tangential topography.[56;57]

Tangential topographical data at 2mm, 4mm and 6mm and along 5 meridians (0, 45, 90, 135, and 180) degree meridian was analysed. I examined areas under the upper lid because it was hypothesised that the putative mechanical and hypoxia effects in this region might be associated with structural and sensory changes. There was no change in the topography from baseline to two weeks any of the sensory effects were not occurring because of the changes to the surface.

Corneal thickness was monitored at baseline and at the 2 week visit. I used the Visante™ OCT to examine meridonial corneal and epithelial thickness in contact lens wearers. The cornea is hypothesised to be in a chronic state of hypoxia under the eyelid and especially the upper eyelid and there is limited evidence of how the corneal structure is influenced in this region.[58;59] This experiment addresses this issue by using high resolution OCT imaging of the corneal structure and examining if there are any changes to the corneal and epithelial thickness while wearing daily wear silicone hydrogels.

Doughty et al. reported in a study using meta-analysis that normal value of central corneal thickness (CCT) in adult human eyes is 0.535 mm which is higher than the 0.518 mm that was considered normal by Mishima.[60] They reported CCT data from literature over a period of 30 years. Overall, studies using slit lamp based pachymetry were reported to show a marginally lower CCT values (average 0.530mm) compared to ultrasound based studies (average 0.544).[61]

Contact lenses have been reported to alter corneal thickness.[62;63] Short- term contact lens wear for a period of 3 hours to 3 months is associated with an increase in corneal thickness [64-68] Few studies report a decrease in corneal thickness in individuals wearing contact lenses for several years.[69;70] After 18 months of wearing contact lenses, corneal thinning was seen in some patients and corneal thickening was seen in others.[71] Doughty et al.[61] summarized data from various studies and reported that an 8% increase in CCT

was expected after wearing hydrogel lenses.[72-76] A larger increase in CCT was reported with overnight wear of contact lenses.[77-80] The average CCT was reported to be 0.532 mm from studies where baseline and experimental values were measured with contact lenses.[75;79;81]

I examined corneal and epithelial thickness in participants wearing silicone hydrogel lenses (Acuvue Advance, PureVision) for a period of two weeks on a daily wear basis. Corneal and epithelial thickness was measured at baseline and after 2weeks of lens wear. Meridonial thickness was measured along horizontal and vertical meridian and at 3 points along each meridian (-3 mm, Apex, and 3 mm). There was a significant difference in the corneal thickness when comparing the silicone hydrogel lenses. There was significant corneal thinning along the superior meridian, at 2 weeks compared to baseline, in wearers of both steeper lenses and in wearers of the flatter AA. In wearers of the flat AA lenses there was more epithelial thinning at the 2 weeks in the superior cornea. However, a limitation of the corneal thickness measurements is perhaps that the baseline measurements were found to be different with the two lenses between the two phases indicating that perhaps a two day washout was not sufficient. In addition, however because the paired statistical tests used examined the mean differences (and not the difference between the means) and these were significant, perhaps in this instance the baseline difference is relatively unimportant.

It has been reported that some degree of corneal staining occurs with contact lens wear.[82-84] The prevalence of corneal staining is reported to be 4 to 79% in normal, non-contact lens wearing patients.[85-87] Factors that are related to corneal staining include the contact lens materials, daily wearing time, care system and contact lens deposition.[84;88] Studies on wearers of hydrogel contact lenses have suggested that front surface dehydration of the lens leads to an absorption of liquid from the post-lens tear film and subsequent corneal staining. [88;89] However there are reports that high water content and silicone hydrogel contact lenses are protective against hypoxia because they provide high oxygen levels to the cornea, which might perhaps help in maintaining epithelial cell viability.[90;91] There is also evidence of the

presence of corneal staining due to the interactions of the silicone hydrogel lenses and preserved care systems.[92;93]

I found nearly all corneal staining was micropunctate as indicated by the low average staining scores. There was no significant difference between lenses and over time in the global staining scores (GSS). It has been reported that contact lens deposition is related to corneal staining and this is perhaps mainly due to the disruption of the mucin layer of the tear film. There was mild to moderate deposition on the contact lens surface and therefore, perhaps the reason in my thesis that there was so little staining was that lens deposition was low or the subjects wore the lenses on a daily wear basis. The use of an unpreserved peroxide system could also have contributed to the lack of corneal staining.

Studies have reported that the most common reason for lapsed contact lens wear is discomfort.[3;94-98] Among the many reasons for discomfort with silicone hydrogel lens wear, the physiological change to the conjunctival tissue and its response might be an important factor to consider but this has not been studied extensively.[99-101] The conjunctival staining and indentation are common conjunctival changes during contact lens wear.[102;103] and the wearers are usually asymptomatic. The conjunctival indentation is seen as a thin band of fluorescein pooling. Studies have also reported the conjunctival histological changes with soft contact lens wear with dry eyes.[104-106]

It is believed that perhaps due to the interaction of the lens edge with the ocular surface, particularly in continuous wear of higher modulus silicone hydrogel lenses the superficial layers of conjunctival cells delaminate.[107] Lofstrom and Kruse[107] reported that of the 32 eyes fit with lotrafilcon A or balafilcon A contact lenses, 11 (34%) were found to have CEF (conjunctival epithelial flaps). The authors reported that the majority of CEF was observed in subjects wearing the lotrafilcon A lens, and that this lens edge had a chisel-shaped edge design, compared with the rounded edge design of the balafilcon A lens. I did not observe any conjunctival epithelial flaps in this study perhaps due to shorter duration of lens wear and also that the lenses were worn on a daily wear basis.

There are no published reports of the conjunctival epithelial thinning underneath and adjacent to the contact lens edge. In this study I measured the conjunctival thickness adjacent and beneath to the contact lens edge to see if the mechanical pressure had any effect on the conjunctival epithelial thickness. The most thinning was found with the tighter fitting AA lens under the lens edge in the inferior quadrant where Kessing's space may be minimal and the least amount of thinning was with the flatter fitting PV lenses. These results indicate that it is not modulus that perhaps causes conjunctival epithelial thinning but that there is statically significant association between steeper lens fit instead. This result does align with the conjunctival staining and indentation found with AA lenses.

Subjective grading of the conjunctival indentation and staining is commonly carried out by using slit lamp microscopy with yellow filter.[108-110] Recent evidence suggests a relationship between conjunctival staining and dry eye,[111] contact lens designs and fit[112-114] and contact lens care systems.[115] Conjunctival staining is observed in soft contact lens wearers.[103;107;111;114] Lakkis et al. reported 62% of contact lens wearers had a greater than grade 1 conjunctival staining (0-4 scale) compared to 12% in non-contact lens wearing group. They also reported that conjunctival staining was associated with symptoms of dryness and itchiness.[112] Du toit et al. studied 150 presbyopes and they reported that 9% had conjunctival staining greater than grade 1 (0-4 scale) and this increased to 20% with soft contact lens wear.[116]

The aetiology of the conjunctival staining may perhaps be related to unstable tear film and dry eyes.[89;117-119] Lens edges, contact lens modulus and inappropriate lens fit can also cause lens related conjunctival staining.[107;120] In the study reported in chapter 5, there was an increase in the conjunctival staining with all the lenses at the 2 week visit compared to the baseline. The wearers of steeper fitting lenses of AA and PV showed a significantly higher conjunctival staining for all the lenses at the 2 week visit.

Conjunctival indentation is most likely to be related to improper lens fit, edge design of the contact lens and modulus of the lens material. Pressure from the upper lid during blink might result the indentation to

be most commonly seen in the superior quadrant.[97;107;121;122] Indentation might also be caused by individual factors such as loosely adherent conjunctiva.[107] The results from my study indicated that conjunctival indentation is related to the tightness of the lens and not the modulus. It appears that perhaps the tight edge of the lens forms an imprint on the bulbar conjunctiva where as a flatter lens edge sits parallel to the bulbar conjunctiva not inducing conjunctival indentation.

Previous studies that indicate that stiffer lenses with higher modulus of elasticity produce greater conjunctival indentation and other conjunctival effects such as conjunctival flaps are reported only in extended wear studies.[121-123] In this daily wear study, wearers of galyfilcon A (Acuvue Advance) lenses had higher rates of lens indentation compared to balafilcon (PureVision) lenses which are stiffer. Therefore, the modulus of lens is perhaps not a factor in daily wear in causing conjunctival indentation.

Limbal staining may be due to a poor lens cornea fitting relationship that might be related to the lens base curve and also the diameter. In this study, a trace amount of limbal staining was observed in the superior quadrant in wearers of higher modulus lenses.

Perhaps the most noticeable changes seen of the eye wearing contact lenses are those that impact the bulbar and limbal vasculature. Various lens related factors have been reported to affect the vasculature including hypoxia,[124-126] poorly fitting lenses,[127] mechanical effects,[124] edge suction and trauma [128]Aakre et al.[129] studied a group of 49 contact lens wearers wearing a variety of low transmissibility hydrogel lenses on a daily wear basis, and 30 of them were refitted with either with lotrafilcon A or balafilcon A on a continuous wear schedule and the rest of them were asked to continue with their habitual lens wear. The results were an increase in bulbar hyperemia in the low transmissibility lens wearing group.

I evaluated bulbar and limbal hyperemia of 30 neophytes after 2 weeks of daily lens wear. There was a significant increase in bulbar hyperemia at the nasal and temporal locations for both baseline and 2 weeks with AA (lower modulus) and PV (higher modulus) lenses. However, at the temporal location the bulbar

hyperemia was significantly reduced in the temporal location perhaps due to the higher oxygen transmission of the lenses. Limbal hyperemia has been also associated with wearing low oxygen transmissibility lenses there is a recent report that 31% to 35% of contact lens wearers had limbal redness of grade one or greater, compared to 5% of non lens wearers.[130] Limbal redness has also been reported to increase during sleep and it has also been shown that using low oxygen transmissibility lenses increases limbal redness after only 4 hours, and this persisted until the next morning. Papas et al. reported a study using nitrogen-filled goggles to reduce the oxygen availability to the anterior eye and they demonstrated that limbal vasculature responded to the hypoxia.[131]

I examined that there was no significant difference in limbal hyperemia while wearing steeper and flatter base curves lenses and also there was no effect with lens wear of higher and lower modulus materials. In my study I found an increase in limbal hyperemia over the 2 weeks in the nasal and temporal locations only. However, since this study is acute (2 weeks) it might be of interest to see if the hyperemia increased significantly with prolonged use of lenses and whether it was the lower Dk of AA or some other difference that was responsible for this reddening effect.

Red blood cell velocity was measured. There are reports of strong associations between hypoxic effects of the contact lens wear and bulbar and conjunctival hyperemia.[125;131-133] Contact lens wear has been associated with initiating neovascularization or growth of new blood vessels and this is perhaps due to chronic hypoxia, injury and inflammation.[134] Vessel dilation is also hypothesised to be one of the causes of new vessel growth and has been shown to decrease blood flow and blood velocity.[125] The chronic level of vessel dilation in soft lens wearers is a cause for concern as persistent dilation of the limbal vessels may be a precursor to new blood vessel growth. In this study I showed a decrease in the red blood cell velocity in wearers of the lower modulus AA lenses with both base curves. This result suggests that mechanical compression on the conjunctival tissue due to a tighter lens with lower modulus might have an effect on the blood velocity. This further supports the evidence that the contact lens may perhaps

interfere with the content of the blood vessel. However, increasing the oxygen permeability of contact lenses and perhaps changing the lens design may reduce the eye's vascular response.[135;136]

Assessment of subjective comfort relating to contact lens wear can be made using descriptive items [137] and variety of scales including visual analogue scales (VAS).[138-142] The subjective assessment of contact lens wearers' symptoms such as ocular comfort and quality of vision is as important as the clinical assessment by practitioners. Visual analog scales have been used in experiments for gathering subjective information in clinical trials.[143-145] Studies have revealed that VAS is the most accurate form of subjective measurement and their reliability and responsiveness have been established.[142;146]

Contact lens related dry eye is a very common clinical problem and is associated with reduced wearing time and also lens discontinuation. Orsborn et al.[147] reported that 18 to 30% of soft contact lens patients had symptoms of dry eye. 12 to 21% of these subjects reduced contact lens wearing time due to the related symptoms and 6 to 9% discontinued lens wear. Doughty et al.[148] reported that almost 50% of soft contact lens wearers report symptoms of dryness.

Symptoms of dryness at insertion, 2 and 6 hours were reported by subjects wearing the lenses used in my study. Increased dryness at the end of 6 hours was also reported. It was observed that lower modulus AA lenses were perceived to be the least dry and higher modulus PV lenses were reported to be the driest at both baseline and at the 2 week visit. This difference was both statistically and clinically significant. This may be related to the wetting agent used with the AA lens in addition to the previously mentioned differences between theses lenses.

The other common problems associated with contact lens wear other than dryness is the burning sensation with the lenses. Silicone hydrogel lens wearers in the present study reported no difference in the sensation of burning with the different lenses.

It has been reported that stiffer materials may provide improved vision because of decreased lens flexure.[149] Since contact lenses rest directly on the eye, flexure, decentration and tear lens formation are possible and these can impact the vision.[3;150] In this study there was a significant association between modulus and time of day. The subjective ratings of vision did not change significantly between time of day with lower modulus (AA) lenses. The rating of vision was highest for the higher modulus (PV) lenses at insertion and decreased 6 hours after insertion and this could perhaps be due to the aspheric optics of this lens.

The associations observed between the clinical and sensory variables at the baseline and the 2 week period with the study lenses were of interest, so the other important question addressed in this experiment was whether end of the day subjective variables were associated with clinical variables. There have been number of reports on end of the day dryness and discomfort with the contact lens wear and associated contact lens discontinuation.[38;151-154] A few studies have reported that there is little difference between the silicone hydrogel lens wear and the conventional low-Dk hydrogel wear [98;155] but there are reports that patients wearing silicone hydrogels have higher levels of comfort.[130;156;157]

In the study reported in Chapter 5, I examined the associations between the clinical variables at the baseline visit, and the sensory variables at 2 weeks. This would perhaps be of importance to contact lens practitioners to help them choose an optimal trail lens based on the sensory variables reported by the subjects at the end of two weeks. In the summary paragraphs that are to follow, the results are organised based on the lens types and base cures.

In wearers of tighter fitting AA 8.3 lenses there was a low association between superior limbal and bulbar hyperemia and sensory variables of discomfort, dryness and burning at the end of 2 weeks. Superior limbal staining in wearers of AA 8.3 was also associated with discomfort and dryness. Red blood cell velocity had a high association to dryness and discomfort with the AA 8.3 lens. This perhaps indicates the

importance of optimal lens fit as a tight fitting contact lens might interfere with the content of blood vessel.

The wearers of the tight fitting PV 8.3 lens showed moderate association between limbal and bulbar hyperemia and the sensory variables of discomfort and burning at the end of 2 weeks. Wearers of flatter fitting AA 8.7 and PV 8.6 did not show any systematic associations between the clinical and sensory variables. No systematic associations were observed between any other clinical and sensory variables at 2 weeks.

When comparing the baseline clinical variables to the end of the day sensory variables, lens wearers of AA 8.3 had lower associations between topographic changes along the 90 degree meridian to the sensory variables of dryness, discomfort and vision at the end of the day. Blood flow had moderate association with the sensation of discomfort at the end of the day. In wearers of the flatter fitting AA 8.7 lens there were moderate associations between the lens fitting characteristics at baseline and sensory variables at the end of the day. Lens movement, lens lag and horizontal lens centration were also significantly associated with vision at the end of the day. Blood flow was associated with the sensation of dryness in those wearing AA 8.7 lens. In wearers of PV 8.3 lenses there was a moderate association between superior conjunctival epithelial thinning and burning. No systematic correlations were observed between the clinical and sensory variables in wearers of PV 8.6 lenses.

There were no systematic effects seen when comparing the clinical variables to sensory variables at 2 weeks and this could perhaps be due to an adaptation effect. However, there were some correlations seen when comparing the clinical variables at the baseline to 2 weeks. The conjunctival epithelial thickness in wearers of the steeper AA 8.3 lens at baseline was moderately correlated to superior bulbar hyperemia at the 2 weeks. In wearers of the flatter AA 8.7 there were lower correlations between the fitting characteristics (lens movement and lens lag) and corneal and epithelial thickness along the 90 degree

meridian, and between superior limbal and bulbar hyperemia. In wearers of PV 8.3 and PV 8.6 there were no systematic correlations.

In conclusion, the end of day sensory variables at two weeks was not strongly associated with the clinical variables measured at baseline. There appeared to be random association occasionally seen between some clinical and sensory variables but no systematic associations emerged. I thought this comparison would be useful for contact lens practitioners; to be able to predict how the lens would feel after 2 weeks of lens wear based on clinical measures collected on the first day of lens wear seem to be a worthwhile outcome to pursue.

Associations between outcome and predictor variables were explored in order, primarily, to assess whether early data may be usefully related to later data (either, for example "acute" same day morning vs. afternoon or "chronic" baseline vs. 2 week). There is a fundamental difficulty in doing exploratory correlation analyses in that by chance alone one might expect 5 out of 100 significant associations (using an 0.05 significance level). There were many more correlations than would be anticipated by chance alone that were significant and often the correlations appeared to be in physiologically plausible clusters, e.g., vascular outcomes. These suggest that the conclusions drawn should not be regarded with too much caution, although, type 1 errors are always a real possibility. In addition, almost none of the correlations reported were very "strong". This is not unexpected; these were physiological and clinical variables, many notorious for being highly variable (e.g., the subjective ratings) and so the absolute size of the correlations should not detract too much from the interpretations of the collection of the associations I found.

This too seems to be a potentially useful thing to know. If important 2 week clinical results can be predicted on day 1 of lens wear, many long term complications might be eliminated. In lens wearers of steeper fitting AA 8.3 and PV 8.3, vascular and staining outcomes were significantly associated with measures of lens fit and corneal topography. Superior conjunctival compression was observed in wearers

of these lenses and this was associated with superior conjunctival indentation and bulbar hyperaemia. RBC velocity at baseline correlated with limbal and conjunctival staining at 2 weeks. The ocular effects on the vasculature of the bulbar conjunctival with different lens materials needs to be elucidated since complications with contact lenses continue to be reported.

Chronic level of vessel dilation with contact lens wear is a cause of concern as persistent vessel dilation indicates an inflammatory response and may be precursor to new vessel growth and changes in the ocular surface. Red blood cell velocity measured in this study perhaps showed an effect on the sensory parameters such as discomfort and dryness. Although decrease in limbal redness and inflammatory response in the cornea are reported with silicone hydrogel lens wear perhaps more attention should be focused on the bulbar area of the conjunctiva since this study indicates an effect of RBC velocities suggesting an ocular response due to mechanical or inflammatory effects.

In summary, discomfort with contact lenses is a complex issue to resolve since it appears to be related to number of factors such as vascular, structural changes with lens wear, physiological changes and lens fitting characteristics. Lens materials, whether they are high or low modulus, high or low water content, with various wetting properties perhaps play a role in affecting comfort. A balance among all these factors must be achieved in order to optimize lens comfort.

Appendix A

Results from chapter 5

Table shows mean and standard deviation of corneal thickness at baseline with AA 8.3, AA 8.7, PV 8.3 and PV 8.6 lenses along 0, 45, 90 and 135 degree meridian at 7 locations.

Lens	Loc	Position						
	Deg	-3	-2	-1	0	1	2	3
AA 8.3	0	600.4±47.5	565.59±43.7	549.05±40.1	547.93±38.4	546.95±39.2	561.63±39.2	586.09±47.0
	45	592.00±45.8	558.05±40.7	543.44±39.5	543.59±37.3	543.59±37.3	549.07±38.6	570.39±43.1
	90	646.39±45.5	599.23±42..3	568.49±39.8	546.9±38.9	547.26±37.7	552.82±38.5	575.83±39.5
	135	651.52±48.8	601.71±43.7	567.77±40.6	549.94±40.2	547.45±36.9	550.83±39.2	571.58±40.7
AA 8.7	0	561.70±41.6	588.31±45.5	638.00±51.6	648.81±62.5	599.91±54.3	566.48±46.2	550.15±40.7
	45	570.63±37.7	604.79±42.2	658.29±45.1	643.31±54.3	591.96±45.7	559.85±45.4	545.19±40.0
	90	554.01±37.1	579.33±36.5	621.44±40.1	670.66±34.7	647.25±45.7	602.26±42.7	571.21±40.3
	135	553.07±37.8	575.44±38.7	612.09±40.6	665.65±43.3	654.31±45.6	604.17±42.6	568.13±39.4
PV 8.3	0	639.56±48.6	650.48±52.3	598.31±45.8	563.92±40.0	547.78±37.5	547.11±38.4	547.63±39.2
	45	652.07±50.7	652.07±50.7	587.89±44.9	557.44±41.7	542.36±37.7	541.21±36.3	541.21±36.3
	90	614.16±46.1	663.48±38.4	643.91±45.6	598.24±42.3	566.51±40.1	547.15±39.6	546.54±38.5
	135	613.95±45.1	666.72±46.3	653.78±48.3	603.32±46.4	565.39±41.4	548.09±38.5	544.96±37.7
PV 8.6	0	544.22±39.1	545.38±39.4	559.70±43.0	585.58±50.0	634.76±55.8	659.15±53.2	605.56±48.1
	45	544.31±35.5	548.09±37.75	563.19±41.6	592.09±47.4	646.77±47.0	656.42±48.6	599.06±44.2
	90	549.37±36.7	544.12±38.27	550.73±38.2	575.00±40.0	612.89±45.3	662.05±32.3	652.92±43.4
	135	547.81±38.4	545.19±36.91	552.57±37.7	574.05±42.1	612.04±44.5	661.71±43.2	649.58±45.9

Table shows mean and standard deviation of corneal thickness at 2 weeks with AA 8.3, AA 8.7, PV 8.3 and PV 8.6 lenses along 0, 45, 90 and 135 degree meridian at 7 locations.

Lens	Loc	Position						
	Deg.	-3	-2	-1	0	1	2	3
AA 8.3	0	653.90±50.3	602.14±42.8	567.28±40.0	548.61±39.2	546.27±38.9	546.93±39.4	559.72±43.7
	45	646.33±43.1	594.24±38.3	559.70±37.9	554.55±36.9	542.87±37.7	542.87±37.7	549.03±38.0
	90	668.62±48.2	645.60±47.1	599.12±40.4	567.31±39.9	546.57±37.9	545.49±36.7	552.82±37.2
	135	666.49±48.1	651.07±54.3	602.12±47.7	566.17±42.5	547.51±40.2	546.39±37.3	551.89±37.5
AA 8.7	0	548.88±38.9	562.85±43.4	591.48±49.3	640.93±56.9	645.23±58.7	597.13±51.7	563.49±43.9
	45	549.14±35.4	567.91±37.2	601.30±42.8	653.63±46.0	643.43±53.5	593.01±46.7	559.49±43.3
	90	545.59±37.6	552.97±36.0	578.72±36.8	624.81±38.7	662.17±33.5	648.84±45.7	601.41±41.9
	135	542.89±39.6	550.29±37.2	572.84±39.8	612.63±41.8	663.59±39.8	653.55±46.6	602.79±42.3
PV 8.3	0	589.69±47.83	640.02±54.7	652.42±53.2	600.36±46.1	566.07±42.5	548.04±39.3	545.51±39.7
	45	597.22±46.0	647.18±47.9	645.63±44.7	590.55±41.6	557.42±38.7	542.11±38.4	541.54±37.0
	90	576.76±39.9	616.87±41.6	660.29±38.3	646.42±44.5	598.72±41.1	567.05±38.8	547.91±39.6
	135	572.71±40.7	614.29±44.7	662.39±43.1	649.43±48.9	601.26±45.0	563.95±41.0	547.09±38.1
PV 8.6	0	546.06±39.7	543.89±38.8	547.99±39.4	564.36±41.2	593.05±46.2	642.33±51.5	662.32±53.5
	45	544.61±41.2	541.16±39.7	546.21±38.5	563.47±40.8	593.29±45.8	645.46±41.3	654.41±51.0
	90	568.46±40.2	546.04±39.6	545.92±40.1	552.39±39.9	577.37±40.4	615.14±42.9	665.23±32.5
	135	565.29±39.0	545.29±38.6	543.51±41.3	552.49±40.7	567.61±42.0	614.68±45.8	671.07±29.4

Table shows mean and standard deviation of epithelial thickness at baseline with AA 8.3, AA 8.7, PV 8.3 and PV 8.6 lenses along 0, 45, 90 and 135 degree meridian at 7 locations.

Lens	Loc	Position						
	Deg.	-3	-2	-1	0	1	2	3
AA 8.3	0	54.55±1.7	55.97±1.5	57.57±2.5	56.26±3.2	54.55±2.4	55.57±1.9	54.59±1.5
	45	54.82±1.4	56.94±2.0	57.21±2.1	55.99±2.4	55.43±2.1	54.66±2.0	54.94±1.5
	90	55.05±2.2	55.08±1.9	58.01±2.8	56.26±2.7	55.45±2.4	54.47±2.1	52.92±2.6
	135	55.22±1.5	56.18±2.6	58.00±2.4	56.42±2.8	56.15±2.4	55.26±2.0	54.63±2.0
AA 8.7	0	54.24±1.3	55.19±1.5	56.68±2.5	56.47±2.7	55.89±2.4	54.71±2.1	55.32±1.6
	45	55.18±1.3	56.13±2.5	58.44±3.2	55.41±2.4	55.63±2.8	55.12±2.5	54.71±1.8
	90	55.79±1.4	54.72±1.2	58.70±2.8	56.95±3.3	55.89±2.7	54.91±2.7	53.98±2.9
	135	55.74±1.5	57.04±2.3	57.98±2.2	56.85±3.2	56.12±3.0	55.15±2.1	54.74±2.0
PV 8.3	0	54.81±1.5	55.78±1.8	56.52±2.2	56.61±2.8	55.92±2.7	54.32±2.0	54.95±1.4
	45	55.04±1.4	56.14±2.0	57.86±2.6	57.02±2.8	55.92±2.4	55.43±2.3	54.63±1.7
	90	55.69±1.7	55.11±2.0	58.64±2.6	56.24±2.7	55.62±2.3	54.88±1.5	53.90±2.0
	135	55.09±1.7	57.21±2.5	58.00±2.8	56.01±2.6	55.96±2.4	55.71±2.3	54.21±2.0
PV 8.6	0	54.75±1.5	55.95±1.8	56.34±2.2	56.15±2.8	55.79±2.7	54.96±1.9	54.64±1.2
	45	54.94±1.4	55.98±2.0	58.05±3.5	56.48±2.2	56.00±2.9	54.92±1.7	54.91±1.4
	90	55.15±1.7	54.49±2.1	59.05±3.1	55.66±2.4	55.25±2.6	54.68±2.0	52.60±2.7
	135	54.59±2.5	57.36±2.0	57.35±2.5	56.28±2.8	56.29±2.5	55.23±2.1	54.34±1.4

Table shows mean and standard deviation of epithelial thickness at 2 weeks with AA 8.3, AA 8.7, PV 8.3 and PV 8.6 lenses along 0, 45, 90 and 135 degree meridian at 7 locations.

Lens	Loc	Position						
	Deg.	-3	-2	-1	0	1	2	3
AA 8.3	0	54.74±1.9	56.42±1.7	56.93±1.9	57.08±3.2	55.52±2.6	54.96±1.9	55.59±1.2
	45	54.73±1.6	56.36±1.9	57.60±2.4	56.37±3.1	55.46±2.4	55.23±2.2	55.49±1.7
	90	55.75±1.7	55.23±2.0	55.54±2.8	56.18±3.1	56.16±3.2	55.31±2.0	53.14±2.9
	135	55.28±1.7	57.17±2.3	58.58±2.2	56.83±2.5	56.18±2.7	54.99±1.6	54.02±1.8
AA 8.7	0	54.77±1.9	55.62±1.8	56.18±2.0	56.24±3.0	55.83±2.4	55.11±2.4	55.14±1.5
	45	54.98±1.7	56.34±2.4	57.61±2.8	55.78±2.6	55.04±2.8	55.10±2.0	55.67±1.9
	90	56.37±1.7	55.01±2.0	59.54±3.9	56.64±3.1	55.92±2.5	55.17±2.0	53.94±2.6
	135	55.06±1.5	57.04±2.8	58.44±2.5	56.31±3.0	55.69±2.5	54.97±1.8	54.18±1.9
PV 8.3	0	55.11±1.4	56.27±2.4	56.07±2.9	55.21±3.2	55.21±2.5	54.76±2.4	54.57±2.7
	45	54.49±1.6	55.35±2.1	57.19±2.8	55.74±2.9	55.19±2.9	54.86±2.7	54.72±1.7
	90	55.48±1.9	55.10±2.2	58.65±3.8	56.06±2.8	54.65±2.4	54.28±2.6	53.38±2.1
	135	55.51±1.5	56.95±2.1	56.78±2.4	55.97±3.2	55.63±2.8	55.41±2.1	54.27±1.4
PV 8.6	0	54.64±1.8	54.35±2.0	56.39±1.9	56.02±2.9	55.54±2.9	54.68±2.3	54.78±1.5
	45	54.99±1.7	56.31±2.4	57.81±1.9	55.48±2.3	54.94±3.0	54.88±2.2	54.13±1.8
	90	55.21±1.6	54.75±1.7	57.41±2.3	55.92±2.8	55.33±2.8	54.72±2.1	51.52±3.9
	135	55.05±1.7	57.32±2.3	57.96±2.6	56.20±3.4	56.48±2.4	55.65±1.9	54.54±1.6

Appendix B

RMS AND CONDITIONS

Nov 11, 2011

This is a License Agreement between jyotsna maram ("You") and Elsevier ("Elsevier") provided by Copyright Clearance Center ("CCC"). The license consists of your order details, the terms and conditions provided by Elsevier, and the payment terms and conditions.

All payments must be made in full to CCC. For payment instructions, please see information listed at the bottom of this form.

Supplier

Elsevier Limited
The Boulevard,Langford Lane
Kidlington,Oxford,OX5 1GB,UK

Registered Company Number

1982084

Customer name

jyotsna maram

Customer address

unit 8, 453 albert street

waterloo, ON n2l5a7

License number

2783210806298

License date

Nov 06, 2011

Licensed content publisher

Elsevier

Licensed content publication

Progress in Retinal and Eye Research

Licensed content title

Recent developments in optical coherence tomography for imaging the retina

Licensed content author

Mirjam E.J. van Velthoven,Dirk J. Faber,Frank D. Verbraak,Ton G. van Leeuwen,Marc D. de Smet

Licensed content date

January 2007

Licensed content volume number26

Licensed content issue number1

Number of pages21

Start Page57

End Page77

Type of Use

reuse in a thesis/dissertation

Portion

figures/tables/illustrations

Number of figures/tables/illustrations

1

Format

electronic

Are you the author of this Elsevier article?

No

Will you be translating?

No

Order reference number

Title of your thesis/dissertation

Anterior segment imaging using optical coherence tomographers to examine soft lens fitting characteristics and comfort

Expected completion date

Nov 2011

Estimated size (number of pages)250

Elsevier VAT number

GB 494 6272 12

Permissions price

0.00 USD

VAT/Local Sales Tax

0.0 USD / 0.0 GBP

Total

0.00 USD

Terms and Conditions

INTRODUCTION

1. The publisher for this copyrighted material is Elsevier. By clicking "accept" in connection with completing this licensing transaction, you agree that the following terms and conditions apply to this transaction (along with the Billing and Payment terms and conditions established by Copyright Clearance Center, Inc. ("CCC"), at the time that you opened your Rightslink account and that are available at any time at http://myaccount.copyright.com).

GENERAL TERMS

2. Elsevier hereby grants you permission to reproduce the aforementioned material subject to the terms and conditions indicated.

3. Acknowledgement: If any part of the material to be used (for example, figures) has appeared in our publication with credit or acknowledgement to another source, permission must also be sought from that source. If such permission is not obtained then that material may not be included in your publication/copies. Suitable acknowledgement to the source must be made, either as a footnote or in a reference list at the end of your publication, as follows:

"Reprinted from Publication title, Vol /edition number, Author(s), Title of article / title of chapter, Pages No., Copyright (Year), with permission from Elsevier [OR APPLICABLE SOCIETY COPYRIGHT OWNER]." Also Lancet special credit - "Reprinted from The Lancet, Vol. number, Author(s), Title of article, Pages No., Copyright (Year), with permission from Elsevier."

4. Reproduction of this material is confined to the purpose and/or media for which permission is hereby given.

5. Altering/Modifying Material: Not Permitted. However figures and illustrations may be altered/adapted minimally to serve your work. Any other abbreviations, additions, deletions and/or any other alterations shall be made only with prior written authorization of Elsevier Ltd. (Please contact Elsevier at permissions@elsevier.com)

6. If the permission fee for the requested use of our material is waived in this instance, please be advised that your future requests for Elsevier materials may attract a fee.

7. Reservation of Rights: Publisher reserves all rights not specifically granted in the combination of (i) the license details provided by you and accepted in the course of this licensing transaction, (ii) these terms and conditions and (iii) CCC's Billing and Payment terms and conditions.

8. License Contingent Upon Payment: While you may exercise the rights licensed immediately upon issuance of the license at the end of the licensing process for the transaction, provided that you have disclosed complete and accurate details of your proposed use, no license is finally effective unless and until full payment is received from you (either by publisher or by CCC) as provided in CCC's Billing and Payment terms and conditions. If full payment is not received on a timely basis, then any license preliminarily granted shall be deemed automatically revoked and shall be void as if never granted. Further, in the event that you breach any of these terms and conditions or any of CCC's Billing and Payment terms and conditions, the license is automatically revoked and shall be void as if never granted. Use of materials as described in a revoked license, as well as any use of the materials beyond the scope of an unrevoked license, may constitute copyright infringement and publisher reserves the right to take any and all action to protect its copyright in the materials.

9. Warranties: Publisher makes no representations or warranties with respect to the licensed material.

10. Indemnity: You hereby indemnify and agree to hold harmless publisher and CCC, and their respective officers, directors, employees and agents, from and against any and all claims arising out of your use of the licensed material other than as specifically authorized pursuant to this license.

11. No Transfer of License: This license is personal to you and may not be sublicensed, assigned, or transferred by you to any other person without publisher's written permission.

12. No Amendment Except in Writing: This license may not be amended except in a writing signed by both parties (or, in the case of publisher, by CCC on publisher's behalf).

13. Objection to Contrary Terms: Publisher hereby objects to any terms contained in any purchase order, acknowledgment, check endorsement or other writing prepared by you, which terms are inconsistent with these terms and conditions or CCC's Billing and Payment terms and conditions. These terms and conditions, together with CCC's Billing and Payment terms and conditions (which are incorporated herein), comprise the entire agreement between you and publisher (and CCC) concerning this licensing transaction. In the event of any conflict between your obligations established by these terms and conditions and those established by CCC's Billing and Payment terms and conditions, these terms and conditions shall control.

14. Revocation: Elsevier or Copyright Clearance Center may deny the permissions described in this License at their sole discretion, for any reason or no reason, with a full refund payable to you. Notice of such denial will be made using the contact information provided by you. Failure to receive such notice will not alter or invalidate the denial. In no event will Elsevier or Copyright Clearance Center be responsible or liable for any costs, expenses or damage incurred by you as a result of a denial of your permission request, other than a refund of the amount(s) paid by you to Elsevier and/or Copyright Clearance Center for denied permissions.

LIMITED LICENSE

The following terms and conditions apply only to specific license types:

15. **Translation**: This permission is granted for non-exclusive world **English** rights only unless your license was granted for translation rights. If you licensed translation rights you may only translate this content into the languages you requested. A professional translator must perform all translations and reproduce the content word for word preserving the integrity of the article. If this license is to re-use 1 or 2 figures then permission is granted for non-exclusive world rights in all languages.

16. **Website**: The following terms and conditions apply to electronic reserve and author websites:
Electronic reserve: If licensed material is to be posted to website, the web site is to be password-protected and made available only to bona fide students registered on a relevant course if:
This license was made in connection with a course,
This permission is granted for 1 year only. You may obtain a license for future website posting,
All content posted to the web site must maintain the copyright information line on the bottom of each image,
A hyper-text must be included to the Homepage of the journal from which you are licensing at http://www.sciencedirect.com/science/journal/xxxxx or the Elsevier homepage for books at http://www.elsevier.com , and
Central Storage: This license does not include permission for a scanned version of the material to be stored in a central repository such as that provided by Heron/XanEdu.

17. **Author website** for journals with the following additional clauses:

All content posted to the web site must maintain the copyright information line on the bottom of each image, and
he permission granted is limited to the personal version of your paper. You are not allowed to download and post the published electronic version of your article (whether PDF or HTML, proof or final version), nor may you scan the printed edition to create an electronic version,
A hyper-text must be included to the Homepage of the journal from which you are licensing at http://www.sciencedirect.com/science/journal/xxxxx , As part of our normal production process, you will receive an e-mail notice when your article appears on Elsevier's online service ScienceDirect (www.sciencedirect.com). That e-mail will include the article's Digital Object Identifier (DOI). This number provides the electronic link to the published article and should be included in the posting of your personal version. We ask that you wait until you receive this e-mail and have the DOI to do any posting.
Central Storage: This license does not include permission for a scanned version of the material to be stored in a central repository such as that provided by Heron/XanEdu.

18. **Author website** for books with the following additional clauses:
Authors are permitted to place a brief summary of their work online only.
A hyper-text must be included to the Elsevier homepage at http://www.elsevier.com

All content posted to the web site must maintain the copyright information line on the bottom of each image
You are not allowed to download and post the published electronic version of your chapter, nor may you scan the printed edition to create an electronic version.
Central Storage: This license does not include permission for a scanned version of the material to be stored in a central repository such as that provided by Heron/XanEdu.

19. **Website** (regular and for author): A hyper-text must be included to the Homepage of the journal from which you are licensing at http://www.sciencedirect.com/science/journal/xxxxx. or for books to the Elsevier homepage at http://www.elsevier.com

20. **Thesis/Dissertation**: If your license is for use in a thesis/dissertation your thesis may be submitted to your institution in either print or electronic form. Should your thesis be published commercially, please reapply for permission. These requirements include permission for the Library and Archives of Canada to supply single copies, on demand, of the complete thesis and include permission for UMI to supply single copies, on demand, of the complete thesis. Should your thesis be published commercially, please reapply for permission.

21. **Other Conditions**:

v1.6

If you would like to pay for this license now, please remit this license along with your payment made payable to "COPYRIGHT CLEARANCE CENTER" otherwise you will be invoiced within 48 hours of the license date. Payment should be in the form of a check or money order referencing your account number and this invoice number RLNK500659209. Once you receive your invoice for this order, you may pay your invoice by credit card. Please follow instructions provided at that time.

Make Payment To:
Copyright Clearance Center
Dept 001
P.O. Box 843006
Boston, MA 02284-3006

For suggestions or comments regarding this order, contact RightsLink Customer Support: customercare@copyright.com or +1-877-622-5543 (toll free in the US) or +1-978-646-2777.

Gratis licenses (referencing $0 in the Total field) are free. Please retain this printable license for your reference. No payment is required.

Dear Jyotsna,

Thank you for your e-mail. You may use the image from Contact Lens Spectrum in your dissertation provided that you include the following verbiage with the image: Reprinted with permission of Contact Lens Spectrum, Copyright Wolters Kluwer Pharma Solutions, Inc. All rights reserved.

Thanks,
Lisa

Lisa Starcher
Managing Editor
Contact Lens Spectrum
Wolters Kluwer Pharma Solutions VisionCare Group
323 Norristown Road
Suite 200
Ambler, PA 19002
215 367-2168
215 827-5390 fax
Lisa.starcher@wolterskluwer.com
www.clspectrum.com

Dear Jyotsna

We hereby grant you permission to reprint the below mentioned material at no charge **in your thesis** subject to the following conditions:

1. If any part of the material to be used (for example, figures) has appeared in our publication with credit or acknowledgement to another source, permission must also be sought from that source. If such permission is not obtained then that material may not be included in your publication/copies.

2. Suitable acknowledgment to the source must be made, either as a footnote or in a reference list at the end of your publication, as follows:

   R20;This article was published in Publication title, Vol number, Author(s), Title of article, Page Nos, **Copyright British Contact Lens Association** (Year).”

3. Your thesis may be submitted to your institution in either print or electronic form.

4. Reproduction of this material is confined to the purpose for which permission is hereby given.

5. This permission is granted for non-exclusive world **English** rights only. For other languages please reapply separately for each one required. Permission excludes use in an electronic form other than submission. Should you have a specific electronic project in mind please reapply for permission.

6. This includes permission for the Library and Archives of Canada to supply single copies, on demand, of the complete thesis. Should your thesis be published commercially, please reapply for permission.

Yours sincerely

Laura Gould

Rights Associate

Global Rights Department

T: +44 (0)1865 843857

E: L.Gould@elsevier.com **Your future requests will be handled more quickly if you complete the online form at** www.elsevier.com/permissions

-----Original Message-----
From: mjyotsna@sciborg.uwaterloo.ca [mailto:mjyotsna@sciborg.uwaterloo.ca]
Sent: 16 November 2011 15:46
To: Health Permissions (ELS-PHI)
Subject: Copyright for images - book- silicone hydrogels : the rebirth of continous wear contact lenses

Respected Sir/madam

This is regarding permission for using few images from the book-

(silicone hydrogels : the rebirth of continuous wear contact lenses)

edited by D Sweeney, to be used in my PhD thesis.The images used are

from page 13 and page 6 of the first chapter. Please let me know the

procedure and how to go about it.

Thank you

Jyotsna

License Details

This is a License Agreement between jyotsna maram ("You") and Elsevier ("Elsevier"). The license consists of your order details, the terms and conditions provided by Elsevier, and the payment terms and conditions.

Get the printable license.

License Number	2783210806298
License date	Nov 06, 2011
Licensed content publisher	Elsevier
Licensed content publication	Progress in Retinal and Eye Research
Licensed content title	Recent developments in optical coherence tomography for imaging the retina
Licensed content author	Mirjam E.J. van Velthoven,Dirk J. Faber,Frank D. Verbraak,Ton G. van Leeuwen,Marc D. de Smet
Licensed content date	January 2007
Licensed content volume number	26
Licensed content issue number	1
Number of pages	21
Type of Use	reuse in a thesis/dissertation
Portion	figures/tables/illustrations
Number of figures/tables/illustrations	1
Format	electronic
Are you the author of this Elsevier article?	No
Will you be translating?	No
Order reference number	
Title of your thesis/dissertation	Anterior segment imaging using optical coherence tomographers to examine soft lens fitting characteristics and comfort
Expected completion date	Nov 2011
Estimated size (number of pages)	250
Elsevier VAT number	GB 494 6272 12
Permissions price	0.00 USD
VAT/Local Sales Tax	0.0 USD / 0.0 GBP
Total	0.00 USD

Bibliography

References – Chapter 1

1. Wichterleo O. Clinical experiences with hydrogel contact lenses. *CeskoslovenskÃ¡ oftalmologie* 1964;**20**:393-9.

2. Holden BA, Stephenson A, Stretton S, Sankaridurg PR, O'Hare N, Jalbert I et al. Superior epithelial arcuate lesions with soft contact lens wear. *Optom Vis Sci* 2001;**78**:9-12.

3. Brautaset RL, Nilsson M, Leach N, Miller WL, Gire A, Quintero S et al. Corneal and conjunctival epithelial staining in hydrogel contact lens wearers. *Eye Contact Lens* 2008;**34**:312-6.

4. Sorbara L, Jones L, Williams-Lyn D. Contact lens induced papillary conjunctivitis with silicone hydrogel lenses. *Cont Lens Anterior Eye* 2009;**32**:93-6.

5. Dumbleton K. Noninflammatory silicone hydrogel contact lens complications. *Eye Contact Lens* 2003;**29**:S186-S189.

6. Sankaridurg PR, Sweeney DF, Holden BA, Naduvilath T, Velala I, Gora R et al. Comparison of adverse events with daily disposable hydrogels and spectacle wear - Results from a 12-month prospective clinical trial. *Ophthalmology* 2003;**110**:2327-34.

7. Holden BA, Mertz GW. Critical oxygen levels to avoid corneal edema for daily and extended wear contact lenses. *Invest Ophthalmol Vis Sci* 1984;**25**:1161-7.

8. Tighe B. Silicone hydrogels:strucure, properties and behaviour. *Silicone Hydrogels: Continuous-WearContact Lenses, 2nd ed.Edinburgh: Butterworth-Heinemann; British Contact LensAssociation;* 2004;1-27.

9. Tighe B. In: Sweeney D ed. Oxford, Butterworth-Heinemann, 2000: 1-21.

10. Morgan PB, Woods CA. International contact lens prescribing. *Cont Lens Spect* 2006;**22**:34-8.

11. Woods CA, Jones DA, Jones LW, Morgan PB. A seven year survey of the contact lens prescribing habits of Canadian optometrists. *Optom Vis Sci* 2007;**84**:505-10.

12. Maldonado-Codina C, Morgan PB, Efron N, Efron S. Comparative clinical performance of rigid versus soft hyper Dk contact lenses used for continuous wear. *Optom Vis Sci* 2005;**82**:536-48.

13. Chalmers RL, Dillehay S, Long B, Barr JT, Bergenske P, Donshik P et al. Impact of previous extended and daily wear schedules on signs and symptoms with high Dk lotrafilcon A lenses. *Optom Vis Sci* 2005;**82**:549-54.

14. Fonn D, MacDonald KE, Richter D, Pritchard N. The ocular response to extended wear of a high Dk silicone hydrogel contact lens. *Clin Exp Optom* 2002;**85**:176-82.

15. Morgan PB, Efron N, Maldonado-Codina C, Efron S. Adverse events and discontinuations with rigid and soft hyper Dk contact lenses used for continuous wear. *Optom Vis Sci* 2005;**82**:528-35.

16. Morgan PB, Efron N, Brennan NA, Hill EA, Raynor MK, Tullo AB. Risk factors for the development of corneal infiltrative events associated with contact lens wear. *Invest Ophthalmol Vis Sci* 2005;**46**:3136-43.

17. Stapleton F, Stretton S, Papas E, Skotnitsky C, Sweeney DF. Silicone hydrogel contact lenses and the ocular surface. *Ocul Surf* 2006;**4**:24-43.

18. Santodomingo-Rubido J, Wolffsohn J, Gilmartin B. Conjunctival epithelial flaps with 18 months of silicone hydrogel contact lens wear. *Eye Contact Lens* 2008;**34**:35-8.

19. Brennan NA, Efron N. Symptomatology of HEMA contact lens wear. *Optom Vis Sci* 1989;**66**:834-8.

20. Fonn D. Targeting contact lens induced dryness and discomfort: what properties will make lenses more comfortable. *Optom Vis Sci* 2007;**84**:279-85.

21. Fonn D. Dryness with contact lenses and dry eye: are they the same or different? *Eye Contact Lens* 2009;**35**:219.

22. Nomura K, Nakao M, Matsubara K. Subjective symptom of eye dryness and lifestyle factors with corneal neovascularization in contact lens wearers. *Eye Contact Lens* 2004;**30**:95-8.

23. Pritchard N, Fonn D, Brazeau D. Discontinuation of contact lens wear: a survey. *Int Cont Lens Clin* 1999;**26**:157-62.

24. Orsborn G, Zantos SG. Practitioner survey: management of dry-eye symptoms in soft lens wearers. *Contact Lens Spectrum* 1989;**4**:23-6.

25. Fonn D. Preventing contact lens dropouts. *Contact Lens Spectrum* 2002;**17**:26-32.

26. Morgan P. Is the UK contact lens market healthy? *Optician* 2001;**5795**:22-6.

27. Weed K, Fonn D, Potvin R. Discontinuation ofcontact lens wear. *Optom Vis Sci* 1993;**70**.

28. Young G. Soft lens fitting reassessed. *Contact Lens Spectrum* 1992;**7**:56-61.

29. Dumbleton KA, Chalmers RL, McNally J, Bayer S, Fonn D. Effect of lens base curve on subjective comfort and assessment of fit with silicone hydrogel continuous wear contact lenses. *Optom Vis Sci* 2002;**79**:633-7.

30. Young G, Holden B, Cooke G. Influence of soft contact lens design on clinical performance. *Optom Vis Sci* 1993;**70**:394-403.

31. Morgan PB, Efron N. In vivo dehydration of silicone hydrogel contact lenses. *Eye Contact Lens* 2003;**29**:173-6.

32. Jones LW, Keir N, Situ P, Fonn D. The impact of post-insertion time on corneal staining and comfort with group II hydrogel materials disinfected with various lens care regimens. *Invest Ophthalmol Vis.Sci.* 2005;**46**.

33. Meadows D. Measuring wettability. *Contact Lens Spectrum* 2005;**20**:7-8.

34. Peterson RC, Fonn D, Woods CA, Jones L. Impact of a rub and rinse on solution-induced corneal staining. *Optom Vis Sci* 2010;**87**:1030-6.

35. Sorbara L, Peterson R, Woods C, Fonn D. Multipurpose disinfecting solutions and their interactions with a silicone hydrogel lens. *Eye Contact Lens* 2009;**35**:92-7.

36. Jones L, Senchyna M, Glasier MA, Schickler J, Forbes I, Louie D et al. Lysozyme and lipid deposition on silicone hydrogel contact lens materials. *Eye Contact Lens* 2003;**29**:S75-S79.

37. Heynen M, Lorentz H, Srinivasan S, Jones L. Quantification of non-polar lipid deposits on senofilcon a contact lenses. *Optom Vis Sci* 2011;**88**:1172-9.

38. Glasson M, Stapleton F, Willcox M. Lipid, lipase and lipocalin differences between tolerant and intolerant contact lens wearers. *Curr Eye Res* 2002;**25**:227-35.

39. Pritchard N, Fonn D, Weed K. Ocular and subjective responses to frequent replacement of daily wear soft contact lenses. *CLAO J* 1996;**22**:53-9.

40. Efron N, Brennan NA, Bruce AS, Duldig DI, Russo NJ. Dehydration of hydrogel lenses under normal wearing conditions. *CLAO J.* 1987;**13**:152-6.

41. Efron N, Young G. Dehydration of hydrogen contact lenses in vitro and in vivo. *Ophthalmic Physiol Opt* 1988;**8**:253-6.

42. Andrasko G. The amount and time course of soft contact lens dehydration. *J Am Optom Assoc* 1982;**53**:207.

43. Morgan PB, Efron N, Morgan SL, Little SA. Hydrogel contact lens dehydration in controlled environmental conditions. *Eye Contact Lens* 2004;**30**:99-102.

44. Efron N, Brennan NA, O'Brien KA, Murphy PJ. Surface hydration of hydrogel contact lenses. *Clin Exp Optom* 1986;**69**:219-22.

45. Golding TR, Harris MG, Smith RC, Brennan NA. Soft lens movement: effects of humidity and hypertonic saline on lens settling. *Acta Ophthalmol Scand* 1995;**73**:139-44.

46. Lira M, Santos L, Azeredo J, Yebra-Pimentel E, Real O. The effect of lens wear on refractive index of conventional hydrogel and silicone-hydrogel contact lenses: a comparative study. *Cont Lens Anterior Eye* 2008;**31**:89-94.

47. Boswall GJ, Ehlers WH, Luistro A, Worrall M, Donshik PC. A comparison of conventional and disposable extended wear contact lenses. *CLAO J* 1993;**19**:158-65.

48. Suchecki JK, Ehlers WH, Donshik PC. A comparison of contact lens-related complications in various daily wear modalities. *CLAO J* 2000;**26**:204-13.

49. Tighe B. In: Sweeney D, ed. D. Sweeney ed. Oxford, Butterworth-Heinemann, 2004: 1-27.

50. Nicolson PC, Vogt J. Soft contact lens polymers: An evolution. *Biomaterials* 2001;**22**:3273-83.

51. Weikart CM, Matsuzawa Y, Winterton L, Yasuda HK. Evaluation of plasma polymer-coated contact lenses by electrochemical impedance spectroscopy. *J Biomed Mater Res* 2001;**54**:597-607.

52. Li L, Wang JH, Xin Z. Synthesis and biocompatibility of a novel silicone hydrogel containing phosphorylcholine. *European Polymer Journal* 2011;**47**:1795-803.

53. Karlgard CCS, Sarkar DK, Jones LW, Moresoli C, Leung KT. Drying methods for XPS analysis of PureVisionâ„¢, FocusÂ® Night&Dayâ„¢ and conventional hydrogel contact lenses. *Applied Surface Science* 2004;**230**:106-14.

54. Cheng L, Muller SJ, Radke CJ. Wettability of silicone-hydrogel contact lenses in the presence of tear-film components. *Curr Eye Res* 2004;**28**:93-108.

55. Sharma A, Khanna R, Reiter G. A thin film analog of the corneal mucus layer of the tear film: An enigmatic long range non-classical DLVO interaction in the breakup of thin polymer films. *Colloids and Surfaces B: Biointerfaces* 1999;**14**:223-35.

56. Haddad M, Morgan PB, Kelly JM, Maldonado-Codina C. A novel on-eye wettability analyzer for soft contact lenses. *Optom Vis Sci* 2011;**88**:E1188-E1195.

57. Lin MC, Svitova TF. Contact lenses wettability in vitro: effect of surface-active ingredients. *Optom Vis Sci* 2010;**87**:440-7.

58. Lorentz H, Rogers R, Jones L. The impact of lipid on contact angle wettability. *Optom Vis Sci* 2007;**84**:946-53.

59. Guillon JP. Non-invasive tearscope plus routine for contact lens fitting. *Cont Lens Anterior Eye* 1998;**21**:31-40.

60. Elliott M, Fandrich H, Simpson T, Fonn D. Analysis of the repeatability of tear break-up time measurement techniques on asymptomatic subjects before, during and after contact lens wear. *Cont Lens Anterior Eye* 1998;**21**:98-103.

61. Bruce AS, Mainstone JC, Golding TR. Analysis of tear film breakup on Etafilcon A hydrogel lenses. *Biomaterials* 2001;**22**:3249-56.

62. Golding TR, Bruce AS, Mainstone JC. Relationship between tear-meniscus parameters and tear-film breakup. *Cornea* 1997;**16**:649-61.

63. Tutt R, Bradley A, Begley C, Thibos LN. Optical and visual impact of tear break-up in human eyes. *Invest Ophthalmol Vis Sci* 2000;**41**:4117-23.

64. Glasson MJ, Stapleton F, Keay L, Sweeney D, Willcox MD. Differences in clinical parameters and tear film of tolerant and intolerant contact lens wearers. *Invest Ophthalmol Vis Sci* 2003;**44**:5116-24.

65. Guillon M, Maissa C. Use of silicone hydrogel material for daily wear. *Cont Lens Anterior Eye* 2007;**30**:5-10.

66. Maldonado-Codina C, Morgan PB, Schnider CM, Efron N. Short-term physiologic response in neophyte subjects fitted with hydrogel and silicone hydrogel contact lenses. *Optom Vis Sci* 2004;**81**:911-21.

67. Nichols JJ, Sinnott LT. Tear film, contact lens, and patient-related factors associated with contact lens-related dry eye. *Invest Ophthalmol Vis Sci* 2006;**47**:1319-28.

68. Luensmann D, Jones L. Albumin adsorption to contact lens materials: a review. *Cont Lens Anterior Eye* 2008;**31**:179-87.

69. Emch AJ, Nichols JJ. Proteins identified from care solution extractions of silicone hydrogels. *Optom Vis Sci* 2009;**86**:E123-E131.

70. Bontempo AR, Rapp J. Lipid deposits on hydrophilic and rigid gas permeable contact lenses. *CLAO J* 1994;**20**:242-5.

71. Zhao Z, Carnt NA, Aliwarga Y, Wei X, Naduvilath T, Garrett Q et al. Care regimen and lens material influence on silicone hydrogel contact lens deposition. *Optom Vis Sci* 2009;**86**:251-9.

72. Franklin V, Horne A, Jones L, Tighe B. Early deposition trends on group I (Polymacon and Tetrafilcon A) and group III (Bufilcon A) materials. *CLAO J* 1991;**17**:244-8.

73. Jones L, Franklin V, Evans K, Sariri R, Tighe B. Spoilation and clinical performance of monthly vs. three monthly Group II disposable contact lenses. *Optom Vis Sci* 1996;**73**:16-21.

74. Solomon OD, Freeman MI, Boshnick EL, Cannon WM, Dubow BW, Kame RT et al. A 3-year prospective study of the clinical performance of daily disposable contact lenses compared with frequent replacement and conventional daily wear contact lenses. *CLAO J* 1996;**22**:250-7.

75. Minarik L, Rapp J. Protein deposits on individual hydrophilic contact lenses: effects of water and ionicity. *CLAO J* 1989;**15**:185-8.

76. Young G, Bowers R, Hall B, Port M. Clinical comparison of Omafilcon A with four control materials. *CLAO J* 1997;**23**:249-58.

77. Prager MD, Quintana RP. Radiochemical studies on contact lens soilation. II. Lens uptake of cholesteryl oleate and dioleoyl phosphatidylcholine. *J Biomed Mater Res* 1997;**37**:207-11.

78. Brennan NA, Coles ML, Connor HR, McIlroy RG. A 12-month prospective clinical trial of comfilcon A silicone-hydrogel contact lenses worn on a 30-day continuous wear basis. *Cont Lens Anterior Eye* 2007;**30**:108-18.

79. Papas E, Vajdic C, Austen R, Hickson S, Rypdal H, Holden BA. The Influence of Oxygen Transmissibility on the Limbal Vascular-Response During Contact-Lens Wear. *Invest Ophthalmol Vis.Sci.* 1995;**36**:S629.

80. Covey M, Sweeney DF, Terry R, Sankaridurg PR, Holden BA. Hypoxic effects on the anterior eye of high-Dk soft contact lens wearers are negligible. *Optom Vis Sci* 2001;**78**:95-9.

81. Sweeney DF, Gauthier C, Terry R, Chong MS, Holden BA. The Effects of Long-Term Contact-Lens Wear on the Anterior Eye. *Invest Ophthalmol Vis.Sci.* 1992;**33**:1293.

82. Holden BA, Sweeney DF, Vannas A, Nilsson KT, Efron N. Effects of long-term extended contact lens wear on the human cornea. *Invest Ophthalmol Vis Sci* 1985;**26**:1489-501.

83. Skotnitsky C, Sankaridurg PR, Sweeney DF, Holden BA. General and local contact lens induced papillary conjunctivitis (CLPC). *Clin Exp Optom* 2002;**85**:193-7.

84. Young G, Garofalo R, Harmer O, Peters S. The effect of soft contact lens care products on lens modulus. *Cont Lens Anterior Eye* 2010;**33**:210-4.

85. Dumbleton K. Adverse events with silicone hydrogel continuous wear. *Cont Lens Anterior Eye* 2002;**25**:137-46.

86. Skotnitsky CC, Naduvilath TJ, Sweeney DF, Sankaridurg PR. Two presentations of contact lens-induced papillary conjunctivitis (CLPC) in hydrogel lens wear: local and general. *Optom Vis Sci* 2006;**83**:27-36.

87. Tan J, Keay L, Jalbert I, Naduvilath TJ, Sweeney DF, Holden BA. Mucin balls with wear of conventional and silicone hydrogel contact lenses. *Optom Vis Sci* 2003;**80**:291-7.

88. Morgan PB, Efron N. Comparative clinical performance of two silicone hydrogel contact lenses for continuous wear. *Clin Exp Optom* 2002;**85**:183-92.

89. Graham AD, Truong TN, Lin MC. Conjunctival epithelial flap in continuous contact lens wear. *Optom Vis Sci* 2009;**86**:e324-e331.

90. Guillon M, Maissa C. Bulbar conjunctival staining in contact lens wearers and non lens wearers and its association with symptomatology. *Cont Lens Anterior Eye* 2005;**28**:67-73.

91. Lofstrom T, Kruse A. A conjunctival response to silicone hydrogel lens wear. *Contact Lens Spectrum* 2005;**20**:42-4.

92. Santodomingo-Rubido J, Wolffsohn J, Gilmartin B. Conjunctival epithelial flaps with 18 months of silicone hydrogel contact lens wear. *Eye and Contact Lens* 2008;**34**:35-8.

93. Lofstrom T, Kruse A. A conjunctival response to silicone hydrogel lens wear. *Contact Lens Spectrum* 2005;**20**:42-4.

94. Veys J, Meyler J, Davies I. Essential contact lens practice - Part 11. *Optician.* 2008;**235**:32-7.

95. Veys J, Meyler J, Davies I. Essential contact lens practice - Part 12. *Optician.* 2008;**235**:28-37.

96. Santodomingo-Rubido J, Rubido-Crespo MJ. The clinical investigation of the base curve and comfort rate of a new prototype silicone hydrogel contact lens. *Eye Contact Lens* 2008;**34**:146-50.

97. Woods R. Quantitative slit lamp observations in contact lens practice. *Journal of the British Contact Lens Association* 1989;**1989**:42-5.

98. Larke J.K. *The Eye in Contact Lens Wear*. 1977.

99. Young G. Evaluation of soft contact lens fitting characteristics. *Optom Vis Sci* 1996;**73**:247-54.

100. GonzÃ¡lez-Cavada J, Corral O, NiÃ±o A, Estrella MA, Fuentes JA, Madrid-Costa D. Base curve influence on the fitting and comfort of the Senofilcon a contact lens. *J Optom* 2009;**2**:90-3.

101. Patel S, Mackay C, McCallum G. The clinical evaluation of hydrogel lens back optic zone radius according to 3 commercially available procedures. *Journal of the British Contact Lens Association* 1988;**11**:17-24.

102. Tranoudis I, Efron N. Tensile properties of soft contact lens materials. *Contact Lens and Anterior Eye* 2004;**27**:177-91.

103. Lowther GE, Tomlinson A. Critical base curve and diameter interval in the fitting of spherical soft contact lenses. *Am J Optom Physiol Opt* 1981;**58**:355-60.

104. Garner LF. Sagittal height of the anterior eye and contact lens fitting. *Am J Optom Physiol Opt* 1982;**59**:301-5.

105. Young G. Ocular sagittal height and soft contact lens fit. *J Brit Contact Lens Assoc* 1992;**15**:45-9.

106. Sorbara L, Maram J, Fonn D, Woods C, Simpson T. Metrics of the normal cornea: anterior segment imaging with the Visante OCT. *Clin Exp Optom* 2010;**93**:150-6.

107. Dumbleton K, Keir N, Moezzi A, Feng Y, Jones L, Fonn D. Objective and subjective responses in patients refitted to daily-wear silicone hydrogel contact lenses. *Optom Vis Sci* 2006;**83**:758-68.

108. Liesegang TJ. Physiologic changes of the cornea with contact lens wear. *CLAO J* 2002;**28**:12-27.

109. Efron N. Vascular response of the cornea to contact lens wear. *J Am Optom Assoc* 1987;**58**:836-46.

110. Holden BA, Sweeney DF, Vannas A, Nilsson KT, Efron N. Effects of Long-Term Extended Contact-Lens Wear on the Human Cornea. *Invest Ophthalmol Vis.Sci.* 1985;**26**:1489-501.

111. Hamano H, Watanabe K, Hamano T, Mitsunaga S, Kotani S, Okada A. A study of the complications induced by conventional and disposable contact lenses. *CLAO journal* 1994;**20**:103-8.

112. Stocker EG, Schoessler JP. Corneal endothelial polymegathism induced by PMMA contact lens wear. *Investigative Ophthalmology and Visual Science* 1985;**26**:857-63.

113. Binder PS. The physiologic effects of extended wear soft contact lenses. *Ophthalmology* 1980;**87**:745-9.

114. Papas EB, Vajdic CM, Austen R, Holden BA. High-oxygen-transmissibility soft contact lenses do not induce limbal hyperaemia. *Curr Eye Res* 1997;**16**:942-8.

115. Dumbleton KA, Chalmers RL, Richter DB, Fonn D. Vascular response to extended wear of hydrogel lenses with high and low oxygen permeability. *Optom Vis Sci* 2001;**78**:147-51.

116. Papas E. On the relationship between soft contact lens oxygen transmissibility and induced limbal hyperaemia. *Exp Eye Res* 1998;**67**:125-31.

117. Polverini PJ. The pathophysiology of angiogenesis. *Crit Rev Oral Biol Med* 1995;**6**:230-47.

118. Guillon M, MaÃ¯ssa C. Long-term effects of the extended wear of senofilcon A silicone hydrogel contact lenses on ocular tissues. *Optometry* 2010;**81**:671-9.

119. Riley C, Young G, Chalmers R. Prevalence of ocular surface symptoms, signs, and uncomfortable hours of wear in contact lens wearers: The effect of refitting with daily-wear silicone hydrogel lenses (senofilcon A). *Eye and Contact Lens* 2006;**32**:281-6.

120. Coles M, Brennan N, Jaworski A. ocular signs and symptoms in patients completing 3 years with silicone hydrogel lenses in 30-day continuous wear. *Optom Vis Sci* 2001;**201**.

121. Holden BA, Sweeney DF. The Significance of the Microcyst Response - A Review. *Optom.Vis.Sci.* 1991;**68**:703-7.

122. Holden BA. The Glenn A. Fry Award lecture 1988: The ocular response to contact lens wear. *Optom.Vis.Sci.* 1989;**66**:717-33.

123. Holden BA, Sweeney DF, Vannas A. Prediction of extended wear microcyst response on the basis of mean overnight corneal response in an unrelated sample of non-wearers. *Invest Ophthalmol Vis Sci* 1985;**26**:1489-501.

124. Keay L, Sweeney DF, Jalbert I, Skotnitsky C, Holden BA. Microcyst response to high Dk/t silicone hydrogel contact lenses. *Optom Vis Sci* 2000;**77**:582-5.

125. Cotsarelis G, Cheng SZ, Dong G, Sun TT, Lavker RM. Existence of slow-cycling limbal epithelial basal cells that can be preferentially stimulated to proliferate: Implications on epithelial stem cells. *Cell* 1989;**57**:201-9.

126. Zieske JD. Perpetuation of stem cells in the eye. *Eye* 1994;**8**:163-9.

127. Ladage PM, Ren DH, Petroll WM, Jester JV, Bergmanson JP, Cavanagh HD. Effects of eyelid closure and disposable and silicone hydrogel extended contact lens wear on rabbit corneal epithelial proliferation. *Invest Ophthalmol Vis Sci* 2003;**44**:1843-9.

128. Ladage PM, Jester JV, Petroll WM, Bergmanson JP, Cavanagh HD. Vertical movement of epithelial basal cells toward the corneal surface during use of extended-wear contact lenses. *Invest Ophthalmol Vis Sci* 2003;**44**:1056-63.

129. O'Leary DJ, Madgewick R, Wallace J, Ang J. Size and number of epithelial cells washed from the cornea after contact lens wear. *Optom Vis Sci* 1998;**75**:692-6.

130. Imayasu M, Shiraishi A, Ohashi Y, Shimada S, Cavanagh HD. Effects of multipurpose solutions on corneal epithelial tight junctions. *Eye and Contact Lens* 2008;**34**:50-5.

131. McCanna DJ, Harrington KL, Driot JY, Ward KW, Tchao R. Use of a human corneal epithelial cell line for screening the safety of contact lens care solutions in vitro. *Eye and Contact Lens* 2008;**34**:6-12.

132. Nomura K, Nakao M, Matsubara K. Subjective symptom of eye dryness and lifestyle factors with corneal neovascularization in contact lens wearers. *Eye Contact Lens* 2004;**30**:95-8.

133. Murphy PJ, Patel S, Marshall J. The effect of long-term, daily contact lens wear on corneal sensitivity. *Cornea* 2001;**20**:264-9.

134. Polse KA. Etiology of corneal sensitivity changes accompanying contact lens wear. *Investigative Ophthalmology and Visual Science* 1978;**17**:1202-6.

135. Ladage PM, Jester JV, Petroll WM, Bergmanson JP, Cavanagh HD. Vertical movement of epithelial basal cells toward the corneal surface during use of extended-wear contact lenses. *Invest Ophthalmol Vis Sci* 2003;**44**:1056-63.

136. Cavanagh HD, Ladage PM, Li SL, Yamamoto K, Molai M, Ren DH et al. Effects of daily and overnight wear of a novel hyper oxygen-transmissible soft contact lens on bacterial binding and corneal epithelium: A 13-month clinical trial. *Ophthalmology* 2002;**109**:1957-69.

137. Ren DH, Yamamoto K, Ladage PM, Molai M, Li L, Petroll WM et al. Adaptive effects of 30-night wear of hyper-O2 transmissible contact lenses on bacterial binding and corneal epithelium: A 1-year clinical trial. *Ophthalmology* 2002;**109**:27-39.

138. Ren DH, Petroll WM, Jester JV, Cavanagh HD. The effect of rigid gas permeable contact lens wear on proliferation of rabbit corneal and conjunctival epithelial cells. *CLAO J* 1999;**25**:136-41.

139. Li L, Ren DH, Ladage PM, Yamamoto K, Petroll WM, Jester JV et al. Annexin V binding to rabbit corneal epithelial cells following overnight contact lens wear or eyelid closure. *CLAO J* 2002;**28**:48-54.

140. Stapleton F, Kasses S, Bolis S, Keay L. Short term wear of high Dk soft contact lenses does not alter corneal epithelial cell size or viability. *Br J Ophthalmol* 2001;**85**:143-6.

141. O'Leary DJ, Wilson G, Henson DB. The effect of anoxia on the human corneal epithelium. *Am J Optom Physiol Opt* 1981;**58**:472-6.

142. Wilson FM. Adverse external ocular effects of topical ophthalmic therapy: an epidemiologic, laboratory, and clinical study. *Trans Am Ophthalmol Soc* 1983;**81**:854-965.

143. Ladage PM, Yamamoto K, Ren DH, Li L, Jester JV, Petroll WM et al. Effects of rigid and soft contact lens daily wear on corneal epithelium, tear lactate dehydrogenase, and bacterial binding to exfoliated epithelial cells. *Ophthalmology* 2001;**108**:1279-88.

144. Perez JG, Meijome JMG, Jalbert I, Sweeney DF, Erickson P. Corneal epithelial thinning profile induced by long-term wear of hydrogel lenses. *Cornea* 2003;**22**:304-7.

145. Patel SV, McLaren JW, Hodge DO, Bourne WM. Confocal microscopy in vivo in corneas of long-term contact lens wearers. *Invest Ophthalmol Vis Sci* 2002;**43**:995-1003.

146. Tsubota K, Yamada M. Corneal epithelial alterations induced by disposable contact lens wear. *Ophthalmology* 1992;**99**:1193-6.

147. Bergmanson JP, Ruben CM, Chu LW. Epithelial morphological response to soft hydrogel contact lenses. *Br J Ophthalmol* 1985;**69**:373-9.

148. Ladage PM, Ren DH, Petroll WM, Jester JV, Bergmanson JP, Cavanagh HD. Effects of eyelid closure and disposable and silicone hydrogel extended contact lens wear on rabbit corneal epithelial proliferation. *Invest Ophthalmol Vis Sci* 2003;**44**:1843-9.

149. Swarbrick HA, Wong G, O'Leary DJ. Corneal response to orthokeratology. *Optom Vis Sci* 1998;**75**:791-9.

150. Ruiz-Montenegro J, Mafra CH, Wilson SE, Jumper JM, Klyce SD, Mendelson EN. Corneal topographic alterations in normal contact lens wearers. *Ophthalmology* 1993;**100**:128-34.

151. Albietz JM. Conjunctival histologic findings of dry eye and non-dry eye contact lens wearing subjects. *CLAO J* 2001;**27**:35-40.

152. Yeniad B, Yigit B, Issever H, Kozer B. Effects of contact lenses on corneal thickness and corneal curvature during usage. *Eye Contact Lens* 2003;**29**:223-9.

153. Jalbert I, Sweeney DF, Stapleton F. The effect of long-term wear of soft lenses of low and high oxygen transmissibility on the corneal epithelium. *Eye* 2009;**23**:1282-7.

154. Efron N. Contact lens-induced changes in the anterior eye as observed in vivo with the confocal microscope. *Prog Retin Eye Res* 2007;**26**:398-436.

155. Miller D. Contact lens-induced corneal curvature and thickness changes. *Arch Ophthalmol* 1968;**80**:430-2.

156. Kok JH, Hilbrink HJ, Rosenbrand RM, Visser R. Extended-wear of high oxygen-permeable quantum contact lenses. *Int Ophthalmol* 1992;**16**:123-7.

157. Sanaty M, Temel A. Corneal curvature changes in soft and rigid gas permeable contact lens wearers after two years of lens wear. *CLAO J* 1996;**22**:186-8.

158. Levenson DS. Changes in corneal curvature with long-term PMMA contact lens wear. *CLAO J* 1983;**9**:121-5.

159. Mandell RB. Methods to measure the peripheral corneal curvature. Part one: Photokeratoscopy. *J Am Optometric Assoc* 1961;**33**:137-9.

160. Moezzi AM, Fonn D, Simpson TL, Sorbara L. Contact lens-induced corneal swelling and surface changes measured with the Orbscan II corneal topographer. *Optom Vis Sci* 2004;**81**:189-93.

161. Yaylali V, Kaufman SC, Thompson HW. Corneal thickness measurements with the Orbscan Topography System and ultrasonic pachymetry. *J Cataract Refract Surg* 1997;**23**:1345-50.

162. Liu Z, Pflugfelder SC. The effects of long-term contact lens wear on corneal. *Ophthalmology* 2000;**107**:105-11.

163. Cho P, Lam AK, Mountford J, Ng L. The performance of four different corneal topographers on normal human corneas and its impact on orthokeratology lens fitting. *Optom Vis Sci* 2002;**79**:175-83.

164. Tang W, Collins MJ, Carney L, Davis B. The accuracy and precision performance of four videokeratoscopes in measuring test surfaces. *Optom Vis Sci* 2000;**77**:483-91.

165. Cho P, Lam AK, Mountford J, Ng L. The performance of four different corneal topographers on normal human corneas and its impact on orthokeratology lens fitting. *Optom Vis Sci* 2002;**79**:175-83.

166. Fonn D, du T, Simpson TL, Vega JA, Situ P, Chalmers RL. Sympathetic swelling response of the control eye to soft lenses in the other eye. *Invest Ophthalmol Vis Sci* 1999;**40**:3116-21.

167. Harris HG, Sarver MD, Brown LR. Corneal edema with hydrogel lenses and eye closure: Time course. *Am J Optom Physiol Opt* 1981;**58**:18-20.

168. Harvitt DM, Bonanno JA. Re-evaluation of the oxygen diffusion model for predicting minimum contact lens Dk/t values needed to avoid corneal anoxia. *Optom.Vis.Sci.* 1999;**76**:712-9.

169. Holden BA, McNally JJ, Mertz GW, Swarbrick HA. Topographical corneal oedema. *Acta Ophthalmol (Copenh)* 1985;**63**:684-91.

170. Bergenske P, Mueller N, Caroline P, Smythe J, Mai-Le K. Uniformity of overnight corneal swelling with extended wear contact lenses. *Optom Vis Sci* 2001;**78**.

171. Hamano H, Maeda N, Hamano T, Mitsunaga S, Kotani S. Corneal thickness change induced by dozing while wearing hydrogel and silicone hydrogel lenses. *Eye Contact Lens* 2008;**34**:56-60.

172. Steffen RB, Schnider CM. The impact of silicone hydrogel materials on overnight corneal swelling. *Eye Contact Lens* 2007;**33**:115-20.

173. Sridharan R, Swarbrick H. Corneal response to short-term orthokeratology lens wear. *Optom Vis Sci* 2003;**80**:200-6.

174. Villasenor RA, Santos VR, Cox KC, Harris DF, Lynn M, Waring GO. Comparison of Ultrasonic Corneal Thickness Measurements Before and During Surgery in the Prospective Evaluation of Radial Keratotomy (Perk) Study. *Ophthalmology* 1986;**93**:327-30.

175. Reinstein DZ, Silverman RH, Trokel SL, Coleman DJ. Corneal Pachymetric Topography. *Ophthalmology* 1994;**101**:432-8.

176. Pavlin CJ, Harasiewicz K, Sherar MD, Foster ES. Clinical Use of Ultrasound Biomicroscopy. *Ophthalmology* 1991;**98**:287-95.

177. Pavlin CJ, Foster FS. Ultrasound biomicroscopy. High-frequency ultrasound imaging of the eye at microscopic resolution. *Radiol Clin North Am* 1998;**36**:1047-58.

178. Dorairaj S, Liebmann JM, Ritch R. Quantitative evaluation of anterior segment parameters in the era of imaging. *Trans Am Ophthalmol Soc* 2007;**105**:99-108.

179. Azen SP, Burg KA, Smith RE, Maguen E. A comparison of three methods for the measurement of corneal thickness. *Invest Ophthalmol Vis Sci* 1979;**18**:535-8.

180. Cotinat J. [Specular microscopy of the corneal endothelium]. *J Fr Ophtalmol* 1999;**22**:255-61.

181. Eisner G. A contact lens for endothelial and epithelial specular microscopy. *J Am Intraocul Implant Soc* 1983;**9**:470-1.

182. Christensen A, Narvaez J, Zimmerman G. Comparison of central corneal thickness measurements by ultrasound pachymetry, konan noncontact optical pachymetry, and orbscan pachymetry. *Cornea* 2008;**27**:862-5.

183. Sallet G. Comparison of optical and ultrasound central corneal pachymetry. *Bull Soc Belge Ophtalmol* 2001;35-8.

184. Chan T, Payor S, Holden BA. Corneal thickness profiles in rabbits using an ultrasonic pachometer. *Invest Ophthalmol Vis Sci* 1983;**24**:1408-10.

185. Gifford P, Alharbi A, Swarbrick HA. Corneal thickness changes in hyperopic orthokeratology measured by optical pachometry. *Invest Ophthalmol Vis Sci* 2011;**52**:3648-53.

186. Gonzalez-Perez J, Gonzalez-Meijome JM, Rodriguez A, Parafita MA. Central corneal thickness measured with three optical devices and ultrasound pachometry. *Eye Contact Lens* 2011;**37**:66-70.

187. Karimian F, Feizi S, Doozandeh A, Faramarzi A, Yaseri M. Comparison of corneal tomography measurements using Galilei, Orbscan II, and Placido disk-based topographer systems. *J Refract Surg* 2011;**27**:502-8.

188. Oliveira CM, Ribeiro C, Franco S. Corneal imaging with slit-scanning and Scheimpflug imaging techniques. *Clin Exp Optom* 2011;**94**:33-42.

189. Arce CG, Soriano ES, Weisenthal RW, Hamilton SM, Rocha KM, Alzamora JB et al. Calculation of intraocular lens power using Orbscan II quantitative area topography after corneal refractive surgery. *J Refract Surg* 2009;**25**:1061-74.

190. Birnbaum F, Schwartzkopff J, Bohringer D, Reinhard T. The Intrastromal Corneal Ring in Penetrating Keratoplasty-Long-term Results of a Prospective Randomized Study. *Cornea* 2011;**30**:780-3.

191. Myrowitz EH, Melia M, O'Brien TP. The relationship between long-term contact lens wear and corneal thickness. *CLAO J.* 2002;**28**:217-20.

192. Cho P, Lam AK, Mountford J, Ng L. The performance of four different corneal topographers on normal human corneas and its impact on orthokeratology lens fitting. *Optom.Vis.Sci.* 2002;**79**:175-83.

193. Fakhry MA, Artola A, Belda JI, Ayala MJ, Alio JL. Comparison of corneal pachymetry using ultrasound and Orbscan II. *J Cataract Refract Surg* 2002;**28**:248-52.

194. Cho P, Cheung SW. Repeatability of corneal thickness measurements made by a scanning slit topography system. *Ophthalmic Physiol Opt* 2002;**22**:505-10.

195. Gonzalez-Meijome JM, Cervino A, Yebra-Pimentel E, Parafita MA. Central and peripheral corneal thickness measurement with Orbscan II and topographical ultrasound pachymetry. *J Cataract Refract Surg* 2003;**29**:125-32.

196. Huang D, Swanson EA, Lin CP, Schuman JS, Stinson WG, Chang W et al. Optical Coherence Tomography. *Science* 1991;**254**:1178-81.

197. Fujimoto JG, Bouma B, Tearney GJ, Boppart SA, Pitris C, Southern JF et al. New technology for high-speed and high-resolution optical coherence tomography. *Ann N Y Acad Sci* 1998;**838**:95-107.

198. Rogowska J, Bryant CM, Brezinski ME. Cartilage thickness measurements from optical coherence tomography. *J Opt Soc Am A Opt Image Sci Vis* 2003;**20**:357-67.

199. Baba T, Moriyama M, Nishimuta A, Mochizuki M. Retinal detachment due to a retinal break in the macular atrophy of a myopic choroidal neovascularization. *Ophthalmic Surg Lasers Imaging* 2007;**38**:242-4.

200. Brown JC, Solomon SD, Bressler SB, Schachat AP, DiBernardo C, Bressler NM. Detection of diabetic foveal edema: contact lens biomicroscopy compared with optical coherence tomography. *Arch Ophthalmol* 2004;**122**:330-5.

201. Browning DJ, Fraser CM. Optical coherence tomography to detect macular edema in the presence of asteroid hyalosis. *Am J Ophthalmol* 2004;**137**:959-61.

202. Costa RA, Jorge R, Calucci D, Melo LA, Cardillo JA, Scott IU. Intravitreal bevacizumab (avastin) for central and hemicentral retinal vein occlusions: IBeVO study. *Retina* 2007;**27**:141-9.

203. Miura M, Mori H, Watanabe Y, Usui M, Kawana K, Oshika T et al. Three-dimensional optical coherence tomography of granular corneal dystrophy. *Cornea* 2007;**26**:373-4.

204. Radhakrishnan S, Rollins AM, Roth JE, Yazdanfar S, Westphal V, Bardenstein DS et al. Real-time optical coherence tomography of the anterior segment at 1310 nm. *Arch Ophthalmol* 2001;**119**:1179-85.

205. Savini G, Barboni P, Zanini M. Tear meniscus evaluation by optical coherence tomography. *Ophthalmic Surg Lasers Imaging* 2006;**37**:112-8.

206. Sebag J. Seeing the invisible: the challenge of imaging vitreous. *J Biomed Opt* 2004;**9**:38-46.

207. Sin S, Simpson TL. The repeatability of corneal and corneal epithelial thickness measurements using optical coherence tomography. *Optom Vis Sci* 2006;**83**:360-5.

208. Tearney GJ, Brezinski ME, Southern JF, Bouma BE, Boppart SA, Fujimoto JG. Optical biopsy in human gastrointestinal tissue using optical coherence tomography. *Am J Gastroenterol* 1997;**92**:1800-4.

209. Holtzman JS, Osann K, Pharar J, Lee K, Ahn YC, Tucker T et al. Ability of Optical Coherence Tomography to Detect Caries Beneath Commonly Used Dental Sealants. *Lasers Surg Med* 2010;**42**:752-9.

210. Barwari K, de Bruin DM, Cauberg ECC, Faber DJ, van Leeuwen TG, Wijkstra H et al. Advanced Diagnostics in Renal Mass Using Optical Coherence Tomography: A Preliminary Report. *J Endourol* 2011;**25**:311-5.

211. Francis GS, Evans AC, Arnold DL. Neuroimaging in Multiple-Sclerosis. *Int Rev Neurobiol* 1995;**13**:147-71.

212. Izatt JA, Hee MR, Swanson EA, Lin CP, Huang D, Schuman JS et al. Micrometer-scale resolution imaging of the anterior eye in vivo with optical coherence tomography. *Arch Ophthalmol* 1994;**112**:1584-9.

213. Azzolini C, Patelli F, Brancato R. Correlation between optical coherence tomography data and biomicroscopic interpretation of idiopathic macular hole. *Am J Ophthalmol* 2001;**132**:348-55.

214. Konno S, Akiba J, Sato E, Kuriyama S, Yoshida A. OCT in successful surgery of retinal detachment associated with optic nerve head pit. *Ophthalmic Surgery and Lasers* 2000;**31**:236-9.

215. Stanga PE, Bird AC. Optical coherence tomography (OCT): principles of operation, technology, indications in vitreoretinal imaging and interpretation of results. *Int Ophthalmol* 2001;**23**:191-7.

216. Azzolini C, Pierro L, Codenotti M, Brancato R. OCT images and surgery of juvenile macular retinoschisis. *Eur J Ophthalmo* 1997;**7**:196-200.

217. Wang Y, Bower BA, Izatt JA, Tan O, Huang D. In vivo total retinal blood flow measurement by Fourier domain Doppler optical coherence tomography. *J Biomed Opt* 2007;**12**:041215.

218. Fujimoto JG, Brezinski ME, Tearney GJ, Boppart SA, Bouma B, Hee MR et al. Optical biopsy and imaging using optical coherence tomography. *Nat Med* 1995;**1**:970-2.

219. Schmitt JM, Yadlowsky MJ, Bonner RF. Subsurface imaging of living skin with optical coherence microscopy. *Dermatology* 1995;**191**:93-8.

220. Jaffe GJ, Caprioli J. Optical coherence tomography to detect and manage retinal disease and glaucoma. *American Journal of Ophthalmology* 2004;**137**:156-69.

221. Muscat S, McKay N, Parks S, Kemp E, Keating D. Repeatability and reproducibility of corneal thickness measurements by optical coherence tomography. *Invest Ophthalmol Vis Sci* 2002;**43**:1791-5.

222. Wang J, Aquavella J, Palakuru J, Chung S, Feng C. Relationships between central tear film thickness and tear menisci of the upper and lower eyelids. *Invest Ophthalmol Vis Sci* 2006;**47**:4349-55.

223. Wang J, Fonn D, Simpson TL, Jones L. The measurement of corneal epithelial thickness in response to hypoxia using optical coherence tomography. *Am J Ophthalmol* 2002;**133**:315-9.

224. Bagayev SN, Gelikonov VM, Gelikonov GV, Kargapoltsev ES, Kuranov RV, Razhev AM et al. Optical coherence tomography for in situ monitoring of laser corneal ablation. *J Biomed Opt* 2002;**7**:633-42.

225. Haque S, Fonn D, Simpson T, Jones L. Corneal and epithelial thickness changes after 4 weeks of overnight corneal refractive therapy lens wear, measured with optical coherence tomography. *Eye Contact Lens* 2004;**30**:189-93.

226. Baikoff G. Anterior segment OCT and phakic intraocular lenses: a perspective. *J Cataract Refract Surg* 2006;**32**:1827-35.

227. Bayraktar S, Bayraktar Z. Central corneal thickness and intraocular pressure relationship in eyes with and without previous LASIK: comparison of Goldmann applanation tonometer with pneumatonometer. *Eur J Ophthalmol* 2005;**15**:81-8.

228. Bitton E, Keech A, Simpson T, Jones L. Variability of the analysis of the tear meniscus height by optical coherence tomography. *Optom Vis Sci* 2007;**84**:903-8.

229. Bizheva K, Povazay B, Hermann B, Sattmann H, Drexler W, Pehamberger H. Compact, broad-bandwidth fiber laser for sub-2-ìm axial resolution optical coherence tomography in the 1300-nm wavelength region. *Opt Lett* 2003;**28**:709.

230. Dawczynski J, Koenigsdoerffer E, Augsten R, Strobel J. Anterior optical coherence tomography: a non-contact technique for anterior chamber evaluation. *Graefes Arch Clin Exp Ophthalmol* 2007;**245**:423-5.

231. Dunne MC, Davies LN, Wolffsohn JS. Accuracy of cornea and lens biometry using anterior segment optical coherence tomography. *J Biomed Opt* 2007;**12**:064023.

232. El M, Baudouin C. [Tear meniscus in Visante OCT]. *J Fr Ophtalmol* 2007;**30**:559.

233. Feng Y, Simpson TL. Comparison of human central cornea and limbus in vivo using optical coherence tomography. *Optom Vis Sci* 2005;**82**:416-9.

234. Feng Y, Simpson TL. Corneal, limbal, and conjunctival epithelial thickness from optical coherence tomography. *Optom Vis Sci* 2008;**85**:E880-E883.

235. Fishman GR, Pons ME, Seedor JA, Liebmann JM, Ritch R. Assessment of central corneal thickness using optical coherence tomography. *J Cataract Refract Surg* 2005;**31**:707-11.

236. Garcia JP, Garcia PM, Buxton DE, Panarelli A, Rosen RB. Imaging through opaque corneas using anterior segment optical coherence tomography. *Ophthalmic Surg Lasers Imaging* 2007;**38**:314-8.

237. Radhakrishnan S, Goldsmith J, Huang D, Westphal V, Dueker DK, Rollins AM et al. Comparison of optical coherence tomography and ultrasound biomicroscopy for detection of narrow anterior chamber angles. *Archives of Ophthalmology* 2005;**123**:1053-9.

238. Kalev-landoy M, Day AC, Cordeiro MF, Migdal C. Optical coherence tomography in anterior segment imaging. *Acta Ophthalmol Scand* 2007;**85**:427-30.

239. Zhang Q, Jin W, Wang Q. Repeatability, reproducibility, and agreement of central anterior chamber depth measurements in pseudophakic and phakic eyes: Optical coherence tomography versus ultrasound biomicroscopy. *J Cataract Refract Surg* 2010;**36**:941-6.

240. Wirbelauer C, Karandish A, Haberle H, Pham DT. Noncontact goniometry with optical coherence tomography. *Arch Ophthalmol* 2005;**123**:179-85.

241. Simpson T, Fonn D. Optical coherence tomography of the anterior segment. *Ocul Surf* 2008;**6**:117-27.

242. Konstantopoulos A, Hossain P, Anderson DF. Recent advances in ophthalmic anterior segment imaging: a new era for ophthalmic diagnosis? *Br J Ophthalmol* 2007;**91**:551-7.

243. McLaren JW, Nau CB, Erie JC, Bourne WM. Corneal thickness measurement by confocal microscopy, ultrasound, and scanning slit methods. *American Journal of Ophthalmology* 2004;**137**:1011-20.

244. Cheng ACK, Lam DSC, McLaren JW, Nau CB, Erie JC, Bourne WM. Corneal thickness measurement by confocal microscopy, ultrasound, and scanning slit methods [3] (multiple letters). *American Journal of Ophthalmology* 2005;**139**:391-2.

245. Bechmann M, Thiel MJ, Neubauer AS, Ullrich S, Ludwig K, Kenyon KR et al. Central corneal thickness measurement with a retinal optical coherence tomography device versus standard ultrasonic pachymetry. *Cornea* 2001;**20**:50-4.

246. Doughty MJ, Zaman ML. Human corneal thickness and its impact on intraocular pressure measures: a review and meta-analysis approach. *Surv Ophthalmol* 2000;**44**:367-408.

247. Prospero P, Rocha KM, Smith SD, Krueger RR. Central and peripheral corneal thickness measured with optical coherence tomography, Scheimpflug imaging, and ultrasound pachymetry in normal, keratoconus-suspect, and post-laser in situ keratomileusis eyes. *J Cataract Refract Surg* 2009;**35**:1055-62.

248. Wang J, Fonn D, Simpson TL. Topographical thickness of the epithelium and total cornea after hydrogel and PMMA contact lens wear with eye closure. *Invest Ophthalmol Vis Sci.* 2003;**44**:1070-4.

249. Wang J, Fonn D, Simpson TL, Sorbara L, Kort R, Jones L. Topographical thickness of the epithelium and total cornea after overnight wear of reverse-geometry rigid contact lenses for myopia reduction. *Invest Ophthalmol Vis Sci* 2003;**44**:4742-6.

250. Wang J, Simpson TL, Fonn D. Objective measurements of corneal light-backscatter during corneal swelling, by optical coherence tomography. *Invest Ophthalmol Vis Sci* 2004;**45**:3493-8.

251. Hutchings N, Simpson TL, Hyun C, Moayed AA, Hariri S, Sorbara L et al. Swelling of the human cornea revealed by high-speed, ultrahigh-resolution optical coherence tomography. *Invest Ophthalmol Vis Sci* 2010;**51**:4579-84.

252. Dementyev DD, Kourenkov VV, Rodin AS, Fadeykina TL, Diaz M. Retinal nerve fiber layer changes after LASIK evaluated with optical coherence tomography. *J Refract Surg* 2005;**21**:S623-S627.

253. Li Y, Netto MV, Shekhar R, Krueger RR, Huang D. A longitudinal study of LASIK flap and stromal thickness with high-speed optical coherence tomography. *Ophthalmology* 2007;**114**:1124-32.

254. Wang J, Thomas J, Cox I. Corneal light backscatter measured by optical coherence tomography after LASIK. *J Refract Surg* 2006;**22**:604-10.

255. Wirbelauer C, Pham DT. Continuous monitoring of corneal thickness changes during LASIK with online optical coherence pachymetry. *J Cataract Refract Surg* 2004;**30**:2559-68.

256. Mishima S, Gasset A, Klyce J, Baum JL. Determination of tear volume and tear flow. *Investigative ophthalmology* 1966;**5**:264-76.

257. Nichols JJ, Sinnott LT. Tear film, contact lens, and patient-related factors associated with contact lens-related dry eye. *Invest Ophthalmol Vis Sci* 2006;**47**:1319-28.

258. Palakuru JR, Wang J, Aquavella JV. Effect of blinking on tear dynamics. *Investigative Ophthalmology and Visual Science* 2007;**48**:3032-7.

259. Azartash K, Kwan J, Paugh JR, Nguyen AL, Jester JV, Gratton E. Pre-corneal tear film thickness in humans measured with a novel technique. *Molecular Vision* 2011;**17**:756-67.

260. King-Smith PE, Fink BA, Fogt N, Nichols KK, Hill RM, Wilson GS. The thickness of the human precorneal tear film: evidence from reflection spectra. *Invest Ophthalmol Vis Sci* 2000;**41**:3348-59.

261. Prydal JI, Artal P, Woon H, Campbell FW. Study of human precorneal tear film thickness and structure using laser interferometry. *Invest Ophthalmol Vis Sci* 1992;**33**:2006-11.

262. Wang J, Fonn D, Simpson TL, Jones L. Precorneal and pre- and postlens tear film thickness measured indirectly with optical coherence tomography. *Invest Ophthalmol Vis Sci* 2003;**44**:2524-8.

263. Wang J, Aquavella J, Palakuru J, Chung S. Repeated measurements of dynamic tear distribution on the ocular surface after instillation of artificial tears. *Invest Ophthalmol Vis Sci* 2006;**47**:3325-9.

264. Lee R, Ahmed I. Anterior Segment Optical Coherence Tomography: Non-contact High Resolution Imaging of the Anterior Chamber. *Techniques in Ophthalmology* 2006;**4**:120-7.

265. Li H, Leung CK, Wong L, Cheung CY, Pang CP, Weinreb RN et al. Comparative Study of Central Corneal Thickness Measurement with Slit-Lamp Optical Coherence Tomography and Visante Optical Coherence Tomography. *Ophthalmology* 2007.

266. Prakash G, Agarwal A, Jacob S, Kumar DA, Agarwal A, Banerjee R. Comparison of fourier-domain and time-domain optical coherence tomography for assessment of corneal thickness and intersession repeatability. *Am J Ophthalmol* 2009;**148**:282-90.

267. Puvanathasan P, Forbes P, Ren Z, Malchow D, Boyd S, Bizheva K. High-speed, high-resolution Fourier-domain optical coherence tomography system for retinal imaging in the 1060 nm wavelength region. *Opt Lett* 2008;**33**:2379-81.

268. Bizheva K, Lee P, Sorbara L, Hutchings N, Simpson T. In vivo volumetric imaging of the human upper eyelid with ultrahigh-resolution optical coherence tomography. *J Biomed Opt* 2010;**15**:040508.

269. Hariri S, Moayed AA, Dracopolos A, Hyun C, Boyd S, Bizheva K. Limiting factors to the OCT axial resolution for in-vivo imaging of human and rodent retina in the 1060nm wavelength range. *Optics Express* 2009;**17**:24304-16.

270. Young G, Schnider C, Hunt C, Efron S. Corneal topography and soft contact lens fit. *Optom Vis Sci* 2010;**87**:358-66.

271. Read SA, Collins MJ, Iskander DR, Davis BA. Corneal topography with Scheimpflug imaging and videokeratography: Comparative study of normal eyes. *J Cataract Refract Surg* 2009;**35**:1072-81.

272. Wan SC, Cho P. A comparative study of the performance of different corneal topographers on children with respect to orthokeratology practice. *Optom.Vis.Sci.* 2005;**82**:420-7.

273. Chui WS, Cho P. A comparative study of the performance of different corneal topographers on children with respect to orthokeratology practice. *Optom Vis Sci* 2005;**82**:420-7.

274. Kruse DE, Silverman RH, Fornaris RJ, Jackson Coleman D, Ferrara KW. A swept-scanning mode for estimation of blood velocity in the microvasculature. *IEEE Transactions on Ultrasonics, Ferroelectrics, and Frequency Control* 1998;**45**:1437-43.

275. Yazdanfar S, Rollins AM, Izatt JA. In vivo imaging of human retinal flow dynamics by color Doppler optical coherence tomography. *Arch Ophthalmol* 2003;**121**:235-9.

276. Matthiessen ET, Zeitz O, Richard G, Klemm M. Reproducibility of blood flow velocity measurements using colour decoded Doppler imaging. *Eye* 2004;**18**:400-5.

277. Lemaillet P, Duncan DD, Lompado A, Ibrahim M, Nguyen QD, Ramella-Roman JC. Retinal spectral imaging and blood flow measurement. *Invest Ophthalmol Vis Sci* 2010;**3**:255-65.

278. Tanaka T, Riva C, Ben Sira I. Blood velocity measurements in human retinal vessels. *Science* 1974;**186**:830-1.

279. Cioffi GA, Alm A. Measurement of ocular blood flow. *Br J Ophthalmol* 2001;**10**:S62-S64.

280. de Jong FJ, Vernooij MW, Ikram MK, Ikram MA, Hofman A, Krestin GP et al. Arteriolar Oxygen Saturation, Cerebral Blood Flow, and Retinal Vessel Diameters. The Rotterdam Study. *Ophthalmology* 2008;**115**:887-92.

281. Japee SA, Ellis CG, Pittman RN. Flow visualization tools for image analysis of capillary networks. *FASEB Journal* 1998;**12**.

282. Lesk MR, Wajszilber M, Deschenes MC. The effects of systemic medications on ocular blood flow. *Can J Ophthalmol* 2008;**43**:351-5.

283. Riva CE, Grunwald JE, Sinclair SH, Petrig BL. Blood velocity and volumetric flow rate in human retinal vessels. *Invest Ophthalmol Vis Sci* 1985;**26**:1124-32.

284. Eden E, Waisman D, Rudzsky M, Bitterman H, Brod V, Rivlin E. An automated method for analysis of flow characteristics of circulating particles from in vivo video microscopy. *IEEE Transactions on Medical Imaging* 2005;**24**:1011-24.

285. Steinman DA, Taylor CA. Flow imaging and computing: Large artery hemodynamics. *Ann Biomed Eng* 2005;**33**:1704-9.

286. Piovella C. In vivo observations of the microcirculation of the bulbar conjunctiva in migraneous. *Res Clin Stud Headache* 1970;**3**:277-93.

287. Duench S. Development of Novel Techniques for Measuring Bulbar Conjunctival Red Blood Cell Velocity, Oximetry and Redness. 118-136. 2009. University of Waterloo.

References – Chapter 2

1. Holden BA, Mertz GW, McNally JJ. Corneal swelling response to contact lenses worn under extended wear conditions. *Investigative Ophthalmology and Visual Science* 1983;**24**:218-26.

2. Wang J, Fonn D, Simpson TL. Topographical thickness of the epithelium and total cornea after hydrogel and PMMA contact lens wear with eye closure. *Invest Ophthalmol Vis Sci.* 2003;**44**:1070-4.

3. Haque S, Jones L, Simpson T. Thickness mapping of the cornea and epithelium using optical coherence tomography. *Optom Vis Sci* 2008;**85**:E963-E976.

4. Li Y, Netto MV, Shekhar R, Krueger RR, Huang D. A longitudinal study of LASIK flap and stromal thickness with high-speed optical coherence tomography. *Ophthalmology* 2007;**114**:1124-32.

5. Maldonado MJ, Ruiz-Oblitas L, Munuera JM, Aliseda D, Garcia-Layana A, Moreno-Montanes J. Optical coherence tomography evaluation of the corneal cap and stromal bed features after laser in situ keratomileusis for high myopia and astigmatism. *Ophthalmology* 2000;**107**:81-7.

6. Fam HB, Lim KL, Reinstein DZ. Orbscan global pachymetry: analysis of repeated measures. *Optom Vis Sci* 2005;**82**:1047-53.

7. Wang J, Fonn D, Simpson TL, Jones L. Relation between optical coherence tomography and optical pachymetry measurements of corneal swelling induced by hypoxia. *Am J Ophthalmol* 2002;**134**:93-8.

8. Gordon A, Boggess EA, Molinari JF. Variability of ultrasonic pachometry. *Optom Vis Sci* 1990;**67**:162-5.

9. Reinstein DZ, Silverman RH, Rondeau MJ, Coleman DJ. Epithelial and corneal thickness measurements by high-frequency ultrasound digital signal processing. *Ophthalmology* 1994;**101**:140-6.

10. Amano S, Honda N, Amano Y, Yamagami S, Miyai T, Samejima T et al. Comparison of central corneal thickness measurements by rotating Scheimpflug camera, ultrasonic pachymetry, and scanning-slit corneal topography. *Ophthalmology* 2006;**113**:937-41.

11. Bechmann M, Thiel MJ, Neubauer AS, Ullrich S, Ludwig K, Kenyon KR et al. Central corneal thickness measurement with a retinal optical coherence tomography device versus standard ultrasonic pachymetry. *Cornea* 2001;**20**:50-4.

12. Drexler W. Ultrahigh-resolution optical coherence tomography. *J Biomed Opt* 2004;**9**:47-74.

13. Kaluzny BJ, Kaluzny JJ, Szkulmowska A, Gorczynska I, Szkulmowski M, Bajraszewski T et al. Spectral optical coherence tomography - A novel technique for cornea imaging. *Cornea* 2006;**25**:960-5.

14. Sin S, Simpson TL. The repeatability of corneal and corneal epithelial thickness measurements using optical coherence tomography. *Optom Vis Sci* 2006;**83**:360-5.

15. Stanga PE, Bird AC. Optical coherence tomography (OCT): principles of operation, technology, indications in vitreoretinal imaging and interpretation of results. *Int Ophthalmol* 2001;**23**:191-7.

16. Wang M, Luo R, Liu Y. [Optical coherence tomography and its application in ophthalmology]. *Yan Ke Xue Bao* 1998;**14**:116-20, 115.

17. Fujimoto JG. Optical coherence tomography for ultrahigh resolution in vivo imaging. *Nat.Biotechnol.* 2003;**21**:1361-7.

18. Simpson T, Fonn D. Optical coherence tomography of the anterior segment. *Ocular Surface* 2008;**6**:117-27.

19. Leung CKS, Choi N, Weinreb RN, Liu S, Ye C, Liu L et al. Retinal nerve fiber layer imaging with spectral-domain optical coherence tomography: Pattern of RNFL defects in glaucoma. *Ophthalmology* 2010;**117**:2337-44.

20. Kiernan DF, Mieler WF, Hariprasad SM. Spectral-Domain Optical Coherence Tomography: A Comparison of Modern High-Resolution Retinal Imaging Systems. *American Journal of Ophthalmology* 2010;**149**:18-31.

21. Matonti F, Hoffart L, Alessi G, Baeteman C, Trichet E, Madar J et al. Spectral-domain optical coherence tomography in anterior segment imaging: The 3rd dimension. *Journal Francais d'Ophtalmologie* 2009;**32**:727-34.

22. Haque S, Fonn D, Simpson T, Jones L. Corneal and epithelial thickness changes after 4 weeks of overnight corneal refractive therapy lens wear, measured with optical coherence tomography. *Eye Contact Lens* 2004;**30**:189-93.

23. Haque S, Simpson T, Jones L. Corneal and epithelial thickness in keratoconus: a comparison of ultrasonic pachymetry, Orbscan II, and optical coherence tomography. *J Refract Surg* 2006;**22**:486-93.

24. Muscat S, McKay N, Parks S, Kemp E, Keating D. Repeatability and reproducibility of corneal thickness measurements by optical coherence tomography. *Invest Ophthalmol Vis Sci* 2002;**43**:1791-5.

25. Mohamed S, Lee GK, Rao SK, Wong AL, Cheng AC, Li EY et al. Repeatability and reproducibility of pachymetric mapping with Visante anterior segment-optical coherence tomography. *Invest Ophthalmol Vis Sci* 2007;**48**:5499-504.

26. Wildner K, Muller M, Dawczynski J, Strobel J. [Comparison of the corneal thickness as measured by Visante anterior segment OCT versus ultrasound technique]. *Klin Monatsbl Augenheilkd* 2007;**224**:832-6.

27. Li H, Leung CK, Wong L, Cheung CY, Pang CP, Weinreb RN et al. Comparative Study of Central Corneal Thickness Measurement with Slit-Lamp Optical Coherence Tomography and Visante Optical Coherence Tomography. *Ophthalmology* 2008;**115**:796-801.

28. Lee R, Ahmed IIK. Anterior segment optical coherence tomography: Non-contact high resolution imaging of the anterior chamber. *Techniques in Ophthalmology* 2006;**4**:120-7.

29. Asai-Coakwell M, Backhouse C, Casey RJ, Gage PJ, Lehmann OJ. Reduced human and murine corneal thickness in an Axenfeld-Rieger syndrome subtype. *Invest Ophthalmol Vis Sci* 2006;**47**:4905-9.

30. Aurich H, Wirbelauer C, Jaroszewski J, Hartmann C, Pham DT. Continuous measurement of corneal dehydration with online optical coherence pachymetry. *Cornea* 2006;**25**:182-4.

31. Feng Y, Varikooty J, Simpson TL. Diurnal variation of corneal and corneal epithelial thickness measured using optical coherence tomography. *Cornea* 2001;**20**:480-3.

32. Haque S, Fonn D, Simpson T, Jones L. Corneal refractive therapy with different lens materials, part 1: corneal, stromal, and epithelial thickness changes. *Optom Vis Sci* 2007;**84**:343-8.

33. Doughty MJ, Zaman ML. Human corneal thickness and its impact on intraocular pressure measures: A review and meta-analysis approach. *Survey of Ophthalmology* 2000;**44**:367-408.

34. Wong ACM, Wong CC, Yuen NSY, Hui SP. Correlational study of central corneal thickness measurements on Hong Kong Chinese using optical coherence tomography, Orbscan and ultrasound pachymetry. *Eye* 2002;**16**:715-21.

35. Marsich MM, Bullimore MA. The repeatability of corneal thickness measures. *Cornea* 2000;**19**:792-5.

36. Bechmann M, Thiel MJ, Roesen B, Ullrich S, Ulbig MW, Ludwig K. Central corneal thickness determined with optical coherence tomography in various types of glaucoma. *British Journal of Ophthalmology* 2000;**84**:1233-7.

37. Gordon MO, Beiser JA, Brandt JD, Heuer DK, Higginbotham EJ, Johnson CA et al. The Ocular Hypertension Treatment Study: Baseline factors that predict the onset of primary open-angle glaucoma. *Archives of Ophthalmology* 2002;**120**:714-20.

38. Zhao PS, Wong TY, Wong WL, Saw SM, Aung T. Comparison of central corneal thickness measurements by Visante anterior segment optical coherence tomography with ultrasound pachymetry. *Am J Ophthalmol* 2007;**143**:1047-9.

39. Moezzi AM, Sin S, Simpson TL. Novel pachometry calibration. *Optom Vis Sci* 2006;**83**:366-71.

40. Wolffsohn JS, Peterson RC. Anterior ophthalmic imaging. *Clin Exp Optom* 2006;**89**:205-14.

41. Edmund C, la C. Some components affecting the precision of corneal thickness measurement performed by optical pachometry. *Acta Ophthalmol (Copenh)* 1986;**64**:499-503.

42. Lattimore MR, Kaupp S, Schallhorn S, Lewis R. Orbscan pachymetry: implications of a repeated measures and diurnal variation analysis. *Ophthalmology* 1999;**106**:977-81.

43. Madgula IM, Kotta S. Stratus optical coherence tomogram III: a novel, reliable and accurate way to measure corneal thickness. *Indian J Ophthalmol* 2007;**55**:301-3.

44. Olsen T, Nielsen CB, Ehlers N. On the optical measurement of a corneal thickness. I. Optical principle and sources of error. *Acta Ophthalmol (Copenh)* 1980;**58**:760-6.

45. Bland J, Altman DG. Statistical methods for assessing agreement between two methods of clinical measurement. *Lancet* 1986;307-10.

46. Dunn G. Regression models for method comparison data. *Journal of Biopharmaceutical Statistics* 2007;**17**:739-56.

47. Hutchings N, Simpson TL, Hyun C, Moayed AA, Hariri S, Sorbara L et al. Swelling of the human cornea revealed by high-speed, ultrahigh-resolution optical coherence tomography. *Invest Ophthalmol Vis Sci* 2010;**51**:4579-84.

48. Lu F, Xu S, Qu J, Shen M, Wang X, Fang H et al. Central corneal thickness and corneal hysteresis during corneal swelling induced by contact lens wear with eye closure. *Am J Ophthalmol* 2007;**143**:616-22.

49. Larsen M, Wang M, Sander B. Overnight thickness variation in diabetic macular edema. *Invest Ophthalmol Vis Sci* 2005;**46**:2313-6.

50. Bayraktar S, Bayraktar Z. Central corneal thickness and intraocular pressure relationship in eyes with and without previous LASIK: comparison of Goldmann applanation tonometer with pneumatonometer. *Eur J Ophthalmol* 2005;**15**:81-8.

51. Grewal DS, Brar GS, Grewal SP. Assessment of central corneal thickness in normal, keratoconus, and post-laser in situ keratomileusis eyes using Scheimpflug imaging, spectral domain optical coherence tomography, and ultrasound pachymetry. *J Cataract Refract Surg* 2010;**36**:954-64.

52. Yenerel NM, Kucumen RB, Gorgun E. Changes in corneal biomechanics in patients with keratoconus after penetrating keratoplasty. *Cornea* 2010;**29**:1247-51.

53. Vasudevan B, Simpson TL, Sivak JG. Regional variation in the refractive-index of the bovine and human cornea. *Optom Vis Sci* 2008;**85**:977-81.

54. Patel S. Some theoretical factors governing the accuracy of corneal-thickness measurement. *Ophthalmic Physiol Opt* 1981;**1**:193-203.

55. Mandell RB. Corneal power correction factor for photorefractive keratectomy. *J Refract Corneal Surg* 1994;**10**:125-8.

56. Dunne MC, Davies LN, Wolffsohn JS. Accuracy of cornea and lens biometry using anterior segment optical coherence tomography. *J Biomed Opt* 2007;**12**:064023.

57. Monteiro PML, Hull CC. The effect of videokeratoscope faceplate design on radius of curvature maps. *Ophthalmic Physiol Opt* 2007;**27**:76-84.

58. Prospero P, Rocha KM, Smith SD, Krueger RR. Central and peripheral corneal thickness measured with optical coherence tomography, Scheimpflug imaging, and ultrasound pachymetry

in normal, keratoconus-suspect, and post-laser in situ keratomileusis eyes. *J Cataract Refract Surg* 2009;**35**:1055-62.

59. Patel S, Alio JL, Artola A. Changes in the refractive index of the human corneal stroma during laser in situ keratomileusis. Effects of exposure time and method used to create the flap. *J Cataract Refract Surg* 2008;**34**:1077-82.

60. Feng Y, Simpson TL. Comparison of human central cornea and limbus in vivo using optical coherence tomography. *Optom Vis Sci* 2005;**82**:416-9.

References- Chapter 3

1. Modis L, Langenbucher A, Seitz B. Evaluation of normal corneas using the scanning-slit topography/pachymetry system. *Cornea* 2004;**23**:689-94.

2. Hee MR, Puliafito CA, Duker JS, Schuman JS, Swanson EA, Fujimoto JG. Topography of diabetic macular edema with optical coherence tomography. *Ophthalmology* 1998;**105**:360-70.

3. Rutledge BK, Puliafito CA, Duker JS, Cox MS. Optical coherence tomography of the macular lesions associated with optic nerve pits. *Ophthalmology* 1996;**103**:1047-53.

4. Schuman JS, Hee MR, Puliafito CA, Wong C, Pedut-Kloizman T, Swanson EA et al. Quantification of nerve fibre thickness in normal and glaucomatous eyes using optical coherence tomography. *Arch Ophthalmo* 1995;**113**:586-96.

5. Schuman JS, Puliafito CA, Fujimoto JG. *Optical coherence tomography of ocular diseases*. 2 ed. Thorofare, NJ: SLACK, 2004.

6. Toth CA, Birngruber R, Boppart SA, Hee MR, Fujimoto JG, Swanson EA et al. Argon laser retinal lesions evaluated in vivo by optical coherence tomography. *Am J Ophthalmol* 1997;**123**:188-98.

7. Wilkins JR, Puliafito CA, Hee MR, Duker JS, Reichel E, Coker JG et al. Characterization of epi-retinal membranes using optical coherence tomography. *Ophthalmology* 1996;**103**:2142-51.

8. Wheeler NC, Morantes CM, Kristensen RM, Pettit TH, Lee DA. Reliability coefficients of three corneal pachymeters. *Am J Ophthalmol* 1992;**113**:645-51.

9. Jalbert I, Stapleton F, Papas E, Sweeney DF, Coroneo M. In vivo confocal microscopy of the human cornea. *Br J Ophthalmol* 2003;**87**:225-36.

10. Avitabile T, Marano F, Uva MG, Reibaldi A. Evaluation of central and peripheral corneal thickness with ultrasound biomicroscopy in normal and keratoconic eyes. *Cornea* 1997;**16**:639-44.

11. Yaylali V, Kaufman SC, Thompson HW. Corneal thickness measurements with the Orbscan Topography System and ultrasonic pachymetry. *J Cataract Refract Surg* 1997;**23**:1345-50.

12. Izatt JA, Hee MR, Swanson EA, Lin CP, Huang D, Schuman JS et al. Micrometer-scale resolution imaging of the anterior eye in vivo with optical coherence tomography. *Arch Ophthalmol* 1994;**112**:1584-9.

13. Muscat S, McKay N, Parks S, Kemp E, Keating D. Repeatability and reproducibility of corneal thickness measurements by optical coherence tomography. *Invest Ophthalmol Vis Sci* 2002;**43**:1791-5.

14. Wong AC, Wong CC, Yuen NS, Hui SP. Correlational study of central corneal thickness measurements on Hong Kong Chinese using optical coherence tomography, Orbscan and ultrasound pachymetry. *Eye* 2002;**16**:715-21.

15. Hirano K, Ito Y, Suzuki T, Kojima T, Kachi S, Miyake Y. Optical coherence tomography for the noninvasive evaluation of the cornea. *Cornea* 2001;**20**:281-9.

16. Huang D, Li Y, Radhakrishnan S. Optical coherence tomography of the anterior segment of the eye. *Ophthalmol Clin North Am* 2004;**17**:1-6.

17. Lee R, Ahmed I. Anterior Segment Optical Coherence Tomography: Non-contact High Resolution Imaging of the Anterior Chamber. *Techniques in Ophthalmology* 2006;**4**:120-7.

18. Li H, Leung CK, Wong L, Cheung CY, Pang CP, Weinreb RN et al. Comparative Study of Central Corneal Thickness Measurement with Slit-Lamp Optical Coherence Tomography and Visante Optical Coherence Tomography. *Ophthalmology* 2007.

19. Radhakrishnan S, Rollins AM, Roth JE, Yazdanfar S, Westphal V, Bardenstein DS et al. Real-time optical coherence tomography of the anterior segment at 1310 nm. *Arch Ophthalmol* 2001;**119**:1179-85.

20. Feng Y, Varikooty J, Simpson TL. Diurnal variation of corneal and corneal epithelial thickness measured using optical coherence tomography. *Cornea* 2001;**20**:480-3.

21. Haque S, Fonn D, Simpson T, Jones L. Corneal and epithelial thickness changes after 4 weeks of overnight corneal refractive therapy lens wear, measured with optical coherence tomography. *Eye Contact Lens* 2004;**30**:189-93.

22. Haque S, Simpson T, Jones L. Corneal and epithelial thickness in keratoconus: a comparison of ultrasonic pachymetry, Orbscan II, and optical coherence tomography. *J Refract Surg* 2006;**22**:486-93.

23. Wang J, Fonn D, Simpson TL. Topographical thickness of the epithelium and total cornea after hydrogel and PMMA contact lens wear with eye closure. *Invest Ophthalmol Vis Sci* 2003;**44**:1070-4.

24. Gonzalez-Meijome JM, Cervino A, Yebra-Pimentel E, Parafita MA. Central and peripheral corneal thickness measurement with Orbscan II and topographical ultrasound pachymetry. *J Cataract Refract Surg* 2003;**29**:125-32.

25. Gonzalez-Perez J, Gonzalez-Meijome JM, Rodriguez A, Parafita MA. Central corneal thickness measured with three optical devices and ultrasound pachometry. *Eye Contact Lens* 2011;**37**:66-70.

26. Bland J, Altman DG. Statistical methods for assessing agreement between two methods of clinical measurement. *Lancet* 1986;307-10.

27. Lin LI. A concordance correlation-coefficient to evaluate reproducibility. *Biometrics* 1989;**45**:255-68.

28. Izatt JA, Hee MR, Swanson EA, Lin CP, Huang D, Schuman JS et al. Micrometer-scale resolution imaging of the anterior eye in vivo with optical coherence tomography. *Arch Ophthalmol* 1994;**112**:1584-9.

29. Bechmann M, Thiel MJ, Neubauer AS, Ullrich S, Ludwig K, Kenyon KR et al. Central corneal thickness measurement with a retinal optical coherence tomography device versus standard ultrasonic pachymetry. *Cornea* 2001;**20**:50-4.

30. Sin S, Simpson TL. The repeatability of corneal and corneal epithelial thickness measurements using optical coherence tomography. *Optom Vis Sci* 2006;**83**:360-5.

31. Wang J, Aquavella J, Palakuru J, Chung S, Feng C. Relationships between central tear film thickness and tear menisci of the upper and lower eyelids. *Invest Ophthalmol Vis Sci* 2006;**47**:4349-55.

32. Wirbelauer C, Pham DT. Continuous monitoring of corneal thickness changes during LASIK with online optical coherence pachymetry. *J Cataract Refract Surg* 2004;**30**:2559-68.

33. Prakash G, Agarwal A, Jacob S, Kumar DA, Agarwal A, Banerjee R. Comparison of fourier-domain and time-domain optical coherence tomography for assessment of corneal thickness and intersession repeatability. *Am J Ophthalmol* 2009;**148**:282-90.

34. Mohamed S, Lee GK, Rao SK, Wong AL, Cheng AC, Li EY et al. Repeatability and reproducibility of pachymetric mapping with Visante anterior segment-optical coherence tomography. *Invest Ophthalmol Vis Sci* 2007;**48**:5499-504.

35. Li Y, Shekhar R, Huang D. Corneal pachymetry mapping with high-speed optical coherence tomography. *Ophthalmology* 2006;**113**:792-9.

36. Marsich MW, Bullimore MA. The repeatability of corneal thickness measures. *Cornea* 2000;**19**:792-5.

37. Sander B, Larsen M, Thrane L, Hougaard JL, JÃ¸rgensen TM. Enhanced optical coherence tomography imaging by multiple scan averaging. *Br J Ophthalmol* 2005;**89**:207-12.

References- Chapter 4

1. Guillon M, Maissa C. Bulbar conjunctival staining in contact lens wearers and non lens wearers and its association with symptomatology. *Cont Lens Anterior Eye* 2005;**28**:67-73.

2. Graham AD, Truong TN, Lin MC. Conjunctival epithelial flap in continuous contact lens wear. *Optom.Vis.Sci.* 2009;**86**:E324-E331.

3. Santodomingo-Rubido J, Wolffsohn J, Gilmartin B. Conjunctival epithelial flaps with 18 months of silicone hydrogel contact lens wear. *Eye Contact Lens* 2008;**34**:35-8.

4. KaÅ‚uzny BJ, Kaluzny JJ, Szkulmowska A, GorczyÅ„ska I, Szkulmowski M, Bajraszewski T et al. Spectral optical coherence tomography: A new imaging technique in contact lens practice. *Ophthalmic and Physiol Opt* 2006;**26**:127-32.

5. Mountford J, Cho P, Chui WS. Is fluorescein pattern analysis a valid Method of assessing the accuracy of reverse geometry lenses for orthokeratology? *Clin Exp Optom* 2005;**88**:33-8.

6. Young G. Ocular sagittal height and soft contact lens fit. *J Brit Contact Lens Assoc* 1992;**15**:45-9.

7. Gonzalez-Meijome JM, CerviÃ A, Carracedo G, Queiros A, Garcia-LÃ¡zaro S, Ferrer-Blasco T. High-Resolution Spectral Domain Optical Coherence Tomography Technology for the Visualization of Contact Lens to Cornea Relationships. *Cornea* 2010;**29**:1359-67.

8. Cho P, Cheung SW, Mountford J, White P. Good clinical practice in orthokeratology. *Cont Lens Anterior Eye* 2008;**31**:17-28.

9. Sridharan R, Swarbrick H. Corneal response to short-term orthokeratology lens wear. *Optom Vis Sci* 2003;**80**:200-6.

10. Swarbrick HA, Wong G, O'Leary DJ. Corneal response to orthokeratology. *Optom Vis Sci* 1998;**75**:791-9.

11. Fujimoto JG, Bouma B, Tearney GJ, Boppart SA, Pitris C, Southern JF et al. New technology for high-speed and high-resolution optical coherence tomography. *Ann N Y Acad Sci* 1998;**838**:95-107.

12. Huang D, Swanson EA, Lin CP, Schuman JS, Stinson WG, Chang W et al. Optical Coherence Tomography. *Science* 1991;**254**:1178-81.

13. Fercher AF, Drexler W, Hitzenberger CK, Lasser T. Optical coherence tomography - Principles and applications. *Reports on Progress in Physics* 2003;**66**:239-303.

14. Drexler W, Morgner U, Ghanta RK, Kartner FX, Schuman JS, Fujimoto JG. Ultrahigh-resolution ophthalmic optical coherence tomography. *Nat Med* 2001;**7**:502-7.

15. Drexler W, Fujimoto JG. State-of-the-art retinal optical coherence tomography. *Prog Retin Eye Res* 2008;**27**:45-88.

16. Ho J, Witkin AJ, Liu J, Chen Y, Fujimoto JG, Schuman JS et al. Documentation of intraretinal retinal pigment epithelium migration via high-speed ultrahigh-resolution optical coherence tomography. *Ophthalmology* 2011;**118**:687-93.

17. Wang Y, Lu A, Gil-Flamer J, Tan O, Izatt JA, Huang D. Measurement of total blood flow in the normal human retina using Doppler Fourier-domain optical coherence tomography. *Br J Ophthalmol* 2009;**93**:634-7.

18. Kaluzny JJ, Wojtkowski M, Sikorski BL, Szkulmowski M, Szkulmowska A, Bajraszewski T et al. Analysis of the outer retina reconstructed by high-resolution, three-dimensional spectral domain optical coherence tomography. *Ophthalmic Surg Lasers and Imaging* 2008;**39**:S30-S36.

19. Yasuno Y, Yamanari M, Kawana K, Miura M, Fukuda S, Makita S et al. Visibility of trabecular meshwork by standard and polarization-sensitive optical coherence tomography. *J Biomed Opt* 2010;**15**:161-67.

20. Potsaid B, Baumann B, Huang D, Barry S, Cable AE, Schuman JS et al. Ultrahigh speed 1050nm swept source/Fourier domain OCT retinal and anterior segment imaging at 100,000 to 400,000 axial scans per second. *Opt Express* 2010;**18**:20029-48.

21. Schuman JS, Hee MR, Arya AV, Pedut-Kloizman T, Puliafito CA, Fujimoto JG et al. Optical coherence tomography: a new tool for glaucoma diagnosis. *Curr Opin Ophthalmol* 1995;**6**:89-95.

22. Izatt JA, Hee MR, Swanson EA, Lin CP, Huang D, Schuman JS et al. Micrometer-scale resolution imaging of the anterior eye in vivo with optical coherence tomography. *Arch Ophthalmol* 1994;**112**:1584-9.

23. Leung CKS, Choi N, Weinreb RN, Liu S, Ye C, Liu L et al. Retinal nerve fiber layer imaging with spectral-domain optical coherence tomography: Pattern of RNFL defects in glaucoma. *Ophthalmology* 2010;**117**:2337-44.

24. Aref AA, Budenz DL. Spectral domain optical coherence tomography in the diagnosis and management of glaucoma. Ophthalmic surgery, lasers & imaging : the official journal of the International Society for Imaging in the Eye 2010;**41 Suppl**:S15-S27.

25. Kiernan DF, Mieler WF, Hariprasad SM. Spectral-Domain Optical Coherence Tomography: A Comparison of Modern High-Resolution Retinal Imaging Systems. *Am J Ophthalmol* 2010;**149**:18-31.

26. Matonti F, Hoffart L, Alessi G, Baeteman C, Trichet E, Madar J et al. Spectral-domain optical coherence tomography in anterior segment imaging: The 3rd dimension. *Journal Francais d'Ophtalmologie* 2009;**32**:727-34.

27. Gora M, Karnowski K, Szkulmowski M, Kaluzny BJ, Huber R, Kowalczyk A et al. Ultra high-speed swept source OCT imaging of the anterior segment of human eye at 200 kHz with adjustable imaging range. *Opt Express* 2009;**17**:14880-94.

28. Choma MA, Sarunic MV, Yang C, Izatt JA. Sensitivity advantage of swept source and Fourier domain optical coherence tomography. *Opt Express* 2003;**11**:2183-9.

29. Lim H, Mujat M, Kerbage C, Lee ECW, Chen Y, Chen TC et al. High-speed imaging of human retina in vivo with swept-source optical coherence tomography. *Opt Express* 2006;**14**:12902-8.

30. Wojtkowski M, Srinivasan VJ, Ko TH, Fujimoto JG, Kowalczyk A, Duker JS. Ultrahigh-resolution, high-speed, Fourier domain optical coherence tomography and methods for dispersion compensation. *Opt Express* 2004;**12**:2404-22.

31. Wojtkowski M, Bajraszewski T, Targowski P, Kowalczyk A. Real-time in vivo imaging by high-speed spectral optical coherence tomography. *Opt Lett* 2003;**28**:1745-7.

32. Wang Y, Nelson JS, Chen Z, Reiser BJ, Chuck RS, Windeler RS. Optimal wavelength for ultrahigh-resolution optical coherence tomography. *Opt Express* 2003;**11**:1411-7.

33. Hall LA, Young G, Wolffsohn JS, Riley C. The Influence of Corneo-Scleral Topography on Soft Contact Lens Fit. *Invest Ophthalmol Vis Sci* 2011.

34. Shen M, Cui L, Riley C, Wang MR, Wang J. Characterization of soft contact lens edge fitting using ultra-high resolution and ultra-long scan depth optical coherence tomography. *Invest Ophthalmol Vis Sci* 2011;**52**:4091-7.

References- Chapter 5

1. Young G, Coleman S. Poorly fitting soft lenses affect ocular integrity. *CLAO J* 2001;**27**:68-74.

2. Young G. Evaluation of soft contact lens fitting characteristics. *Optom Vis Sci* 1996;**73**:247-54.

3. Young G, Holden B, Cooke G. Influence of soft contact lens design on clinical performance. *Optom Vis Sci* 1993;**70**:394-403.

4. Anna sulley. Soft contact lens fitting. *Contact lens fitting today* 2005;46-51.

5. Young G. Exploring the relationship between materials and ocular health and comfort. *Contact Lens Spectrum* 2007;**Special Edition**:37-40.

6. Efron N, Young G. Dehydration of hydrogen contact lenses in vitro and in vivo. *Ophthalmic Physiol Opt* 1988;**8**:253-6.

7. Douthwaite WA. Initial selection of soft contact lenses based on corneal characteristics. *CLAO J* 2002;**28**:202-5.

8. Andrasko G. The amount and time course of soft contact lens dehydration. *J Am Optom Assoc* 1982;**53**:207.

9. Dumbleton KA, Chalmers RL, McNally J, Bayer S, Fonn D. Effect of lens base curve on subjective comfort and assessment of fit with silicone hydrogel continuous wear contact lenses. *Optom Vis Sci* 2002;**79**:633-7.

10. Young G, Schnider C, Hunt C, Efron S. Corneal topography and soft contact lens fit. *Optom Vis Sci* 2010;**87**:358-66.

11. Fonn D, Dumbleton K, Papas E. Conjunctival appearance related to silicone hydrogel lens wear. *Contact Lens Spectrum* 2005;**20**:46-52.

12. Fonn D. Targeting contact lens induced dryness and discomfort: what properties will make lenses more comfortable. *Optom Vis Sci* 2007;**84**:279-85.

13. Begley CG, Barr JT, Edrington TB, Long WD, McKenney CD, Chalmers RL. Characteristics of corneal staining in hydrogel contact lens wearers. *Optom Vis Sci* 1996;**73**:193-200.

14. Orsborn GN, Zantos SG. Corneal desiccation staining with thin high water content contact lenses. *CLAO J* 1988;**14**:81-5.

15. Fonn D, Dumbleton K. Dryness and discomfort with silicone hydrogel contact lenses. *Eye Contact Lens* 2003;**29**:S101-S104.

16. Richdale K, Sinnott LT, Skadahl E, Nichols JJ. Frequency of and factors associated with contact lens dissatisfaction and discontinuation. *Cornea* 2007;**26**:168-74.

17. Stahl U, Willcox M, Stapleton F. Role of hypo-osmotic saline drops in ocular comfort during contact lens wear. *Contact Lens and Anterior Eye* 2010;**33**:68-75.

18. Ozkan J, Papas E. Lubricant effects on low dk and silicone hydrogel lens comfort. *Optom.Vis.Sci.* 2008;**85**:773-7.

19. du Toit R, Pritchard N, Heffernan S, Simpson T, Fonn D. A comparison of three different scales for rating contact lens handling. *Optom Vis Sci* 2002;**79**:313-20.

20. Young G, Efron N. Characteristics of the pre-lens tear film during hydrogel contact lens wear. *Ophthalmic Physiol Opt* 1991;**11**:53-8.

21. Nichols KK, Nichols JJ, Mitchell GL. The lack of association between signs and symptoms in patients with dry eye disease. *Cornea* 2004;**23**:762-70.

22. Glasson MJ, Stapleton F, Keay L, Sweeney D, Willcox MD. Differences in clinical parameters and tear film of tolerant and intolerant contact lens wearers. *Invest Ophthalmol Vis Sci* 2003;**44**:5116-24.

23. McNamara NA, Polse KA, Brand RJ, Graham AD, Chan JS, McKenney CD. Tear mixing under a soft contact lens: effects of lens diameter. *Am J Ophthalmol* 1999;**127**:659-65.

24. Paugh JR, Stapleton F, Keay L, Ho A. Tear exchange under hydrogel contact lenses: methodological considerations. *Invest Ophthalmol Vis Sci* 2001;**42**:2813-20.

25. French K. Part2-Mechanical behaviour and modulus. *Optician* 2005;**230**.

26. Stapleton F, Stretton S, Papas E, Skotnitsky C, Sweeney DF. Silicone hydrogel contact lenses and the ocular surface. *Ocular Surface* 2006;**4**:24-43.

27. Skotnitsky C, Sankaridurg PR, Sweeney DF, Holden BA. General and local contact lens induced papillary conjunctivitis (CLPC). *Clin Exp Optom* 2002;**85**:193-7.

28. Dumbleton K. Noninflammatory silicone hydrogel contact lens complications. *Eye Contact Lens* 2003;**29**:S186-S189.

29. Liesegang TJ. Physiologic changes of the cornea with contact lens wear. *CLAO J* 2002;**28**:12-27.

30. Holden BA, Sweeney DF, Vannas A, Nilsson KT, Efron N. Effects of long-term extended contact lens wear on the human cornea. *Invest Ophthalmol Vis Sci* 1985;**26**:1489-501.

31. Whiting MAN, Raynor MK, Morgan PB, Galloway P, Tole DM, Tullo A. Continuous wear silicone hydrogel contact lenses and microbial keratitis. *Eye* 2004;**18**:935-7.

32. Collins MJ, Buehren T, Trevor T, Statham M, Hansen J, Cavanagh DA. Factors influencing lid pressure on the cornea. *Eye Contact Lens* 2006;**32**:168-73.

33. Collins MJ, Buehren T, Bece A, Voetz SC. Corneal optics after reading, microscopy and computer work. *Acta Ophthalmol Scand* 2006;**84**:216-24.

34. Holden BA, Stephenson A, Stretton S, Sankaridurg PR, O'Hare N, Jalbert I et al. Superior epithelial arcuate lesions with soft contact lens wear. *Optom Vis Sci* 2001;**78**:9-12.

35. Bruce AS, Mainstone JC, Golding TR. Analysis of tear film breakup on Etafilcon A hydrogel lenses. *Biomaterials* 2001;**22**:3249-56.

36. Efron N, Morgan PB, Hill EA, Raynor MK, Tullo AB. The size, location, and clinical severity of corneal infiltrative events associated with contact lens wear. *Optom.Vis.Sci.* 2005;**82**:519-27.

37. Liesegang TJ. Physiologic changes of the cornea with contact lens wear. *CLAO J* 2002;**28**:12-27.

38. Maldonado-Codina C, Morgan PB, Schnider CM, Efron N. Short-term physiologic response in neophyte subjects fitted with hydrogel and silicone hydrogel contact lenses. *Optom Vis Sci* 2004;**81**:911-21.

39. Erickson P, Comstock TL, Zantos SG. Is the superior cornea continuously swollen? *Clin Exp Optom* 2002;**85**:168-71.

40. Lin MC, Soliman GN, Song MJ, Smith JP, Lin CT, Chen YQ et al. Soft contact lens extended wear affects corneal epithelial permeability: hypoxic or mechanical etiology? *Cont Lens Anterior Eye* 2003;**26**:11-6.

41. Yeniad B, Yigit B, Issever H, Kozer B. Effects of contact lenses on corneal thickness and corneal curvature during usage. *Eye Contact Lens* 2003;**29**:223-9.

42. Herse P, Akakura N, Ooi C. Topographical corneal edema. An update. *Acta Ophthalmol (Copenh)* 1993;**71**:539-43.

43. Zantos SG, Holden BA. Ocular changes associated with continuous wear of contact lenses. *Aust J Optom* 1978;**61**:418-26.

44. Benjamin WJ, Rasmussen MA. Oxygen consumption of the superior cornea following eyelid closure. *Acta Ophthalmologica* 1988;**66**:309-12.

45. Benjamin WJ, Ruben CM. Human corneal oxygen demands at superior, central, and inferior sites. *J Am Optom Assoc* 1995;**66**:423-8.

46. Josephson JE. A corneal irritation uniquely produced by hydrogel lathed lenses and its resolution. *J Am Optom Assoc* 1978;**49**:869-70.

47. Efron N. Vascular response of the cornea to contact lens wear. *J Am Optom Assoc* 1987;**58**:836-46.

48. Sweeney DF, Gauthier C, Terry R, Chong MS, Holden BA. The Effects of Long-Term Contact-Lens Wear on the Anterior Eye. *Invest Ophthalmol Vis.Sci.* 1992;**33**:1293.

49. Stapleton F, Stretton S, Papas E, Skotnitsky C, Sweeney DF. Silicone hydrogel contact lenses and the ocular surface. *Ocul Surf* 2006;**4**:24-43.

50. Sweeney DF. The Max Schapero Memorial Award Lecture 2004: contact lenses on and in the cornea, what the eye needs. *Optom Vis Sci* 2006;**83**:133-42.

51. Dumbleton KA, Woods CA, Jones LW, Fonn D. Comfort and adaptation to silicone hydrogel lenses for daily wear. *Eye Contact Lens* 2008;**34**:215-23.

52. Dumbleton K, Keir N, Moezzi A, Feng Y, Jones L, Fonn D. Objective and subjective responses in patients refitted to daily-wear silicone hydrogel contact lenses. *Optom Vis Sci* 2006;**83**:758-68.

53. Morgan PB, Efron N. Comparative clinical performance of two silicone hydrogel contact lenses for continuous wear. *Clin Exp Optom* 2002;**85**:183-92.

54. Fonn D, MacDonald KE, Richter D, Pritchard N. The ocular response to extended wear of a high Dk silicone hydrogel contact lens. *Clin Exp Optom* 2002;**85**:176-82.

55. Morgan P, Efron N. A decade of contact lens prescribing trends in the United Kingdom (1996-2005). *Cont Lens Anterior Eye* 2006;**29**:59-68.

56. Brennan NA, Coles MLC, Comstock TL, Levy B. A 1-year prospective clinical trial of balafilcon A (PureVision) silicone-hydrogel contact lenses used on a 30-day continuous wear schedule. *Ophthalmology* 2002;**109**:1172-7.

57. Brennan NA, Coles ML, Ang JH. An evaluation of silicone-hydrogel lenses worn on a daily wear basis. *Clin Exp Optom* 2006;**89**:18-25.

58. Szczotka-Flynn L, Diaz M. Risk of corneal inflammatory events with silicone hydrogel and low dk hydrogel extended contact lens wear: a meta-analysis. *Optom Vis Sci* 2007;**84**:247-56.

59. Dumbleton K, Fonn D, Jones L, Williams-Lyn D. Severity and management of CL related complications with continuous wear of high DK silicone hydrogel lenses. *Optom Vis Sci* 2000;**77**:216.

60. Morgan P. Is the UK contact lens market healthy? *Optician* 2001;**5795**:22-6.

61. Fonn D. Dryness with contact lenses and dry eye: are they the same or different? *Eye Contact Lens* 2009;**35**:219.

References- Chapter 6

1. Young G, Coleman S. Poorly fitting soft lenses affect ocular integrity. *CLAO J* 2001;**27**:68-74.

2. Young G. Evaluation of soft contact lens fitting characteristics. *Optom Vis Sci* 1996;**73**:247-54.

3. Young G, Holden B, Cooke G. Influence of soft contact lens design on clinical performance. *Optom Vis Sci* 1993;**70**:394-403.

4. Veys J, Meyler J, Davies I. Essential contact lens practice - Part 11. *Optician.* 2008;**235**:32-7.

5. Veys J, Meyler J, Davies I. Essential contact lens practice - Part 12. *Optician.* 2008;**235**:28-37.

6. Moezzi AM, Sin S, Simpson TL. Novel pachometry calibration. *Optom Vis Sci* 2006;**83**:366-71.

7. Hutchings N, Simpson TL, Hyun C, Moayed AA, Hariri S, Sorbara L et al. Swelling of the human cornea revealed by high-speed, ultrahigh-resolution optical coherence tomography. *Invest Ophthalmol Vis Sci* 2010;**51**:4579-84.

8. Lu F, Xu S, Qu J, Shen M, Wang X, Fang H et al. Central corneal thickness and corneal hysteresis during corneal swelling induced by contact lens wear with eye closure. *Am J Ophthalmol* 2007;**143**:616-22.

9. Larsen M, Wang M, Sander B. Overnight thickness variation in diabetic macular edema. *Invest Ophthalmol Vis Sci* 2005;**46**:2313-6.

10. Bayraktar S, Bayraktar Z. Central corneal thickness and intraocular pressure relationship in eyes with and without previous LASIK: comparison of Goldmann applanation tonometer with pneumatonometer. *Eur J Ophthalmol* 2005;**15**:81-8.

11. Li Y, Netto MV, Shekhar R, Krueger RR, Huang D. A longitudinal study of LASIK flap and stromal thickness with high-speed optical coherence tomography. *Ophthalmology* 2007;**114**:1124-32.

12. Grewal DS, Brar GS, Grewal SP. Assessment of central corneal thickness in normal, keratoconus, and post-laser in situ keratomileusis eyes using Scheimpflug imaging, spectral domain optical coherence tomography, and ultrasound pachymetry. *J Cataract Refract Surg* 2010;**36**:954-64.

13. Yenerel NM, Kucumen RB, Gorgun E. Changes in corneal biomechanics in patients with keratoconus after penetrating keratoplasty. *Cornea* 2010;**29**:1247-51.

14. Haque S, Fonn D, Simpson T, Jones L. Corneal and epithelial thickness changes after 4 weeks of overnight corneal refractive therapy lens wear, measured with optical coherence tomography. *Eye Contact Lens* 2004;**30**:189-93.

15. Fatt I, Harris MG. Refractive index of the cornea as a function of its thickness. *Am J Optom Arch Am Acad Optom* 1973;**50**:383-6.

16. Vasudevan B, Simpson TL, Sivak JG. Regional variation in the refractive-index of the bovine and human cornea. *Optom Vis Sci* 2008;**85**:977-81.

17. Patel S. Some theoretical factors governing the accuracy of corneal-thickness measurement. *Ophthalmic Physiol Opt* 1981;**1**:193-203.

18. Mandell RB. Corneal power correction factor for photorefractive keratectomy. *J Refract Corneal Surg* 1994;**10**:125-8.

19. Patel S. Refractive index of the mammalian cornea and its influence during pachometry. *Ophthalmic and Physiological Optics* 1987;**7**:503-6.

20. Patel S, Alio JL, Artola A. Changes in the refractive index of the human corneal stroma during laser in situ keratomileusis. Effects of exposure time and method used to create the flap. *J Cataract Refract Surg* 2008;**34**:1077-82.

21. Leonard DW, Meek KM. Refractive indices of the collagen fibrils and extrafibrillar material of the corneal stroma. *Biophys J* 1997;**72**:1382-7.

22. Clark BA, Carney LG. Refractive index and reflectance of the anterior surface of the cornea. *Am J Optom Arch Am Acad Optom* 1971;**48**:333-43.

23. Dunne MC, Davies LN, Wolffsohn JS. Accuracy of cornea and lens biometry using anterior segment optical coherence tomography. *J Biomed Opt* 2007;**12**:064023.

24. Monteiro PML, Hull CC. The effect of videokeratoscope faceplate design on radius of curvature maps. *Ophthalmic Physiol Opt* 2007;**27**:76-84.

25. Prospero P, Rocha KM, Smith SD, Krueger RR. Central and peripheral corneal thickness measured with optical coherence tomography, Scheimpflug imaging, and ultrasound pachymetry in normal, keratoconus-suspect, and post-laser in situ keratomileusis eyes. *J Cataract Refract Surg* 2009;**35**:1055-62.

26. Sin S, Simpson TL. The repeatability of corneal and corneal epithelial thickness measurements using optical coherence tomography. *Optom Vis Sci* 2006;**83**:360-5.

27. Feng Y, Varikooty J, Simpson TL. Diurnal variation of corneal and corneal epithelial thickness measured using optical coherence tomography. *Cornea* 2001;**20**:480-3.

28. Wang J, Aquavella J, Palakuru J, Chung S, Feng C. Relationships between central tear film thickness and tear menisci of the upper and lower eyelids. *Invest Ophthalmol Vis Sci* 2006;**47**:4349-55.

29. Wirbelauer C, Pham DT. Continuous monitoring of corneal thickness changes during LASIK with online optical coherence pachymetry. *J Cataract Refract Surg* 2004;**30**:2559-68.

30. Wang J, Fonn D, Simpson TL. Topographical thickness of the epithelium and total cornea after hydrogel and PMMA contact lens wear with eye closure. *Invest Ophthalmol Vis Sci.* 2003;**44**:1070-4.

31. Sander B, Larsen M, Thrane L, Hougaard JL, JÃ¸rgensen TM. Enhanced optical coherence tomography imaging by multiple scan averaging. *Br J Ophthalmol* 2005;**89**:207-12.

32. Muscat S, McKay N, Parks S, Kemp E, Keating D. Repeatability and reproducibility of corneal thickness measurements by optical coherence tomography. *Invest Ophthalmol Vis Sci* 2002;**43**:1791-5.

33. Bechmann M, Thiel MJ, Neubauer AS, Ullrich S, Ludwig K, Kenyon KR et al. Central corneal thickness measurement with a retinal optical coherence tomography device versus standard ultrasonic pachymetry. *Cornea* 2001;**20**:50-4.

34. Prakash G, Agarwal A, Jacob S, Kumar DA, Agarwal A, Banerjee R. Comparison of fourier-domain and time-domain optical coherence tomography for assessment of corneal thickness and intersession repeatability. *Am J Ophthalmol* 2009;**148**:282-90.

35. Mohamed S, Lee GK, Rao SK, Wong AL, Cheng AC, Li EY et al. Repeatability and reproducibility of pachymetric mapping with Visante anterior segment-optical coherence tomography. *Invest Ophthalmol Vis Sci* 2007;**48**:5499-504.

36. Li Y, Shekhar R, Huang D. Corneal pachymetry mapping with high-speed optical coherence tomography. *Ophthalmology* 2006;**113**:792-9.

37. Schwallie JD, Bauman RE. Fitting characteristics of Dailies daily disposable hydrogel contact lenses. *CLAO J.* 1998;**24**:102-6.

38. Dumbleton KA, Woods CA, Jones LW, Fonn D. Comfort and adaptation to silicone hydrogel lenses for daily wear. *Eye Contact Lens* 2008;**34**:215-23.

39. Graham AD, Truong TN, Lin MC. Conjunctival epithelial flap in continuous contact lens wear. *Optom Vis Sci* 2009;**86**:e324-e331.

40. Dumbleton K, Woods C, Jones L, Richter D, Fonn D. Comfort and Vision with Silicone Hydrogel Lenses: Effect of Compliance. *Optom Vis Sci* 2010;**87**:421-5.

41. Young G. Soft lens fitting reassessed. *Contact Lens Spectrum* 1992;**7**:56-61.

42. Dumbleton KA, Chalmers RL, McNally J, Bayer S, Fonn D. Effect of lens base curve on subjective comfort and assessment of fit with silicone hydrogel continuous wear contact lenses. *Optom Vis Sci* 2002;**79**:633-7.

43. Brennan NA, Coles ML, Ang JH. An evaluation of silicone-hydrogel lenses worn on a daily wear basis. *Clin Exp Optom* 2006;**89**:18-25.

44. Martin DK. Empirical analysis of the motion of soft contact lenses across the human eye. *Australas Phys Eng Sci Med* 1987;**10**:214-20.

45. Wolffsohn JS, Hunt OA, Basra AK. Simplified recording of soft contact lens fit. *Cont Lens Anterior Eye* 2009;**32**:37-42.

46. Young G. Ocular sagittal height and soft contact lens fit. *J Brit Contact Lens Assoc* 1992;**15**:45-9.

47. Bruce AS. Influence of corneal topography on centration and movement of low water content soft contact lenses. *Int Cont Lens Clin* 1994;**21**:45-9.

48. Roseman MJ, Frost A, Lawley ME. Effects of base curve on the fit of thin, mid-water contact lenses. *Int Cont Lens Clin* 1993;**20**:95-101.

49. Garner LF. Sagittal height of the anterior eye and contact lens fitting. *Am J Optom Physiol Opt* 1982;5**9**:301-5.

50. Bibby MM. Sagittal depth considerations in the selection of the base curve radius of a soft contact lens. *Am J Optom Physiol Opt* 1979;5**6**:407-13.

51. McMonnies CW, Ho A. Responses to a dry eye questionnaire from a normal population. *J Am Optom Assoc* 1987;**58**:588-91.

52. Craig JP, Tomlinson A. Age and gender effects on the normal tear film. *Adv Exp Med Biol* 1998;**438**:411-5.

53. Fonn D, Situ P, Simpson T. Hydrogel lens dehydration and subjective comfort and dryness ratings in symptomatic and asymptomatic contact lens wearers. *Optom Vis Sci* 1999;**76**:700-4.

54. Fonn D, Dumbleton K, Jones L, du T, Sweeney D. Silicone hydrogel material and surface properties. *Contact Lens Spectrum* 2002;**17**:24-8.

55. Sorbara L, Fonn D, Holden BA, Wong R. Centrally fitted versus upper lid-attached rigid gas permeable lenses. part II. a comparison of the clinical performance. *Int Cont Lens Clin* 1996;**23**:121-7.

56. Cho P, Lam AK, Mountford J, Ng L. The performance of four different corneal topographers on normal human corneas and its impact on orthokeratology lens fitting. *Optom Vis Sci* 2002;**79**:175-83.

57. Tang W, Collins MJ, Carney L, Davis B. The accuracy and precision performance of four videokeratoscopes in measuring test surfaces. *Optom Vis Sci* 2000;**77**:483-91.

58. Liesegang TJ. Physiologic changes of the cornea with contact lens wear. *CLAO J* 2002;**28**:12-27.

59. Benjamin WJ, Rasmussen MA. Oxygen consumption of the superior cornea following eyelid closure. *Acta Ophthalmol (Copenh)* 1988;**66**:309-12.

60. MISHIMA S. Corneal thickness. *Survey of Ophthalmology* 1968;**13**:57-96.

61. Doughty MJ, Zaman ML. Human corneal thickness and its impact on intraocular pressure measures: a review and meta-analysis approach. *Surv Ophthalmol* 2000;**44**:367-408.

62. Mandell RB, Polse KA, Fatt I. Corneal swelling caused by contact lens wear. *Arch Ophthalmol* 1970;**83**:3-9.

63. Snyder AC, Schoessler JP. Corneal thickness changes associated with daily and extended contact lens wear. *Am J Optom Physiol Opt* 1983;**60**:830-8.

64. Carney LG. Hydrophilic lens effects on central and peripheral corneal thickness and corneal topography. *Am J Optom Physiol Opt* 1975;**52**:521-3.

65. Bonanno JA, Polse KA. Central and peripheral corneal swelling accompanying soft lens extended wear. *Am J Optom Physiol Opt* 1985;**62**:74-81.

66. Harris HG, Sarver MD, Brown LR. Corneal edema with hydrogel lenses and eye closure: Time course. *Am J Optom Physiol Opt* 1981;**58**:18-20.

67. Miller D. Contact lens-induced corneal curvature and thickness changes. *Arch Ophthalmol* 1968;**80**:430-2.

68. Iskeleli G, Oral AY, Celikkol L. Changes in corneal radius and thickness in response to extended wear of rigid gas permeable contact lenses. *CLAO J* 1996;**22**:133-5.

69. GuÌˆrdal C, Aydin S, KirimliogÌŒlu H, Toprak E, SÌ§engoÌˆr T. Effects of extended-wear soft contact lenses on the ocular surface and central corneal thickness. *Ophthalmologica* 2003;**217**:329-36.

70. Yaylali V, Kaufman SC, Thompson HW. Corneal thickness measurements with the Orbscan Topography System and ultrasonic pachymetry. *J Cataract Refract Surg* 1997;**23**:1345-50.

71. Liu Z, Pflugfelder SC. The effects of long-term contact lens wear on corneal thickness, curvature, and surface regularity. *Ophthalmology* 2000;**107**:105-11.

72. Bailey IL, Carney LG. Corneal changes from hydrophilic contact lenses. *Am J Optom Arch Am Acad Optom* 1973;**50**:299-304.

73. Binder PS, Worthen DM. Clinical evaluation of continuous-wear hydrophilic lenses. *Am J Ophthalmol* 1977;**83**:549-53.

74. Bucci FA, Myers PJ, Evans RE, Tanner JB, Moody KJ, Lopatynsky MO. Clinical and overnight corneal swell comparison of the 1-Day Acuvue lens versus the Medalist, Surevue, Biomedics, and Acuvue lenses. *CLAO J* 1997;**23**:103-12.

75. Cho P, Lam C. Factors affecting the central corneal thickness of Hong Kong-Chinese. *Curr Eye Res* 1999;**18**:368-74.

76. Garner LF, Caithness HA. The effect of fenestrating soft contact lenses on corneal swelling. *Am J Optom Physiol Opt* 1981;**58**:189-92.

77. Cox I, Ames K. Effect of eye patching on the overnight corneal swelling response with rigid contact lenses. *Optom Vis Sci* 1989;**66**:207-8.

78. Holden BA, Mertz GW. Critical oxygen levels to avoid corneal edema for daily and extended wear contact lenses. *Invest Ophthalmol Vis Sci* 1984;**25**:1161-7.

79. Holden BA, Sweeney DF, Lahood D, Kenyon E. Corneal Deswelling Following Overnight Wear of Rigid and Hydrogel Contact-Lenses. *Curr Eye Res* 1988;**7**:49-53.

80. Kenyon E, Polse KA, Seger RG. Influence of wearing schedule on extended-wear complications. *Ophthalmology* 1986;**93**:231-6.

81. El H, Leach NE. Central and peripheral corneal thickness changes induced by "on K", steep, and flat contact lens wear. *J Am Optom Assoc* 1975;**46**:296-302.

82. Kline LN, DeLuca TJ, Fishberg GM. Corneal staining relating to contact lens wear. *J Am Optom Assoc* 1979;**50**:353-7.

83. Begley CG, Barr JT, Edrington TB, Long WD, McKenney CD, Chalmers RL. Characteristics of corneal staining in hydrogel contact lens wearers. *Optom Vis Sci* 1996;**73**:193-200.

84. Orsborn GN, Zantos SG. Corneal desiccation staining with thin high water content contact lenses. *CLAO J* 1988;**14**:81-5.

85. Korb DR, Korb JM. Corneal staining prior to contact lens wearing. *J Am Optom Assoc* 1970;**41**:228-32.

86. Schwallie JD, McKenney CD, Long WD, McNeil A. Corneal staining patterns in normal non-contact lens wearers. *Optom Vis Sci* 1997;**74**:92-8.

87. Dundas M, Walker A, Woods RL. Clinical grading of corneal staining of non-contact lens wearers. *Ophthalmic Physiol Opt* 2001;**21**:30-5.

88. Guillon JP, Guillon M, Malgouyres S. Corneal desiccation staining with hydrogel lenses: tear film and contact lens factors. *Ophthalmic Physiol Opt* 1990;**10**:343-50.

89. Nichols JJ, Sinnott LT. Tear film, contact lens, and patient-related factors associated with contact lens-related dry eye. *Invest Ophthalmol Vis Sci* 2006;**47**:1319-28.

90. Ichijima H, Yokoi N, Nishizawa A, Kinoshita S. Fluorophotometric assessment of rabbit corneal epithelial barrier function after rigid contact lens wear. *Cornea* 1999;**18**:87-91.

91. Stapleton F, Kasses S, Bolis S, Keay L. Short term wear of high Dk soft contact lenses does not alter corneal epithelial cell size or viability. *Br J Ophthalmol* 2001;**85**:143-6.

92. Peterson RC, Fonn D, Woods CA, Jones L. Impact of a rub and rinse on solution-induced corneal staining. *Optom Vis Sci* 2010;**87**:1030-6.

93. Sorbara L, Peterson R, Woods C, Fonn D. Multipurpose disinfecting solutions and their interactions with a silicone hydrogel lens. *Eye Contact Lens* 2009;**35**:92-7.

94. Pritchard N, Fonn D. Dehydration, lens movement and dryness ratings of hydrogel contact lenses. *Ophthalmic Physiol Opt* 1995;**15**:281-6.

95. Pritchard N, Fonn D, Weed K. Ocular and subjective responses to frequent replacement of daily wear soft contact lenses. *CLAO J* 1996;**22**:53-9.

96. Pritchard N, Fonn D, Brazeau D. Discontinuation of contact lens wear: a survey. *Int Cont Lens Clin* 1999;**26**:157-62.

97. Covey M, Sweeney DF, Terry R, Sankaridurg PR, Holden BA. Hypoxic effects on the anterior eye of high-Dk soft contact lens wearers are negligible. *Optom Vis Sci* 2001;**78**:95-9.

98. Fonn D, Dumbleton K. Dryness and discomfort with silicone hydrogel contact lenses. *Eye Contact Lens* 2003;**29**:S101-S104.

99. Larke JR, Hirji NK. Some clinically observed phenomena in extended contact lens wear. *British Journal of Ophthalmology* 1979;**63**:475-7.

100. Efron N, Al Dossari M, Pritchard N. Confocal Microscopy of the Bulbar Conjunctiva in Contact Lens Wear. *Cornea* 2010;**29**:43-52.

101. Skotnitsky CC, Naduvilath TJ, Sweeney DF, Sankaridurg PR. Two presentations of contact lens-induced papillary conjunctivitis (CLPC) in hydrogel lens wear: local and general. *Optom Vis Sci* 2006;**83**:27-36.

102. Guillon M, Maissa C. Bulbar conjunctival staining in contact lens wearers and non lens wearers and its association with symptomatology. *Contact Lens and Anterior Eye* 2005;**28**:67-73.

103. Brautaset RL, Nilsson M, Leach N, Miller WL, Gire A, Quintero S et al. Corneal and conjunctival epithelial staining in hydrogel contact lens wearers. *Eye Contact Lens* 2008;**34**:312-6.

104. Adar S, Kanpolat A, Surucu S, Ucakhan OO. Conjunctival impression cytology in patients wearing contact lenses. *Cornea* 1997;**16**:289-94.

105. Albietz JM. Conjunctival histologic findings of dry eye and non-dry eye contact lens wearing subjects. *CLAO J* 2001;**27**:35-40.

106. Begley CG, Chalmers RL, Abetz L, Venkataraman K, Mertzanis P, Caffery BA et al. The relationship between habitual patient-reported symptoms and clinical signs among patients with dry eye of varying severity. *Invest Ophthalmol Vis Sci* 2003;**44**:4753-61.

107. Lofstrom T, Kruse A. A conjunctival response to silicone hydrogel lens wear. *Contact Lens Spectrum* 2005;**20**:42-4.

108. Marner K, NORN MS. Vital staining properties of neutral red. Vital staining of cornea and conjunctiva. *Acta Ophthalmol (Copenh)* 1978;**56**:742-50.

109. Keir N, Woods CA, Dumbleton K, Jones L. Clinical performance of different care systems with silicone hydrogel contact lenses. *Contact Lens and Anterior Eye* 2010;**33**:189-95.

110. Bron AJ, Evans VE, Smith JA. Grading of corneal and conjunctival staining in the context of other dry eye tests. *Cornea* 2003;**22**:640-50.

111. Eliason JA, Maurice DM. Staining of the conjunctiva and conjunctival tear film. *Br J Ophthalmol* 1990;**74**:519-22.

112. Lakkis C, Brennan NA. Bulbar conjunctival fluorescein staining in hydrogel contact lens wearers. *CLAO J* 1996;**22**:189-94.

113. Efron N, Veys J. Ocular Integrity Can be Compromised by Defects in Disposable Contact-Lenses. *Invest Ophthalmol Vis Sci* 1992;**33**:1293.

114. Guillon M, Maissa C. Bulbar conjunctival staining in contact lens wearers and non lens wearers and its association with symptomatology. *Cont Lens Anterior Eye* 2005;**28**:67-73.

115. Paugh JR, Brennan NA, Efron N. Ocular response to hydrogen peroxide. *Am J Optom Physiol Opt* 1988;**65**:91-8.

116. du T, Situ P, Simpson T, Fonn D. The effects of six months of contact lens wear on the tear film, ocular surfaces, and symptoms of presbyopes. *Optom Vis Sci* 2001;**78**:455-62.

117. Holly FJ. Tear film physiology. *Am J Optom Physiol Opt* 1980;**57**:252-7.

118. Begley CG, Chalmers RL, Liu H, Smith JA, Edrington TB, Simpson TL et al. From tear instability to dry eye: A unifying hypothesis. *Invest Ophthalmol Vis.Sci.* 2005;**46**.

119. Begley CG, Chalmers RL, Abetz L, Venkataraman K, Mertzanis P, Caffery BA et al. The relationship between habitual patient-reported symptoms and clinical signs among patients with dry eye of varying severity. *Invest Ophthalmol Vis Sci* 2003;**44**:4753-61.

120. Holden BA, Stephenson A, Stretton S, Sankaridurg PR, O'Hare N, Jalbert I et al. Superior epithelial arcuate lesions with soft contact lens wear. *Optom Vis Sci* 2001;**78**:9-12.

121. Santodomingo-Rubido J, Wolffsohn J, Gilmartin B. Conjunctival epithelial flaps with 18 months of silicone hydrogel contact lens wear. *Eye Contact Lens* 2008;**34**:35-8.

122. Stapleton F, Dart J, Minassian D. Nonulcerative complications of contact lens wear: Relative risks for different lens types. *Arch Ophthalmol* 1992;**110**:1601-6.

123. Lakkis C, Vincent S. Clinical Investigation of Asmofilcon A Silicone Hydrogel Lenses. *Optom Vis Sci* 2009;**86**:350-6.

124. Guillon M, Bilton S, Bleshoy H, Guillon JP, Lydon DPM. Limbal changes associated with hydrogelcontact lens wear. *Journal of the British Contact Lens Association* 1985;**8**:15-9.

125. Efron N. Vascular response of the cornea to contact lens wear. *J Am Optom Assoc* 1987;**58**:836-46.

126. Papas E. On the relationship between soft contact lens oxygen transmissibility and induced limbal hyperaemia. *Exp Eye Res* 1998;**67**:125-31.

127. McMonnies CW, Chapman-Davies A, Holden BA. The vascular response to contact lens wear. *Am J Optom Physiol Opt* 1982;**59**:795-9.

128. McMonnies CW, Chapman-Davies A. Assessment of conjunctival hyperemia in contact lens wearers. Part II. *Am J Optom Physiol Opt* 1987;**64**:251-5.

129. Aakre BM, Ystenaes AE, Doughty MJ, Austrheim Ã, Westerfjell B, Lie MT. A 6-month follow-up of successful refits from daily disposable soft contact lenses to continuous wear of high-Dk silicone-hydrogel lenses. *Ophthalmic and Physiological Optics* 2004;**24**:130-41.

130. Chalmers RL, Dillehay S, Long B, Barr JT, Bergenske P, Donshik P et al. Impact of previous extended and daily wear schedules on signs and symptoms with high Dk lotrafilcon A lenses. *Optom Vis Sci* 2005;**82**:549-54.

131. Papas EB. The role of hypoxia in the limbal vascular response to soft contact lens wear. *Eye Contact Lens* 2003;**29**:S72-S74.

132. Papas EB, Vajdic CM, Austen R, Holden BA. High-oxygen-transmissibility soft contact lenses do not induce limbal hyperaemia. *Curr Eye Res* 1997;**16**:942-8.

133. Dumbleton KA, Chalmers RL, Richter DB, Fonn D. Vascular response to extended wear of hydrogel lenses with high and low oxygen permeability. *Optom Vis Sci* 2001;**78**:147-51.

134. Shah SS, Yeung KK, Weissman BA. Contact lens-related deep stromal vascularization. *Int Cont Lens Clin* 1998;**25**:128-36.

135. Fonn D, Sweeney D, Holden BA, Cavanagh D. Corneal oxygen deficiency. *Eye Contact Lens* 2005;**31**:23-7.

136. Stapleton F, Stretton S, Papas E, Skotnitsky C, Sweeney DF. Silicone hydrogel contact lenses and the ocular surface. *Ocul Surf* 2006;**4**:24-43.

137. Efron N, Brennan NA, Currie JM, Fitzgerald JP, Hughes MT. Determinants of the Initial Comfort of Hydrogel Contact-Lenses. *Am J Optom Physiol Opt* 1986;**63**:819-23.

138. La Hood D. Edge shape and comfort or rigid lenses. *Am J Optom Physiol Opt* 1988;**65**:613-8.

139. Edwards N. Re: "A critical review of visual analogue scales in the measurement of clinical phenomena". *Research in nursing & health* 1991;**14**:81.

140. McCormack HM, Horne DJ, Sheather S. Clinical applications of visual analogue scales: a critical review. *Psychological medicine* 1988;**18**:1007-19.

141. du Toit R, Pritchard N, Heffernan S, Simpson T, Fonn D. A comparison of three different scales for rating contact lens handling. *Optom Vis Sci* 2002;**79**:313-20.

142. Papas EB, Schultz BL. Repeatability and comparison of visual analogue and numerical rating scales in the assessment of visual quality. *Ophthalmic Physiol Opt* 1997;**17**:492-8.

143. Carta A, Braccio L, Belpoliti M, Soliani L, Sartore F, Gandolfi SA et al. Self-assessment of the quality of vision: Assosciation of questionnaire score with objective clinical tests. *Curr Eye Res* 1998;**17**:506-11.

144. Woods CA, Cumming B. The impact of test medium on use of visual analogue scales. *Eye and Contact Lens* 2009;**35**:6-10.

145. Grunberg SM, Groshen S, Steingass S, Zaretsky S, Meyerowitz B. Comparison of conditional quality of life terminology and visual analogue scale measurements. *Qual Life Res* 1996;**5**:65-72.

146. McCormack HM, Horne DJ, Sheather S. Clinical applications of visual analogue scales: a critical review. *Psychological medicine* 1988;**18**:1007-19.

147. Orsborn G, Zantos SG. Practitioner survey: management of dry-eye symptoms in soft lens wearers. *Contact Lens Spectrum* 1989;**4**:23-6.

148. Doughty MJ, Fonn D, Richter D, Simpson T, Caffery B, Gordon K. A patient questionnaire approach to estimating the prevalence of dry eye symptoms in patients presenting to optometric practices across Canada. *Optom.Vis.Sci.* 1997;**74**:624-31.

149. Tighe B. In: Sweeney D ed. Oxford, Butterworth-Heinemann, 2000: 1-21.

150. Young G, Garofalo R, Harmer O, Peters S. The effect of soft contact lens care products on lens modulus. *Cont Lens Anterior Eye* 2010;**33**:210-4.

151. Morgan P. Is the UK contact lens market healthy? *Optician* 2001;**5795**:22-6.

152. Glasson MJ, Keay L, Willcox MDP. Understanding the reasons why some patients are Intolerant to soft contact lens wear. *Invest Ophthalmol Vis.Sci.* 2000;**41**:S73.

153. Situ P, Fonn D, Pritchard N, Simpson T. Dryness, comfort levels and lens dehydration in symptomatic and non-symptomatic hydrogel lens wearers. *Invest Ophthalmol Vis.Sci.* 1997;**38**:657.

154. Situ P, Simpson TL, Fonn D. Clinical measures do not discriminate symptomatic and asymptomatic contact lens wearers. *Invest Ophthalmol Vis.Sci.* 1999;**40**:S909.

155. Coles M, Brennan N, Jaworski A. ocular signs and symptoms in patients completing 3 years with silicone hydrogel lenses in 30-day continuous wear. *Optom Vis Sci* 2001;**201**.

156. Brennan NA, Coles MLC, Comstock TL, Levy B. A 1-year prospective clinical trial of balafilcon A (PureVision) silicone-hydrogel contact lenses used on a 30-day continuous wear schedule. *Ophthalmology* 2002;**109**:1172-7.

157. Dumbleton K, Keir N, Moezzi A, Feng Y, Jones L, Fonn D. Objective and subjective responses in patients refitted to daily-wear silicone hydrogel contact lenses. *Optom Vis Sci* 2006;**83**:758-68.